University of Canterbury

Department of Civil and Natural Resources Engineering

Experimental Study on the Seismic Performance of Low Damage Systems for Non-structural Light Framed Plasterboard Partition Walls

ENEQ690 Master's Thesis

Master's Candidate:

Joshua Mulligan (64560538)

Supervisor:

Timothy Sullivan

Co-Supervisor:

Rajesh Dhakal

ABSTRACT

Field surveys and experimental studies have shown that light steel or timber framed plasterboard partition walls are particularly vulnerable to earthquake damage prompting the overarching objective of this research, which is to further the development of low damage seismic systems for non-structural partition walls in order to facilitate their adoption by industry to assist with reducing the losses associated with the maintenance and repair cost of buildings across their design life. In particular, this study focused on the behaviour of steel-framed partition walls systems with novel detailing that aim to be "low-damage" designed according to common practice for walls used in commercial and institutional buildings in New Zealand. This objective was investigated by (1) investigating the performance of a flexible track system proposed by researchers and industry by experimental testing of full-scale specimens; (2) investigating the performance of the seismic gap partition wall systems proposed in a number of studies, further developed in this study with input from industry, by experimental testing of full-scale specimens; and (3) investigating the potential implications of using these systems compared with traditionally detailed partition wall systems within multi-storey buildings using the Performance Based Earthquake Engineering loss assessment methodology.

Three full-scale testing frames were designed in order to replicate, under controlled laboratory conditions, the effects of seismic shaking on partition walls within multi-storey buildings by the application of quasi-static uni-directional cyclic loading imposing an inter-storey drift. The typical configuration for test specimens was selected to be a unique "y-shape", including one angled return wall, with typical dimensions of approximately 2400 mm along the main wall and 600 mm along (approximately) the returns walls with a height of 2405 mm from floor to ceiling. The specimens were aligned within test frames at an oblique angle to the direction of loading in order to investigate bi-directional effects.

Three wall specimens with flexible track detailing, two identical plane specimens and the third including a doorway, were tested. The detailing involved removing top track anchors within the proximity of wall intersections, thus allowing the tracks to 'bow' out at these locations. Although the top track anchors were specified to be removed the proximity of wall intersections, a construction error was made whereby a single top track slab to concrete anchor was left in at the three-way wall junction. Despite this error, the experimental testing was deemed worthwhile since such errors will also occur in practice and because the behaviour of the wall can be examined with this fixing in mind. The specimens also included an acoustic/fire sealant at the top lining to floor boundary. In addition to providing drift capacities, the force-displacement behaviour is also reported, the dissipated energy was computed, and the parameters of the Wayne-Stewart hysteretic model were fitted to the results. The

specimen with the door opening behaved significantly different to the plane specimens: damage to the doorway specimen began as cracking of the wallboard propagating from the corners of the doorway following which the L- and Y- shaped junctions behaved independently, whereas damage to the plane specimens began as cracking of the wallboard at the top of the L-junction and wall system deformed as a single unit. The results suggest that bi-directional behaviour is important even if its impact cannot be directly quantified by the experiments conducted. Damage to sealant implies that the bond between plasterboard and sealant is important for its seismic performance. Careful quality control is advised as defects in the bond may significantly impact its ability to withstand seismic movement.

Two specimens with seismic gap detailing were tested: a steel stud specimen and a timber stud specimen. Observed drift capacities were significantly greater than traditional plasterboard partition systems. Equations were used to predict the drift at which damage state 1 (DS1) and damage state 2 (DS2) would initiate. The equation used to estimate the drift at the onset of DS1 accurately predicted the onset of plaster cracking but overestimated the drift at which the gap filling material was damaged. The equation used to predict the onset of DS2 provided a lower bound for both specimens and also when used to predict results of previous experimental tests on seismic gap systems. The gap-filling material reduced the drift at the onset of DS1, however, it had a beneficial effect on the re-centring behaviour of the linings. Out-of-plane displacements and return wall configuration did not appear to significantly impact the onset of plaster cracking in the specimens.

A loss assessment according to the PBEE methodology was conducted on four steel MRF case study buildings: (1) a 4-storey building designed for the Christchurch region, (2) a 4-storey building designed for the Wellington region, (3) a 12-storey building designed for the Christchurch region, and (4) a 12-storey building designed for the Wellington region. The fragility parameters for a traditional partition system, the flexible track partition system, and the seismic gap steel stud and timber stud partition systems were included within the loss assessment. The order (lowest to highest) of each system in terms of the expected annual losses of each building when incorporating the system was, (1) the seismic gap timber stud system, (2) the seismic gap steel stud system, (3) the traditional/baseline system, and (4) the flexible track system.

For the seismic gap timber stud system, which incurred the greatest reduction in expected annual losses for each case study building, the reduction in expected annual losses in comparison to the losses found when using the traditional system ranged from a 5% to a 30% reduction. This reinforces the fact that while there is a benefit to the using low damage partition systems in each building the extent of reduction in expected annual losses is significantly dependent on the particular building design and its location.

The flexible track specimens had larger repair costs at small hazard levels compared to the traditional system but smaller repair costs at larger hazard levels. However, the resulting expected annual losses for the flexible track system was higher than the traditional system which reinforces findings from past studies which observed that the greatest contribution to expected annual losses arises from low to moderate intensity shaking seismic events (low hazard levels).

ACKNOWLEDGEMENTS

I would like to extend my sincere gratitude to my primary supervisor Professor Timothy Sullivan whose oversight, expertise, and support ensured this project stayed on course towards a good result even considering the many obstacles encountered along the way. I would also like to thank my secondary supervisor professor Rajesh Dhakal for his insight and attention to detail which has added considerable value to this study at critical stages.

I wish to extend my thanks to Hans Gerlich and Frank Kang (Winstone Wallboards Ltd.) for providing building materials, labour, and practical advice during the design and preparation of the partition wall systems tested within this study. Their willingness to collaborate and input was particularly helpful during the experimental specimen design and construction phases of this study.

The help of the technical staff working in the laboratory is also very much appreciated. I would like to thank all of the staff and technicians who were involved in this research. In particular I would like to thank Anne Mackenzie, the structures lab engineering manager; Mosese Fifita & John Maley, the appointed technicians for this project; Michael Weaver & Peter Coursey, for their help with instrumentation and software; and David MacPherson (technical services manager). Without their technical knowledge, experience, and practical skill the objectives of this project would not have been able to be realized.

I would also like to gratefully acknowledge the funding support offered by the International Collaborative Research program of the Disaster Prevention Research Institute, Kyoto University under Project Number 28W-03 (PI: Timothy Sullivan), the NZ Property Council, and Quake Centre. This project was also partially supported by QuakeCoRE, a New Zealand Tertiary Education Commission-funded Centre. And give my thanks also to several industry partners; RONDO Ltd.; Winston Wallboards Ltd.; Dunning Thornton Consultants; and Holmes Consulting.

In addition, I would also like to thank Amir Orumiyehei for the valuable input he provided to the analytical modelling stages of this study. For information on ground motion records and building components (quantity, fragility, and consequence functions), as used within the building modelling and analysis stages of this project, made possible with Amir's assistance, refer to the site from following the link below:

https://wiki.canterbury.ac.nz/display/QuakeCore/Project%2b17137%2b-%2bUsage%2bof%2bSeismic%2bLoss%2bAssessment%2bto%2bMotivate%2bHigh%2bPerformance%2bBuilding%2bSolutions

Finally, I would like to thank my wife, Hayley, for her continual support and encouragement.

TABLE OF CONTENTS

TABLE OF FIGURES

TABLE OF TABLES

1. INTRODUCTION

1.1 Overview

As has been shown by field observation (Whitman *et al.* 1973, Taghavi and Miranda 2003, Dhakal 2010), experimental studies (Davies *et al.* 2011, Restrepo and Bersofsky 2011, Tasligedik *et al.* 2015), and analytical studies (Arifin *et al.* 2017, Yeow *et al.* 2018) the behaviour of partition wall systems subject to seismic loading has a significant effect on the repair cost of building systems following earthquake ground motions due to their susceptibility to incur damage requiring repair under relatively small inter-storey drifts. Therefore, the overall objective of this research project is to further the development of low damage seismic systems for non-structural partition walls to facilitate their adoption by industry to assist with reducing the losses associated with the maintenance and repair cost of buildings across their design life. In particular, this study focuses on the behaviour of steel-framed partition walls systems with novel detailing that aim to be "low-damage" and are designed according to common practice for walls used in commercial and institutional buildings in New Zealand.

This chapter introduces the context and motivation of the research conducted within this study. The design and typical detailing of partition walls is discussed particularly as it pertains to typical construction within commercial buildings in New Zealand; a brief overview is provided of the performance of plasterboard partition walls as observed by field observations and reconnaissance reports following earthquake events, highlighting the vulnerability of plasterboard partitions when subject earthquake loading; an overview of the Pacific Earthquake Engineering Research (PEER) Centre's Performance Based Earthquake Engineering (PBEE) methodology is provided due to its significance in quantifying the performance of non-structural partition walls in the context of buildings systems; a summary of the research relating to the seismic behaviour of light framed gypsum partition walls is given demonstrating the need for extensive testing on low damage seismic solutions for partition walls; and finally as justified by the discussions provided, the research objectives and scope will be presented in the context of current literature.

1.2 Characteristics of Partition Walls

1.2.1 Plasterboard Background

Due to its ease of installation, familiarity, fire performance, and acoustic performance, gypsum wall board (also known as drywall or plasterboard) is ubiquitous in construction. The main advantages of gypsum board over other wall linings include its relatively low cost, ease of installation, fire-resistance, sound attenuation, and availability. Technological advancements mean that a wide array of boards are available to that are able to achieve a number of performance criteria. Plasterboard is now the most

common internal wall lining surface in residential and commercial construction Internationally and in New Zealand.

Winstone Wallboards is the only manufacturer of gypsum plasterboard in New Zealand and the largest marketer of drywall systems and associated products and services. The company manufactures products under the GIB® brand.

1.2.2 Standard Construction of Partition Walls

The construction of partition walls differs for residential and commercial construction. In residential buildings partitions may be used as both vertical and horizontal load resisting elements as well as to provide partitioned spaces. Unlike residential buildings partition walls are not designed to be part of the primary gravity or lateral load resisting system as the design forces in commercial buildings using conventional structural systems are much higher than the forces a partition wall system can be expected to resist. Therefore, as per NZS1170.5 Section 8, these walls are considered a non-structural component because they are designed to carry limited gravity or lateral loads in addition to their own weight.

The design of partition walls in residential buildings is done according to NZS 3604:2011 (Standards New Zealand 2011), which is used to design most homes and low-rise timber-framed buildings in New Zealand. Wall framing typically consists of 2.4 m high 100 x 50 mm studs with 100 x 50 mm top and bottom plates. Studs are generally spaced at a maximum of 600 mm centres with dwangs (horizontal timber blocking) in horizontal rows at 800 mm maximum centres, or as required, to provide edge fixing for sheet lining materials or to support internal joinery (Standards New Zealand 2011). The GIB® Site Guide (2014) outlines the correct procedure for the installation of plasterboard in walls and ceilings. For walls, plasterboard sheets may be installed horizontally or vertically. The sheets may be fastened to the framing around the perimeter with screws or nails at 300 mm centres and to intermediate studs and nogs with screws, nails, or adhesive at 300 mm centres (Figure 1.1). For bracing elements, the perimeter fastener spacing typically is reduced to 150 mm centres and hold-down brackets are introduced. Steel framed plasterboard partitions are also used; however, timber framed walls are more common. Control joints to relieve stresses imposed by structural movement (due to changes in temperature, changes in humidity, and wind forces) are also required at a maximum of 12 m centres along continuous lengths of wall. Once the linings are installed the joints between sheets must be finished appropriately to provide strength and resistance to cracking. This is done using joint tape and compound (typically plaster based compound or an air-drying compound) in two to three coats depending on the level of finish required. External and internal corners are finished with paper or metal trims in place of tape. The topcoat is then typically sanded before the wall is painted.

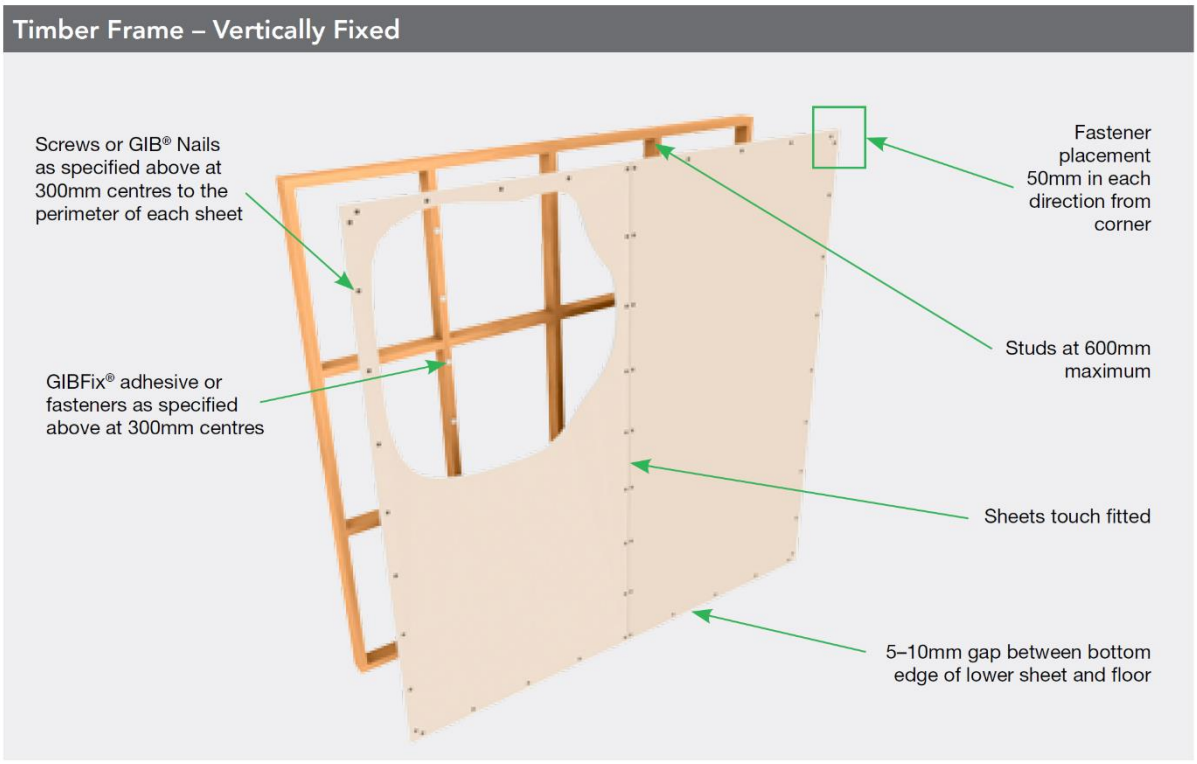

Figure 1.1 Typical New Zealand timber framed residential partition wall as per GIB® Site Guide (2014)

Wall systems in commercial buildings are typically constructed using light-frame construction materials, the most common being wood or steel framing lined with gypsum wall board. Due to its low weight versus wood framing, the variability of moisture content wood framing, and its non-combustibility steel framing is the preferred option in large commercial structures. Light steel framed plasterboard walls are typically constructed using U-shaped base track fixed directly to the floor slab. Another U-shaped track is fixed to the upper floor slab. Stud members are placed vertically, and friction fitted between the two tracks, typically at 600 mm centres. The tracks along with the studs compose the frame of the wall. Gypsum wall board panels, typically 13 mm to 16 mm thick, are then attached to the studs using self-drilling screws. There are several alternate configurations provided by manufacturers for steel-framed partition wall systems for commercial systems designed to satisfy various performance objectives including, fire rating, acoustic rating, water resistance, impact resistance, to name a few. The systems differ in the type, thickness, and number of layers of gypsum board, fastener sizes, and stud size and type. The acoustic rating of a partition may also be increased by installing insulating material between the studs or by using specialist channels and clips to create a physical break across the partition. They also vary in tracks sizes; however, 64 x 34 x 0.55 mm steel studs and 64 x 30 x 0.55 mm steel tracks are the most common for non-loadbearing walls with few exceptions. The configuration and detailing of a typical 60 minute fire resistance rating (FRR) non-loadbearing wall from GIB Fire Rated Systems (2012), GBS 60, is shown in Figure 1.2. Typical details for the junctions between intersecting

walls are shown in Figure 1.4. The dimensions and specifications of the GBS 60 wall components are as follows:

- Steel studs are 64 x 34 x 0.55 mm nominal with 6 mm lips spaced at 600 mm centres.
- Steel tracks are 64 x 30 x 0.55 mm nominal fixed at top and bottom boundaries.
- 15 mm expansion gap must be provided between the top track and top of studs.
- Studs are not fastened to the tracks and are only held in place by clamping/grip of the tracks.
- Recommended maximum height is 2700mm. For higher walls, specific engineering design is required.
- One layer of 13mm GIB Fyreline® Plasterboard (proprietary fire-retardant plasterboard) is used each side of frame. They must be aligned vertically, touch fitted, and fixed hard to the floor.
- Sheathing to stud connectors are 25 mm x 6g GIB® Grabber® Drywall Self Tapping Screws spaced at 300 mm centres up each stud, 12 mm from sheet edges, and 50 mm from sheet ends.
- Linings may be fastened to the top and bottom tracks provided the fasteners do not connect the studs and the tracks.
- All screw heads must be stopped, and all sheets joints tape reinforced in accordance with the GIB® Site Guide (2014).
- Control joints as shown in Figure 1.3 are required at 9 m centres. Note that these control joints are designed to accommodate small building movements that are likely to result from the variations in temperature and humidity; and are not designed to accommodate structural movements.

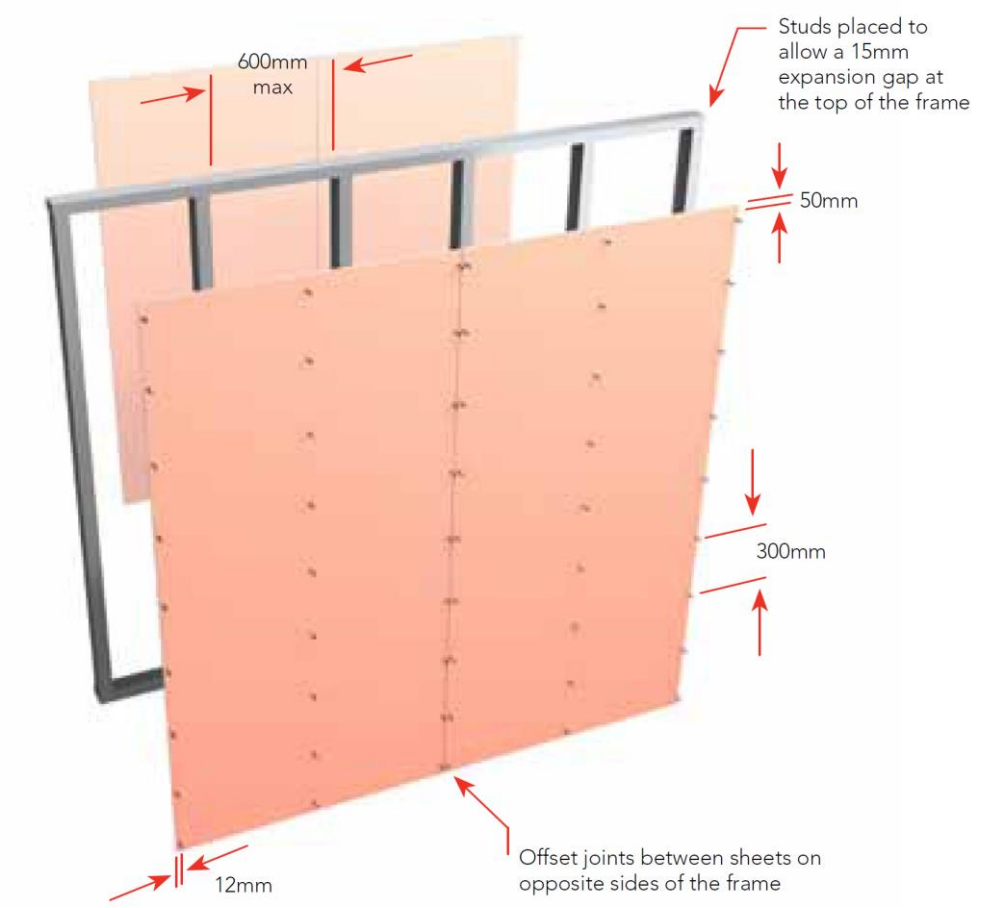

Figure 1.2 Typical New Zealand steel framed partition, GBS 60 from GIB Fire rated systems manual (Winstone Wallboards 2012)

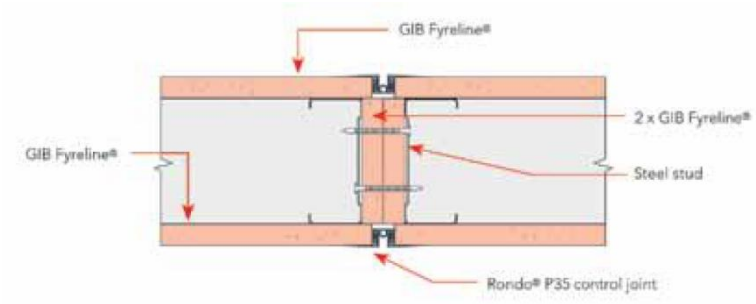

Figure 1.3 Typical New Zealand steel framed partition control joint detail, GBS 60 from GIB Fire rated systems manual (Winstone Wallboards 2012)

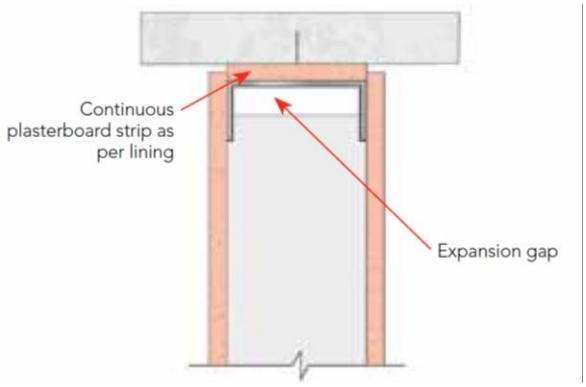

(a) Connection to top slab (option 1)

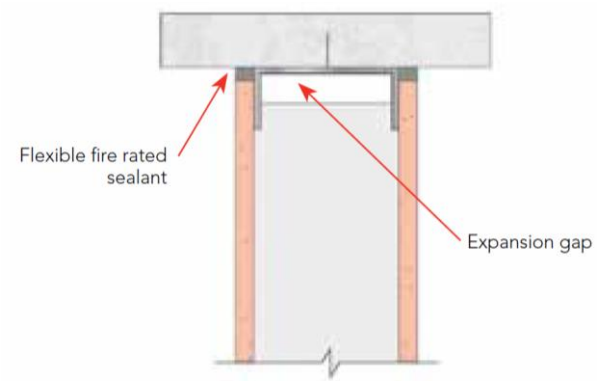

(b) Connection to top (option 2)

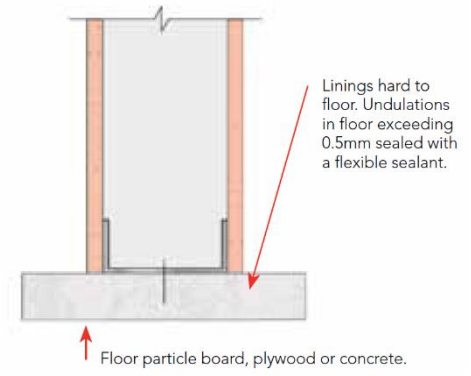

(c) Connection to floor slab

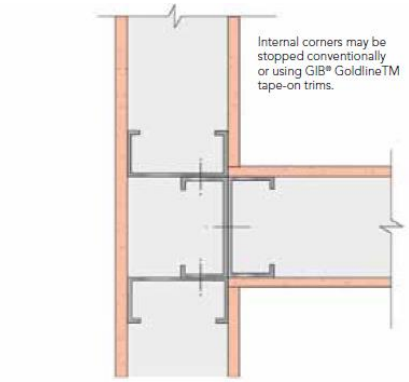

(d) T-junction detail (option 1)

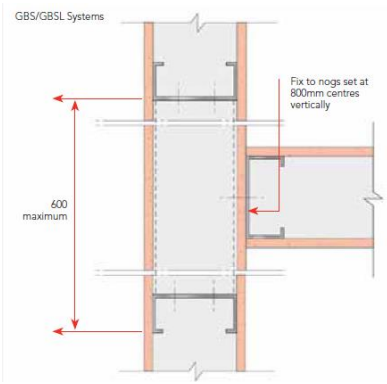

(e) T-junction detail (option 2)

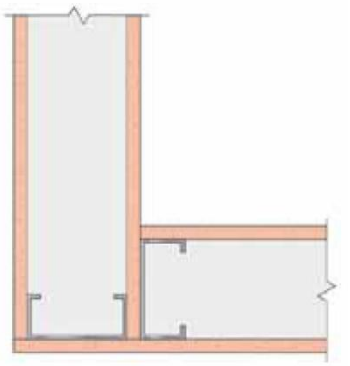

(f) L-junction detail

Figure 1.4 GIB® Fire Rated Systems (2012) recommended details

1.3 Performance of Standard Partitions in Previous Earthquakes

1.3.1 9th of February 1971 San Fernando Earthquake

The 1971 San Fernando earthquake (also known as the Sylmar earthquake), a 6.7 on the moment magnitude scale, occurred in the San Gabriel Mountains in southern California. The earthquake cost 64 people their lives and created physical losses estimated at more than 500 million U.S. dollars (USGS 1971). Whitman *et al.* (1973) documented the degree of damage experienced by high-rise buildings in the Los Angeles area during the earthquake and compiled damage statistics based upon this documentation. The study encompassed buildings having 5 or more storeys only in an area south of the epicentre which experienced a Modified Mercialli Intensity of ground shaking of VI or greater (area shown in Figure 1.5). The modified Mercalli scale describes the intensity of earthquakes in a qualitative way, based on the relative amount of damage that structures undergo during an earthquake, using a scale of I to XII. The damage in this area ranged from none to extreme and contained buildings constructed before the advent of earthquake design requirements as well as buildings designed and constructed in accordance with modern requirements (applicable at the time).

Of the 1650 buildings having 5 or more storeys believed to be present in the area, damage was documented for about 370. The modified Mercalli intensity was assigned to each sub-area to indicate the level of ground shaking experienced by each building. The number of high-rise buildings documented by this study differentiated by number of storeys, date of construction, and level of ground shaking experienced is shown in Table 1.1.

Table 1.1 Number of high-rise buildings documented and reported by Whitman *et al.* (1973) within sub-regions affected by MMI earthquake intensities VI, VII, and VIII

	Pre-1933			Post-1947		
No. Storeys	VI	VII	VIII	VI	VII	VIII
5 to 7	10	33	0	14	41	12
8 to 13	9	78	0	28	70	4
14 to 18	0	2	0	12	19	0
19+	0	1	0	3	26	0
Total	19	114	0	57	156	16

A detailed damage study was conducted for a limited number of buildings. This included measuring partition lengths from tenant drawings and determining the type of partitions used. Unit costs of various types of partitions were obtained from the owners and some cases with the help of partition contractors and gypsum and plaster manufacturers.

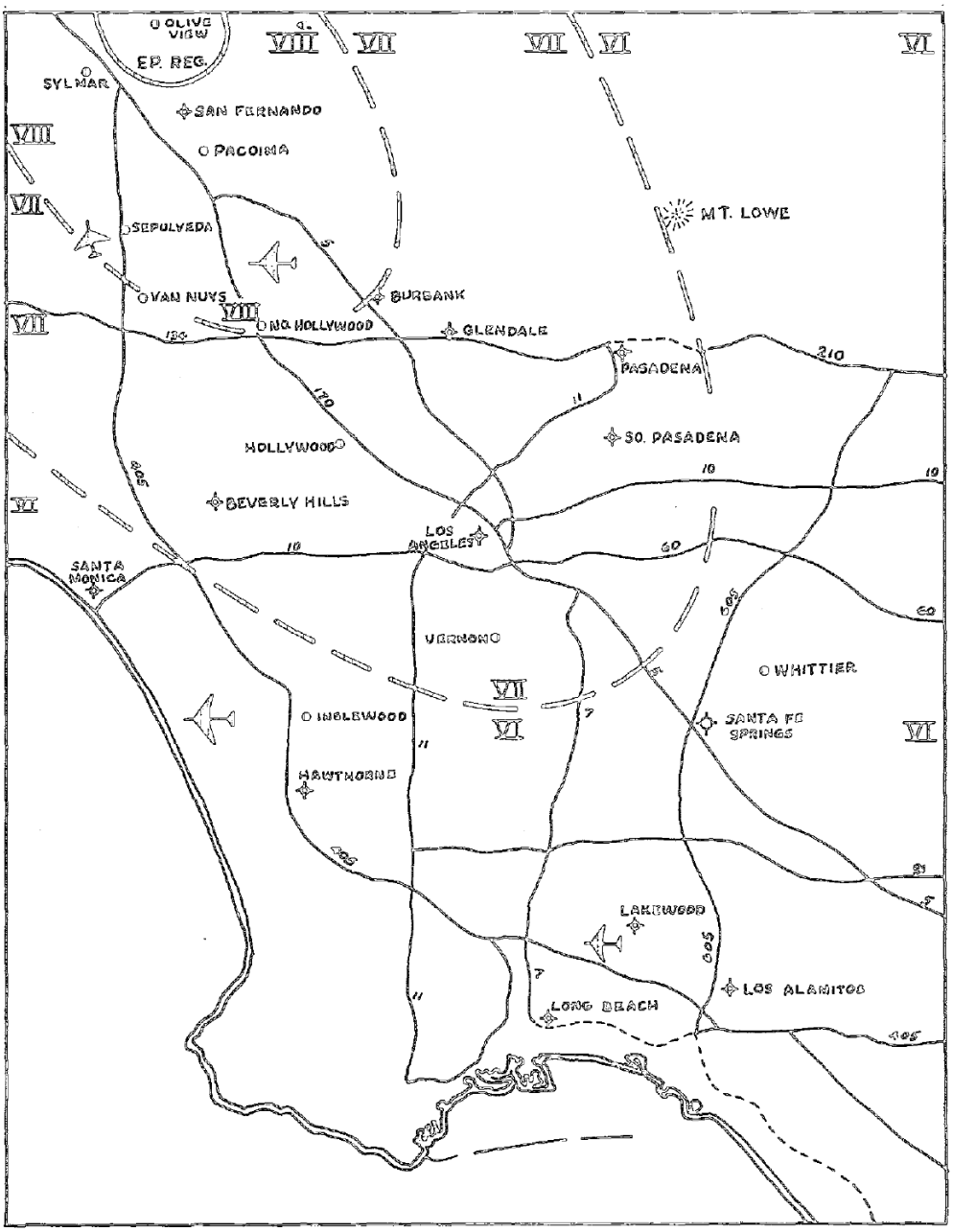

Figure 1.5 Geographical area of study with zones of Modified Mercalli Intensity (Whitman *et al.* 1973)

The report noted that in general for buildings in intensity zone VI, the damage was about 5% structural, 5% elevators, and 90% partitions and finish. For newer buildings in zone VII, these numbers were approximately 20% structural, 5% mechanical, 10% elevators, and 65% partitions and finish. In zone VII, even though the total dollars spent for repairs increased, the percentage of these repairs spent on structural damage decreased compared to zone VI.

76 buildings located in MMI zone VI had complete damage information. Buildings in this zone experienced a damage ratio (ratio of cost of repair to building replacement cost) of 0.15%. Upon examination of the component damage ratios it was noted that painting, partitions, and glass were the

major damage components, while structural damage, mechanical damage, electrical damage, and elevator damage were negligible. In addition, the study noted that the damage is closely related to the inter-storey displacement and the flexibility of the partition walls and glass panels. Whitman *et al.* (1973) noted that improving the flexibility of the partition wall and glass panels may be one of the most effective ways to reduce the total damage in MMI VI. Additionally they made the observation that buildings built pre–1933 behaved better than those built post-1947 which they suggested may be because modern partition wall and glass panel construction is weaker than older construction and/or old buildings are stiffer and therefore attract less inter-storey drift. 275 buildings located in MMI zone VII had complete damage information and only 20% of buildings were free from damage. A study of the mean component damage shows that painting and partition walls still accounted for the major part of the repair cost, but structural and elevator damage both represented sizable portions.

1.3.2 28th of February 2001 Nisqually Earthquake

The moment magnitude M_w 6.8 Nisqually earthquake occurred in the Puget Sound area of Washington State. It is expected that a large amount of the two billion USD (estimated) loss incurred as a result of the Nisqually earthquake can be attributed to non-structural components (Filiatrault *et al.* 2001). From A report by Filiatrault *et al.* (2001), detailing observations made during a field reconnaissance, show that a large portion of the reported loss associated with the Nisqually earthquake was related to the damage to non-structural components. Cracking in interior wall finishes was seen in many buildings during the reconnaissance. In many cases cracking was observed as diagonal cracks at upper corners of doors and window openings and at the intersection between walls and beams. An example of cracking at the intersection of beams observed by Filiatrault *et al.* (2001) is shown in Figure 1.6a. One interesting observation made during the reconnaissance at Kent Regional District Center was vertical cracks at the upper corners of almost all of the interior doors in the building (Figure 1.6b), and, as shown, these cracks were predominantly only on one side. Vertical cracks in of wall finish materials at the intersection of perpendicular walls was also seen in a number of buildings. An example of this type of cracking was observed at the Supreme Court located in the Temple of Justice Building in Olympia (Figure 1.6c). In addition, a substantial amount of cracking of interior finish materials was observed along stairwells.

(a)

(c) (d)

Figure 1.6 Damage to interior walls and finishing in buildings following the 2001 Nisqually earthquake (Filiatrault *et al.* 2001) (a) cracking to finishing at junctions of beams, (b) cracking of plasterboard and finishing above a doorway, and (c) cracking of plasterboard and finishing at wall intersections.

1.3.3 27th of February 2010 Chile Earthquake

The M_w 8.8 offshore Maule, Chile earthquake occurred on the 27th of February 2010 and caused widespread damage in most residential, commercial, industrial, and office buildings. Miranda *et al.* (2012) conducted a field reconnaissance examining non-structural systems in the major affected cities

within a week following the earthquake event and summarized damage to non-structural components in different building types.

Much of of the reported loss associated with the earthquake was attributed to damage to non-structural systems, including damage to partitions, which was widespread in residential and office buildings. The typical damage experienced by partitions included cracking of the finishing materials and of the wallboards. Miranda *et al.* (2012) noted that, particularly for newer buildings, the damage to partition walls and other drift sensitive non-structural elements should have been limited by drift criteria for specified in Chilean codes, which limit the allowable drifts to 0.3%.

During this earthquake 130 hospitals were located within the affected areas and 62% of these suffered non-structural damage requiring repairs. The most common non-structural damage was fallen objects, such as ceiling tiles, partition walls, monitor support units, toppling of shelves, and other objects that were not adequately anchored. Partition walls in newer hospital were typically constructed of light gauge steel studs and only moderate damage, requiring local repairs, was observed at drifts of 0.5-0.7%.

Figure 1.7 Plaster damage and separation of gypsum panes above a door opening in a newer private hosptital (Miranda *et al.* 2012).

1.3.4 4th of September 2010 Darfield Earthquake

The 4th September 2010 M_w 7.1 earthquake, which struck Darfield caused widespread damage. The earthquake had a perceived intensity of MMI X. Of the estimated 4 billion dollar loss incurred from the earthquake and the subsequent aftershocks was attributed to the losses associated with damage to non-structural components and building contents (Dhakal 2010). Although there was only noticeable structural damage in a small proportion of buildings, damage to non-structural components and building contents was observed in almost all buildings and in many cases, there was more damage to non-

structural components than structural components with the exception of old and un-retrofitted unreinforced masonry buildings (Dhakal 2010).

The damage caused to partition walls and internal linings was commonly observed as cracks initiating from door and window corners. In many buildings, aftershocks caused additional damage to partitions and there were also reports of new cracks appearing in walls and internal linings and existing cracks widening and extending following the aftershocks. Some examples of damage to partition walls and internal linings observed following the earthquake are shown in Figure 1.8.

Figure 1.8 Examples of damage to plasterboard partition walls incurred from the 2010 Darfield Earthquake (Dhakal 2010)

1.3.5 22nd of February 2011 Christchurch Earthquake

The 22 February 2011 Christchurch earthquake caused widespread damage to non-structural components on top of the damage sustained from the 4th of September 2010 earthquake. There were numerous cases of complete failure of partitions in addition to significant and widespread damage exceeding the serviceability limit state. This level of damage has significant economic implications due as it requires costly and time-consuming repairs.

Baird *et al.* (2014) conducted a survey of 217 multi-storey buildings following the M_w 6.3 22nd of February 2011 Christchurch Earthquake in order to quantify damage to buildings based on visual inspection of the exteriors only. In addition, a smaller survey of 150 buildings was made for internal partitions. A summary of the performance of facades and infill systems from damage observed following the earthquake is shown in Figure 1.9 with damage states following those suggested by ASCE (2006): Operational, Immediate Occupancy, Life Safety, and Hazards Reduced. However, partitions were assessed with reference only to the Operational and Immediate Occupancy performance levels: undamaged vs. damaged. Note that as only visual inspections were performed the assessment will have underestimated the true extent of damage as less obvious forms of damage may be present, for example, warped framing and damaged connections.

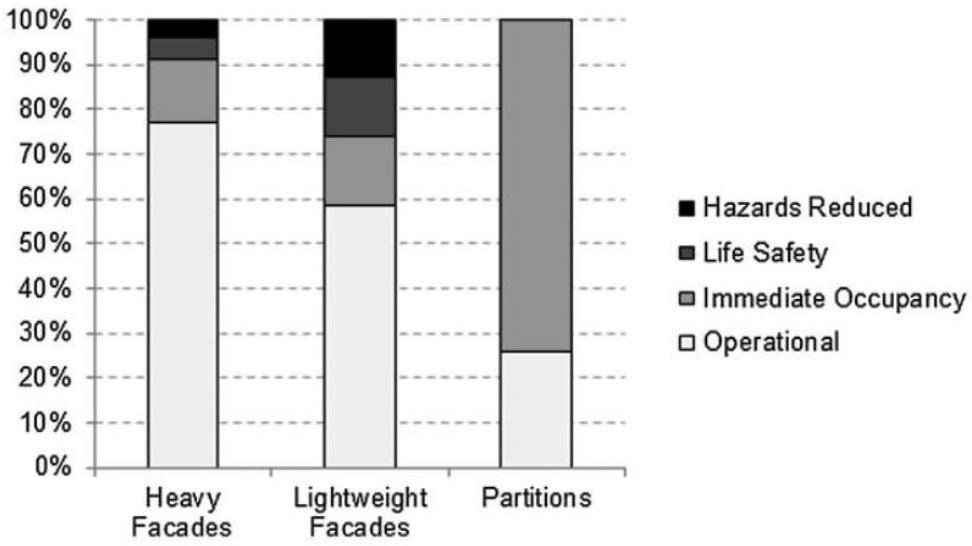

Figure 1.9 Performance of façade and infill systems after the 22nd of February 2011 earthquake retrieved from Baird *et al.* (2014) assessed as per the damage states suggested by ASCE (2006).

As can be seen in Figure 1.9, damage to partitions was widespread. Baird *et al.* (2014) showed that 74% of internally inspected buildings contained some form of damage to the partitions. Baird *et al.* (2014) noted that most of the damage observed was cosmetic and did pose a threat to egress, thus meeting performance level requirements for life safety. The most recurrent damage to partitions observed were:

- Damage to fasteners at the top and bottom track-plasterboard connections;
- Steel-framed partition studs coming out of the top and/or bottom tracks;
- Linings detaching in high stud steel- and timber-framed partition walls (more common for wall heights above 3.0 m);
- And, cracking of the linings around openings and wall penetrations.

Baird *et al.* (2014) concluded that partition walls are particularly susceptible to damage, as demonstrated by the constant repetitive damage caused by Christchurch aftershocks, and because of their high cost of repair, current code requirements do not set a high enough threshold for damage avoidance in order to minimize economic loss.

1.3.6 Study by Taghavi and Miranda (2003)

Taghavi and Miranda (2003) presented a review of the performance of non-structural components in commercial buildings during past earthquakes. The information used to inform the study by Taghavi and Miranda (2003) was partly based of a database developed by Soong *et al.* (1999) , which contained data gathered from more than 40 earthquakes. Taghavi and Miranda (2003) developed a new database with additional information from the authors based on the study of the performance of components in

previous earthquakes. The total number of records is more than 4000. For each record of information there is data relating to four main groups: building information, earthquake information, damage information, and reference information. The authors concluded that most of the economic loss comes from damage to non-structural components and suggested two reasons for this: (1) most of the total construction cost is spent on non-structural components, and (2) damage to non-structural components is more frequent compared to damage to structural components.

Taghavi and Miranda (2003) showed that non-structural components comprise the majority of investment in commercial buildings (Figure 1.10) and that interior construction, which consists of partition walls, doors, wall finishes, ceilings, and floor finishes, comprises 20-30% of the non-structural component cost (Figure 1.11).

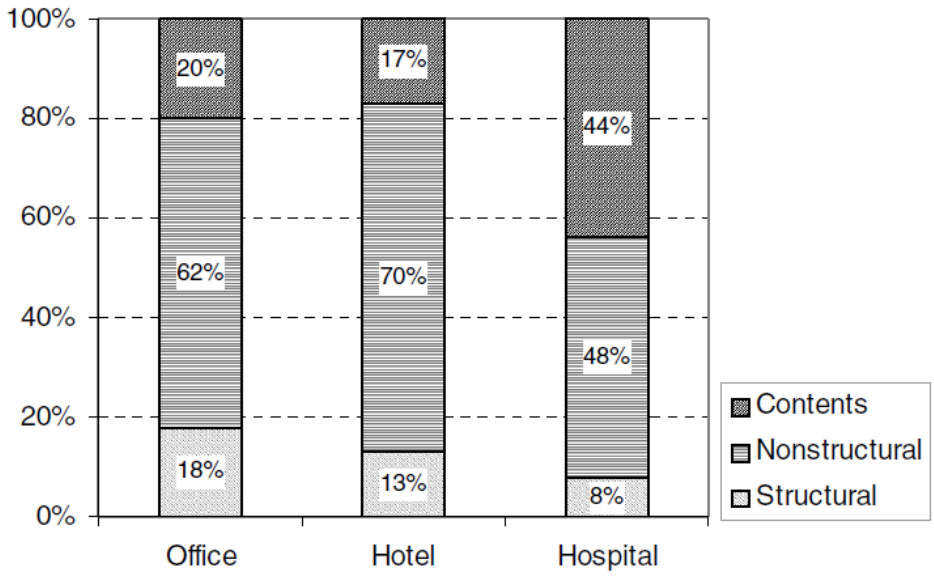

Figure 1.10 Cost breakdown of office buildings, hotels, and hospitals retrieved from Taghavi and Miranda (2003).

It was observed that for plasterboard partitions, damage usually consists of plaster cracking, which is initially easily repaired, but as ground motion intensity increases, the extent of cracking increases and damage is incurred to the wallboard. Damage to wallboards includes cracking, tearing, or dislodging of screws. Taghavi and Miranda (2003) noted that cracks are commonly located at the wall-ceiling junction and at corners of interior door frames. An example of plasterboard damage in a stairwell is shown in Figure 1.12.

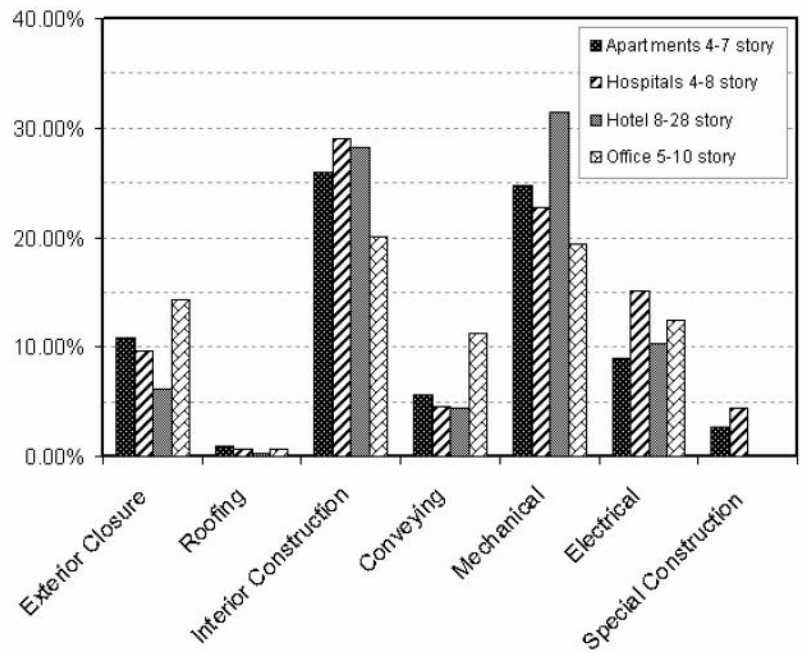

Figure 1.11 Nonstructural components cost breakdown of four sample buildings retrieved from Taghavi and Miranda (2003).

Figure 1.12 Encino Office Park, California, cracking of gypsum wallboard in stairwell. (NISEE Stenibrugge collection, photo by Karl Stenbrugge) retrieved from Taghavi and Miranda (2003).

1.4 Performance Based Earthquake Engineering (PBEE)

1.4.1 Objective

In response to a growing understanding that non-structural elements comprise the majority of investment in buildings and the majority of repair cost following earthquake events (Taghavi and Miranda 2003), the engineering community has moved towards an understanding that it is important to design structural systems for earthquake loads. An overview of the Pacific Earthquake Engineering Research (PEER) Centre's Performance Based Earthquake Engineering (PBEE) methodology is provided herein. This methodology aims to determine the performance of buildings in terms of direct performance metrics relevant to the interests of stakeholders including, estimates of repair costs, casualties, and loss-of-duration. The objective of the PBEE methodology is to estimate the frequency with which these performance measures exceed various levels for a given design at a given location and to create probability distributions of the performance metrics across any planning period of interest. This methodology is an important tool in quantifying the performance of non-structural partition walls in the context of buildings systems.

1.4.2 Methodology

PEER's PBEE approach involves four stages: hazard analysis, structural analysis, damage analysis, and loss analysis (Figure 1.13): Hazard analysis considers the seismic environment and presents it as a hazard curve, which describes the annual frequency with which seismic excitation is estimated to exceed various levels; Structural analysis creates a structural model of the facility to estimate the structural response, measured as an Engineering Demand Parameter (EDP); Damage analysis inputs the EDP into a set of fragility functions, that model the levels of damage in a structural or non-structural component as a function of a particular structural response; Loss analysis is the estimation as a probability, of the performance of the structure, where performance is measure by a particular design variable (dollars, death, downtime).

1.4.3 Damage States and Fragility Functions

Damage to buildings and non-structural components generally occurs as a continuum with the extent of damage increasing with demand. Rather than using a continuum, damage to buildings and non-structural components is described with discreet damage states, which characterize the distinct levels of damage that can develop. Each of these damage states is then associated with a unique set of consequences, which have:

- A unique repair action including an associated repair cost, time, and consequences;
- A unique potential for unsafe placarding;

- And, a unique potential effect on the number of casualties.

Fragility functions are used within the PBEE framework to provide statistical distributions (assumed to be lognormal) indicating the conditional probability of incurring damage to a building component at any given level of demand. For each damage state of a building component the PBEE framework requires there to be a unique fragility function.

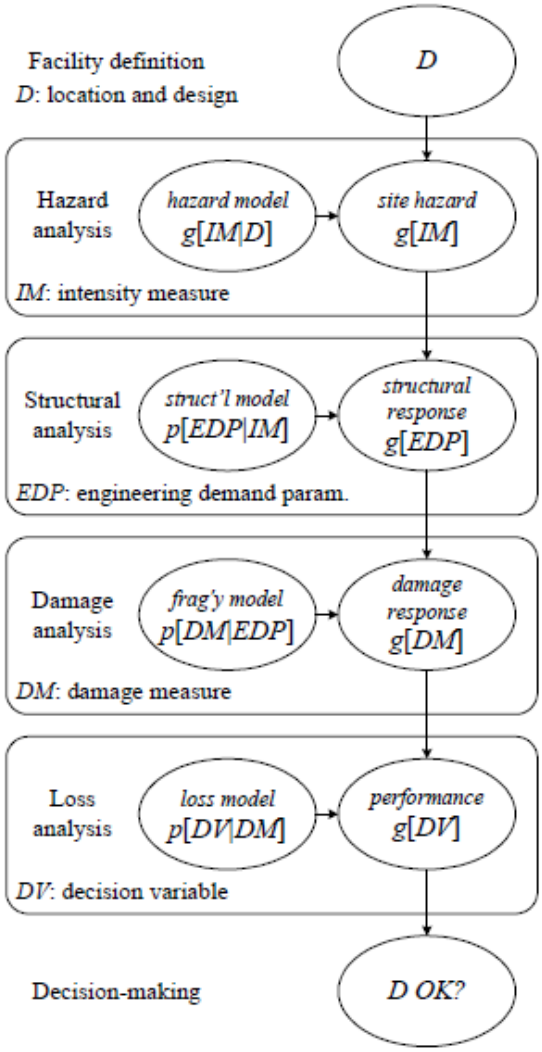

Figure 1.13 PEER analysis methodology retrieved from Porter (2003).

The fragility function for each damage state is defined by a median value, x_m, at which there is a 50% chance that the damage will initiate, and a dispersion, β, which is the standard deviation of the data in the log space and represents the uncertainty that damage will initiate at this level of demand. Dispersion is associated solely with uncertainty in the onset of damage as a function of demand and represents the uncertainty caused by a number of variables, including variability in construction and material quality,

the level of knowledge regarding the likely behaviour of a component subjected to a specified value of demand, and the extent to which the occurrence of damage can be predicted by a single demand parameter. The fragility curve will flatten as the value of β increases, which indicates that the damage state is likely to initiate over a wider range of demands.

For drywall partitions, three damage states are considered defined in terms of the level of repair required, as recommended by FEMA P-58. The three damage states are (1) minor damage characterized by cracking in the drywall paint requiring taping, plastering, and painting; (2) cracking of the drywall panels requiring replacement of panels re-taping, plastering, and painting; and (3) damage to framing requiring both the panels and framing to be replaced and the taping of the panels, plastering, and finally painting. An example of a typical fragility function for drywall partitions is shown in Figure 1.14.

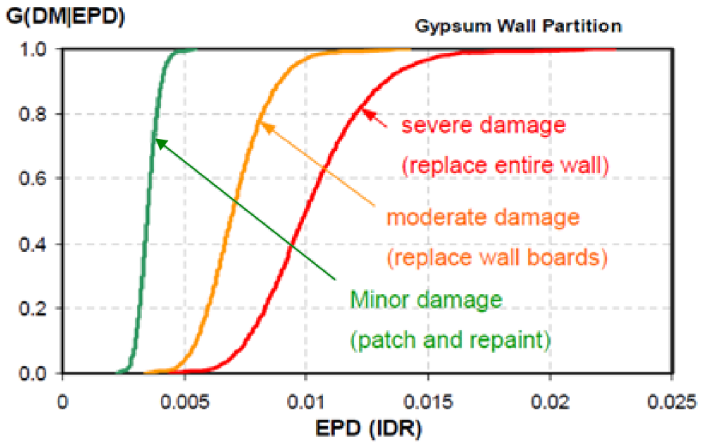

Figure 1.14 Example of EDP to DM fragility curves for drywall partitions retrieved from Deierlein *et al.* (2003).

1.4.4 Repair Costs

The economic cost associated with damage caused by an earthquake event is an important performance measure. Monetary cost can be used to predict the direct economic loss that a region will incur following an earthquake event and can be useful for estimating insurance and comparing risk mitigation programs. In addition, it is crucial to global risk management strategies that the total value of existing structures and their relative materials be established.

In determining the repair costs for a particular component all necessary construction activities required to return the damaged component to its original condition must be considered. It should be noted that these repair actions should not include any works required for bringing a non-conforming component into compliance with newer criteria and should only reflect the work involved in the repair or replacement of a component in relation to its original condition.

1.5 Experimental Testing on Non-structural Drywall Partitions

1.5.1 Early Studies (1971 – 1990)

A significant number of studies have been conducted on the lateral behaviour of light framed gypsum partition walls. The earliest studies focused on investigating the load-deformation characteristics and damage thresholds of partition walls with varying construction typologies and configurations: these early studies included those by Freeman (1971), Rihal (1980), Girard and Tarpy (1982), and Adham *et al.* (1990). These early studies used both quasi-static and dynamic loading and found that cracking at wall penetrations and of paint over fastener heads initiates at very low drifts (~0.25%). The study by Adham *et al.* (1990) focused mainly on light steel framed plasterboard walls design to provide lateral load carrying capacity. Five out of six of the specimens incorporated steel diagonal flat strap braces and are therefore not representative of non-structural partition systems used today. Therefore, no further details on this study have been presented. The studies by Freeman (1971), Rihal (1980), and Girard and Tarpy (1982) are discussed in further detail below.

Freeman (1971) studied 17 different configurations of wall specimens (shown in Table 1.2) under dynamic and quasi-static cyclic loading up to a maximum interstorey drift of 1.56%. Variables included sheathing material, stud material, openings, and stud connectivity. Wall specimens were 8’ (2438 mm) high by 8’ (2438 mm) long and did not have return walls. Note at the end of the wall panels, there was no plasterboard lining to finish the end of the wall, and thus if the lining and studs are detached from the top plate/track, no damage would be observed in the wall. Additionally, no hold down ties were provided at the ends of the specimens, so that they were free to uplift without restraint. The author observed first visible damage to forms as early as 0.13% interstorey drift. In the doorway specimen type 2, A-28, the author observed cracks beginning in the gypsum lining over the doorway at 0.26% drift (Figure 1.15) and that after it had been repaired, this crack reopened at only 0.065% drift. Note the specimens were not painted so this initial form of damage is attributed to cracking in plaster along the joints, screw damage, and cracks in the gypsum board.

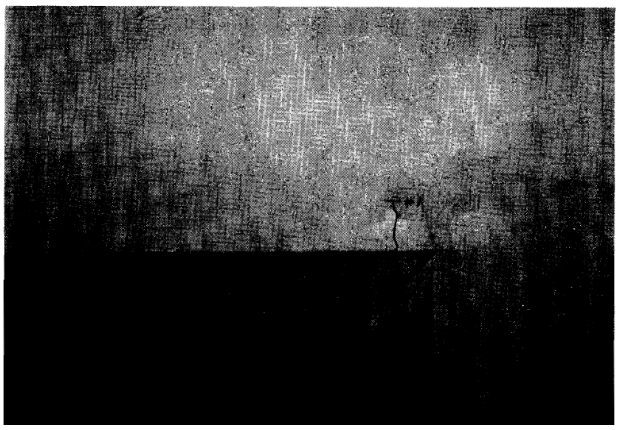

Figure 1.15 Cracking of plasterboard above the door frame observed during the testing of wall type 2 at 0.26% drift by Freeman (1971).

Table 1.2 Description of wall panels tested by Freeman (1971)

Type Number	Wall Material	Stud Material	Wall Openings	Remarks
1	12.7 mm gypsum wall board	92 mm Metal	None	Connection of stud to runner by friction
2	12.7 mm gypsum wall board	92 mm Metal	Door	Connection of stud to runner by friction
3	12.7 mm gypsum wall board	92 mm Metal	None	Connection of stud to runner by friction
4	12.7 mm gypsum wall board	92 mm Metal	Door	Connection of stud to runner by pop-rivets
5	12.7 mm gypsum wall board	50 x 100 mm Timber	None	-
6	12.7 mm gypsum wall board	50 x 100 mm Timber	Door	-
7	12.7 mm plywood	50 x 100 mm Timber	None	8d nails at 305 mm centres
8	203 mm concrete block	-	None	No grout, no reinforcement
9	12.7 mm gypsum wall board	92 mm Metal	None	Same as Type 3 with wallboard screws to runners
10	Plywood and gypsum wallboard	50 x 100 mm Timber	Window	One side plywood and one side wallboard
11	Plaster and gypsum lathe	50 x 100 mm Timber	None	plate and sill bolted to concrete
12	Plaster and gypsum lathe	50 x 100 mm Timber	Door	plate and sill bolted to concrete
17	9.5 mm plywood	50 x 100 mm Timber	None	8d nails at 152 mm centres, blocking at mid-height

Rihal (1980) conducted a series of horizontal racking experiments on 14 partition wall specimens, including a partial height specimen, under quasi-static cyclic loading. The partitions selected for this testing program were typical non-load bearing steel stud partitions with fire rated plasterboard linings. As per the tests conducted by Freeman (1971) the specimens were 8’ (2438 mm) high by 8’ (2438 mm) long and had no return walls or bounding structural elements. Specimens incorporated variations in geometry, placement of wallboard panels (horizontal or vertically placed), connection details at boundaries and openings, taped vs. untapped joints between gypsum wall board and facing panels, loading history, and joint slip at the interface between panels. The general pattern of behaviour of specimens agreed with the results reported by Freeman (1971) in terms of load-deformation behaviour and energy dissipation however the first noticeable partition damage was observed at larger interstorey drift levels of 0.39%. Note as for the tests by the Freeman (1971) the specimens were not painted so this initial form of damage is attributed to cracking in plaster along the joints, screw damage, and cracks in the gypsum board. The information provided within this test on the damage development in the specimen was limited as for the tests by Freeman (1971) with most of the focus of the study being on the load-deformation behaviour and energy dissipation.

Girard and Tarpy (1982) tested 8’ (2438 mm) high by 8’ (2438 mm) long specimens which and had no return walls or bounding structural elements as per the studies by Rihal (1980) and Freeman (1971). A total of seven different specimen types were tested using quasi-static loading. The variation between specimen types included anchorage system, plywood or plasterboard sheathing, fillet welding or screwing steel studs to the tracks, and stud spacing. All specimens had uplift restraints at wall ends. This study was conducted in response to need within industry at the time for the development of design criteria for steel stud shear wall panels with different sheathing materials for inclusion in various design codes. The specimens most like standard gypsum wallboard non-structural partition walls used today (wall type A) experienced initial cracking at 0.40% drift. This initial damage was from cracking of the gypsum wall board between the corner fasters and the edge of the wallboard at the wall ends close to the location of the uplift restraint.

1.5.2 Modern Studies (2007 – Today)

With the development of PBEE following the 1994 Northridge and 1995 Kobe earthquakes, there has been an increased awareness that it is important to design non-structural systems for earthquake loads. Therefore, many modern studies have focused on the damage and repair cost relationship of partitions in order to inform fragility functions and cost functions for the implementation of PBEE. Some of the studies focused on these objectives are those by McMullin and Merrick (2007), Restrepo and Bersofsky (2011), Davies *et al.* (2011), and Jenkins *et al.* (2016).

McMullin and Merrick (2007) conducted a series of 11 tests on full-scale non-structural gypsum wallboard partition walls. The partition walls were all double sided ½" (12.7 mm) gypsum wallboard partition walls with timber framing (typical configuration as per Figure 1.16). The objectives of the tests was to (1) compare the performance of walls using screws or nails to support the wallboard and evaluate the effect of changing fastener spacing; (2) compare the behaviour of walls for monotonic and cyclic loading protocols; and (3) determine the drift at which specific damage thresholds occurred. The authors recognized that one of the key causes of damage to wallboard is the influence of intersecting walls and ceilings, which tend to restrain movement of the sheathing panels relative to the framing. And as the walls are taped and compounded to these orthogonal boundary members cracking and/or crushing is expected to occur at lower levels of drift than for similar walls without such restraints. The wall specimens were therefore built with orthogonal bounding members along the top, bottom, and both ends. A summary of the observed damage is shown in Table 1.3. The first visible damage in the specimens was observed at an average interstorey drift of 0.25% with slight cracking of the panels at the re-entrant corners, followed by increasing damage up to drifts of 2%. They identified that damage thresholds for cyclic loading were very similar, but often occur at lower drifts compared with monotonic loading.

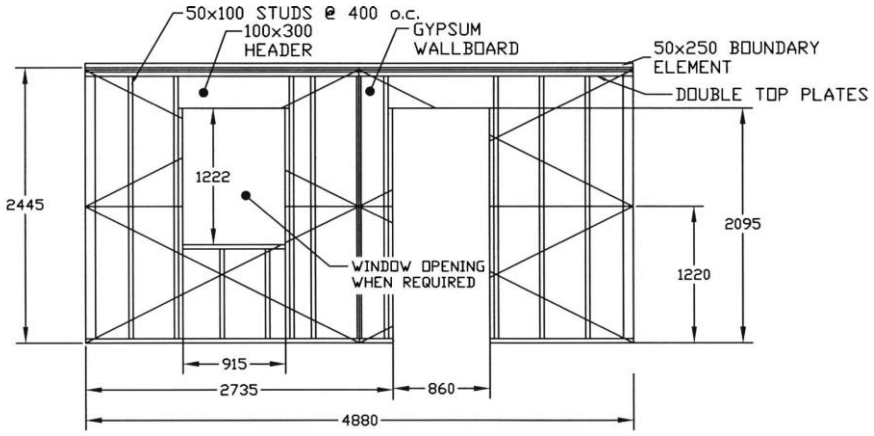

Figure 1.16 Typical specimens tested by McMullin and Merrick (2007).

Table 1.3 Damage thresholds in timber framed partition specimens observed during tests by McMullin and Merrick (2007).

	Occurrence[a]						
	Lowest		Highest[b]		Average[c]		
Damage threshold	Mono.	All	Mono.	All	Mono.	All	Number of cyclic tests when damage occurred in primary loading cycle[d]
Cracking of reentrant corner at opening	0.20	0.12	0.76	0.76	0.29	0.25	6/8
Cracking of paint over fastener head	0.25	0.24	1.25	1.69	0.67	0.64	7/8
Cracking at the vertical end of wall	0.48	0.25	2	3	0.80	0.68	4/7
Local buckling of the wallboard	0.24	0.13	1	2	0.47	0.46	7/7
Damage at the vertical butt joint	0.51	0.39	7	8	0.80	0.67	3/7
Cracking of the tapered wall joint	1.00	0.66	11	16	2.58	1.69	2/3
Crushing of the wallboard	0.25	0.25	1	2	1.13	1.21	6/6
Global buckling	1.44	1.44	5	8	2.02	2.50	4/5

[a]Mono. refers to tests with monotonic loading protocols (sample size=14); and All refers to all tests (sample size=22).

[b]If the value for the highest occurrence is an integer, then the integer is the number of walls that did not experience the damage threshold.

[c]Average occurrence is the average of the walls that did experience a specific damage threshold.

[d]Fraction indicates the number of wall faces with damage event occurring in primary loading cycle divided by the total number of times the damage occurred.

Restrepo and Bersofsky (2011) conducted quasi-static racking tests on eight nearly identical pairs of gypsum wallboard sheathed light gage steel stud partition walls following common United States practices. Each wall consisted of a 4.88 m long 2.44 m tall "web" wall and two return walls 1.2 m long and 2.44 m high. The wall specimens were painted unlike previous studies. The main variables were (1) configuration, including a plain wall specimen (configuration I shown in Figure 1.17), a doorway specimen (configuration II), and a partial height specimen (configuration III); (2) screw spacing; (3) stud thickness and spacing; (4) the presence of vertically slotted tracks at the top of the partition wall; and (5) wallboard thickness. A description of the test specimens is shown in Table 1.4. Damage to the specimens was grouped into three distinct damage states (DS1-3) as recommended by FEMA P-58 (refer to section 1.4.3) and recorded throughout the tests (results shown in Table 1.5). The authors observed that there were very small differences between the behaviour of the pairs of identical specimens. The doorway specimens (configuration II) developed DS1 at a drift of only 0.05%, whereas for configurations I & III DS1 developed at 0.3% drift.

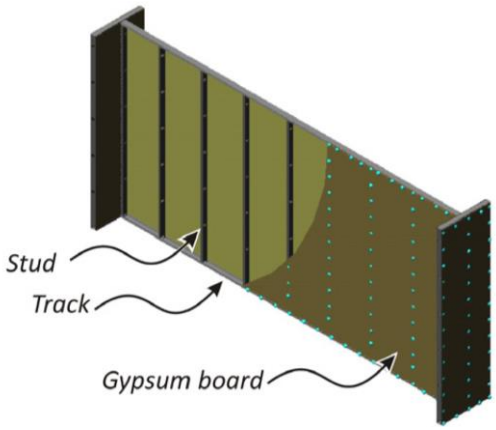

Figure 1.17 Wall configuration I in tests by Restrepo and Bersofsky (2011).

Table 1.4 Description of test specimens in tests by Restrepo and Bersofsky (2011) (test variable shown in bold) retrieved from Restrepo and Bersofsky (2011).

Test	Configuration	Self-drilling screw spacing (mm)	Gypsum board height (m)	Vertical slotted track?	Gypsum board thickness (mm)	Metal stud gage	Stud spacing (mm)
2[a]	I	204	2.44	No	16	25	610
3	**II**	204	2.44	No	16	25	610
4	I	**305**	2.44	No	16	25	610
5	**III**	204	2.04	No	16	25	610
6	I	204	2.44	**Yes**	16	25	610
7	I	204	2.44	No	**13**	25	610
8	I	204	2.44	No	16	**20**	**406**

[a] Tests 1 and 2 were practically identical, but tie down rods yielded in Test 1 voiding the test results.

Table 1.5 Inter-storey drift ratios (%) at the onset of damage states for each specimen tested by Restrepo and Bersofsky (2011) retrieved from Restrepo and Bersofsky (2011).

Test	DS1				DS2		DS3		
	Tape uplift	Drywall cracking	Screw head popping	Small track slip	Drywall buckling	Drywall crushing	Drywall spalling	Steel stud buckling	Large track slip
2	0.3	0.3	0.5		1	1.5	3	3	
3	0.05	0.3				0.5	0.5	1.5	
4	1	0.3					1.5		
5		0.5	0.3					0.75	
6	0.1		0.75					1.5	
7		0.1	0.75	0.5	1		2	2	
8		0.1	0.75	0.3		0.75			1.5

Davies *et al.* (2011) tested 50-full scale partition walls in 22 different configurations, constructed following standard industry construction practices in the United States, using both quasi-static and dynamic protocols and generated data on partition wall in- and out-of-plane seismic behaviour and fragility. The typical specimens were 3708 mm long (12'-2") and 3505 mm high (11'- 6") with 610 mm (2') long return walls at each end making an I-shape and framed with cold-formed steel studs sheathed with 15.9 mm (5/8") plasterboard. Specimens were also painted as per the tests by Restrepo and Bersofsky (2011). The tests were used to populate a seismic fragility database and force-displacement curves for the in-plane wall behaviour in order to determine a set of parameters for a tri-linear hysteretic model aimed at reproducing the mechanical behaviour of the walls. The authors defined a set of damage states (DS) for partitions, similar to those suggested by Taghavi and Miranda (2003), which are shown in Table 1.6. A set of lognormally distributed fragility function parameters for each damage state developed from the experimental results are shown in Table 1.7. Novel specimen detailing aimed at improving the fragility curves for partition specimens were tested. One of these systems is discussed in further detail in Section 1.5.3. The authors recommended that when considering the characteristics of light gauge partitions without information on their detailing to adopt as fragility parameters the median values of 0.35, 0.69, and 1.04%, with logarithmic standard deviations of 0.56, 0.39, and 0.55, for damage states DS_1, DS_2, and DS_3 respectively. Some of the conclusions from this test regime was that the fragility analysis results were comparable to the results from previous experimental observations, and that the logarithmic standard deviations were as high as 0.59 which is consistent with the fact that identical specimens, constructed using the same techniques, identical details, and by the same team, can exhibit failure mechanisms that are completely different.

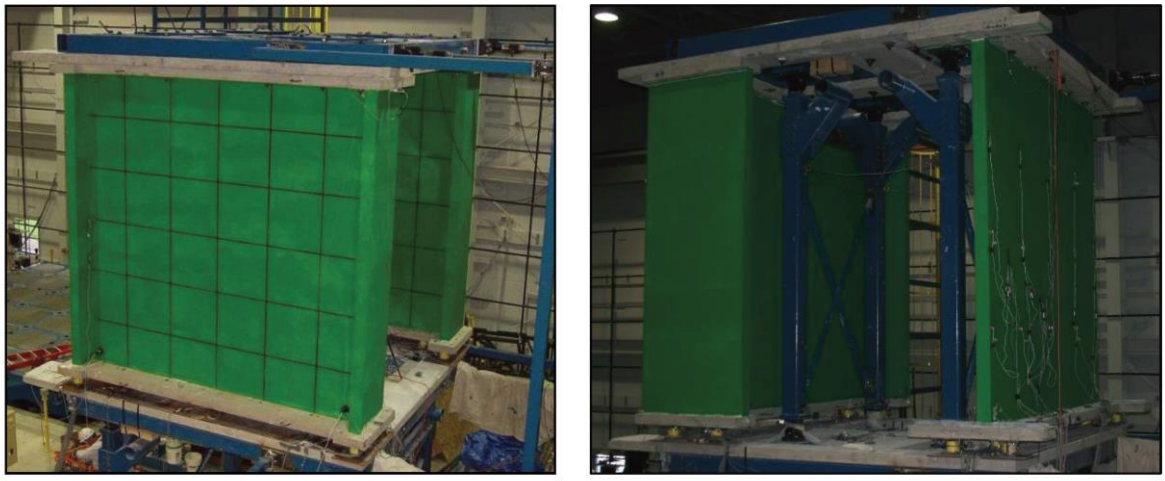

(a) For in-plane testing (b) For out-of-plane testing

Figure 1.18 Photos of typical test specimen configuration for experimental study by Davies *et al.* (2011) (retrieved from Davies *et al.* (2011)).

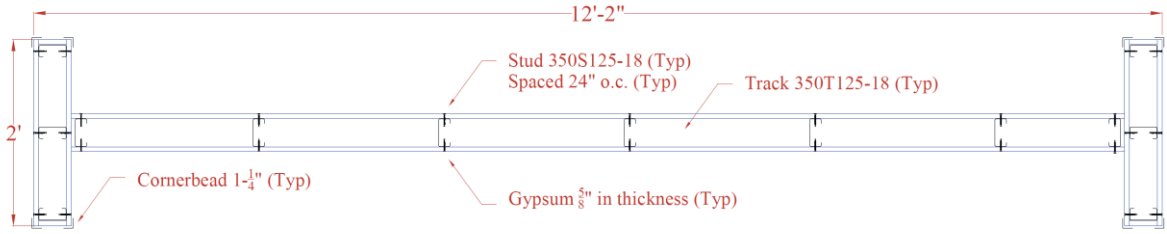

Figure 1.19 Plan schematic of typical test specimen configuration from experimental study by Davies *et al.* (2011) (retrieved from Davies *et al.* (2011)).

Table 1.6 Damage states (DS) for light framed partitions (Davies *et al.* 2011)

Damage State		Description of Damage Associated	Repair Actions
DS_1	Superficial damage to the walls	Cracks along corner beads, cracks along joint paper tape, screws pulled out from connections of gypsum boards to steel framing	Cosmetic repairs, including: replacement of corner beads, replacement of screws pulled out, replacement of joint paper tape, application of joint compound, sanding, and painting
DS_2	Local damage of gypsum wallboards and/or steel frame components	Crushing of wall corners, out-of-plane bending and cracking of gypsum wallboards at wall intersections, damage of screws connecting wallboards to boundary studs, bending of boundary studs, buckling of diagonal braces (partial height partition walls), damage of gypsum wallboards around ceiling connectors or damage induced by ceiling impact	Local repairs, including: repair or replacement of gypsum wallboards, replacement of boundary studs, replacement of seismic braces, replacement of ceiling connectors
DS_3	Severe damage to walls	Tears in steel tracks around connectors of track to concrete slab, track fasteners passing thru track webs, track flanges bent at wall intersections, hinges forming in studs, partition wall collapse	Replacement of partition wall (Steel framing and gypsum wallboards)

Table 1.7 Summary of fragility curve parameters in terms of inter-storey drift (%) (Davies *et al.* 2011)

Group	Sub Group	Description	DS_1		DS_2		DS_3	
			x_m (%)	β	x_m (%)	β	x_m (%)	β
0	0	All speci en data	0.35	0.56	0.69	0.39	1.04	0.55
1	1a	Full-height specimens. Commercial construction practice and slip tracks	0.26	0.45	0.68	0.35	0.75	0.36
	1b	Full-height specimens. Commercial construction practice and partial/full connections	0.27	0.44	0.61	0.41	1.18	0.59
	1c	Full-height specimens. Commercial construction practice (slip tracks and full connection)	0.27	0.43	0.64	0.38	0.96	0.61
2	2a	Full-height specimens. Institutional construction practice and slip tracks	0.36	0.55	0.79	0.34	-	-
	2b	Full-height specimens. Institutional construction practice and partial/full connections	0.40	0.25	0.63	0.43	0.88	0.33
	2c	Full-height specimens. Institutional construction practice (slip tracks and full connection)	0.42	0.31	0.69	0.40	0.98	0.52
3	3	Partial-height specimens	0.74	0.29	1.00	0.33	1.79	0.28
4	4	Specimens including improved corner details	0.34	0.77	-	-	-	-

Jenkins et al (2016), at the University of Reno, Nevada, conducted eight full-scale system level experiments using a two-storey steel braced frame structure (Figure 1.20) under dynamic loading. A variety of different partition wall configurations were tested: including cantilever partial height walls, braced partial height walls, institutional and commercial detailed walls, and a slip track connection developed by Araya-Letelier and Miranda (2012) the details of which are discussed further in Section 1.5.4. The specimen configurations included walls without returns and walls with returns including C-L-, and S-shaped variants. They compared the drifts for which DS1, DS2, and DS3, initiated in this test with results from previous studies and found that DS1 and DS2 began at higher drifts in their experiment than in previous studies and at similar drift levels for DS3. However, for the only specimen type that is full height with conventional detailing incorporating return walls, partition label P8-F, there is no data available. And therefore the results are not comparable to the tests by Davies *et al.* (2011).

Sample Test-bed Pictures: (a, b) north and south bay rooms, (c) full structure, (d) content room, (e) free standing partition walls formulating content room

Figure 1.20 Full-scale shake table testing frame and specimen construction at University of Nevada (Jenkins *et al.* 2016)

1.5.3 Low Damage Systems

Considering the results from recent studies on the seismic performance of non-structural partition walls, which show that they suffer damage at significantly lower drifts than those that damage structural systems, there has been a demand for improved performance of partition walls. Thus, in recent years, researchers have begun to develop low damage systems. From a review of current literature, three promising systems have been identified:

- Sliding/frictional connection.
- Gaps between linings.
- Flexible track system.

1.5.4 Sliding/Frictional Connection

Araya-Letelier and Miranda (2012) developed a sliding/frictional connection for the top-track of partition walls that intends to mitigate the damage to gypsum partitions from seismic events. The main strategy for developing the connection was to isolate the partition from the lateral deformations experienced by the structure. The connection system is shown in Figure 1.21. Component tests and full-scale tests were conducted under cyclic reverse loading to determine the new systems seismic performance. The conventional damage states were used. The drifts associated with the onset of each damage state are shown in Table 1.8. These show that the new connection significantly reduced the damage to partition walls from imposed inter-storey drift. Jenkins *et al.* (2016) conducted system level dynamic tests using the connection detailing suggested by Araya-Letelier and Miranda (2012) and found that damage to the novel slip track partition walls initiated at ~0.6% drift, whereas in Araya-Letelier and Miranda (2012) their tests show DS1 begins at ~2% drift.

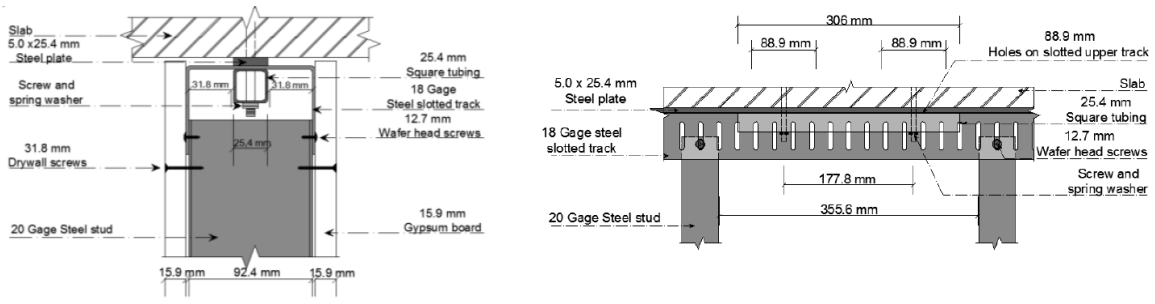

Figure 1.21 Cross section (on the left) and side-view elevation (on the right) of the proposed new sliding/frictional connection (Araya-Letelier and Miranda 2012)

Table 1.8 Storey drift ratio (SDR) associated with each damage state for wall specimen A (conventional) and B (sliding/frictional connection) (Araya-Letelier and Miranda 2012)

Damage State	Wall Specimen A. SDR [%]	Wall Specimen B. SDR [%]
DS1	0.10	2.13
DS2	1.08	2.13
DS3	2.13	2.98

1.5.1 Gaps between linings solution

A common method of isolating structural and non-structural elements from the inter-storey displacements imposed on buildings by earthquake ground motions is to provide seismic gaps. In an effort to isolate the linings of partition walls from structural movements several researchers have suggested partition wall details that incorporate seismic gaps (Lee *et al.* 2007, Magliulo *et al.* 2014, Tasligedik *et al.* 2015, Pali *et al.* 2017, 2018). The studies by Lee *et al.* (2007) and Tasligedik *et al.* (2015) are discussed herein.

Lee et al (2007), inspired by PEER's PBEE methodology, studied the typical Japanese configuration for steel-stud framed interior gypsum drywalls under quasi-static and dynamic loading in order to determine their seismic performance and corresponding repair costs. Test specimens were 2800 mm high and included (1) a plain drywall partition, (2) a wall with a door, and (3) a wall with two intersecting walls at each end. The Japanese method of partition construction is to not screw the vertical studs to the runners (top and bottom tracks) and to attach the wallboard to the studs only. This allows the studs and gypsum board to slide as the runners move with the floor or ceiling. Therefore, the drywall partition is not expected to sustain damage until the side of the drywall partition is constrained by an intersecting wall or structural column. The exception to this is around door framing where the studs are attached directly to the bottom and top runners. Even though there is no code specification on the clearance of drywall partitions, 10-15 mm is usually adopted in Japanese practice. A 15 mm gap was provided between the edge of the specimens and neighbouring columns in this experiment. This corresponds a total gap size of 30 mm and 1.07% (30 mm/2800 mm) of inter-storey drift allowance. The results of the testing showed that the plain drywall partition specimen did not need to be repaired as long as the drift was not greater than 1.0%, because it slid without being damaged; the wall with a door did not need to be repaired as long as the storey drift was not greater than 0.5%, due to cracks appearing at the corners of the door opening; and the wall with intersecting walls experienced onset damage at 0.25%, which is consistent with the results of modern experiments on drywall partitions with intersecting walls. Note that no details were suggested in this study for the provision of seismic gaps at the intersection of return walls.

Tasligedik *et al.* (2015) suggested modifications to the standard detailing of drywall partitions, incorporating seismic gaps, aimed at allowing the partition to accommodate drifts with no or low damage. These modifications were kept simple in order to avoid additional labour, materials, or

complicated details and facilitate their wider adoption by contractors, engineers, or architects. The developed solution was applied in two different ways for steel and timber framed drywalls. The seismic gap specimen details included fire and non-fire rated alternatives. At the horizontal boundary the external studs were attached to the frame but not to the linings; and an additional stud was provided near the external stud to which the linings were attached so that the linings and internal framing would be free to slide within the bottom and top tracks. The details of the low damage steel and timber stud specimens tested in this study are shown in Figure 1.22 and Figure 1.23 respectively. The total horizontal gap in the steel and timber specimens was 40 mm and the clear height between floors was 2550 mm corresponding to a design inter-storey drift of 1.56%. The specimens were tested in-plane as an infill wall within a reinforced concrete moment resisting frame according to a quasi-static loading protocol. In the timber stud specimen closing of the gaps was observed at 1.5% drift and damage first started with cracking of the plaster along the finishing material over fastener heads at 2.0% drift demonstrating significant improvement over traditional detailed partition walls. However, as the specimens tested did not include any specimens with return walls and displacements were applied in-plane only, these details have not been verified for their out-of-plane performance or considering the interaction with return walls.

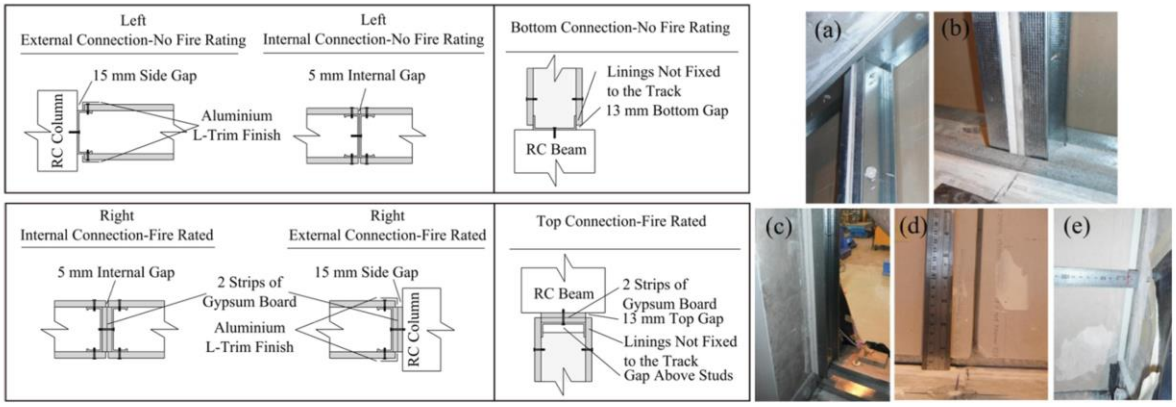

Figure 1.22 Adopted details in the low damage steel framed drywall specimen from study by Tasligedik *et al.* (2015): (a) & (b) fire rated internal stud, (c) fire rated external stud, (d) fire rated internal gap between adjacent linings, and (e) fire rated external gap between the lining and concrete.

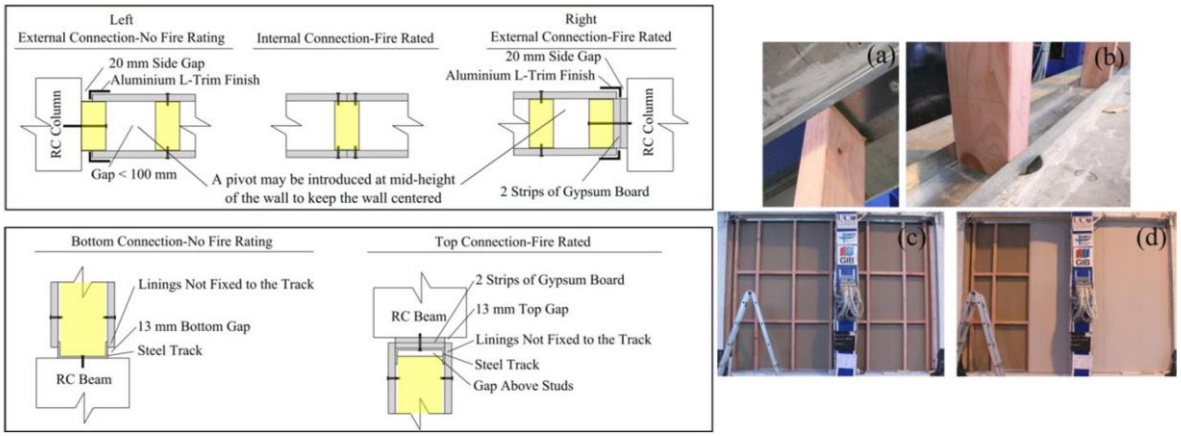

Figure 1.23 Adopted details in the low damage timber framed drywall specimen from study by Tasligedik *et al.* (2015): (a) & (b) friction fitted studs in steel channels, (c) completed frame system after the gypsum lining on the back was attached, and (d) attached linings.

1.5.2 Flexible track system

Included within the series of tests by Davies et al. (2011) were some novel details for improving the performance of partitions including a flexible track system (specimen 34 & 36). Through conversation with the industry it appears that a partially-sliding partition wall system with similar detailing to that tested by Davies et al. (2011) is used in practice. The flexible track system proposed by Davies et al. (2011) increases track flexibility by not using track to concrete slab connectors within 610 mm (2') of wall intersections, thus allowing the tracks to act as a beam to absorb the lateral forces at increasing drifts. Davies et al. (2011) proposed two specimen designs. For the first specimen only the top track anchors were removed, the studs and plasterboard were screwed to the bottom track, and the studs were free to slide within the top track. For the second specimen, both top and bottom anchors were removed in proximity to junctions, and the studs and linings were not connected to the track at the top or bottom, and so were free to slide at both ends. A schematic of the detailing at junctions is shown in Figure 1.24. Damage similar to the conventional system tested by Davies et al. (2011) was observed, however it was observed at higher drift levels. Damage to the specimen with anchors removed at the top only occurred for the first time with joint paper tape detaching from wall intersections at 0.4-0.6% drift; whereas for the specimen with anchors removed at the top and bottom intersection damage was observed first, with joint paper tape detaching from wall intersections at 1.2-1.4% drift. For both specimens DS1 triggers at a larger inter-storey drift than for the standard partition systems. However, as noted by the author, additional practical considerations for this system need to be considered including bi-directional seismic loading (Retamales *et al.* 2013).

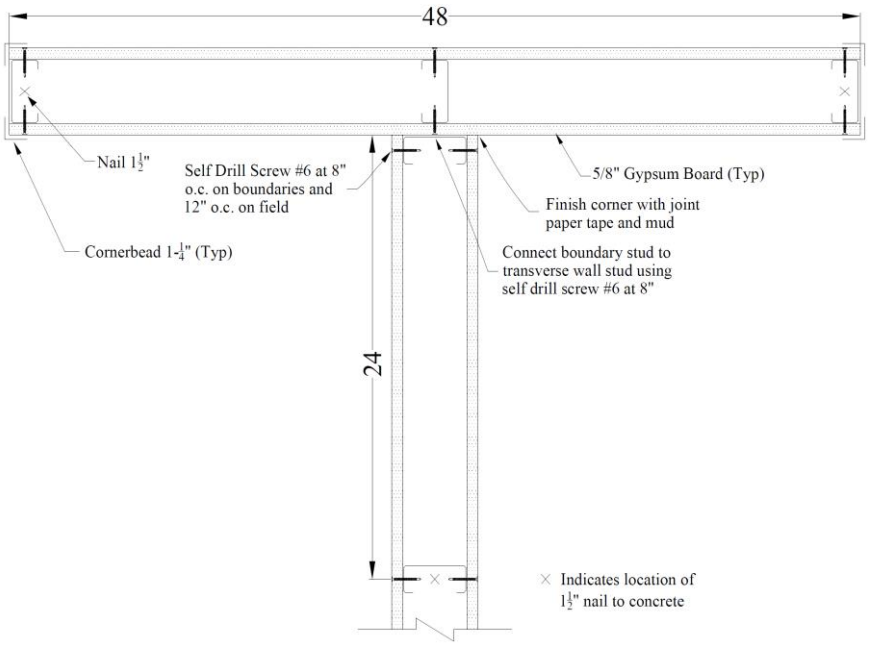

Figure 1.24 Adopted details for flexible track specimens at junction with return walls (dimensions in inches) from study by Davies et al. (2011).

1.6 Research Objectives & Scope

As has been shown by field observation, experimental studies, and analytical studies the behaviour of partition wall systems subject to seismic loading has a significant effect on the repair cost of building systems following earthquake ground motions due to their susceptibility to incur damage requiring repair under relatively small inter-storey drifts. Therefore, the overall objective of this research project is to further the development of low damage seismic systems for non-structural partition walls to facilitate their adoption by industry to assist with reducing the losses associated with the maintenance and repair cost of buildings across their design life. In particular, this study focuses on the behaviour of steel-framed partition walls systems with novel detailing that aim to be "low-damage" and are designed according to common practice for walls used in commercial and institutional buildings in New Zealand. The scope of this study is as follows:

1. Investigate the performance of the flexible track system proposed by Davies *et al.* (2011) and industry by experimental testing of full-scale specimens in order to:
    a. Validate the performance of this system using NZ materials and construction practices.
    b. Derive its fragility function for use within the PBEE framework.
    c. Investigate the performance of the system when tested under uni-directional loading applied at an oblique angle to the wall and with a unique return wall configuration including an angled return wall.
    d. And investigate the behaviour of a fire stop sealant used at the top boundary of the plasterboard linings under quasi-static cyclic loading.
2. Investigate the performance of the seismic gap partition wall systems proposed in a number of studies, in particular the detailing used in Tasligedik *et al.* (2015) further developed in this study with input from industry, by experimental testing of full-scale specimens in order to:
    a. Validate the performance of this system using NZ materials and construction practices.
    b. Investigate the performance of the system when tested under uni-directional loading applied at an oblique angle to the wall and with a unique return wall configuration including an angled return.
    c. Investigate alternate detailing of the specimens including increasing horizontal gap widths, including an intermediate joint, and using timber studs instead of steel studs.
    d. Investigate the behaviour of using an acrylic gap filler within the seismic gaps and its influence on the behaviour of the system under quasi-static loading.

3. Investigate the potential implications of using the systems studied herein compared with traditionally detailed partition wall systems within multi-storey buildings using the PBEE loss assessment method.

2. EXPERIMENTAL PROGRAM & TEST SETUP

2.1 Experimental Program

As outlined in section 1.6 the two low damage systems selected for experimental testing were a seismic gap system and a flexible track system. The details of these two systems are described in Chapters 3 & 4. In order to investigate research objectives 1 & 2 experimental testing is to be conducted on the two systems selected for study. Three flexible track system and two seismic gap systems were tested in total. The experimental program for the tests is shown in Table 2.1.

Table 2.1 Experimental program for full-scale testing of low damage partitions in this study.

Series	Test ID	System	Configuration	Loading	Test Date
A	A1	Flexible Track System	Plain wall	Cyclic	15 April - 5 May
	A2	Flexible Track System	Plain wall	Cyclic	16 May -20 May
	A3	Flexible Track System	Doorway	Cyclic	9 July - 14 July
B	B1	Seismic Gap System	Plain wall	Cyclic	20 - 26 June
	B2	Seismic Gap System	Plain wall	Cyclic	26 June - 3 July

2.2 Test Specimen Configuration

The typical detailing of partition walls is discussed in Section 1.2. The configuration chosen to provide a baseline for the specimens to be tested in this study is a fire rated partition typology from the GIB Fire Rated Systems (2012) manual, GBS60. The details of which are described in Section 1.2. The fire rated wall type was chosen as this represents the detailing of typical full height non-structural partition walls in commercial buildings. The detailing of the flexible track and seismic gap system specimens is further discussed in chapters 3 and 4 however, the detailing of both systems was developed with reference to this baseline specimen typology.

As per research objective 1c and 2b the performance of the systems with unique return wall configurations, including an angled return wall, is to be assessed. The typical configuration for each of the five specimens was therefore selected to be a unique “y-shape” with nominal plan dimensions as shown in Figure 2.2. The configuration for the doorway specimen (Test ID A3) is shown in Figure 2.3. The typical specimens incorporated an approximately 2400 mm long main wall with 600 mm long (approximately) returns walls with a height of 2405 mm between floor and ceiling. Note that the dimensions of each specimen differed slightly depending on their detailing.

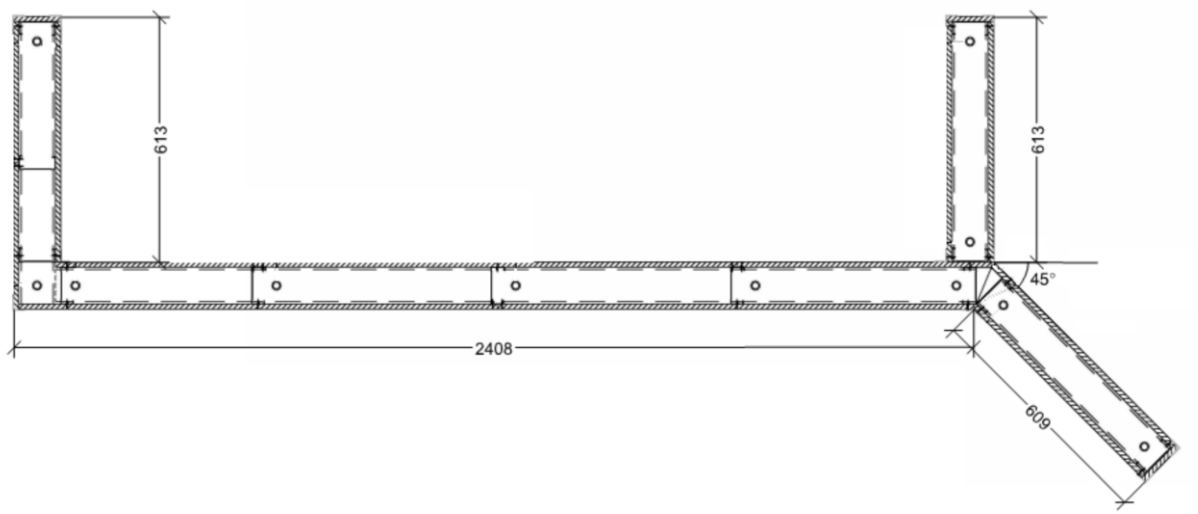

Figure 2.1 Plan view of typical “y-shape” wall configuration for specimens tested within this study and approximate dimensions (in mm).

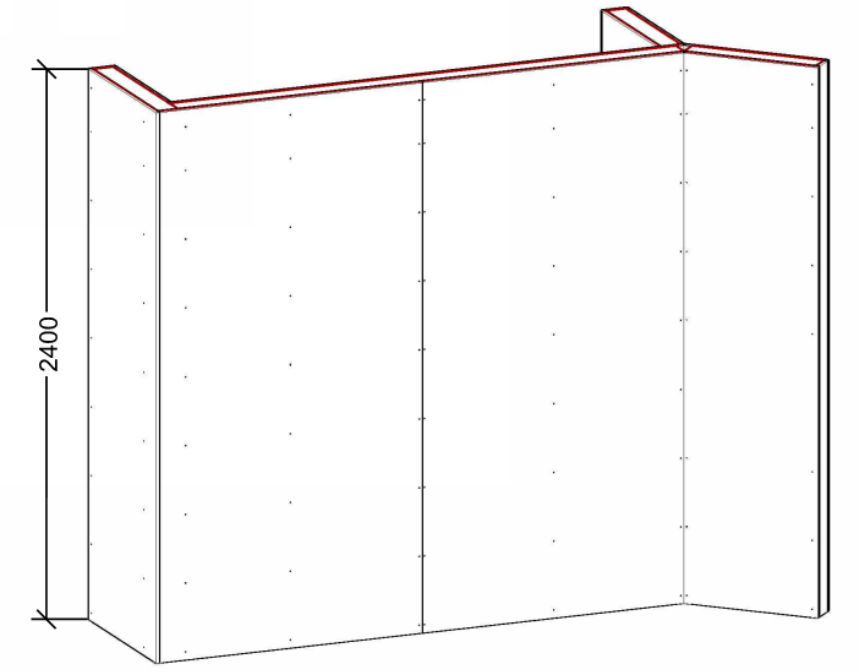

Figure 2.2 Perspective view of typical “y-shape” wall configuration for specimens tested within this study and typical specimen height to top of linings (dimensions in mm).

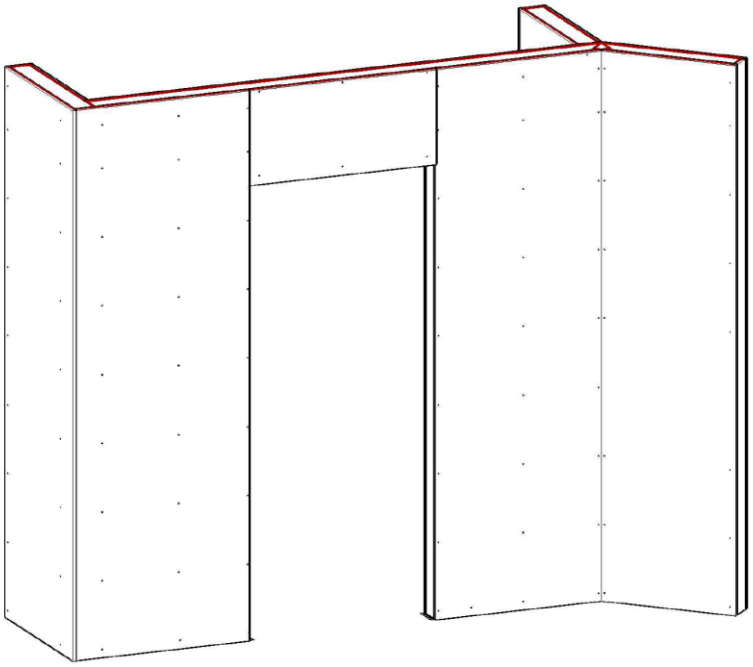

Figure 2.3 Perspective view of flexible track doorway specimen (Test ID A3) configuration.

2.3 Test Setup

2.3.1 Test Frame

A testing frame was designed in order to replicate, under controlled laboratory conditions, the effects of seismic shaking on partition walls within multi-storey buildings. The test frames were designed to simulate seismic shaking through application of quasi-static uni-directional cyclic loading imposing an inter-storey drift equivalent to what would be experienced within multi-storey buildings. Three identical frames were designed as this allowed three partition wall specimens to be installed simultaneously in order to limit the specimen construction time and help meet the time restraints of the project and available time allocated for the lab space.

The frames were designed as steel concentrically braced frames in the across direction and with removable steel braces in the along direction. These braces provided stability to the test frame while the actuator was not attached. Once the actuator was attached to the top slab of the test frames, the braces could be removed, and the frames would be free to displace longitudinally with the actuator displacement. The steel sections used for the frames were all 125 PFC. Top and bottom concrete slabs were constructed of 25 MPa 120 mm thick reinforced concrete slabs reinforced with SE92 mesh at 45 mm cover to centroid from the bottom of the sections. Only one 100 kN actuator was used during the course of the testing. After each test was completed the tested frame was braced and then the actuator was moved over to the next frame. Once the actuator was attached to the frame the longitudinal braces could be removed and testing of the next specimen could begin. The testing setup model is shown in

Figure 2.4 and a photograph of the constructed setup is shown in Figure 2.5. The plan dimensions available within each testing bay for construction of the specimens was 2100 mm by 3175 mm, shown in Figure 2.6, and the clear height between slabs was 2405 mm. The alignment of the specimens to the direction of loading is shown in Figure 2.6 also. The angle θ was equal to 30° for the series A specimens and 35° degrees for the series B specimens. The angle was changed as towards the end of testing specimen A1, the top of the steel frame began to bear against the top of the partition wall specimen, and so the angle was increased to provide a larger gap between the top of the wall and the steel frame for the series B specimens. Structural drawings for the testing frame are shown in Appendix A.

The response of an individual bare frame when subject to a monotonic cycle of 150 mm displacement, corresponding to 6.24% (150 mm / 2405 mm x 100%) drift, is shown in Figure 2.7. The response of the frame was linear with a stiffness of 10.1 N/mm. The noise shown in Figure 2.7 is attributed to the dynamic oscillation of the reaction frame. This occurred due to a combination of the factors including the stiffness of the reaction frame, the high mass of the top slab, gaps at the bolted connections of both the testing frame and the reaction frame, and a relatively high loading rate from the actuator. This noise is deemed to be inconsequential and the mean fit for applied cycle is deemed to be appropriate for use when determining the hysteresis of the specimens.

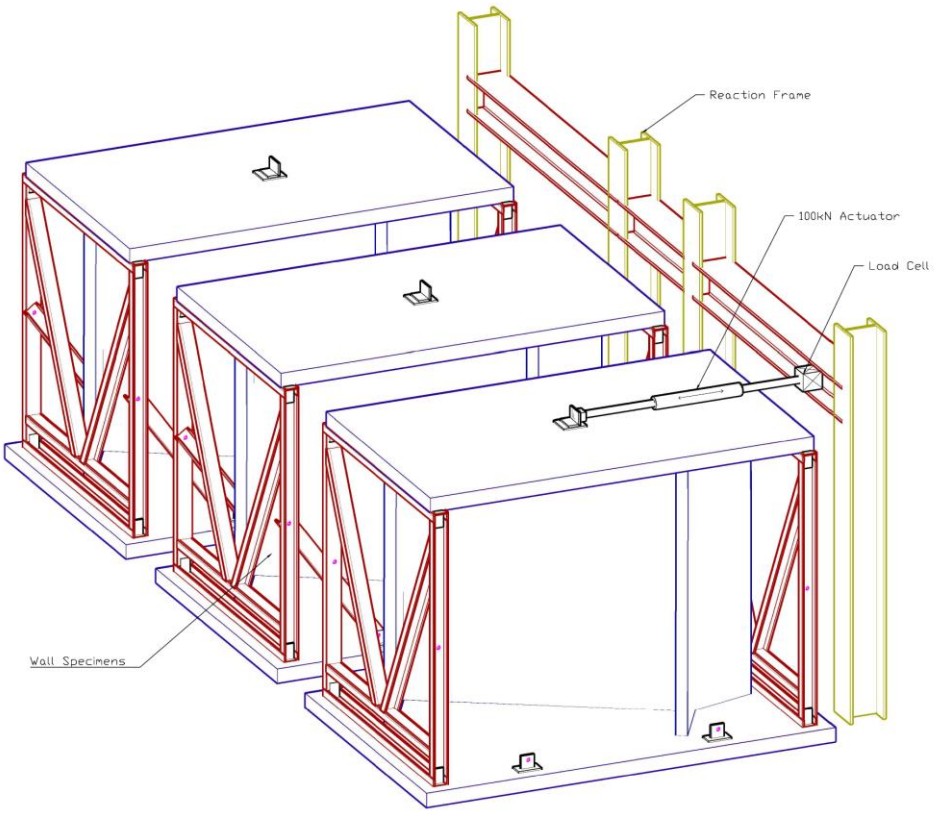

Figure 2.4 3D AutoCAD model of partition testing frame.

Figure 2.5 Photograph of as-built partitions testing setup.

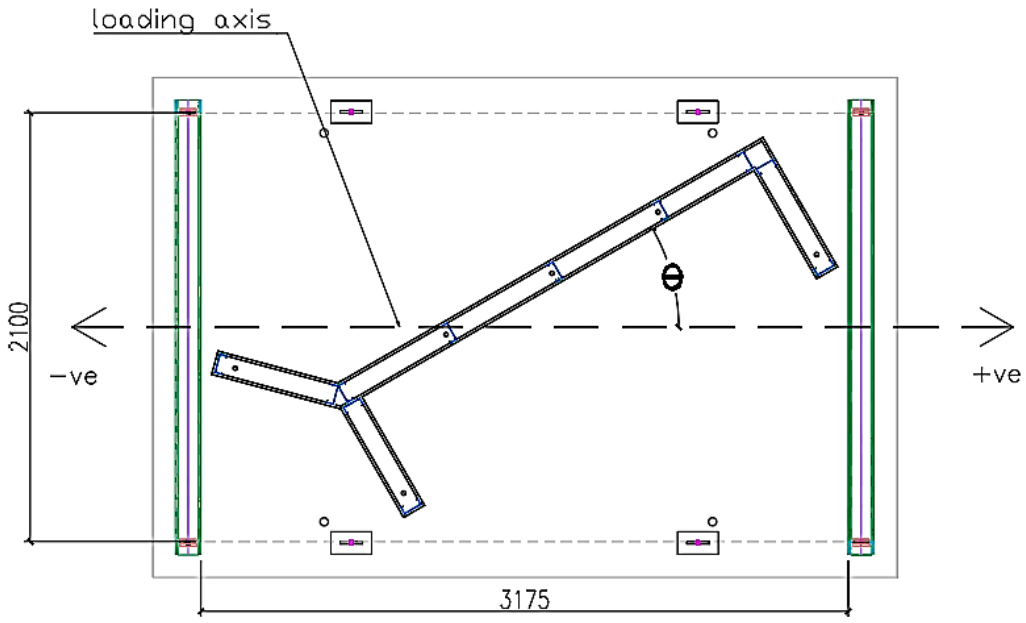

Figure 2.6 Individual test bed plan with dimensions of available space showing typical specimen and orientation to direction of loading (dimensions in mm).(Winstone Wallboards 2014)

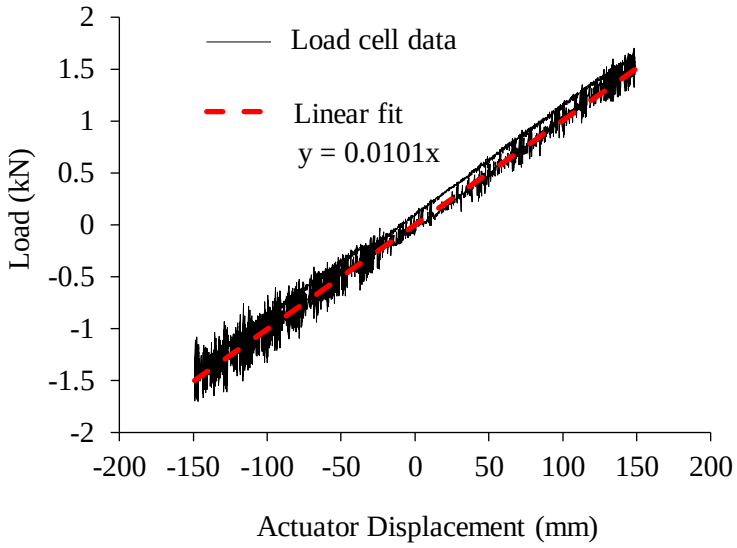

Figure 2.7 Load displacement behaviour of the bare frame.

2.3.2 Load Application

The quasi-static loading protocol used for the test was taken from the FEMA 461 document (Applied Technology Council 2007). The FEMA 461 document was produced in order to provide interim or provisional testing protocols for determining the seismic performance characteristics of structural and non-structural components. The quasi-static cyclic testing protocol is used herein as the aim of these tests is to determine the performance characteristics of a component (non-structural partition) whose behaviour is primarily controlled by the application of seismic-induced forces and displacements.

The FEMA 461 quasi-static cyclic testing protocol consist of slow cyclic application of load or deformation with a predetermined loading pattern. Two types of quasi-static test protocols testing are provided: racking testing and hysteretic testing. Racking testing is performed for components that either are not required to participate in a buildings structural resistance or not provide significant strength or stiffness modification of the building structure. These components will not typically be included in structural analytical models used to predict building performance. Hysteretic testing is performed for components that either are intended to provide structural resistance or significantly alter the strength or stiffness of a building structure. These types of components will typically be included in analytical models used to predict structural performance. As non-structural partition walls are not typically included within the structural model or known to significantly affect building performance, the racking test protocol is used.

FEMA 461 recommends performing an initial monotonic test to provide a baseline for estimating the cumulative damage effect at each damage state and to calibrate the cyclic loading history. However, in order to inform the likely drift at the onset of each damage state, the results of the tests by Restrepo and

Bersofsky (2011) were used. The loading history is defined by the parameters below and depicted in Figure 2.8.

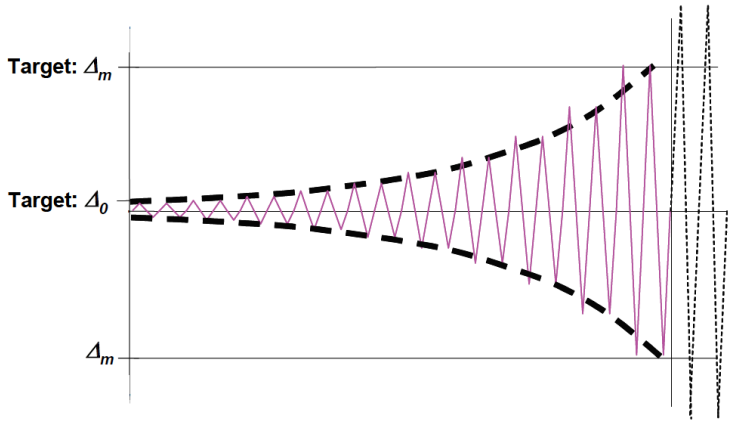

Figure 2.8 FEMA 461 quasi-static cyclic racking protocol parameters (Applied Technology Council 2007)

Δ_0 = target smallest deformation amplitude of the loading history. It must be safely smaller than the amplitude at which the lowest damage state is first observed. At the lowest damage state at least six cycles must have been executed.

Δ_m = target maximum deformation amplitude of the loading history. It is an estimated value of the imposed deformation at which the most severe damage level is expected to initiate. If the most severe damage state has not yet occurred at the target value the loading history should be continued by using further increments of amplitude of $0.3\Delta_m$.

n = the number of steps in the loading history

a_i = the amplitude of the cycles, as they increase in magnitude, i.e., the first amplitude, a_1, is Δ_0.

The amplitude a_{i+1} of the step i+1 (not of each cycle, since each step has two cycles) is given by the following equation:

$$a_{i+1} = 1.4a_i$$

Where a_I is the amplitude of the preceding step, and a_n is the amplitude of the step close to the target, Δ_m, and two cycles are performed for each step in the loading history.

Restrepo and Bersofsky (2011) tested partition wall specimens in-plane that were of similar dimensions to those tested herein (for further details see Section 1.5) and therefore have been used to provide an estimate for the drift at the onset of DS1, which for configuration I of their tests develops at 0.3%. As this protocol requires that before the smallest damage state initiates at least six cycles must have been

executed, the target smallest deformation amplitude, Δ_0, is equal to 1.4^{-6} x Δ_{DS1}. The maximum displacement that we intended to take the partition specimens was to 5% drift, as this would represent the maximum possible drift experienced in a building. Therefore, with the following parameters the inter-storey drift loading history to be applied to the specimens was as shown in Figure 1.

Δ_0 = 0.133*0.3% = 0.04%

Δ_m = 5%

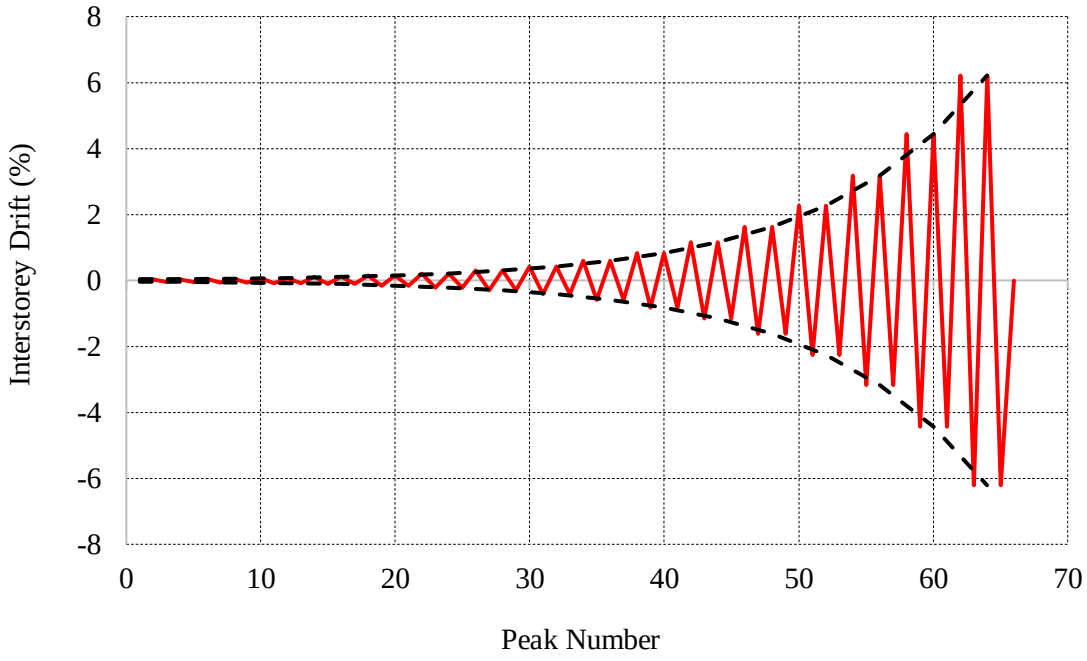

Figure 2.9 FEMA 461 Quasi-static unidirectional deformation-controlled loading history used for experimental testing of partitions.

Table 2.2 FEMA 461 cyclic loading history step amplitudes used for experimental testing of partition walls.

Step	Disp (mm)	Drift (%)
1	0.96	0.04
2	1.3	0.06
3	1.9	0.08
4	2.6	0.11
5	3.7	0.15
6	5.2	0.21
7	7.2	0.3
8	10.1	0.42
9	14.2	0.59
10	19.8	0.82
11	27.8	1.15
12	38.9	1.62
13	54.4	2.26
14	76.2	3.17
15	106.7	4.44
16	149.3	6.21

2.3.3 Instrumentation & Data Logging

The load applied to the specimens was recorded from a 50 kN load cell with an accuracy of ± 3 N. The specimens were instrumented with a combination of linear potentiometers (example of potentiometer layout at a wall junction is shown in Figure 2.10) and cameras. Potentiometers were used to measure the horizontal, vertical and lateral deflections for both specimens. The instrumentation layout for each specimen is shown in chapters 3 and 4 for each system. A series of high contrast points at approximately 75 mm spacing were applied to the surface of the specimens and the camera took pictures of these surfaces at each displacement increment in order to allow particle tracking analysis.

The required inputs for particle tracking analysis are a stream of photographs of the wall's specimens at each increment of loading of the loading protocol. In order to achieve this, cameras were setup initially at three points to take photographs of the specimen from three different angles. However, for simplicity this was reduced to a single camera taking photos of the wall specimens orthogonal to the direction of loading. The results of the particle tracking were not useable to draw informative data on the behaviour of the specimens at the end of the tests. This was because of error in the data recording and insufficient information to perform geometric transformations on the particle records.

Errors in the recording of data included loss of data at some steps of the loading protocol due to malfunction of the camera triggering mechanism; loss of data points on the field of the wall due to lighting issues within the lab space (picture of light coming in from upper windows of the lab shown in Figure 2.12); and also obstructions of people walking past the camera during testing.

As the particle tracking camera was positioned at a right angle to the direction of loading the particle records show the movement of the particles in the direction of loading, and therefore need to be geometrically transformed into the plane of the wall. This requires inputs of the coordinates of several particles within the plane of the wall. These points, however, were not recorded before the start of the testing. The only recorded points at the start of the testing were of the scale picture, which was taken for each specimen with a tape measure along the plane of the wall, as shown in Figure 2.13; which could be used to provide the coordinates of the particles (black dots) adjacent to the tape measure. However, the small number of particle coordinates derived using this method results in an error in the geometric transformation that is too large for the particle tracking results to be meaningful. In addition to the error in the transformation between the oblique plane to in-plane displacements, due to the direction of loading there is significant out-of-plane displacement induced at the top boundary. These out-of-plane displacements mean that the scale varies throughout the testing depending on the height of the particle within the plane of the wall and the error in the results is very significant.

Due to the sources of error in the data recording, the geometric transformation, and the resultant error in the results of the particle tracking analysis, the results were not useable and have not been discussed in subsequent chapters.

Figure 2.10. Example of potentiometer layout at wall intersections to record in-plane and out-of-plane movement.

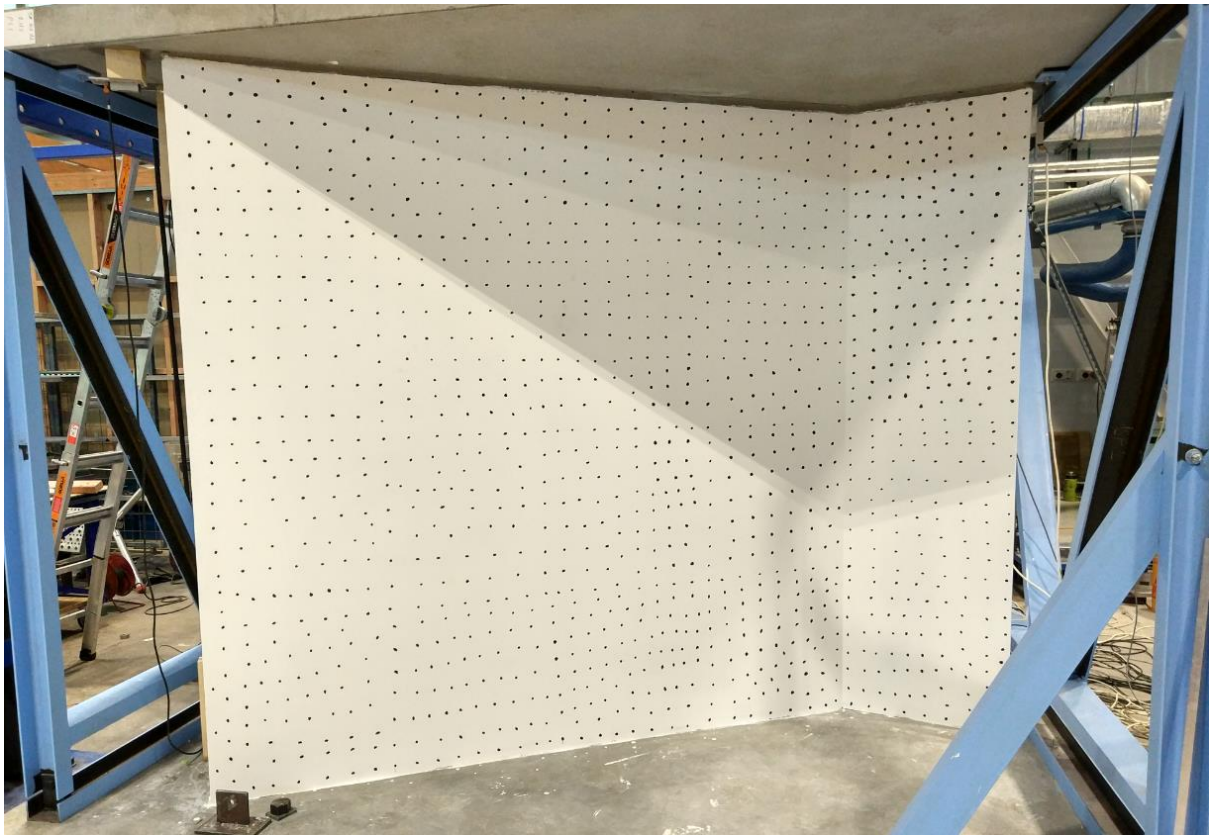

Figure 2.11 Specimen A1 painted black dots for particle tracking analysis.

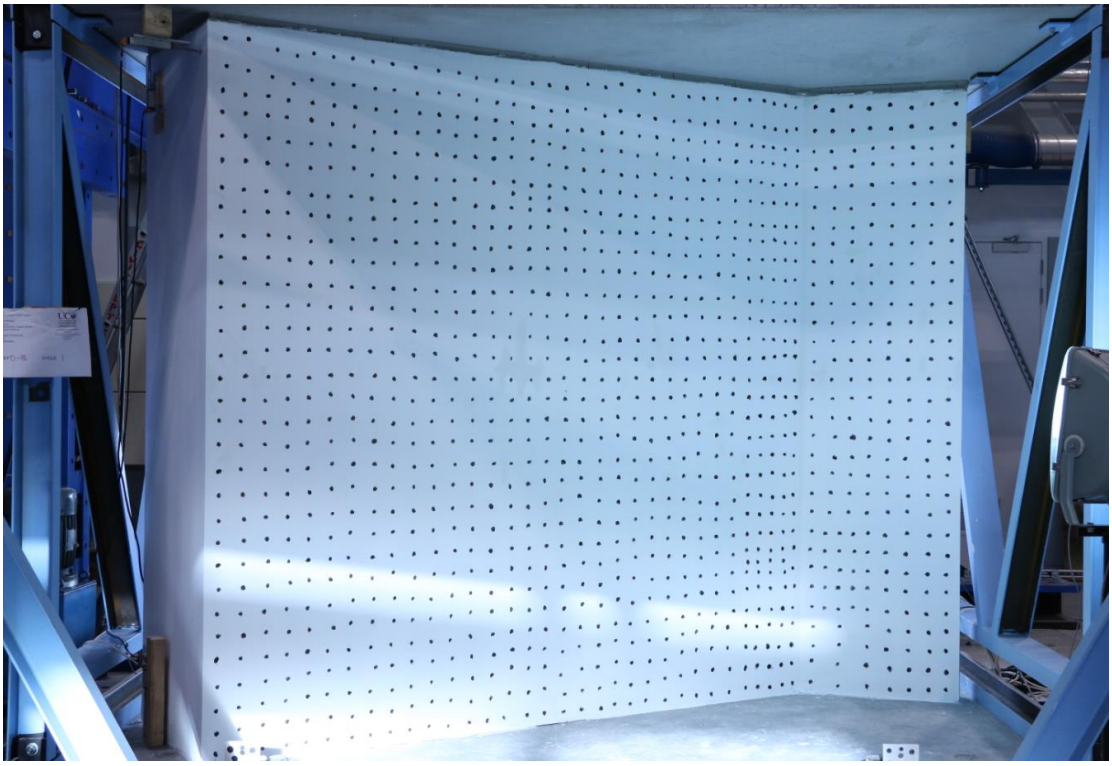

Figure 2.12 Example of lighting issues with particle tracking data (specimen A2).

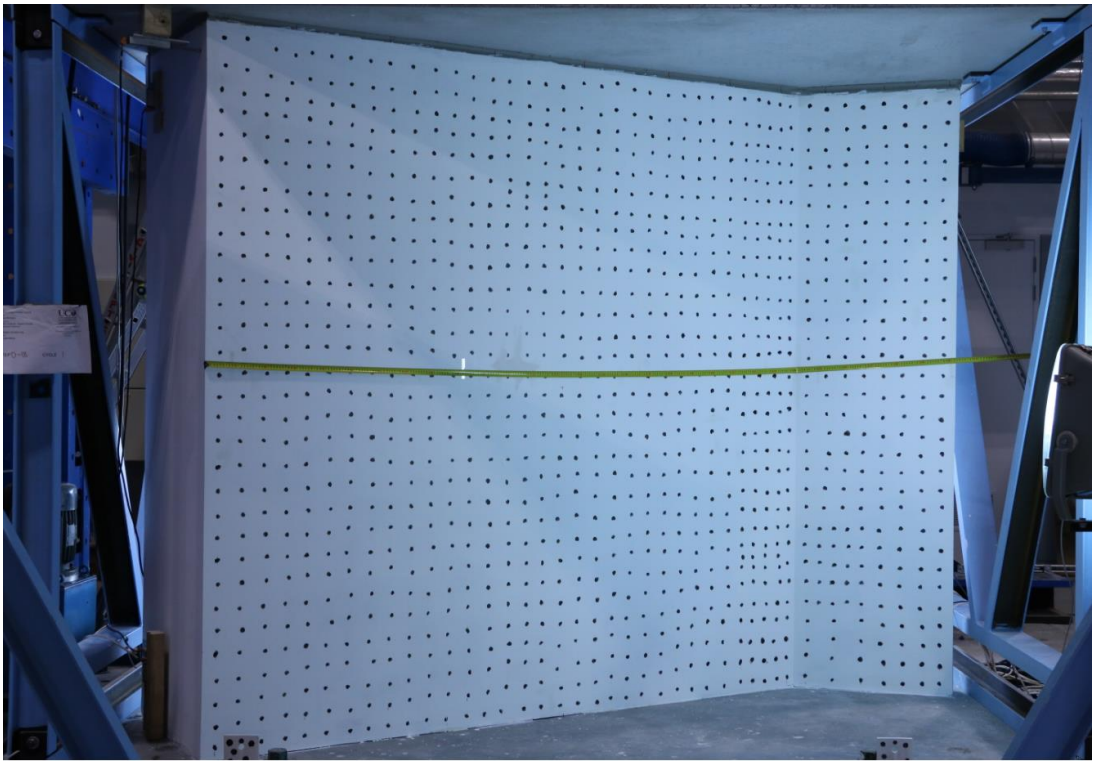

Figure 2.13 Example of scale picture for particle tracking (specimen A2).

3. JOURNAL PAPER ON EXPERIMENTAL SEISMIC PERFORMANCE OF PARTLY-SLIDING PARTITION WALLS

This chapter presents the experimental testing work on the partly-sliding partition wall specimens and is comprised of a journal paper published on said topic in the Journal of Earthquake Engineering (JEE) (Mulligan *et al.* 2020a) formatted for inclusion with this Master's thesis. For the specimen structural drawings and further information on damage observations and potentiometer readings refer to Appendix B.

Experimental Seismic Performance of Partly-Sliding Partition Walls

J. Mulligan, T.J. Sullivan, R.J. Dhakal

Department of Civil and Natural Resource Engineering, University of Canterbury, Christchurch, New Zealand.

ABSTRACT: Plasterboard partition walls typically used in commercial buildings are especially sensitive to earthquakes, with the onset of cosmetic damage initiating at small values of interstorey drift. The most common partition wall systems are constructed of gypsum board attached to either steel or timber framing which is fixed directly to the floor system at the top and bottom interfaces. This study investigates the seismic performance of a novel partly-sliding steel framed partition system examined in the past and used by industry, with minor modifications incorporated within the partition detailing. This novel system involves removing top track anchors within the proximity of wall intersections, thus allowing the tracks to 'bow' out at these locations. In this study three full-scale specimens were subjected to quasi-static cyclic testing; two identical plane specimens and the third including a doorway. The specimens were built in a y-shape and angled at 30° to the direction of applied loading, which allowed bi-direction behaviour to be examined. The specimens included an acoustic/fire sealant. The progression of damage in a partition can be categorized by three sequential damage states associated with distinct levels of repair: superficial damage requiring cosmetic repair (damage state 1 (DS1)), damage requiring local repairs or replacement of only portions of the partition assembly (damage state 2 (DS2)), and severe damage requiring complete removal and replacement of the wall (damage state 3 (DS3)). Damage was first observed as cracking of the wallboard at the wall ends, at external junctions, and propagating from the corners of the door opening. The onset of DS1 and DS2 occurred simultaneously at a median in-plane drift of 0.29%. DS3 was not observable until the linings had been removed at the end of the tests. In addition to providing drift capacities, the force-displacement behaviour is also reported, the dissipated energy was computed, and the parameters of the Wayne-Stewart hysteretic model were fitted to the results. The specimen with the door opening behaved significantly different to the plane specimens: damage to the doorway specimen began as cracking of the wallboard propagating from the corners of the doorway following which the L- and Y- shaped junctions behaved independently, whereas damage to the plane specimens began as cracking of the wallboard at the top of the L-junction and wall system deformed as a single unit. The results suggest that bi-directional behaviour is important even if its impact cannot be directly quantified by this experiment. Damage to sealant implies that the bond between plasterboard and sealant is important for its seismic performance, and careful quality control is advised, as defects in the bond may significantly impact its ability to withstand seismic movement.

Keywords: Plasterboard partition walls; fragility curves; non-structural elements; drywall; acoustic/fire sealant.

3.1 Introduction

It is now widely recognized that the performance of non-structural elements is a crucial component of the performance of building systems during earthquakes (Dhakal 2010). Their performance is vital to maintain continuity of emergency and recovery services, to reduce the likelihood of injury or death, to prevent loss of building function, and to limit the direct and indirect economic losses resulting from earthquake events. Taghavi and Miranda (2003) have shown that non-structural elements comprise the majority of investment in commercial buildings (Figure 3.1). Furthermore, for all building types, interior construction was shown to comprise 20-30% proportion of the non-structural component cost. Partition walls, also known as drywalls, have been shown to significantly contribute to total earthquake losses. Whitman *et al.* (1973) found that in the 1971 San Fernando Earthquake, for buildings in earthquake intensity (MMI) zones VI, VII, and VIII, the damage to partitions contributed approximately 90, 65, and 50% respectively, to the total cost of damage to buildings. They concluded that improving the seismic performance of interior partitions would be one of the most effective ways to reduce the seismic losses in buildings subjected to MMI VI earthquakes. This is because partition walls are especially sensitive to earthquake damage, with the onset of damage initiating at low interstorey drifts of approximately 0.35% according to Davies *et al.* (2011). This level of interstorey drift may be imposed by low intensity ground motions with frequent return periods and this implies frequent repairs after relatively small earthquake events or aftershocks, resulting in significant financial loss (Arifin *et al.* 2017).

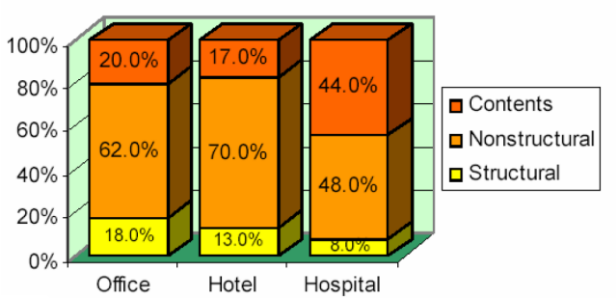

Figure 3.1 Building construction cost distribution of components of three sample buildings as a percentage of total cost (Taghavi and Miranda 2003]

Performance-based earthquake engineering (PBEE), described in the FEMA P58 document (FEMA 2012), provides a framework by which buildings can be designed using performance objectives that are system level in terms of risk of collapse, fatalities, repair costs, and post-earthquake loss of function. In order to provide a rigorous probabilistic assessment of losses, PBEE utilises fragility and loss functions. Fragility functions can provide a probabilistic means of quantifying the likely level of

damage in a component given a particular structural response. The levels of damage are expressed as damage states corresponding to a level of repair and the structural response is quantified by a particular engineering design parameter (EDP) that correlates well with damage. For light framed steel or timber plasterboard partition walls, damage states have shown to correlate best with in-plane interstorey drift (Freeman 1971, Rihal 1980, Taghavi and Miranda 2003).

The earliest experimental investigations on gypsum lined walls, were focused on the load-deformation of shear walls designed to resist lateral loads (Deierlein *et al.*, 2003). The earliest series of tests that the author is aware of on commercial non-structural partition walls was conducted by Lee *et al.* (2007). Lee *et al.* (2007] tested full-scale partitions with lightweight steel framing according to typical Japanese configurations and estimated a damage-repair cost relationship. Overall, the specimens were damage free until up to 0.25% interstorey drift.

Restrepo and Bersofsky (2011) tested 2.4 m high 2.9 m long I-shape partition wall specimens with 1.2 m returns at each end, under quasi-static reversed cyclic displacement based on in-plane loading according to the CUREE loading protocol for wood frame structures (Krawinkler *et al.* 2001). Restrepo and Bersofsky (2011) used the damage state (DS) definition recommended by Taghavi and Miranda (2003) for drywall wood stud partition walls: (1) cracking in plaster and paint, (2) damaged drywall panel, and (3) damage to framing. For conventional steel stud partitions DS1, DS2, and DS3 occurred at drifts of 0.3%, 1%, and 3% respectively.

The most extensive series of experiments into the seismic performance of plasterboard partition walls appears to have been conducted by Davies *et al.* (2011). The authors tested 50 full scale partition walls in 22 different configurations under both quasi-static and dynamic loading and generated data regarding the in- and out-of-plane seismic behaviour. Variables included return wall configurations; partial-height and full-height specimens; alternate junction details; connectivity of studs, tracks, and sheathing; and bookshelf attachments. This data was used to produce a set of fragility parameters, useful for implementation in PBEE analysis of buildings. For the development of the fragility parameters, the authors used damage states previously defined by Taghavi and Miranda (2003). The typical test specimens were 3.5 m high by 3.7 m long. For the test specimens close to NZ commercial partitions, the mean drifts associated with DS1, DS2, and DS3 were 0.26%, 0.68%, and 0.75% respectively. It should be noted that DS3 was triggered at a relatively low drift. This was failure of the track to concrete fasteners at the ends of return walls. The track to concrete fasteners used by were standard powder driven 25 mm (1") fasteners @ 610 mm (24") centres, using a Ramset gun model SA-270 and Ramset .27 caliber shots. Similar fasteners were used by Restrepo and Bersofsky (2011) at a larger spacing (812 mm centres) driven in by a 0.22 caliber nail gun-plus. However, this form of damage was not observed as additional fasteners were placed at the end of return walls.

Included within the series of tests by Davies *et al.* (2011) were some novel details for improving the performance of partitions, including a 'sacrificial corner bead' system (specimen 33 & 35), and a flexible track system (specimen 34 & 36). Other systems have been proposed in the literature for the improvement of the seismic performance of partitions: including a sliding/frictional system developed by Araya-Letelier and Miranda (2012), and a gapped system tested in several studies (Lee *et al.* 2007, Magliulo *et al.* 2014, Tasligedik *et al.* 2015, Pali *et al.* 2017, Pali *et al.* 2018).

The flexible track system proposed by Davies *et al.* (2011) is the focus of this study. Retamales *et al.* (2013) suggested that "practical considerations of the new proposed details would require evaluation of other design constraints including bidirectional seismic loading, acoustic transmission, and fire resistance' and that 'additional tests are required to evaluate their effectiveness'. Through conversation with the industry it appears that a partially-sliding partition wall system with similar detailing to that tested by Davies *et al.* (2011) is used in practice. As such, this work reports an experimental campaign that tests partially sliding partition walls in order to investigate the effect of bi-directional behaviour, angled return walls, and door openings; and to develop fragility functions. The tests aim to investigate the seismic behaviour of fire/acoustic sealant when used in practice at the top lining to floor boundary.

3.2 Details of Partially Sliding Partition Walls

In New Zealand, steel framed drywalls are typically constructed of light gauge steel studs sheathed with gypsum wallboard (GIB) screwed to the framing. There are various alternatives in connections and configurations including, steel framing size and gauge; fastener type, spacing, and location; sheathing type, orientation, and number of layers; top and bottom track anchors; and others. Guidelines are available that recommend different configurations depending on various performance objectives including, fire rating, sound rating, impact resistance, and other special purposes. The configuration chosen to provide a baseline for this experimental study was a fire rated partition typology selected from GIB Fire Rated Systems (GIB 2012), with a 60 minute fire-resistance rating (GBS60). The steel framing consisted of 92 x 34 x 0.5 studs 94 x 30 x 0.5 base tracks provided by RONDO. The framing was sheathed with 13 mm GIB Fyreline®, connected with 25 mm x 6 g GIB Drywall Self Tapping Screws® at 300 mm centres up each stud with an additional screw between the lining and bottom track between each stud. Bottom and top track anchors were HILTI HUS3-H8 x 55 screw anchors at 600 mm centres.

The flexible track system proposed by Davies *et al.* (2011) increases track flexibility by not using track to concrete slab connectors within 610 mm (2') of wall intersections, thus allowing the tracks to 'bow' out. Davies *et al.* (2011) proposed two specimen designs. For the first specimen only the top track anchors were removed, the studs and plasterboard were screwed to the bottom track, and the studs were free to slide within the top track. For the second specimen, both top and bottom anchors were removed

in proximity to junctions, and the studs and linings were not connected to the track at the top or bottom, and so were free to slide at both ends.

The specimen design for this test series, termed "partially-sliding", was developed considering the designs by Davies *et al.* (2011) and in discussion with an industry partner who has been producing a similar system. The design incorporates only minor alterations to the as-built NZ GBS 60 partition wall. The changes are to remove top track fixings within the proximity of return walls, thus allowing the walls to 'bow' out; and to fix the sheathing to the bottom track at 600 mm centres, but not at the top; the objective of this being that the studs are free to slide within the top track while the sheathing remains stationary. The junction details were developed in consultation with industry. The return walls were approximately 600 mm long and were configured in a 'y' shape, with two return walls at a 90° angle to the main wall and one at 45°, as shown in Figure 3.2 & 3.3. This configuration was chosen as no previous studies the author is aware of had considered the impact of oblique walls. In addition, a 25 mm gap at the top of the sheathing was provided and filled with fire sealant, as is common in practice, with tape along the track flanges in order to break the bond between top track and sealant (Figure 3.4). The fire sealant used for this application was HILTI CP606 flexible fire stop sealant. The main difference between this specimen design and the specimens tested by Davies *et al.* (2011) was the junction details. Davies *et al.* (2011) tested an I-shaped specimen with two T-shaped junctions, whereas the specimens studied herein were in a y-shape with one L-junction and one Y-junction. Some other differences from the specimens tested by Davies *et al.* (2011) were that the studs were not fixed to the tracks at any location; and more robust track anchors were utilised to avoid the early anchor failure experienced in both of their tests.

Although the top track anchors were specified to be removed within 600 mm of wall intersections, a construction error was made whereby a single top track slab to concrete anchor was left in at the three-way wall junction (Figure 3.4). The potential impact of this error is discussed when reviewing results. Despite this error, the experimental testing was deemed worthwhile since such errors will also occur in practice and because the behaviour of the wall can be examined with this fixing in mind.

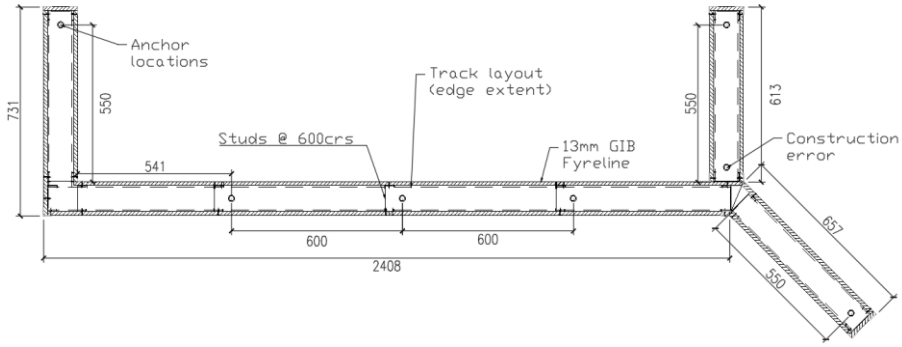

Figure 3.2 Specimen A1 & A2 dimensions with top track anchor locations (dimensions in mm)

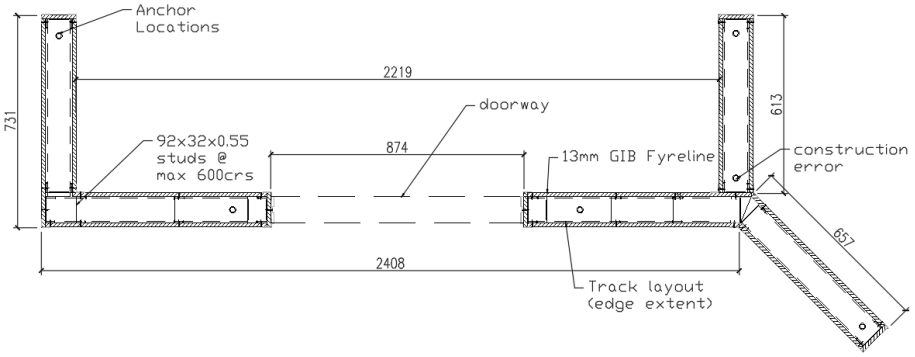

Figure 3.3 Specimen A3 plan dimensions and top track anchor locations (dimensions in mm)

(a) (b)

Figure 3.4 (a) Top slab connection, (b) base slab connection.

3.3 Experimental Test Setup

3.3.1 Testing Frame

The walls were tested in racking in order to simulate the loading experienced by partition walls in commercial buildings. The testing frame was hinged at the top and the bottom in-plane, with diagonal braces to provide stability while the actuator is not attached. The frames are constructed of steel 125PFC members. The top and bottom concrete boundaries are 120 mm thick reinforced concrete slabs, which were selected in order to simulate the most typical boundary conditions and flooring systems in real buildings. The plan dimensions of compartment including the partitions were 3175 mm by 2100 mm, and the clear height was 2405 mm (Figure 3.5a & 3.5b). Three separate frames were constructed, in order to allow swift construction and testing (Figure 3.5c & 3.5d). The response of the bare frame was approximately linear with a stiffness of 10.1 N/mm, as shown in Figure 3.6.

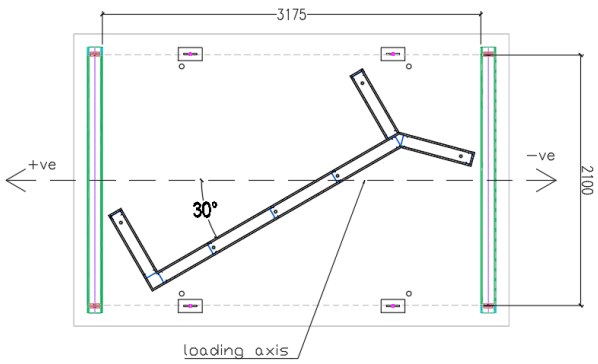

(a)

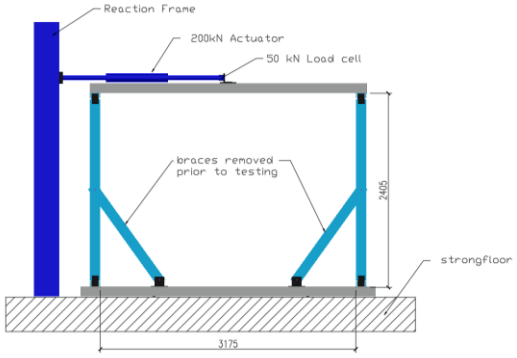

(b)

(c)

(d)

Figure 3.5 (a) Plan of testing frame (mm); (b) Elevation of testing frame (mm); (c) Photograph of setup; (d) Photograph of specimen A3 (doorway specimen).

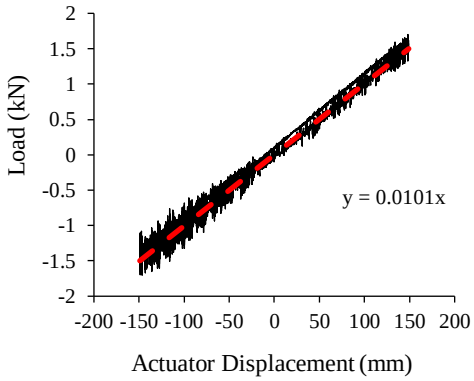

Figure 3.6 Load displacement behaviour of the bare frame

3.3.2 Experimental Program

Three partition wall specimens were tested in this experiment: two (A1 & A2) identical to those shown in Figure 3.2, and a third specimen, A3, that was also identical except that it possessed a door (see Figure 3.3). To assess the impact of bidirectional loading on fragility, the wall specimens were aligned at an angle of 30° to the loading direction, as shown in Figure 3.5a. The specimens were tested according to FEMA 461 deformation-controlled unidirectional quasi-static cyclic protocol (FEMA 2007). The protocol was calibrated based on the results of previous in-plane tests on similarly detailed walls (Restrepo and Bersofsky 2011). The estimated drift for DS1 was 0.3% and the target maximum drift was 5%. Two cycles were applied at each drift amplitude and the drift amplitude of each step was 1.4 times the amplitude of the preceding step. A total of sixteen drift steps were applied, up to a maximum drift of 6.21% (Figure 3.7), which corresponds to a maximum in-plane drift of 5.38% for the wall angled at 30°. Specimens A1 & A2 were tested up to step 15 and specimen A3 was tested up to step 16.

3.3.1 Data Acquisition

The load applied to the specimens was recorded with a 50kN load cell with an accuracy of ± 3N. The specimens were instrumented with a combination of linear potentiometers and cameras. With reference locations shown in Figure 3.8, the general potentiometer layout for the test series is shown in Figure 3.9. For the first specimen 30 potentiometers were used to measure the horizontal, vertical and lateral deflections, however the number of potentiometers was reduced to 23 by the third specimen as some of the instruments were deemed unnecessary. The potentiometers recorded the linear relative displacement between the location they were fixed on the wall and the surface of the concrete slab closest to their location. The cameras were used to record frames at each displacement increment in order to enable particle tracking software analysis. A series of high contrast points at approximately 75mm spacing were applied to the surface of the specimens for this purpose.

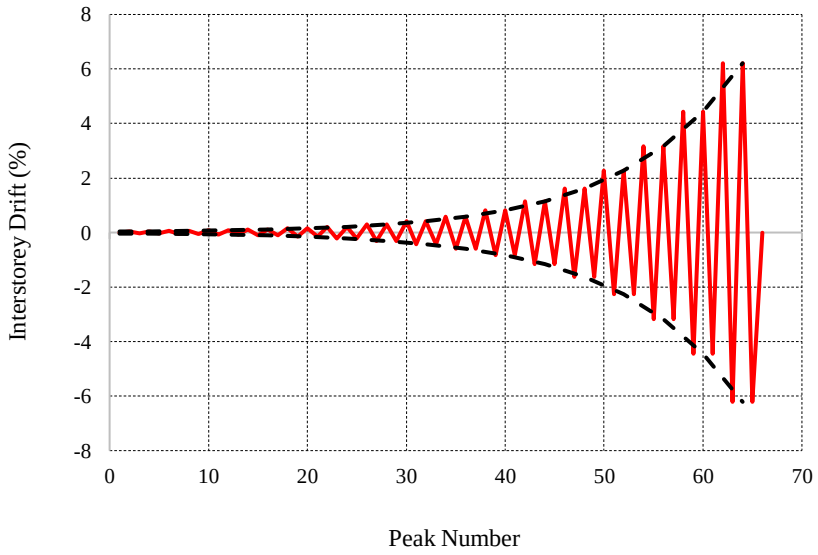

Step	Top Slab Disp (mm)	Drift (%)
1	0.96	0.04
2	1.3	0.06
3	1.9	0.08
4	2.6	0.11
5	3.7	0.15
6	5.2	0.21
7	7.2	0.3
8	10.1	0.42
9	14.2	0.59
10	19.8	0.82
11	27.8	1.15
12	38.9	1.62
13	54.4	2.26
14	76.2	3.17
15	106.7	4.44
16	149.3	6.21

Figure 3.7 FEMA 461 quasi-static cyclic displacement protocol

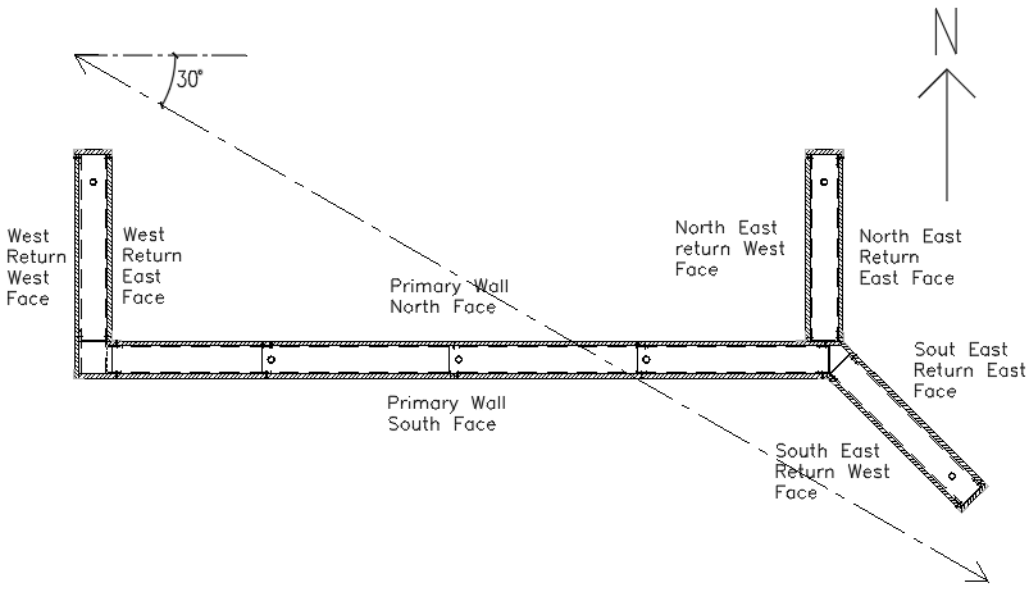

Figure 3.8 Wall specimen showing references for wall locations

3.4 Results

3.4.1 Damage Observations

Damage observations were taken after each step in the loading protocol (Figure 3.7), these included detailed visual inspections and photographs. As only visual observations were made, the point at which the framing was damaged could not be identified until the wallboard began to spall, which happened only in the doorway specimen. Thus, only at the completion of the test could a detailed inspection of the framing be made. The forms of damage observed during the tests are summarised in Table 3.1, along with their associated repair actions. Figure 3.10 illustrates the damage states being referred to in Table 3.1. These are similar to the conventional three damage states suggested by Taghavi and Miranda (2003), but include fire/acoustic sealant debonding as part of DS1. Note that typically failure of track anchors would be included within DS3, but as large anchors were used these did not damage in any case. Damage state 0 has been included to represent damage that is visible but is not considered to need repair depending on the required level of finish and a subjective assessment from the owner. The in-plane drift at which each damage state initiated in the specimens is shown in Table 3.2. Note that for DS3 the values recorded in Table 3.2 represent the final maximum drift the specimen was subject to before an inspection of the internal frame was conducted. The formation of hinges in studs, associated with DS3, was discovered during the inspection performed following the tests, which indicates that the DS was triggered during testing at an unknown drift level. The formation of hinges in studs may be related to popping out screws around the hinge or strength degradation in the hysteresis loops. However, the lowest drift level at which plasterboard panels need to be replaced corresponds to DS2 and as this type of repair work could reveal damaged studs, a lower-bound estimate for DS3 would be to adopt the same drift values as per DS2. The percentage undamaged framing at the end of the test is shown in Table 3.3. This value represents the length of undamaged framing at the end of the test as a percentage of the total original length of framing. Damage to the studs was more pronounced at the ends of walls and near the junctions; and damage to the steel tracks primarily occurred along the top, with more deformation near the junctions.

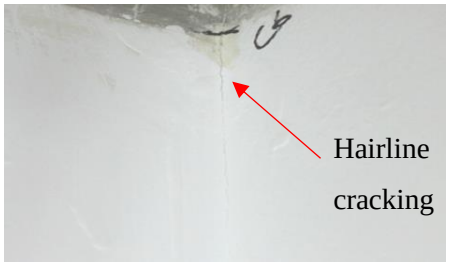

(a) Paint cracking

(b) Sealant de-bonding

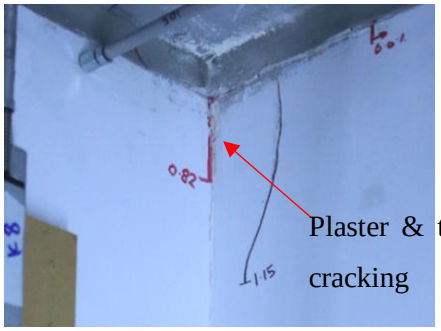

(c) Plaster cracking

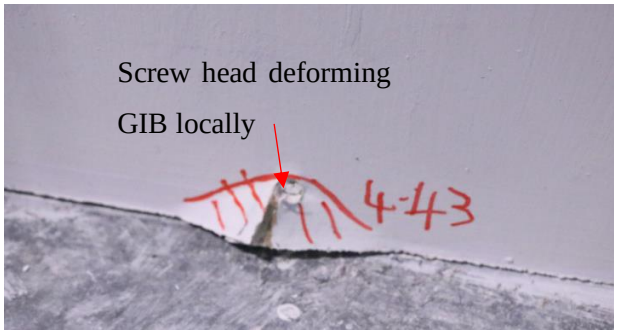

(d) Screw damage

(e) Wallboard damage

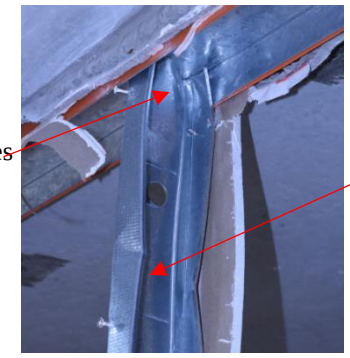

(f) Framing damage

Figure 3.9 Examples of observed damage

Table 3.1 Damage states

Damage State	Description	Repair Action
0	Hairline cracking of paint at joints	Barely visible damage, deemed not requiring repair.
1.a	Sealant de-bonding	Remove and re-apply sealant
1.b	Cracking in plaster and paint along trim	Scrape out minor cracks, and reapply plaster and paint.
1.c	Screw damage, pull through, popping, shearing	Refix or tighten any existing loose fasteners and place additional fasters near original. Finish with plaster, and sand and paint.
2	Wallboard damage - paper face separating, crushing, cracking, spalling	Requires replacement of linings or local repairs of linings. Breakages can be ground out and patch fixed, using plastering and paper tape.
3	Framing damage - flanges bent, buckling, hinging	Both linings and framing must be removed and replaced. Thus, complete demolition and replacement of the wall is required.

Table 3.2 In-plane drift %, r_i, at damage onset and fragility curve parameters.

	A1	A2	A3	x_m	β
DS1	0.36	0.26	0.26	0.29	0.35
DS2	0.36	0.26	0.26	0.29	0.35
DS3	<3.84	<3.84	<5.38	-	-

Table 3.3 Percentage of framing undamaged at the end of testing.

Test	Studs	Top tack	Bottom track
A1	46%	0%	100%
A2	39%	14%	100%
A3	24%	57%	57%

3.4.2 Detailed Damage Progression

The progression of damage in the specimens is detailed in Tables 3.4, 3.5, and 3.6. The drifts presented are the components of the total drift in-plane to the different wall orientations. The locations referred to in these tables are explained in Figure 3.11. Each location refers to any vertical point of the wall within the region defined in Figure 3.11. The damage states defined in Table 3.1 are used, and the entries in these tables represent the loading steps at which each damage state initiated at that location. For specimen A3, locations 4 and 13 refer to the section of wallboard above the doorway (lintel). For DS2, replacement of sealant and re-plastering is implied, therefore when DS2 occurs first or coincidentally with DS1, DS1 is not noted in Tables 3.4, 3.5, and 3.6.

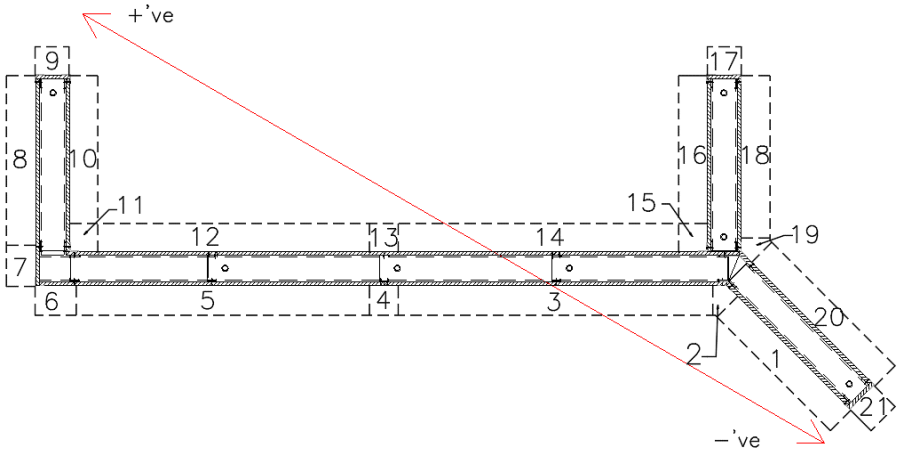

Figure 3.10 Specimen location reference for damage progression tables. Axis of loading a definition of positive loading direction shown in red.

Table 3.4 Detailed damage progression for specimen A1 described in relation to damage states listed in Table 3.1.

	STEP	6	7	8	9	10	11	12	13	14	15
Drift (%)	loading dir.	0.21	0.3	0.42	0.59	0.82	1.15	1.62	2.27	3.17	4.44
	45° wall	0.20	0.29	0.41	0.57	0.79	1.11	1.56	2.19	3.06	4.29
	90° walls	0.11	0.15	0.21	0.30	0.41	0.58	0.81	1.14	1.59	2.22
	long wall	0.18	0.26	0.36	0.51	0.71	1.00	1.40	1.97	2.75	3.85
Location	**1**	-	-	-	-	-	-	-	1a,1c	-	2
	2	-	-	-	-	-	-	-	-	1a	-
	3	-	-	-	-	-	-	1a	1c	-	2
	4	-	-	-	-	-	1c	-	-	1a	2
	5	-	-	-	-	-	1c	-	-	1a	-
	6	-	-	-	-	-	-	-	1a,2	-	1b
	7	-	-	-	-	-	1a, 2		-	-	1c
	8	-	-	-	-	-	-	1a	-	-	-
	9	-	-	-	-	-	1a, 2	-	-	-	-
	10	-	-	-	-	-	-	1c	1a	-	1b
	11	0	-	1a,1b	-	-	-	-	2	-	-
	12	-	-	-	-	1a	-	-	1c,2	-	-
	13	-	-	-	-	-	-	-	1a	-	-
	14	-	-	-	-	-	-	-	1a	-	-
	15	-	0	1a	1b	-	-	-	-	-	2
	16	-	-	-	-	1a	-	-	-	2	-
	17	-	-	-	-	-	-	-	1a,2	-	1b
	18	-	-	-	-	1a	-	-		-	1b
	19	-	-	-	-	-	1b	-		1a	-
	20	-	-	-	-	-	-	-	1c	1a	-
	21	-	-	1a,2	-	-	-	-	-	1a	-

Table 3.5 Detailed damage progression for specimen A2 described in relation to damage states listed in Table 3.1.

	STEP	6	7	8	9	10	11	12	13	14	15
Drift (%)	loading dir.	0.21	0.3	0.42	0.59	0.82	1.15	1.62	2.27	3.17	4.44
	45°	0.20	0.29	0.41	0.57	0.79	1.11	1.56	2.19	3.06	4.29
	90°	0.11	0.15	0.21	0.30	0.41	0.58	0.81	1.14	1.59	2.22
	long wall	0.18	0.26	0.36	0.51	0.71	1.00	1.40	1.97	2.75	3.85
Location	**1**	-	-	-	-	-	-	-	1a	-	1b
	2	-	-	-	-	-	-	-	1a	-	1b
	3	-	-	-	-	-	-	1a	-	-	-
	4	-	-	-	-	-	-	1a	-	-	-
	5	-	-	-	-	-	1a	-	-	-	-
	6	-	-	-	-	-	2	-	-	-	-
	7	-	2	-	-	-	-	-	-	-	-
	8	-	-	-	-	-	1a	-	-	-	-
	9	-	-	-	-	1a	2	-		-	-
	10	-	-	-	-	-	1a	-	-	-	-
	11	-	-	-	-	0	-	-	-	1b	2
	12	-	-	-	1a	-	-	-	-	-	-
	13	-	-	-	-	-	-	-	1a	-	-
	14	-	-	-	-	-	-	-	1a	-	-
	15	-	0	-	-	-	1a,1b	2	-	-	-
	16	-	-	-	-	-	-	2	-	-	-
	17	-	-	-	-	-	-	2	-	-	-
	18	-	-	-	-	-	-	1a	-	2	1c
	19	-	-	-	-	1a	0	-	-	1c	1b,2
	20	-	-	-	-	-	-	1a	-	2	-
	21	-	-	-	2	-	-	-	-	-	-

Table 3.6 Detailed damage progression for specimen A3 described in relation to damage states listed in Table 3.1.

	STEP	6	7	8	9	10	11	12	13	14	15	16
Drift (%)	loading dir.	0.21	0.3	0.42	0.59	0.82	1.15	1.62	2.27	3.17	4.44	6.22
	45° wall	0.20	0.29	0.41	0.57	0.79	1.11	1.56	2.19	3.06	4.29	6.00
	90° walls	0.11	0.15	0.21	0.30	0.41	0.58	0.81	1.14	1.59	2.22	3.11
	long wall	0.18	0.26	0.36	0.51	0.71	1.00	1.40	1.97	2.75	3.85	5.38
Location	**1**	-	-	-	-	-	-	-	-	1a	1c,2	1b
	2	-	-	-	-	-	-	-	-	1a	1b	2
	3	-	-	-	-	-	-	-	-	1a	1b,1c	2
	4	**0**	2	-	-	-	-	-	-	1a, 3*	-	3
	5	-	-	-	-	-	-	-	1a	-	-	-
	6	-	-	-	-	-	-	-	1a	-	1c,2	-
	7	-	-	-	-	-	-	-	1a	2	-	-
	8	-	-	-	-	-	-	-	-	1a,1c	-	-
	9	-	-	-	-	-	1a,2	-	-	-	-	-
	10	-	-	-	-	-	-	-	2	-	-	-
	11	-	-	-	0	1b	2	-	-	-	-	-
	12	-	-	-	-	-	-	-	1a	-	-	1c,2
	13	**0**	2	-	-	-	-	-	1a	-	-	-
	14	-	-	-	-	-	1a	-	-	-	-	1c,2
	15	-	-	-	0	1b	-	2	-	-	-	-
	16	-	-	-	-	-	1a	-	-	-	-	-
	17	-	-	-	-	-	-	1a	-	2	-	-
	18	-	-	-	-	-	1a	-	1b	2	1c	-
	19	-	-	-	-	-	-	-	1b	2	-	-
	20	-	-	-	-	-	1a	-	-	1b	2	-
	21	-	-	-	1b	2	-	-	-	-	-	-

Note: 3* refers to damage of the doorframe at which point the door could not be closed

3.4.3 Behaviour description & discussion

Damage was first observed as cracking of the wallboard at the wall end (location 21) for specimen A1, cracking of the wallboard at the junction (location 7) for specimen A2, and cracking of the wallboard propagating from the corners of the door opening (location 4 and 13) for specimen A3. The onset of DS1 and DS2 occurred simultaneously at a median in-plane drift of 0.29% and DS3 until the lings had been removed at the end of the test (Table 3.2).

The mean damage state parameters and the damage progression was compared with similarly detailed specimens tested by Davies *et al.* (2011). Davies *et al.* (2011) tested two partially sliding specimens (specimen 34 and 36). Specimen 34 was detailed similarly to the specimens tested in this study: with track anchors removed only at the top, and linings fixed to the tracks at the bottom. In this specimen, damage was first observed with cracking of the joint tape at vertical wall junctions and popping out of screws connected at the bottom track; and DS1, DS2, and DS3 initiated at 1.00%, 1.35%, and 1.84% drift respectively. Therefore, damage progression of this specimen was significantly different from the specimens tested herein. This may be attributed to several factors including differing geometry; return

wall configurations; junction details; the presence of a track anchor at the Y-junction; and bi-directional behaviour. The Davies *et al.* (2011) specimens were 3.5 m high and 3.7 m long, with 1.2 m returns at either end forming an I-shape configuration, whereas the specimens tested herein were 2.4 m high and 2.4 m long, with 0.6 m return walls in a y-shape. The junction details were significantly different. In the Davies *et al.* (2011) specimen there was no direct contact between the end of tracks and the linings. It is suspected that the factor providing the largest impact is this difference in detailing of the junctions.

The behaviour at the junctions was important. The first damage observed in specimen A2 was due to the top track pushing against the plasterboard lining and causing it to crack, thus initiating DS2, at a relatively low drift of 0.26%. The damage caused by the ends of track pushing against the lining was also the first damage seen in specimen A1, where the track pushed against the end of the return wall (location 20) at 0.36% drift. For specimen A3, the first observed damage was cracking of the linings at the corners of the doorway opening, however tracks pushing through linings did occur at larger drifts (0.71%). Cracking of linings from contact with track ends occurred at larger drifts for all specimens (locations 7, 8, 16, and 20). As this form of damage was seen consistently in all specimens, it is advised that future works could endeavour to solve this problem by either providing alternate junction details or cutting the top tracks short of the ends of walls and junctions.

The effect of the door opening, in this system, was that instead of damage beginning at the ends of tracks (location 7 or 20), it began through diagonal cracking of the linings at the corners of the door opening on either side of the wall (location 4 and 12). This occurred at similar drifts to the onset of damage in specimens A1 and A2. Damage to other locations, including cracking of the linings, was delayed to higher drifts (0.71%). The 2D particle tracking shows that the doorway specimen behaved significantly different to the specimens without openings. Specimens A1 and A2 deformed very little in-plane, with minimal sliding and rocking, however there was rocking due to out-of-plane displacements. For specimen A3, the plasterboard over the doorway cracked early on, and then either end of the wall (L- and Y-junction) moved as independent sections, with a greater degree of in-plane rocking and sliding. The difference between the behaviour of the specimens is shown in Figure 3.12 and illustrated by the comparative sliding of the long wall in Figure 3.13a, and the in-plane rocking of the 45° wall is shown in Figure 3.13b.

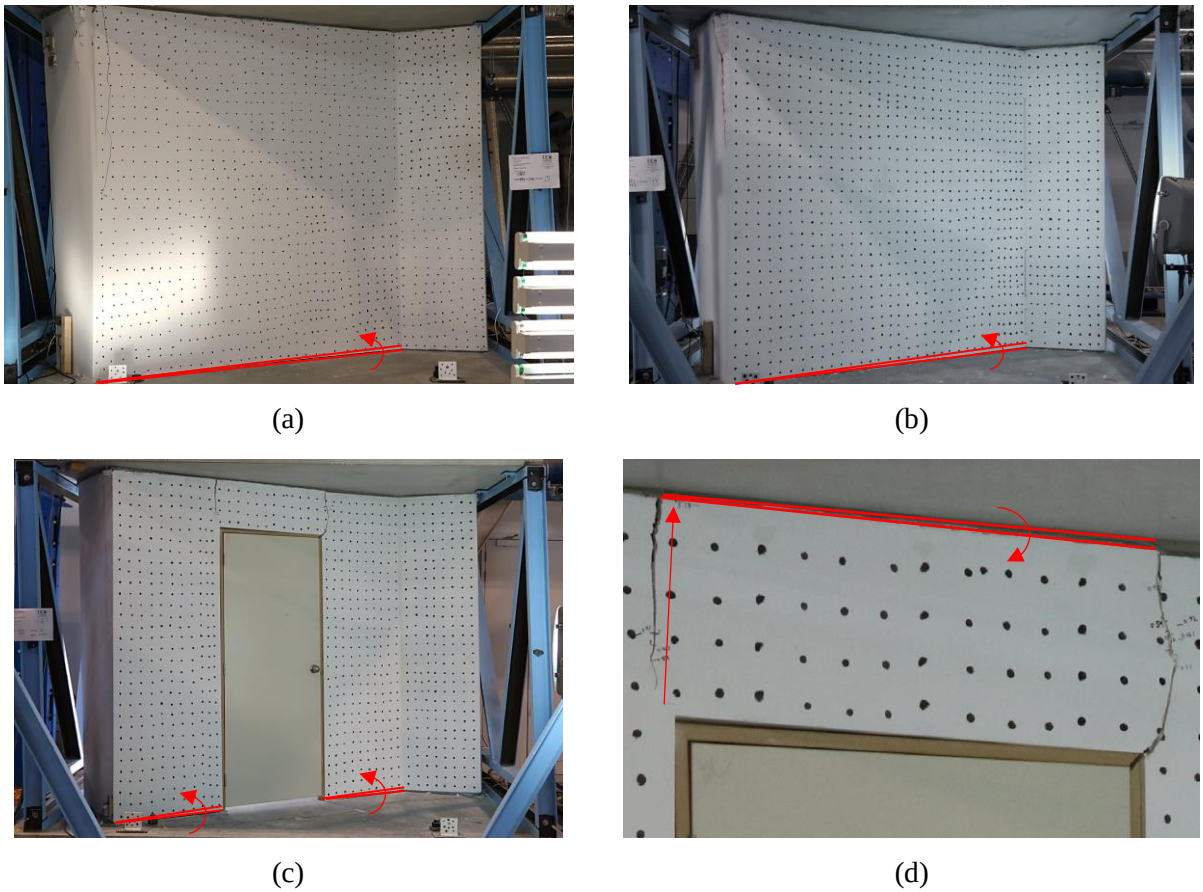

(a) (b)

(c) (d)

Figure 3.11 Visual comparison of the behaviour of specimens at the first peak of loading step 15 (4.44% drift): (a) specimen A1, (b) specimen A2, (c) specimen A3, and (d) specimen A3 showing sealant deformation above doorway.

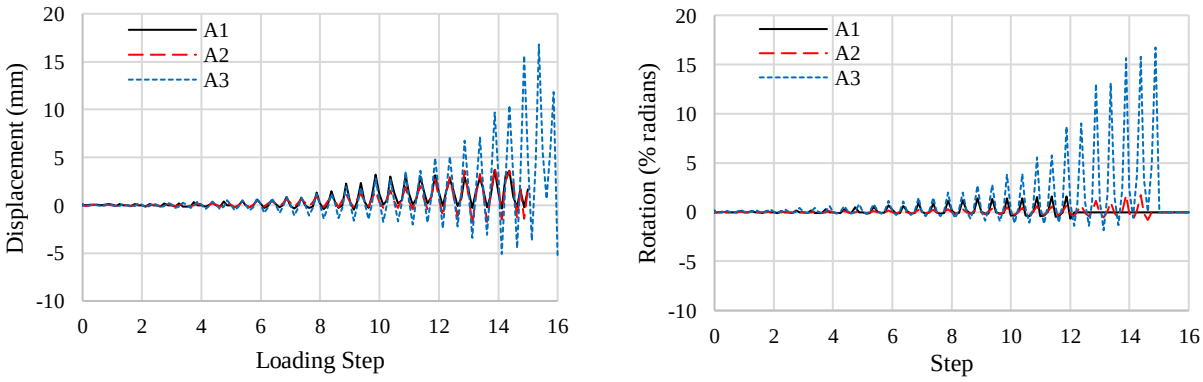

(a) (b)

Figure 3.12 Comparison of behaviour of partition specimens. (a) long wall in-plane sliding and (b) rotation of 45° return wall (*data missing for specimen A1 due to instrumentation failure).

It was intended to investigate the bi-directional behaviour by aligning the specimens at a 30° angle to the direction of loading (Figure 3.5a). As no tests have been conducted on identical specimen's in-plane, a direct comparison cannot be made. However, the specimen detailing is similar to the Davies *et al.*

(2011) specimen subgroup 1a commercial full-height slip track specimens, albeit with different return wall configurations. These specimens showed the onset of DS1 occurring at 0.26% in-plane drift, with no out-of-plane loading. And the median onset of damage for DS1 in this series of tests is 0.29% in-plane drift of the long wall and 0.17% out-of-plane drift along the long wall. Thus, it can be tentatively concluded that the out-of-plane demand did not significantly impact the fragility. Additionally, by comparing the drift at which the ends of the return walls damaged in each specimen (Table 3.7), it can be seen that for locations 9 and 21, this occurred at a similar level of in-plane displacement, even though the walls were at a different angle to the applied loading. This suggests that this form of damage is best correlated to the in-plane displacement of the wall.

Table 3.7 Summary of wallboard damage progression at wall ends

		DS2: Wallboard damage				
	Dir. Of	**Location**	**A1**	**A2**	**A3**	**Mean**
In-plane drift (%)	**90° wall**	9	0.58	0.58	0.58	0.58
	90° wall	17	1.14	0.81	1.59	1.18
	45° wall	21	0.41	0.57	0.79	0.59

Location 17 appeared to perform better in terms of wallboard damage (Table 3.7), which is suspected to be due to the unique Y-shape at the junction and the position of the top track anchors. As the top track anchors are removed from the long wall and the 45° angled wall close to the junction, the track is flexible out-of-plane at these locations. When the specimen is pushed in the positive direction (as defined in Figure 3.11), the top track in the 90° wall pushes at the end (location 17) and the 45° wall will push against the linings (between locations 15 & 19). As the 90° wall is being forced in the positive direction by both the track in the 45° wall and the track in the 90° wall the linings tend to slide and rotate in the direction of loading instead of cracking at location 17. The asymmetric behaviour at the Y-junction is illustrated in Figure 3.14, which shows the relative out-of-plane displacement between the lining and the top slab at the corners of the long wall (location 15/Y-junction). When the wall is pushed in the positive direction, if the long wall is to remain in position, there will be a positive relative out-of-plane displacement reading and vice versa. If the wall moves with the imposed displacement the value of out-of-plane displacement will be zero. This figure shows that the amplitude of the excursions is greater when the wall is pushed in the positive direction demonstrating that the top track is flexing, but when loaded in the negative direction the top track in the long wall is unable to flex giving smaller amplitude readings. As a result the 90° return slides preferentially when loaded in the positive direction to the negative, which is supported by Figure 3.15a and 15b; the long wall slides preferentially in the positive to the negative direction; and the 45° wall rotates when loaded in the positive direction more than the negative (Figure 3.13).

The out-of-plane behaviour at the Y-junction can be contrasted to the out-of-plane relative movement measured at the L-junction (Figures 3.14, shown in red). The movement at the L-junction showed preference to negative displacement for specimen A1 and A2, although specimen A2 was approximately symmetrical for the initial cycles. The data for specimen A3 was lost due to issues with the potentiometer during testing. The preference to negative displacement is attributed to how when loaded in the positive direction the top track of the 90° wall pushes through the end and thus the wall movement is only forced by the top track of the long wall, thus there is larger out-of-plane displacement measured as the wall attempts to remain stationary while the top slab moves. When loaded in the negative direction, the top track of the 90° return pushes against the top track of the long wall such that the wall is forced by both the movement of the 90° return top track and the long wall top track, and there is very little relative displacement between the top slab and the out-of-plane potentiometer.

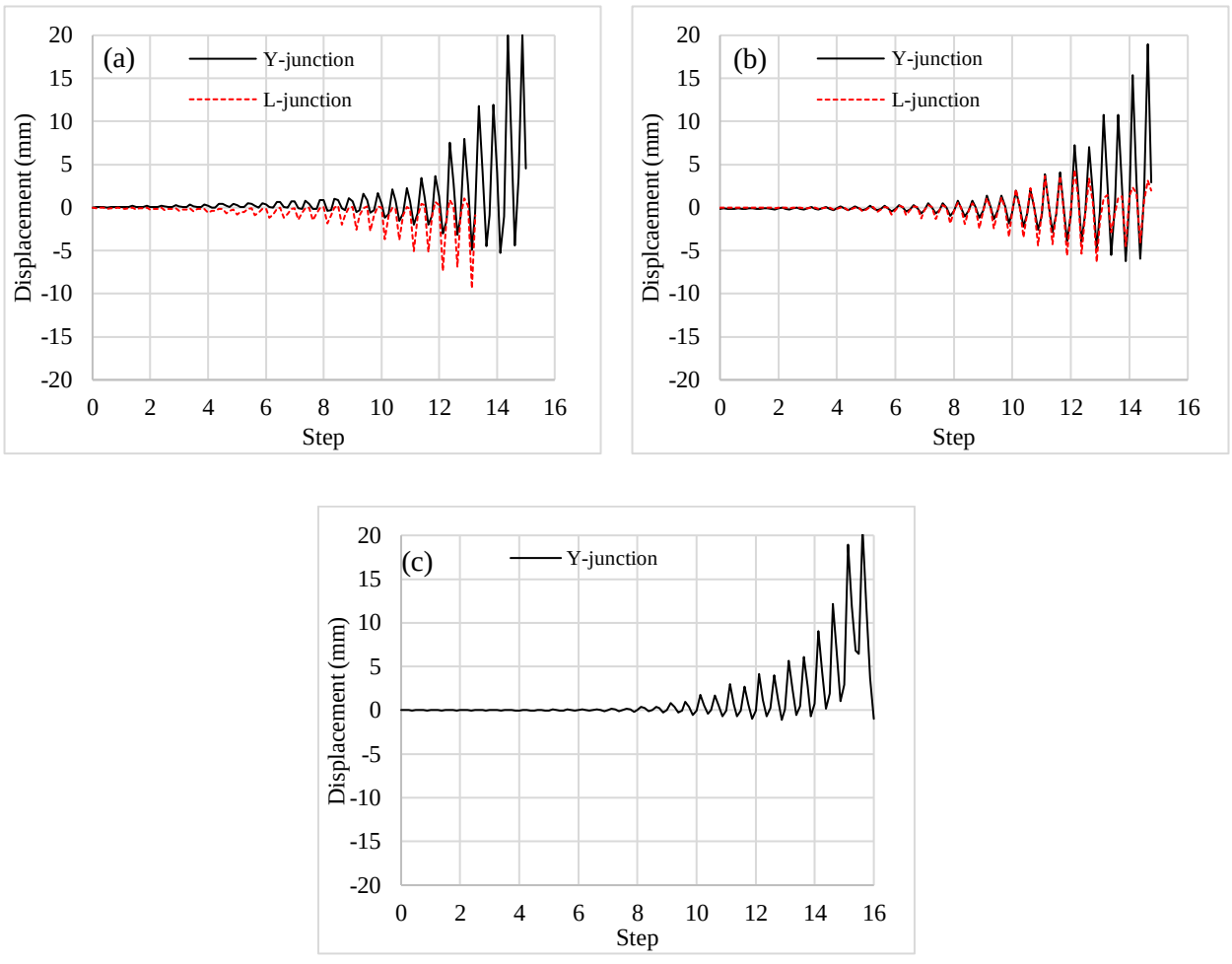

Figure 3.13 Out-of-plane relative displacement at the top of the long wall corners at the Y- and L-junctions for specimen (a) A1 (*data missing due to instrumentation failure) (b) A2, and (c) A3 (*data missing for L-junction due to instrumentation failure).

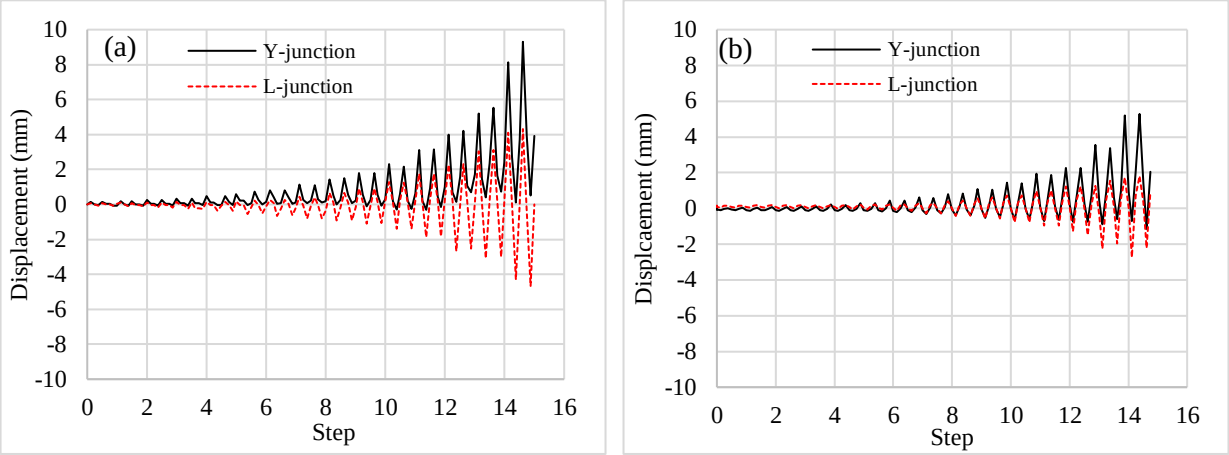

Figure 3.14 In-plane sliding of 90° return walls for specimens (a) A1 and (b) A2.

The effect of the angled return wall has been discussed above. It can also be seen that the junction between the 45° return wall and the main wall or 90° return wall experienced very little damage (location 2 and 19). DS1 initiated in this junction at 1%, 2.75%, and 1.96% drift for specimen A1, A2, and A3 respectively. The resistance to damage at this junction may be attributed to the rigidity of the joint itself. The joint was reinforced with 0.55 bmt galvanised 135° steel angles screwed to the studs at this location, so this may have reduced the differential movement between the wall panels. Figure 3.16c shows that the top track from the long wall and the 45° wall at the Y-junction have pushed hard up against the 90° wall top track at the end of the test. This represents the residual displacement of the joint after a negative loading peak excursion of 150 mm displacement or 6.2% drift. This shows how when loaded in the negative direction the top track of the 90° return wall pushes against the junction, which is attempting to remain stationary as the track anchors at this location are removed. The bending of the flanges at this location is attributed to the fact that the end studs are rigidly attached to the junction and therefore the linings are attempting to remain stationary, while the top track is forced by the anchor at this location to move. It is noted that if the anchor had been removed, this form of damage may have been avoided, and consequently damage at locations 15 and 19 reduced. The relative out-of-plane displacement between the 90° wall and the top slab, measured near location 19 is shown in Figure 3.16d.

No damage was observed along the field of the wall due to the out-of-plane displacements (other than to sealant). This is because the wall is relatively flexible out-of-plane. The influence of bi-directional behaviour becomes important at the junctions between neighbouring walls. The results showed that the behaviour of the wall specimens depends on the direction of loading. The results from the test on specimen A3 suggest that the walls deform as a unit rather than as separate walls. Therefore, bi-directional behaviour is deemed significant, even if its impact cannot be quantified by this test.

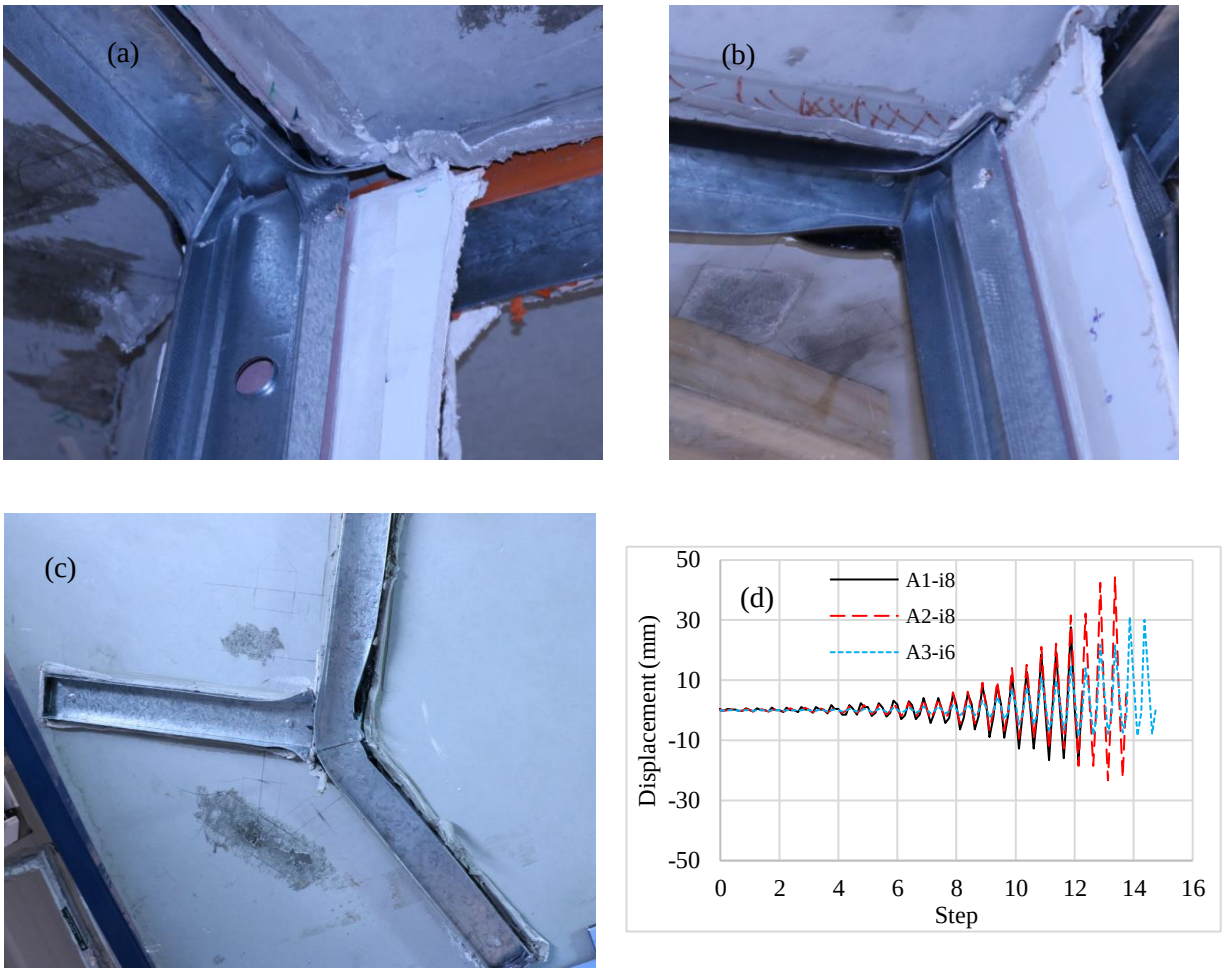

Figure 3.15 Damage to steel tracks at Y-junction for specimen (a) A1 (b) A2, and (c) A3. In particular showing bent flanges of 90° angled wall top track. (d) Shows the out-of-plane relative movement between 90° return wall at location 19 top corner and top slab for the three specimens (*data missing for specimen A1 due to instrumentation failure).

The sealant was applied over a 25mm gap at the top of the linings on all specimens. Sealant damaged at 0.36% (locations 10 and 20), 0.51% (locations 11 and 20), and 0.71% (location 10) in-plane drift for specimens A1, A2, and A3 respectively. The damage at locations 20 (the end of the angled return wall) was coincident with the cracking of the linings, whereas for location 10 the damage was in the sealant bond itself. The damage to the sealant first occurred around areas of high deformability (i.e. at the junctions) at drifts greater than 0.36%, whereas damage to sealant away from junctions typically occurred at higher drifts (0.7-1%) irrespective of whether this was in the primary length of the wall or in a return wall (i.e. in-plane or out-of-plane demand). Damage consisted primarily of separation at the lining interface initially, but for some parts of the wall, at higher drifts, the sealant remained bonded and ruptured in the middle of its depth. This suggests that the bond between the plasterboard and the sealant is very important for the seismic performance, as if the sealant is well-bonded, it can sustain higher demands. It was also noted that after the sealant had cured there was a significant number of defects in the bond to the plasterboard. Therefore, it is advised that careful quality control is maintained

when applying similar products, as defects in the bond may hamper the effectiveness of their fire and acoustic performance and reduce their ability to withstand seismic movement.

3.4.4 Fragility

The most common form of a seismic fragility function is the lognormal cumulative distribution function (CDF):

$$F_d(x) = P[D \geq d|X = x], \quad d \in \{1,2,\dots,Nd\}$$

$$= \phi\left(\frac{\ln(x/\theta_d)}{\beta_d}\right) \quad \textbf{(1)}$$

The experimental results from the test were used to produce a set of fragility curves for the damage states defined in Table 3.1. The three specimens were grouped together to represent the seismic fragility of a partition specimen with an arbitrary configuration (Figure 3.17) and compared with fragility subgroup 1a from the Davies *et al.* (2011) tests. These specimens have similar detailing to the typical NZ partition wall. The in-plane displacement of the primary section of the wall was used as the engineering design parameter (EDP) to correlate between damage and demand, according to Porter *et al.* (2007). The framework proposed by Porter *et al.* (2007) for experimentally determined fragility curves, Method A, was used (Equation 1 & 2), where M is the number of specimens tested to failure; i is the index of the specimens, $i \in \{1,2,\dots,M\}$; ri is the EDP at which damage was observed to occur in specimen i; x_m is the median; β is the random logarithmic standard deviation; and as less than five specimens were tested and the specimens were loaded according to the same protocol, an additional term β_u was introduced according to the guidelines in Porter (2018) and FEMA (2012). This additional term represents uncertainty that the tests represent actual conditions of installation and loading, or uncertainty that the available data are an adequate sample size to accurately represent the true random variable. The fragility parameters for each damage state are shown in Table 3.2.

$$x_m = exp\left(\frac{1}{M}\sum_{i=1}^{M} ln\, r_i\right) \quad \textbf{(2)}$$

$$\beta = \sqrt{\frac{1}{M-1}\left(\sum_{i=1}^{M}\left(\ln\left(\frac{ri}{x_m}\right)\right)^2\right)} \quad \textbf{(3)}$$

$$\beta' = \sqrt{\beta^2 + \beta_u^2} \quad \textbf{(4)}$$

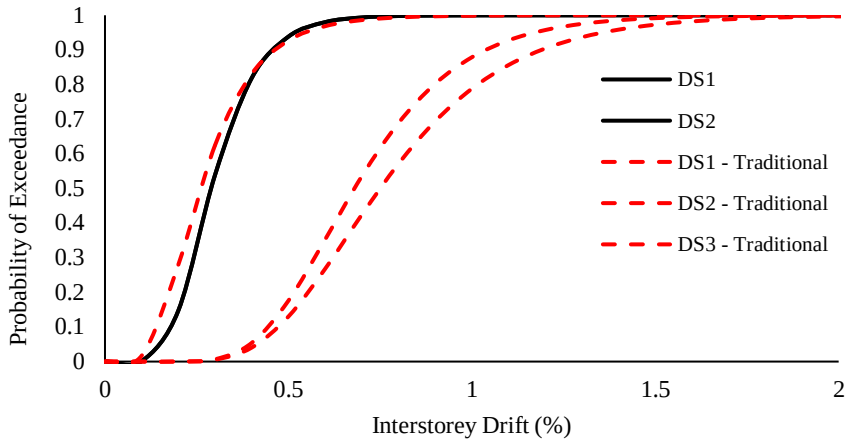

Figure 3.16 Seismic fragility curves superimposed with Davies *et al.* (2011) fragilities for subgroup 1a – full-height commercial slip tracks (red)

The fragility parameters that result from this experiment are not necessarily directly relatable to previous tests. This is because the damage states do not imply the same loss functions. A loss function represents the probable loss associated with a component in the event of an earthquake for each damage state of the component. The repair costs of partitions have been calculated previously, as in Taghavi and Miranda (2003). These estimates are based on the three distinct repair actions: (1) tape and finish and paint with roller on both sides; (2) remove damaged boards on both sides, replace boards, tape and finish, and paint with roller on both sides; and (3) remove damage boards, remove damaged metal frames, replace framing, replace gypsum boards on both sides, tape and finish, and paint with roller on both sides. The estimates for repair cost are made assuming that finishing, replacement of gypsum board, and replacement of framing is required at every location. In particular, for this series of experiments, the wallboard damage was highly localised, and the point at which DS2 has been reported to initiate does not imply the wallboard in every location requires replacement. Therefore, if a loss assessment was conducted using conventional loss functions, it is expected that they would overestimate losses.

3.4.5 Force Displacement Behaviour

The first two specimens, A1 and A2, were identical, but their hysteretic responses were significantly different. It can also be seen that the damage progression in A1 was significantly different from A2 (Table 3.4 and 3.5). The capping forces the two loading directions varied in both specimens, but no significant bias can be seen in either direction. The average capping force in the positive and negative

directions for the three specimens are 9.83 kN at 2.2% and 9.79 kN at 2.19% respectively (Table 3.8). The difference in behaviour may be attributed to a number of factors including variations in material properties and construction quality.

Table 3.8 Ultimate loads

	-ve		+ve	
Specimen	**Max load**	**Drift**	**Max load**	**Drift**
A1	7.59	2.09	9.58	2.14
A2	10.57	2.25	10.37	2.27
A3	11.20	2.25	9.53	2.17

3.4.1 Energy Absorption

The equivalent viscous damping was determined at each cycle according to equation 5 (Calvi *et al.* 2007), and is shown in Figure 3.19b. Where A_h is the energy absorbed during a complete cycle, F_m is the maximum force experienced in the cycle, and Δ_m is the maximum displacement experienced in the cycle. The energy absorbed by the specimen is defined as the area under the force-displacement curve. The hysteretic curves shown in Figure 3.18 were integrated using the trapezium method for each increment in data. The energy dissipated in the two cycles of loading at each amplitude were averaged to attain the average energy dissipation at each step (Figure 3.19a).

$$\xi_{hyst} = \frac{A_h}{2\pi F_m \Delta_m} \quad \textbf{(5)}$$

The data is not available for the small cycles of specimen A1, as there were some issues with the loading and instrumentation setup-early on in the testing. Therefore, calculation of energy dissipation during these early cycles is uncertain. Data is shown for loading cycles 11 to 15, which corresponds to 1.15 to 4.44% drift in the direction of loading.

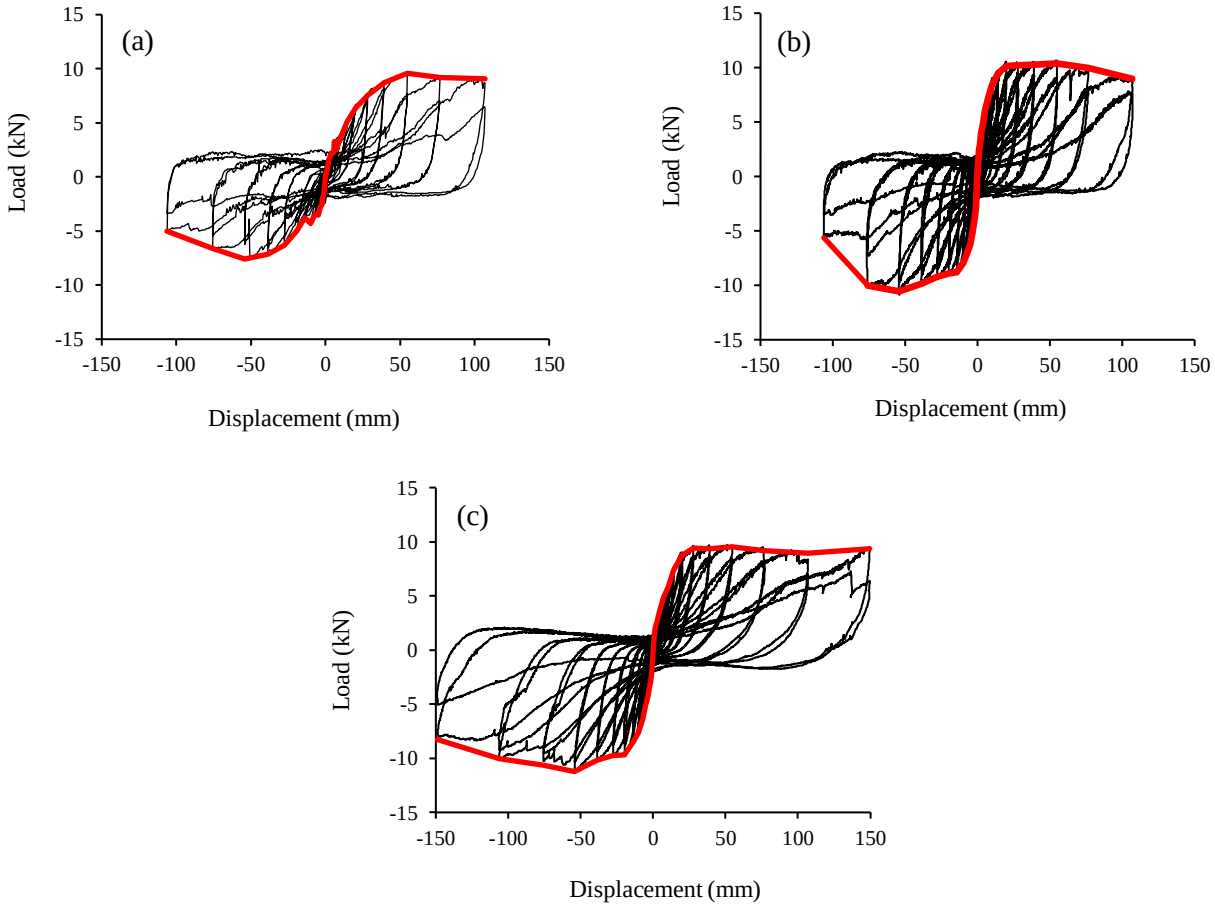

Figure 3.17 Hysteresis results and backbone curves for (a) Specimen 1, (b) Specimen 2, and (c) Specimen 3

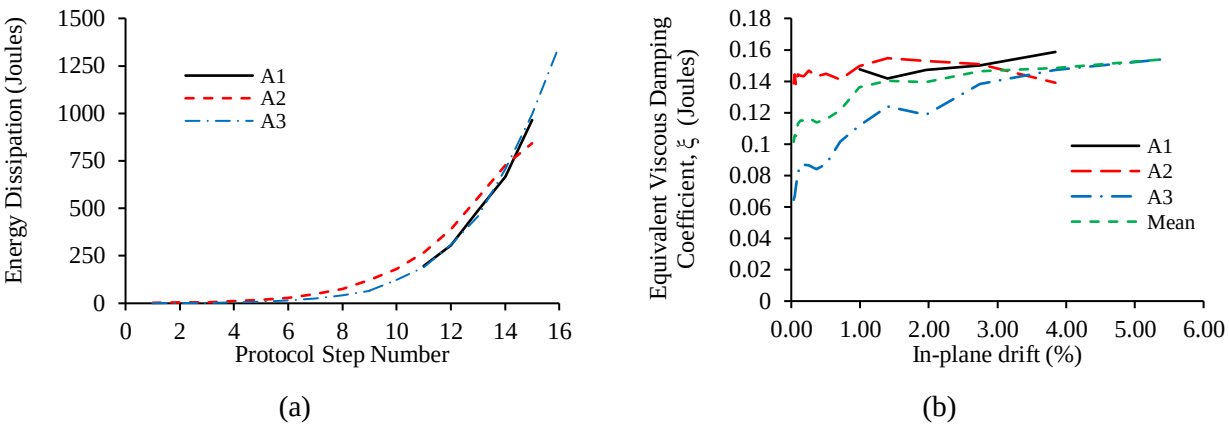

(a) (b)

Figure 3.18 (a) Energy dissipation during each step; (b) Equivalent viscous damping coefficient for each cycle versus in-plane drift demand

3.4.2 Numerical Model Calibration

For numerical investigation purposes, the experimental results were used to calibrate a hysteretic model. Because of the significance of pinching, the hysteresis rule used to describe the behaviour of the

partition specimens was the Wayne Stewart degrading stiffness model (Figure 3.20) available in Ruaumoko 2D [Carr, 2008]. The key parameters of the model are described in Table 3.9.

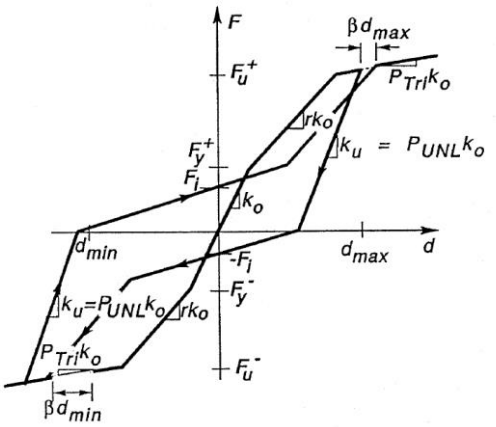

Figure 3.19 Wayne-Stewart Degrading Hysteresis model available in Ruaumoko 2D (Carr 2008)

The first step in calibrating the Wayne Stewart hysteretic model is to determine the backbone curves from the experimental data. The backbone curves were generated by tracking the force associated with the maximum displacement excursions. The idealized force-displacement backbone curve is characterized by eight points, four positive and four negative. The selection of these points is guided by calculating the first derivative of the backbone curve (tangent stiffness). The tri-linear factor beyond the ultimate force is taken as zero for all specimens and the strength degradation was modelled as dependent on ductility. The parameters were then calibrated to each specimen depending on the shape of the curves and the relative energy dissipation between the analytical and experimental results. The final calibrated model factors are shown in Table 3.9, and the corresponding analytical hysteretic curves are plotted against the experimental results in Figure 3.21. A final model representing the mean behaviour across the specimens is illustrated in Figure 3.21d.

Table 3.9 Calibrated Wayne-Stewart Hysteretic model parameters for each specimen

Key Parameters		Specimen			Mean
		1	2	3	
Ko	Stiffness	0.83	1.37	1.10	1.10
PTRI	Tri-linear factor beyond ultimate force or moment	0.00	0.00	0.00	0.00
FU+	Positive ultimate force	9.58	10.37	9.53	9.83
FU-	negative ultimate force	-7.59	-10.57	-11.20	-9.79
M1	ductility at start of degradation	1.74	4.67	2.54	2.98
M2	ductility at finish of degradation	2.84	6.27	5.79	4.97
M3	final fraction of strength	0.80	0.68	0.86	0.78
M4	ductility at 1% of initial strength	-	-	-	-
FY	yield force or moment (>0):	3.03	5.08	5.57	4.56
FI	Intercept force or moment (>0):	1.50	1.50	1.50	1.50
R	Bi-linear factor (<0.9) or Ramberg-Osgood Factor (>1)	0.25	0.32	0.23	0.26
PUNL	unloading stiffness factor (>1):	1.50	1.50	1.50	1.50
GAP+	Initial slackness in positive axis ,Diagonal gap (>0):	0.00	0.00	0.00	0.00
GAP-	Initial slackness in negative axis, Diagonal gap (<0):	0.00	0.00	0.00	0.00
BETA	Softening factor (>=1):	1.03	1.08	1.03	1.05
ALPHA	Pinch power factor (<=1):	0.55	0.60	0.55	0.57
IOP	0 for the unmodified loop, 1 for the modified loop:	1.00	1.00	1.00	1.00

Note: Factors M1 to M4 are parameters corresponding to strength degradation type 1, where strength degradation depends on the ductility

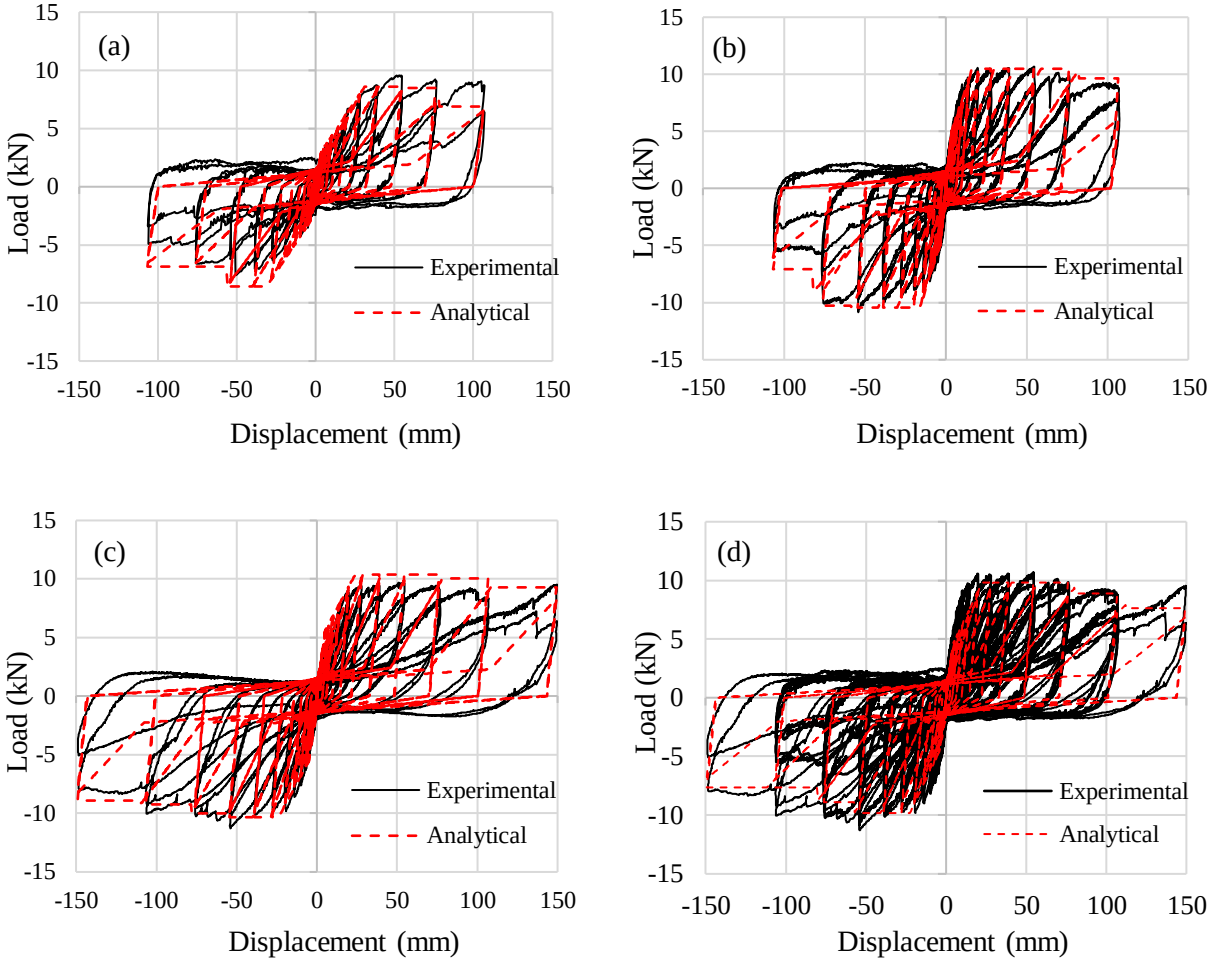

Figure 3.20 Wayne Stewart hysteretic model fit of experimental hysteresis; (a) Specimen A1, (b) Specimen A2, (c) Specimen A3, (d) All specimens with mean parameter model fit

3.5 Conclusions

Three specimens with partly sliding detailing, consisting of top tracks that are not bolted at intersections, were subjected to quasi-static cyclic testing. The specimens were aligned at 30° and the y-shaped configuration meant bi-directional behaviour could be examined. The specimens included an acoustic/fire sealant. Although the top track anchors were specified to be removed within 600 mm of wall intersections, a construction error was made whereby a single top track slab to concrete anchor was left in at the three-way wall junction (Figure 3.4). Despite this error, the experimental testing was deemed worthwhile since such errors will also occur in practice and because the behaviour of the wall can be examined with this fixing in mind.

In addition to providing drift capacities, the force-displacement behaviour has been reported, energy dissipation computed, and parameters of the Wayne-Stewart hysteretic model fitted to the test results. This information may be useful for those interested in undertaking refined analyses of partition walls.

The main findings from this experimental programme are summarised as follows:

- Damage was first observed as cracking of the wallboard at the wall ends, at external junctions, and propagating from the corners of the door opening. The onset of DS1 and DS2 occurred simultaneously at a median in-plane drift of 0.29% and damage state DS3 was not observed until after the linings had been removed at the end of the test, which indicates that the DS was triggered during the testing at an unknown drift level.
- The specimen with the door opening (specimen A3) behaved differently to the plane specimens (specimens A1 & A2). Damage began as cracking of the wallboard propagating from the corners of the doorway, at similar drift levels to specimens A1 and A2. Following the separation of the wallboard above the lintel, the L- and Y- junctions behaved as independent wall sections, and damage elsewhere was delayed.
- No damage was observed along the field of the wall due to out-of-plane displacements (other than to sealant). This is because the wall is relatively flexible out-of-plane. The results showed that the behaviour of the wall specimens depends on the direction of loading and that the walls deform as a unit rather than separately. Therefore, bi-directional behaviour is deemed significant, even if its impact cannot be directly quantified by this test.
- Damage to sealant first occurred around areas of high deformability (i.e. at the junctions) at drifts greater than 0.36%. Whereas damage to sealant away from junctions typically occurred at higher drifts (0.7-1%) irrespective of whether this was in the primary length of the wall or in a return wall (i.e. in-plane or out-of-plane demand). Results suggest that the bond between plasterboard and sealant is important for the seismic performance. It was also noted that after the sealant had cured there was a significant number of defects in the bond to the plasterboard.

Therefore, it is advised that careful quality control is maintained when applying similar products, as defects in the bond may hamper the effectiveness of their fire and acoustic performance and reduce their ability to withstand seismic movement.

3.6 Acknowledgements

The authors gratefully acknowledge the funding support offered by The International Collaborative Research program of the Disaster Prevention Research Institute, Kyoto University under Project Number 28W-03 (PI: Timothy Sullivan), the NZ Property Council, and Quake Centre. This project was also partially supported by QuakeCoRE, a New Zealand Tertiary Education Commission-funded Centre. This is QuakeCoRE publication number 0457'. Thanks also to the industry partners; RONDO; Winston Wallboards; Dunning Thornton Consultants; and Holmes Consulting.

4. JOURNAL PAPER ON EXPERIMENTAL STUDY OF THE SEISMIC PERFORMANCE OF PLASTERBOARD PARTITION WALLS WITH SEISMIC GAPS

This chapter presents the experimental testing work on the partition walls with seismic gaps specimens and is comprised of a journal paper published on said topic in the Bulletin for the New Zealand Society of Earthquake Engineering (BNZSEE) (Mulligan *et al.* 2020b). For construction drawings of the specimens and further information on damage observations and potentiometer readings refer to Appendix C.

EXPERIMENTAL STUDY OF THE SEISMIC PERFORMANCE OF PLASTERBOARD PARTITION WALLS WITH SEISMIC GAPS

Joshua G. Mulligan , Timothy J. Sullivan and Rajesh P. Dhakal

(Submitted *September 2019*; Reviewed *October 2019*; Accepted *February 2020*)

4.1 Abstract

It is now widely recognized that the performance of non-structural elements is crucial to the performance of building systems during earthquakes. Field surveys and experimental studies have shown that light steel or timber framed plasterboard partition walls are particularly vulnerable. The objective of this study is to investigate the seismic performance of a novel seismic gap partition system with angled return walls under quasi-static cyclic loading applied obliquely and to investigate the benefits of using acrylic gap-filler in the seismic gaps. Two specimens were tested: a steel stud specimen and a timber stud specimen. Observed drift capacities were significantly greater than traditional plasterboard partition systems. Equations were used to predict the drift at which damage state 1 (DS1) and damage state 2 (DS2) would initiate. The equation used to estimate the drift at the onset of DS1 accurately predicted the onset of plaster cracking but overestimated the drift at which the gap filling material was damaged. The equation used to predict the onset of DS2 provided a lower bound for both specimens and also when used to predict results of previous experimental tests on seismic gap systems. The gap-filling material reduced the drift at the onset of DS1, however, it had a beneficial effect on the re-centring behaviour of the linings. Out-of-plane displacements and return wall configuration did not appear to significantly impact the onset of plaster cracking in the specimens.

4.2 Introduction

It is now widely recognized that careful consideration of the performance of non-structural elements is crucial for the performance of buildings during earthquakes. Limiting damage to non-structural elements is vital to maintain the continuity of emergency and recovery services, to reduce the likelihood of injury or death, to prevent loss of building function, and to limit the direct and indirect economic losses resulting from earthquake events. Taghavi and Miranda (2003) and Khakurel *et al.* (2020) have shown that non-structural elements comprise the majority of investment in commercial buildings (Figure 4.1) and that interior construction, which includes partitions, doors, wall finishes, ceilings, and floor finishes, comprises 20-30% of the non-structural component cost. Partition walls, also known as drywalls, have been shown to significantly contribute to total earthquake losses (Bradley *et al.* 2009, Dhakal *et al.* 2016). Whitman *et al.* (1973) found that in the 1971 San Fernando Earthquake, for buildings in earthquake intensity (MMI) zones VI, VII, and VIII, the damage to partitions was approximately 90, 65, and 50% respectively of the total cost of damage to buildings. They concluded that improving the seismic performance of interior partitions would be one of the most effective ways to reduce the seismic losses in buildings subjected to MMI VI earthquakes (Whitman *et al.* 1973). This is because partition walls are particularly susceptible to earthquake damage, with the onset of damage initiating at low interstorey drifts of approximately 0.35% (Davies *et al.* 2011). This level of interstorey

drift may be imposed by low intensity ground motions with small return periods and this implies frequent repairs after relatively small earthquake events or aftershocks, resulting in significant financial loss (Dhakal *et al.* 2016, Arifin *et al.* 2017). This was observed in many buildings following the 4th September 2010 Darfield (Canterbury) earthquake, where aftershocks caused new cracks on walls and internal linings to develop and existing cracks to widen and extend (Dhakal 2010). Following the 22 February 2011 Christchurch Earthquake Baird *et al.* (2014) suggested that the repeated damage to partitions from aftershocks, which exceeded the serviceability limit state, implies that current code requirements do not set a high enough threshold for damage avoidance in order to minimize economic loss.

The earliest experimental investigations on gypsum lined walls, were focused on the load-deformation of shear walls designed to resist lateral loads (Freeman 1971, Rihal 1980, Adham *et al.* 1990). However, in order to inform the calibration of models in performance-based earthquake engineering, modern studies began to focus on the damage and repair cost of non-structural partition systems. Lee *et al.* (2007) tested full-scale partitions with lightweight steel framing according to typical Japanese configurations and estimated a damage-repair cost relationship. Overall, the specimens in this study were damage free up to 0.25% interstorey drift. Restrepo and Bersofsky (2011) tested partition wall specimens built according to typical US configurations using the damage state (DS) definitions as provided by Taghavi and Miranda (2003). These damage state definitions are as follows: DS1, cracking in plaster and paint; DS2, damage to drywall panels; and DS3, damage to framing. For the conventional steel stud partitions tested by Restrepo and Bersofsky (2011) DS1, DS2, and DS3 occurred at drifts of 0.3%, 1.0%, and 3.0% respectively.

Although significant research has been conducted on the behaviour of non-structural partition walls subject to in-plane deformations, their behaviour when subjected to out-of-plane displacements has not been studied previously. Previous studies have mainly focused on the out-of-plane behaviour of partitions when subject to acceleration (Davies *et al.* 2011, Jenkins *et al.* 2016). Petrone *et al.* (2016) conducted quasi-static tests on a single vertical "strip" of wall. This carries the assumption that the wall is wide enough in order to neglect the influence of adjacent return walls. In addition, the out-of-plane displacements were applied in a six-point bending scheme and therefore simulated displacements induced by out-of-plane accelerations rather than interstorey drift.

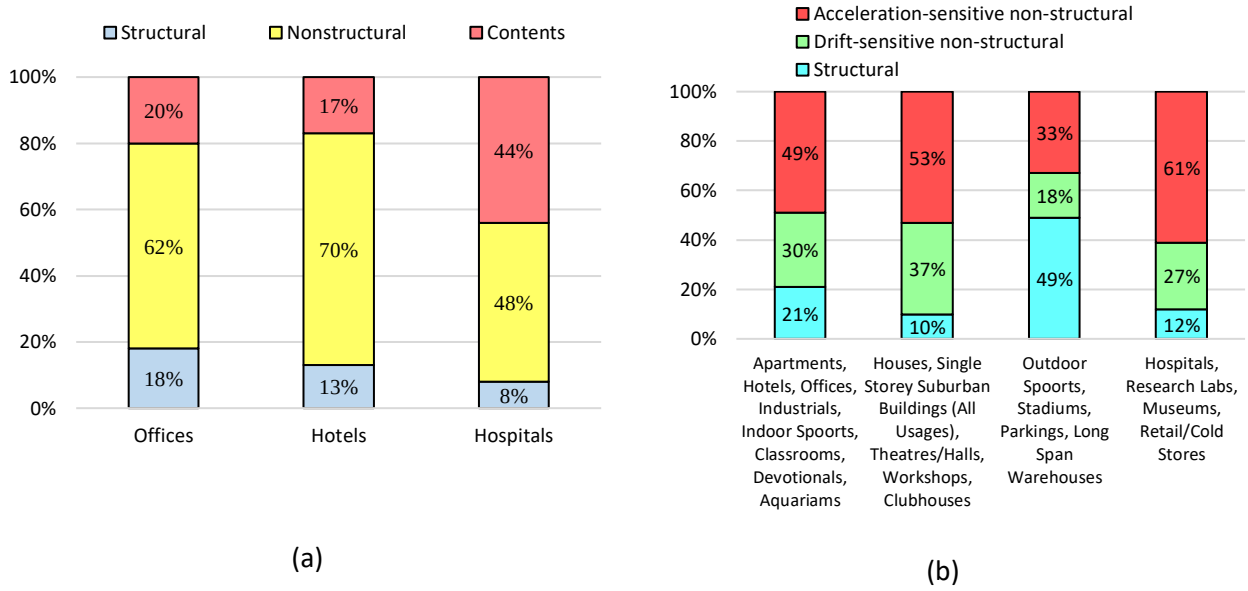

Figure 4.1 Building construction cost distribution of different buildings from (a) Taghavi and Miranda (2003) and (b) Khakurel *et al.* (2020)

Davies *et al.* (2011) conducted an extensive series of experiments into the seismic performance of plasterboard partition walls. The authors tested 50 full scale partition walls in 22 different configurations under both quasi-static and dynamic loading and generated data regarding the in- and out-of-plane seismic behaviour. Variables included return wall configurations; partial-height and full-height specimens; alternate junction details; connectivity of studs, tracks, and sheathing; and bookshelf attachments. This data was used to produce a set of fragility parameters, useful for implementation in Performance Based Earthquake Engineering (PBEE) analysis of buildings. For the development of the fragility parameters, the authors used damage states previously defined by Taghavi and Miranda (2003). For the test specimens most like NZ commercial partitions, the mean drift associated with DS1, DS2, and DS3 was 0.26%, 0.68%, and 0.75% respectively. It should be noted that DS3 was triggered at relatively low drifts. This was due to failure in the track to concrete fasteners, not observed in the tests of Restrepo and Bersofsky (2011) or Lee *et al.* (2007).

Included within the test series of Davies *et al.* (2011) were some novel details for improving the performance of partitions, including a 'sacrificial corner bead' system and a flexible track system. A similar system to this flexible track system was also tested in Mulligan *et al.* (2020a). Other systems have been proposed in the literature for the improvement of the seismic performance of partitions: including a sliding/frictional system developed by Araya-Letelier and Miranda (2012), and a seismic gap system tested in several studies (Lee *et al.* 2007, Magliulo *et al.* 2014, Tasligedik *et al.* 2015, Pali *et al.* 2017, 2018). The seismic gap system tested by Tasligedik *et al.* (2015) offered a DS1 drift capacity of over 2.0%.

The seismic gap specimen details suggested by Tasligedik *et al.* (2015) included fire and non-fire rated alternatives. These details are as shown in Figure 4.2. At the horizontal boundary the external studs were attached to the frame but not to the linings; and an additional stud was provided near the external stud to which the linings were attached so that the linings and internal framing are free to slide within the bottom and top tracks. As the specimens tested in by Tasligedik *et al.* (2015) did not include any specimens with return walls and displacements were applied in-plane only, these details have not been verified for their out-of-plane performance or considering the interaction with return walls. The objective of this study therefore is to investigate the behaviour of partition systems with seismic gaps in configurations that have not previously tested: as an internal partition, without bounding structural members; in a unique y-shape configuration; with one return wall at a 45° angle; and under a quasi-static cyclic loading protocol applied obliquely. In addition, the impact of using a filler material in the seismic gaps is to be investigated.

4.3 Experimental Tests In This Study

4.3.1 Specimen Design

The specimen designs in this study are a variation on the designs detailed in Tasligedik *et al.* (2015), further adapted in this work following discussions and proposals from an industry collaborator. The details proposed by Tasligedik *et al.* (2015) were for infill walls and thus had to be converted to equivalent details for internal partitions walls with no structural boundaries. In particular, the junction details were modified by connecting tracks to the returns and friction fitting the studs within these. Top and bottom track anchors were removed in the proximity of junctions at some locations to allow the tracks to bend. The wallboards were also fitted hard to the floor. The intermediate top and side edges at gap locations were finished with GIB® Goldline® L-Trim. The gaps were also half-filled with GIB® Gap Filler in order to assess the benefits of using filler to improve the aesthetic as an alternative to negative detailing.

The configuration chosen to provide a baseline for the specimens was a fire rated partition typology selected from GIB Fire Rated Systems® (Winstone Wallboards 2012) with a 60 minute fire-resistance rating (GBS60). Two specimens were constructed: a steel stud specimen with a total nominal horizontal gap size of 10 mm provided by two nominal 5 mm gaps at each end (details shown Figures 4.3, 4.5, and 4.6); and a timber stud specimen with a total nominal horizontal gap size of 25 mm provided by two nominal 10 mm gaps at each end and an additional nominal 5 mm gap in an intermediate joint (details shown in Figures 4.4, 4.5, and 4.6). The steel stud specimen framing consisted of 92 x 0.55 bmt studs, 92 x 0.5 bmt stud tracks, and 92 x 1.15 bmt deflection head tracks. The timber stud specimen's framing materials were identical however 90 x 45 timber studs were used instead of 92 x 0.55 bmt steel studs. For both specimens the framing was sheathed with 13 mm GIB Fyreline® connected to the framing

with 25 mm x 6 g GIB Drywall Self Tapping Screws® at 300 mm centres up each stud. Bottom and top tracks were fixed to the top and bottom floor slabs with HILTI HUS3-H 8 x 55 screw anchors at 600 mm centres and were left out at some locations as shown.

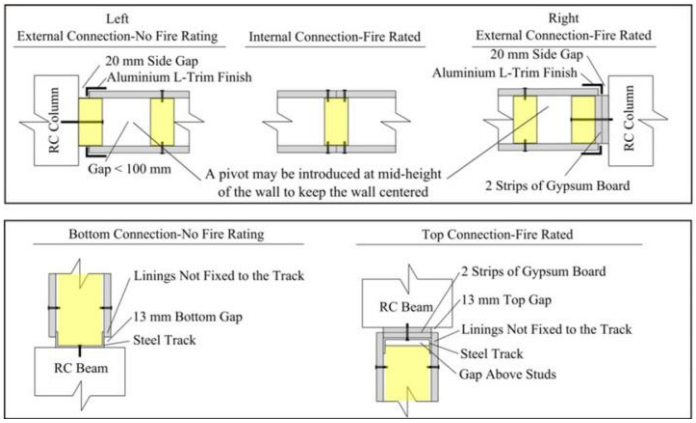

Figure 4.2 Details of low damage timber or steel framed specimens from Tasligedik *et al.* (2015)

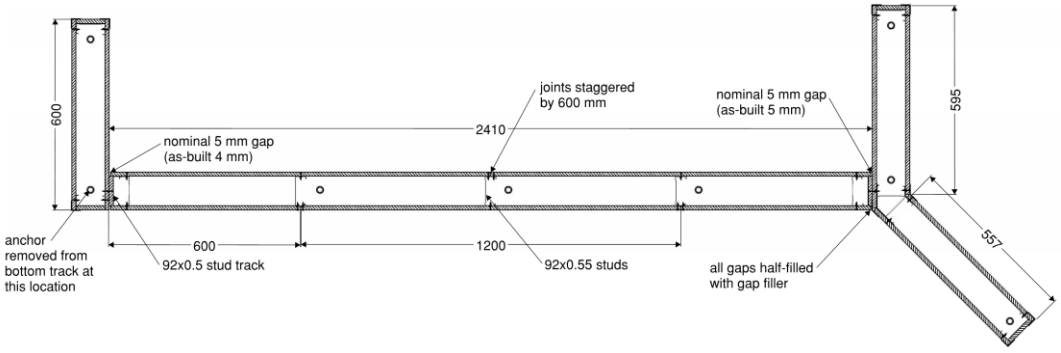

Figure 4.3 Specimen 1 plan - steel stud wall with no intermediate joints.

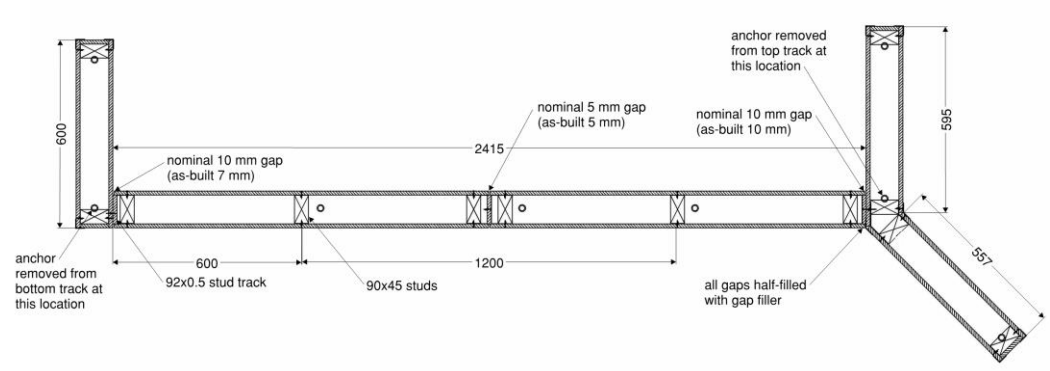

Figure 4.4 Specimen 2 plan – timber stud wall in steel tracks with intermediate joints.

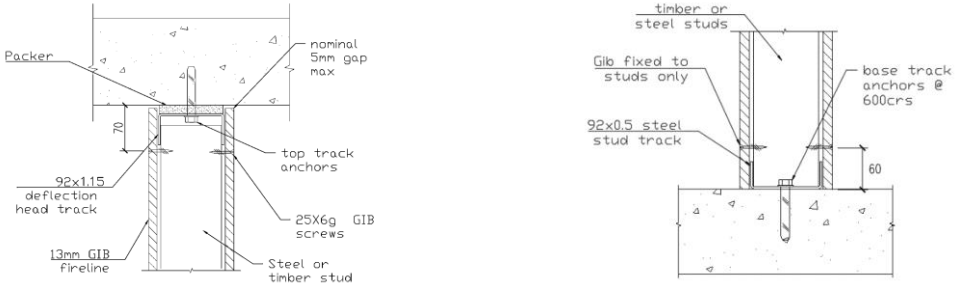

(a) (b)

Figure 4.5 (a) Top slab to track connection (b) Bottom slab to track connection.

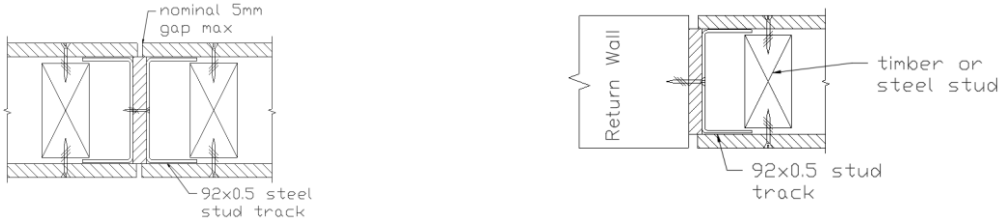

(a) (b)

Figure 4.6 Details of modifications to Tasligedik *et al.* (2015) low damage system (a) intermediate joint detail for Specimen 2 (b) Studs fit within steel tracks at junction for both specimens.

4.3.2 Anticipated Capacity

The in-plane behaviour of the specimens can be predicted assuming that the framing is free to slide within the tracks and that the linings behave as rigid bodies (Figure 4.7). The anticipated in-plane drift capacity for each specimen can be calculated from Equations 1 and 2 as per the deformation behaviour shown in Figure 4.7.

$$D_1 = \frac{\Delta_{Gh}}{h_c} \times 100\% \quad \textbf{(1)}$$

$$D_2 = D_1 + \frac{\Delta_{Gv}}{L} \times 100\% \quad \textbf{(2)}$$

Where D_1 and D_2, are the design lower bound interstorey drift capacity for the damage state 1 and 2 respectively, Δ_{Gh} is the sum of the horizontal gaps along the wall, Δ_{Gv} is the sum of the vertical gap along the wall between the linings and the top and bottom floors, h_c is the clear height between floors (2405 mm), and L is the largest length of panel between joints along the wall. As there is a vertical gap between the linings and floor slab, the linings are able to undergo an additional interstorey drift before a strut will form. It is expected that wallboard damage will take place after the drift calculated from Equation 2 is reached, acknowledging that some of this capacity may be used up by vertical floor

deflections. If significant floor deflections are expected this should be accounted for by reducing Δ_{Gv} accordingly. For specimen 2 the length of panel between joints is reduced due to the presence of an intermediate joint and so it is anticipated that this will increase the drift at which DS2 occurs relative to a wall with gaps only at the ends. The specified gap sizes varied slightly from the design drawings, highlighting the need to allow for construction tolerances. Only the design drift capacities calculated using the as-built dimensions are shown are shown in Table 4.1.

As the plasterboard linings is not directly fixed to the steel tracks at the top or bottom, it is predicted that the plasterboard and internal framing will be free to rotate as the top boundary is displaced. As the mid-height of the wall is composite steel and gypsum board it will be significantly stiffer out-of-plane compared with the top and bottom ends of the wall. Therefore, it is anticipated that the gypsum board and the steel tracks will deform locally at the ends of the walls allowing the internal frame to rotate. The predicted large displacement behaviour of the wall is shown in Figure 4.8. The out-of-plane behaviour will also be influenced by the return walls and the bending of the tracks. However, the interaction between walls loaded out-of-plane and walls loaded in-plane is complex and difficult to simplify by mechanistic models.

Table 4.1 Estimated lower bound drift capacities, Di, from as-built gap sizes.

Specimen	Δ_{Gh} (mm)	Δ_{Gv} (mm)	D_1 (%)	D_2 (%)
1 - Steel Stud	9	5	0.37	0.58
2 - Timber Stud	22	10	0.91	1.75

4.4 Experimental Test Setup

4.4.1 Testing Frame

The walls were tested in racking in order to simulate the seismic loading experienced by internal partition walls in commercial buildings. The testing support frames (Figure 4.9) were hinged at the top and the bottom in the direction of actuator movement, with diagonal braces to provide stability while the actuator was not attached. The frames were constructed of steel 125 PFC members. The top and bottom concrete boundaries were 120 mm thick reinforced concrete. This slab was selected in order to simulate the most typical boundary conditions and flooring systems in real buildings. The plan dimensions of concrete space available to construct the partitions was 3175 mm by 2100 mm, and the clear height was 2405 mm. The response of the bare frame (Figure 4.10) was approximately linear with a stiffness of 10.1 N/mm.

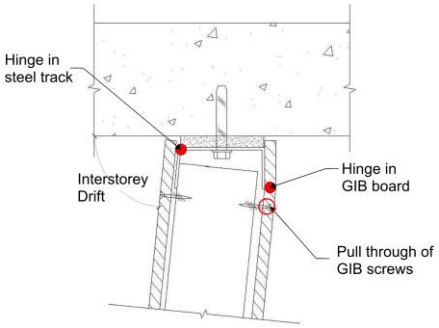

Figure 4.7 Predicted out-of-plane damage at large drift levels at the top and bottom interfaces.

4.4.2 Experimental Program

The specimens were tested according to the FEMA 461 deformation-controlled unidirectional quasi-static cyclic protocol (Applied Technology Council 2007). The protocol was calibrated based on the results of previous in-plane tests for standard partition detailing using the tests by Restrepo and Bersofsky (2011). The estimated drift for DS1 was 0.3% and the target maximum drift was 5%. Two cycles are performed at each loading amplitude. The amplitude of each step is 1.4 times the amplitude of the preceding step.

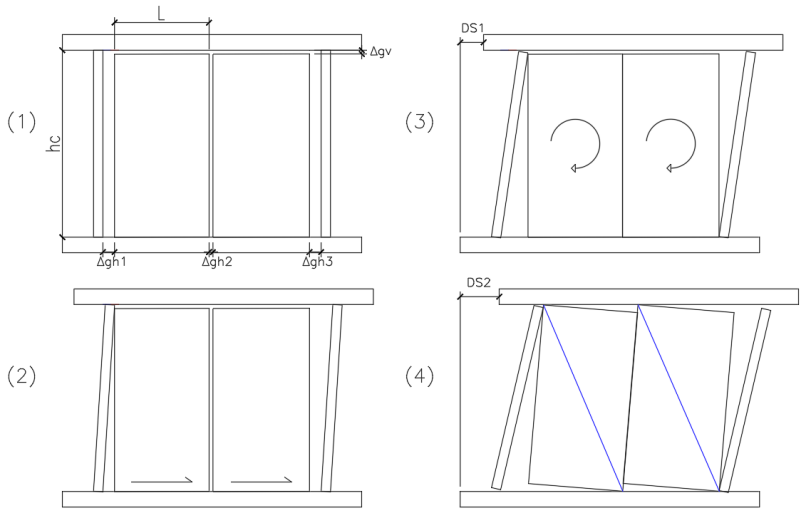

Figure 4.8 Predicted in-plane behaviour of specimens demonstrating estimated lower bound drift capacities for DS1 and DS2

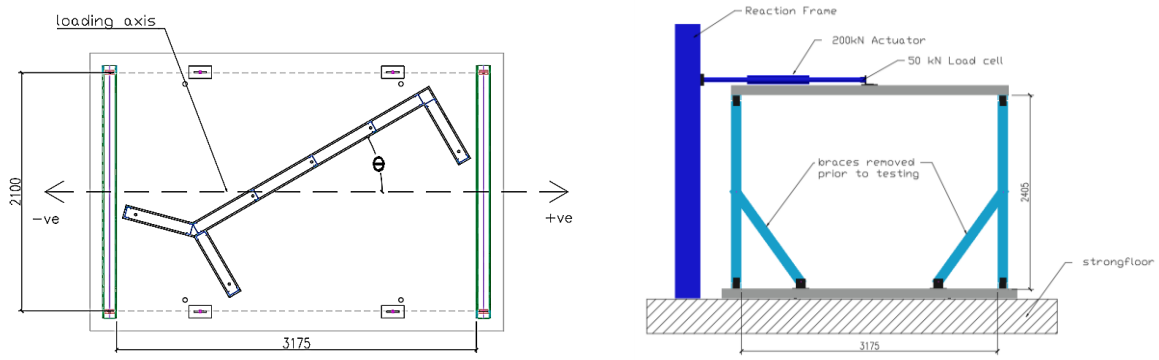

(a) (b)

(c) (d)

Figure 4.9 (a) Plan of testing frame (mm); (b) Elevation of testing frame (mm); (c) Photograph of setup; (d) Photograph of setup with specimen 1 installed.

A total of sixteen loading steps were performed, up to a magnitude of 6.21%, which corresponds to a maximum in-plane drift of 5.09% for walls angled at 35° (Figure 4.11). To assess the impact of bidirectional demands on fragility, the wall specimens were aligned at an angle of 35° to the loading direction, as shown in Figure 4.9a.

4.4.3 Data Acquisition

The load applied to the specimens was recorded from a 50 kN load cell with an accuracy of ± 3 N. The specimens were instrumented with a combination of linear potentiometers and a camera. Potentiometers were used to measure the horizontal, vertical and lateral deflections for both specimens. Specimen 1 used 26 potentiometers and specimen 2 used 29. The instrumentation layout is shown in Figure 4.13 with reference to the location shown in Figure 4.12. A series of high contrast points at approximately 75 mm spacing were applied to the surface of the specimens and the camera took pictures of these surfaces at each displacement increment in order to allow particle tracking analysis.

4.5 Results & Discussion

4.5.1 Damage Observations

Damage observations were taken after each step in the loading protocol (Figure 4.11) and these relied upon visual inspections, physical marking of observed damage, notes, and photographs.

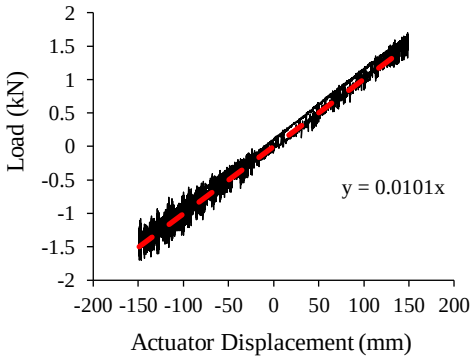

Figure 4.10 Load displacement behaviour of the bare frame.

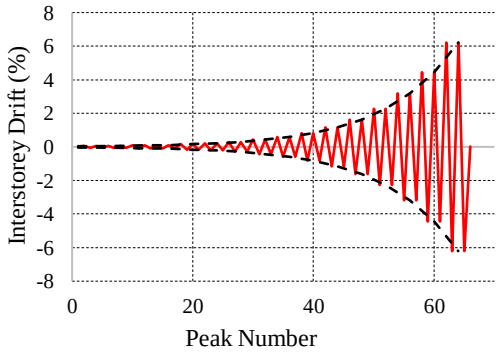

Figure 4.11 FEMA 461 quasi-static cyclic displacement protocol used in these tests.

As only external visual observations could be made, the point at which the framing was damaged could not be identified unless the wallboard began to spall or if sufficient gap sizes developed at joints, which was only the case during the larger cycles. Therefore, the drifts recorded for DS3 correspond to instances in which framing damage could first be observed from visual inspection. Noting that while determining DS3 based on visual observations would be consistent with post-earthquake inspection processes, damage to internal framing may be discovered during repair works for DS2. The forms of damage observed during the tests are summarised in Table 4.2, along with their associated repair actions. Figure 4.14 illustrates the damage states being referred to in Table 4.2. These are similar to the damage state definition defined by Taghavi and Miranda (2003) and include gap-filler debonding as part of DS1. The point at which the gap filler had debonded was chosen as the point at which the material

had fully debonding through the whole depth, and/or was not able to be restored to its original appearance by repainting.

The drift in-plane to the long wall at which each damage state initiated in the specimens is shown in Table 4.3, along with the lower bound predictions for DS1 and DS2. Note that for specimen 2, DS1 initiated due to separation of the gap-filling material at a lower drift than the predicted. However, plaster damage occurred at 0.94% drift which is above the predicted value as expected.

Very little screw connection damage (DS1c) was observed during the test, in particular no popping or pull-through of the fastener heads was observed. The only form of screw connection damage observed was seen during the final loading step of both tests, where at some locations the sheathing had detached from the studs (Figure 4.14d). This occurred primarily along the top and bottom of the boundary studs of the long wall.

Table 4.2. Damage states.

Damage State	Description	Repair Action
0	Hairline cracking of paint at joints	Barely visible damage deemed not requiring repair.
1.a	Sealant de-bonding	Remove and re-apply gap filler
1.b	Cracking in plaster and paint along trim	Scrape out minor cracks and reapply plaster and paint.
1.c	Screw damage - pull through, popping, or shearing	Re-fix or tighten any existing loose fasteners and place additional fasters near original. Finish with plaster, and sand and paint.
2.a	Wallboard damage - paper face separating, crushing, cracking, or spalling	Requires replacement of linings or local repairs of linings. Breakages can be ground out and patch fixed, using plastering and paper tape.
2.b	Residual gap at joints	Replace linings
3	Framing damage - flanges bent, buckling, or hinging	Both linings and framing must be removed and replaced. Thus, complete demolition and replacement of the wall is required.

Table 4.3 In-plane drift (%) at onset of damage.

	Specimen 1		Specimen 2	
DSi	**Predicted**	**Observed**	**Predicted**	**Observed**
1	0.37	0.48	0.91	0.67
2	0.58	0.94	1.74	1.86
3	-	2.6	-	3.64

An additional form of damage was excessive gap size developing at the junction between the long wall and the returns (DS2b). To maintain fire rating at gap locations the linings must overlap the vertical strip of gypsum board by more than 6 mm (according to advice from an industry collaborator). Thus, the linings must be repositioned if the gaps grow such that the required cover is not provided.

Only at the completion of the test could a detailed inspection of the framing be made, the results of which are shown in Table 4.4. This value represents the length of undamaged framing at the end of the test as a percentage of the total original length of framing. Damage to the studs was concentrated at the ends of walls and near the junctions. Damage to the tracks was concentrated along the top with more deformation near junctions.

Table 4.4 Percentage of framing undamaged at the end of testing

Test	Studs	Top track	Bottom track
B1	36%	71%	57%
B2	92%	86%	29%

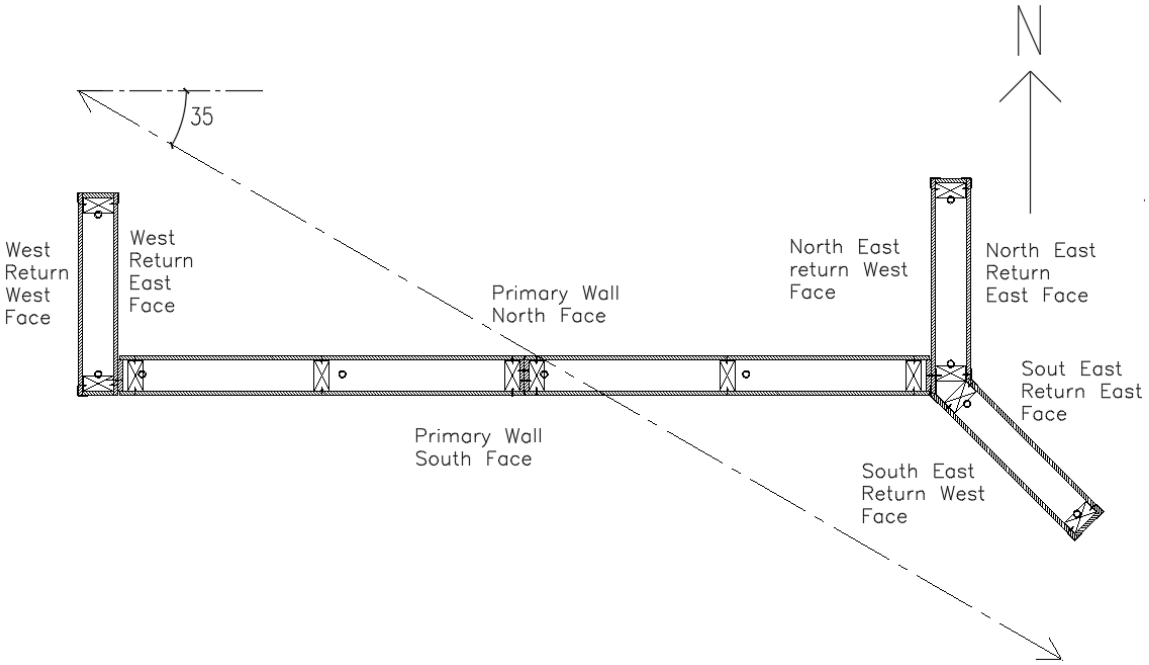

Figure 4.12 Wall specimen showing references for wall locations.

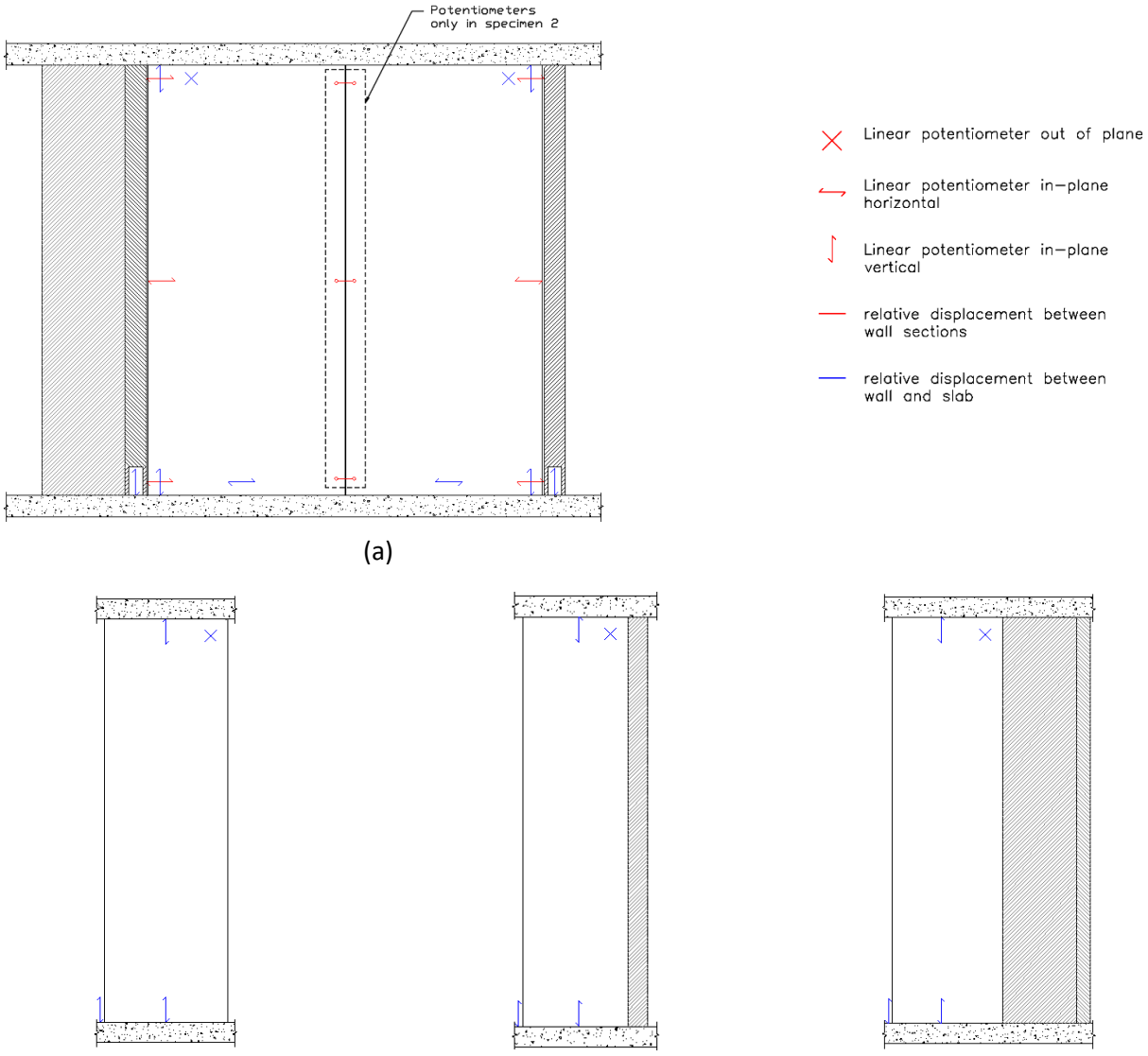

Figure 4.13 Potentiometer layout (a) primary wall north face (b) west return wall west face (c) north east return wall west face (d) south east return wall east face.

(a) Paint cracking

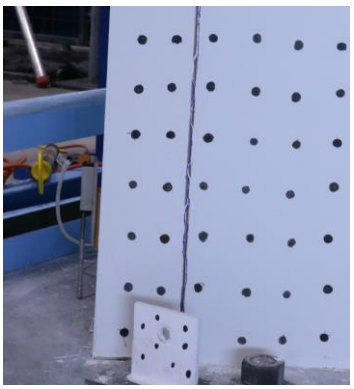

(b) Sealant de-bonding

(c) Plaster cracking

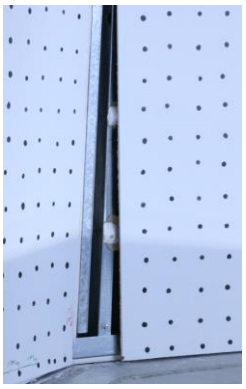

(d) Wallboard detaching

(e) Wallboard damage

(f) Framing damage

Figure 4.14 Examples of specimen damage

4.5.2 Detailed Damage Development

The damage progression for specimen 1 and 2 is shown in Table 4.5 and 4.6 respectively. In these tables the locations 1 to 21 shown in Figure 4.15 have been used when referring to damage. These locations refer to any vertical point within the area shown and represent the panels, joints between panels, and wall ends. The drift values shown in the tables refer to the in-plane drift along the different wall segments. In discussing damage progression below the in-plane drift along the long section of the wall has been used unless otherwise stated.

Both drywalls suffered damage in a similar pattern:

(1) The first signs of damage in both specimens was hairline paint cracking at the joints (DS0). For specimen 1 this occurred at locations 6 and 11 at 0.34% drift, and for specimen 2 at locations 2, 6, 11, and 15 at 0.48% drift. This observation suggests that increasing the width of the joint increases the drift at which the paint along the joints remains undamaged.

(2) The next form of damage to initiate was separation of the gap filling material (DS1a). For specimen 1 this occurred at locations 6, 11, and 15 at 0.48% drift, and for specimen 2 at locations 2, 6, 11, and 15 at 0.67% drift.

(3) The third form of damage to initiate was cracking of the plaster (DS1b) and paint along the trims at joints and edges. For specimen 1 this occurred at location 10 at 0.48% drift, and for specimen 2 at several locations (1, 11, 12, 16, 17, 20, and 21) at 0.94% drift. The design drifts at which the gaps close are 0.37% and 0.91% for specimens 1 and 2 respectively. Thus, plaster damage initiates very soon after the anticipated drift capacity is reached, and the equation used to predict the formation of DS1 provided a close prediction in specimen 1 and specimen 2. Sealant debonding occurred simultaneously with plaster cracking in specimen 1 at 0.37 % drift, but for specimen 2, sealant debonding occurred at 0.67 % drift before plaster cracking at 0.94 %. Therefore, the prediction for DS1 appears to work for plaster cracking, but not for debonding of the gap filler. Thus, it can be inferred that using sealant will reduce the drift at the onset of DS1.

(4) For specimen 1, wallboard damage (DS2a) initiated at locations 10, 11, 15, and 21 at 0.94% in-plane drift, and for specimen 2 at location 10 at 1.86% in-plane drift. The predicted lower bound at which damage to wallboard would occur was 0.58% and 1.74% drift for specimens 1 and 2 respectively. This approximation does not appear to provide a precise estimate of when wallboard damage will initiate, but it did provide a lower bound in both cases.

The rotation of the main wall section was recorded throughout the test. As the gap between the lining and the top floor was ~5 mm, the expected maximum rotation of the linings before crushing occurs could be estimated as (5 mm / 2410 mm) x 100%, which corresponds to 0.21% radians. Figure 4.16a shows that for specimen 1 crushing of the linings should begin at step 11, at which the rotation is a maximum of 0.16% radians. This was confirmed as plasterboard crushing was observed at location 6 (Table 4.5) at step 11. This is earlier than anticipated however this disparity may be attributed to small variations in the gap size between the linings and the top floor. Figure 4.16b shows that the rotation was predominantly fully recovered at equilibrium until larger displacement cycles.

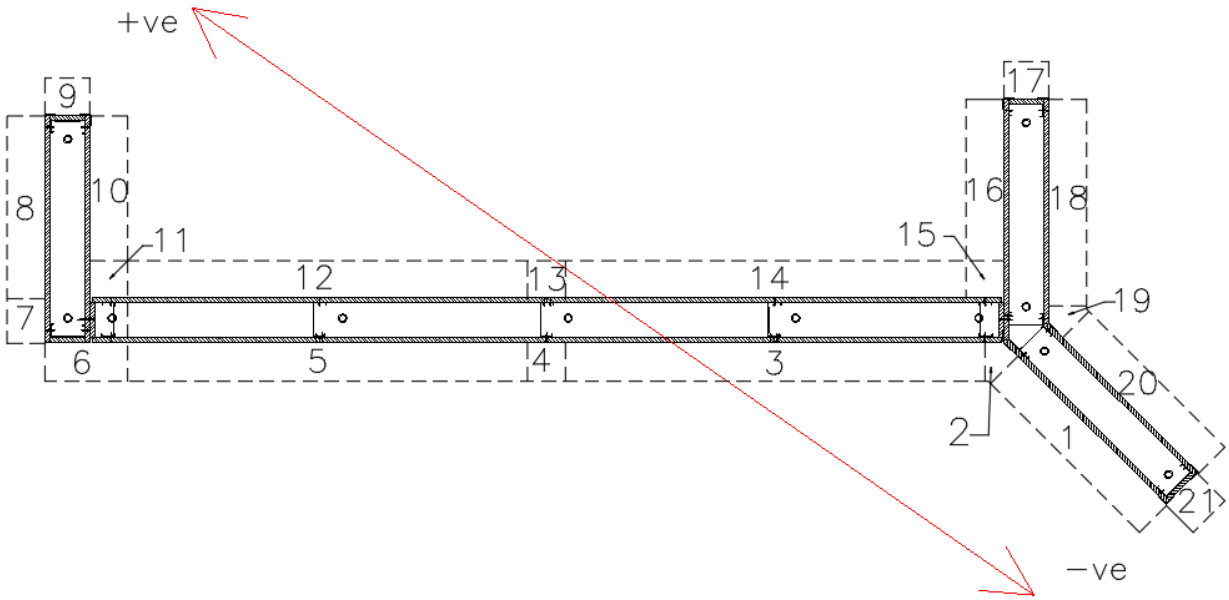

Figure 4.15 Reference locations for damage observations.

Table 4.5 Specimen 1 damage progression.

	STEP	8	9	10	11	12	13	14	15	16
Drift (%)	loading	0.42	0.59	0.82	1.15	1.62	2.27	3.17	4.44	6.21
	45° wall	0.41	0.58	0.81	1.13	1.60	2.23	3.12	4.37	6.12
	90° walls	0.24	0.34	0.47	0.66	0.93	1.30	1.82	2.55	3.56
	long wall	0.34	0.48	0.67	0.94	1.33	1.86	2.60	3.64	5.09
Location	1	-	-	1b	-	-	2a	-	-	-
	2	-	-	-	1a	1b	-	2a	-	1c
	3	-	-	-	-	-	-	-	1b	-
	4	-	-	-	-	-	-	-	-	-
	5	-	-	-	-	-	-	-	-	-
	6	0	1a	-	2b	-	-	1b,2a,3	-	-
	7	-	-	-	-	1b	-	-	-	-
	8	-	-	-	-	1b	-	-	-	-
	9	-	-	-	1b	-	-	-	-	2a
	10	-	-	-	1b,2a	-	-	-	-	1c
	11	0	1a,1b	-	2a	-	2b	3	-	1c
	12	-	-	-	-	-	1b	-	-	1c
	13	-	-	-	-	-	-	-	-	-
	14	-	-	-	-	-	-	-	-	-
	15	-	0,1a	1b	2a	-	-	-	-	-
	16	-	-	-	1b	-	-	2a	-	-
	17	-	-	-	1b	-	-	-	-	2a
	18	-	-	-	-	-	-	1b	2a	-
	19	-	-	0	-	-	-	1b	-	2a
	20	-	-	-	1b,2a	-	-	-	-	-
	21	-	-	-	1b,2a	-	-	-	-	3

Table 4.6 Specimen 2 damage progression

	STEP	8	9	10	11	12	13	14	15	16
Drift (%)	loading	0.42	0.59	0.82	1.15	1.62	2.27	3.17	4.44	6.21
	45° wall	0.41	0.58	0.81	1.13	1.60	2.23	3.12	4.37	6.12
	90° walls	0.24	0.34	0.47	0.66	0.93	1.30	1.82	2.55	3.56
	long wall	0.34	0.48	0.67	0.94	1.33	1.86	2.60	3.64	5.09
Location	1	-	-	-	1b	-	-	2a	-	-
	2	-	0	1a	-	-	-	2b	-	1c
	3	-	-	-	-	-	-	-	-	1b,1c
	4	-	-	0	-	1a	-	2b	-	-
	5	-	-	-	-	-	-	-	-	1b
	6	-	0	1a	-	-	-	2b	2a,3	1c
	7	-	-	-	-	-	1b	2a	3	-
	8	-	-	-	-	-	1b	2a	-	-
	9	-	-	-	-	1b	-	-	3	2a
	10	-	-	-	-	-	1b,2a	-	-	-
	11	-	0	1a	1b	-	-	2b	2a,3	-
	12	-	-	-	1b	-	-	2a	-	-
	13	-	-	0	-	1a	-	2b	-	-
	14	-	-	-	-	-	-	1b,2a	-	-
	15	-	0	1a	-	1b	-	2b	-	-
	16	-	-	-	1b	-	-	-	2a	-
	17	-	-	-	1b	-	-	-	2a	-
	18	-	-	-	-	-	-	1b	2a	-
	19	-	-	-	-	-	-	1b	2a	-
	20	-	-	-	1b	-	-	1b,2a	-	-
	21	-	-	-	1b	-	-	2a	-	-

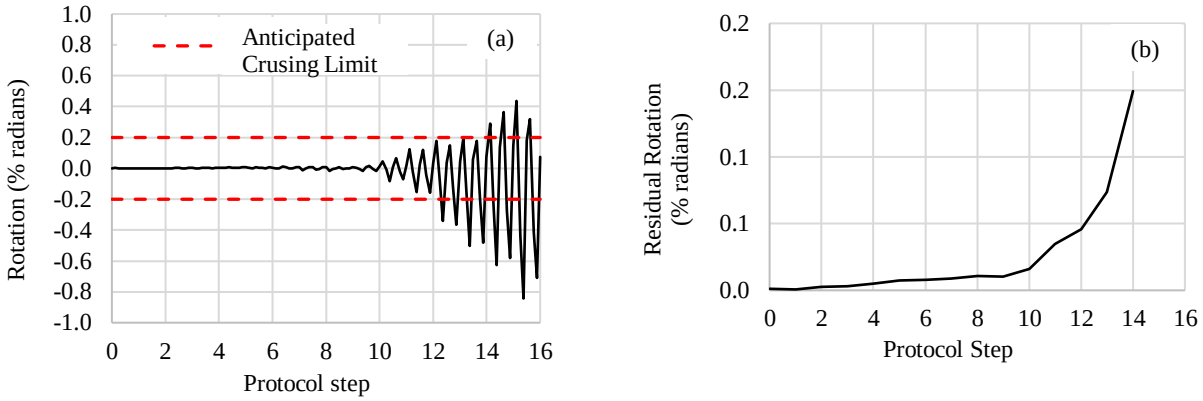

Figure 4.16 Specimen 1 potentiometer readings to record rotation: (a) peak excursions during each step and (b) residual rotation after each step.

(5) The residual gap size developing at the junction between the main wall and the returns was recorded. Figure 4.17a and 4.18a show the sliding of the linings during each cycle and Figure 4.17b and 4.18b show the residual sliding displacement of the linings at the end each cycle. For specimen 1, Figure 4.17b shows that the residual gap exceeded the limiting size for fire performance after step 11, and for specimen 2, Figure 4.18b indicates that there was negligible residual sliding and thus a residual gap should not have developed. However, it was observed that the bottom track withing the North West return wall (location 7) had bent such that at loading step 14 a residual gap was present even though the wallboards had returned to their original position as shown by Figure 4.18b. It can be seen in Figure 4.18 that the sliding of the linings occurred primarily in the positive direction. This is attributed to the bending of the bottom track at location 7, which will have reduced the sliding force imposed upon the linings when displaced in the negative direction.

Assuming both the return walls and the primary wall behave as rigid bodies, a gap forms at the junction of the main wall and return wall as explained in Figure 4.19 for specimen 1. This mechanism shows that the linings and studs slide as the gaps on either side of the wall close. However, when the relative displacement returns to equilibrium, they will not re-centre. The sliding of the main wall section was recorded by potentiometers. It can be seen in Figure 4.17a that at loading step 9, which corresponds to 0.48% drift and a displacement of 11.5 mm, the wall slides approximately half of the total gap size (5mm) in each direction. This is how the wall would be expected to behave if Figure 4.18 is a correct explanation; however, Figure 4.17b shows that the gap re-centres after step 9, and only begins to increase in size at larger cycles, until at step 11, corresponding to 0.94% in-plane drift, the gap is large enough such that the fire performance is hindered. This initial re-centring behaviour may be attributed to the presence of the gap filling material at the junctions. This is supported by the observation that separation of the gap filling material occurs at step 9 after which a gap begins to develop. Two solutions are possible to address the problem of residual gap development: (1) provide additional vertical strips of gypsum lining between adjacent walls and the vertical steel tracks such that a larger gap can be accommodated before the fire performance is hindered or (2) provide a pivot point to force the linings to return to their original position at the end of a loading cycle. The anticipated effect of introducing a pivot to the system is shown and explained in Figure 4.20.

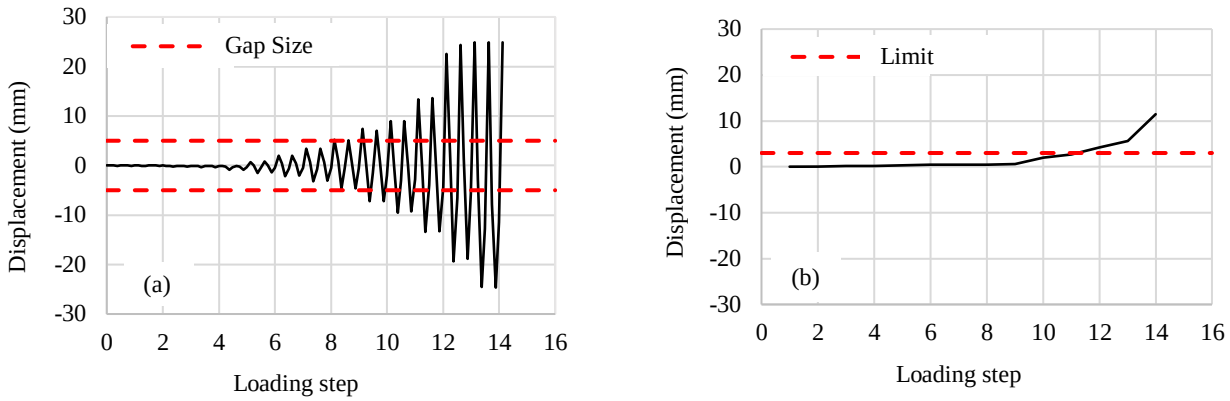

Figure 4.17 Specimen 1 potentiometer readings to record sliding: (a) peak excursions during each step and (b) residual displacement after each step.

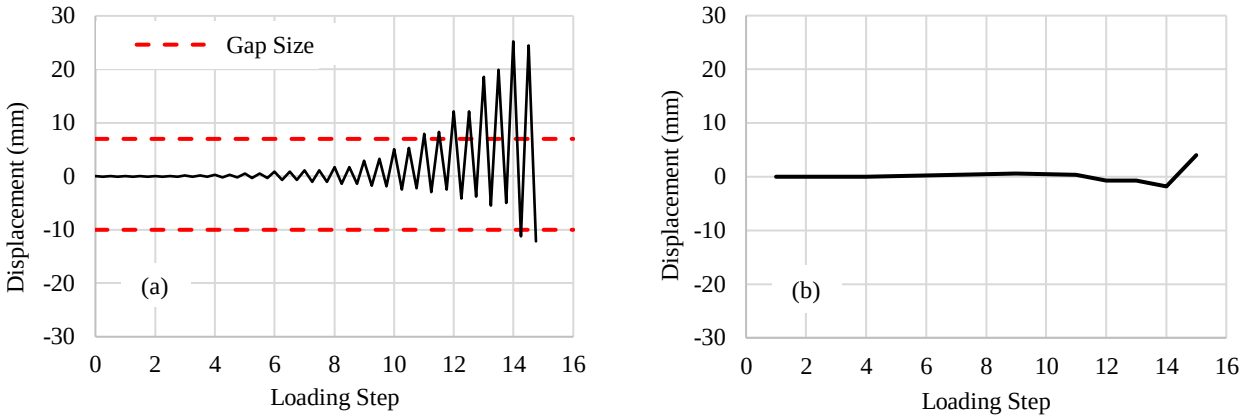

Figure 4.18 Specimen 2 potentiometer readings to record sliding: (a) peak excursions during each step and (b) residual displacement after each step.

(6) The final form of damage to occur was framing damage (DS3). The first observable form of framing damage in specimen 1 was hinging of the vertical steel tracks at locations 6 and 11 at 2.6% drift. This was able to be observed as the gap between the linings and the return wall had grown such that the underlying framing was visible. For specimen 2, damage at locations 6 and 11 was also observed where the flanges of the vertical steel tracks were bent out. Additionally, bottom track damage was observed at locations 7 as the plasterboard had pushed the track flanges flat at this location, and at location 9 where the bottom track flanges were bent in.

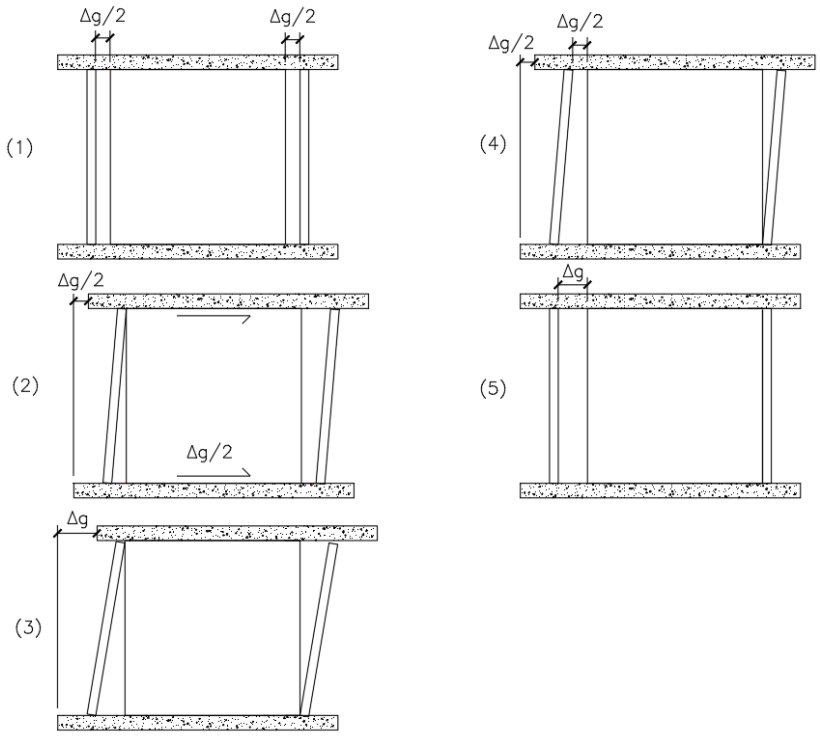

Figure 4.19 Explanation of residual gap formation for a loading sequence of one peak excursion: (1) Initial condition, (2) lateral displacement of Δg/2 imposed on slab and gap on left closes, (3) lateral displacement of Δg imposed on slab, linings slide Δg/2, and gap on right also closes, (4) lateral displacement of slab reduced back to Δg/2, and (5) lateral displacement of slab reduced to zero and residual displacement in wall remains

4.5.1 Force Displacement Behaviour

The hysteretic response for the specimens is shown in Figure 4.21 and the maximum loads presented in Table 4.7. The general pattern of behaviour was that the load and displacement started at zero but thereafter the load was non-zero at zero displacement. This is due to inelastic behaviour. When loaded in the positive direction, the walls had less capacity in all cases. This asymmetric behaviour may be due to a couple of reasons: (1) The asymmetry of the specimens, and (2) bias in the loading; as the loading is first applied in the positive direction for each step the specimen will damage in the first cycle leaving less capacity in the specimen when the loading is reversed. However, as the positive direction had less capacity for both specimens, also under subsequent cycles to the same drift demand, the geometry of the specimen must have been the main factor producing this asymmetric response. The orientation of the specimen to the loading direction is as shown in Figure 4.9a, where θ is 35°.

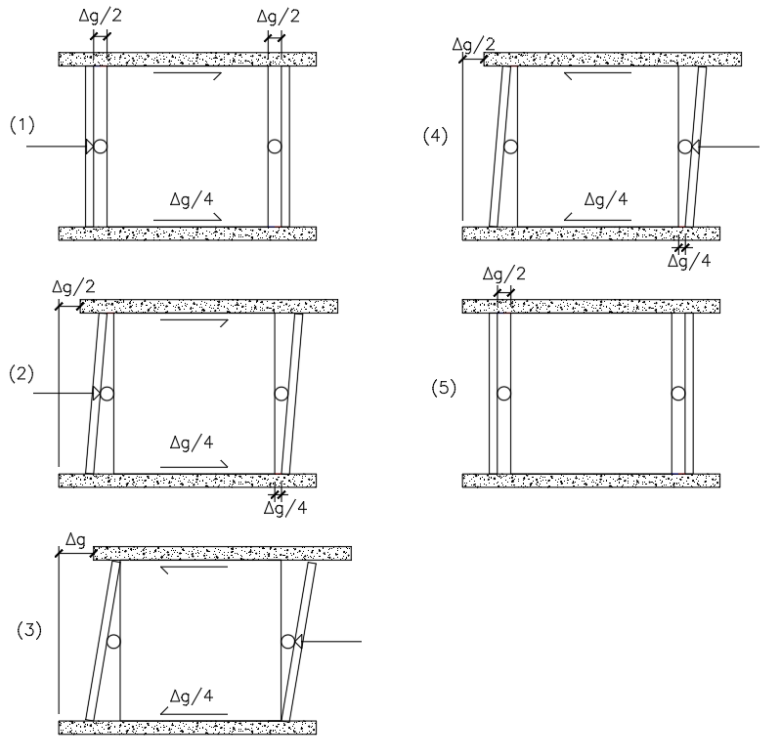

Figure 4.20 Explanation of the effects of introducing a pivot at mid-height on the formation of a residual gap, for a loading sequence of one peak excursion: (1) Initial condition, (2) lateral displacement of Δg/2 imposed on slab and linings slide Δg/4, (3) lateral displacement of Δg imposed on slab and and linings slide Δg/4, (4) lateral displacement of slab reduced back to Δg/2 and linings slide back Δg/4, and (5) lateral displacement of slab reduced to zero and residual linings slide Δg/4 to return to initial position.

Table 7. Maximum load from tests.

	Negative Direction		Positive Direction	
Specimen	**Max Load (kN)**	**Drift (%)**	**Max Load (kN)**	**Drift (%)**
1	12.89	3.13	8.68	2.08
2	12.92	6.18	9.91	5.70

The dissipated energy and equivalent viscous damping at each amplitude of loading was determined. This information may be useful for those interested in undertaking refined analyses on partition walls. The energy absorbed by the specimen is defined as the area within the force-displacement curve. The hysteretic curves shown in Figures 4.21a and 4.21b were integrated using the trapezium method for each increment in data. The energy dissipated in the two cycles of loading was averaged to attain the average energy dissipation at each amplitude. The equivalent viscous damping was determined at each

cycle according to equation 3. Where A_h, is the area within the hysteretic loop, F_m is the force at the displacement of Δm, the maximum imposed displacement in the cycle. Applying this equation led to the values in Figure 4.22.

$$\xi_{hyst} = \frac{A_h}{2\pi F_m \Delta_m} \quad \textbf{(3)}$$

4.5.2 Comparison of Results with Previous Studies

Table 4.8 shows a comparison of the predicted versus observed damage in specimens incorporating seismic gaps from previous studies. In assessing these results, it is important to note how damage observations were made. As it is impractical to take detailed assessments of damage continuously, the damage observations are made at discrete points in the loading history, typically at the end of each loading step. Thus, the accuracy of damage observations will have an error proportional to the step size of the loading protocol. Note that for the studies done by Lee *et al.* (2007) and Magliulo *et al.* (2014) the size of the vertical gap between linings and the support frame was not provided in their report; therefore, predictions could not be made for DS2.

Table 4.8 shows that the prediction for the onset of DS1 based upon the size of the horizontal gaps is accurate across all five experimental tests. While there is an apparent discrepancy between the predicted and observed drift at onset of DS1 for the specimens tested by Tasligedik *et al.* (2015) this can be accounted for by the step size of the loading protocol. The loading protocol used by Tasligedik *et al.* (2015) applied a drift of 1.50% at step 10 and 2.00% at step 11. DS1 was therefore observed following the completion of step 11. This implies that DS1 was triggered between 1.50% and 2.00% drift, which is the range wherein the predicted value lies. The prediction for the onset of DS2 was in all cases below the observed drift. For the specimens tested by Tasligedik *et al.* (2015) the exact drift DS2 initiated is not known as the tests were only run to 2.50% drift, but it can be stated that for at least one of the specimens the wall had greater capacity for DS2 than that predicted. Although the prediction for specimen 2 in this paper significantly underestimated the onset of DS2, the equation did provide a lower bound in all cases albeit a conservative one.

There were a number of differences between specimen designs and method of load application for the four previous studies shown in Table 4.8. While the specimen designs in Lee *et al.* (2007), Magliulo *et al.* (2014), Tasligedik *et al.* (2015), and Pali *et al.* (2018) all incorporated seismic gaps and were constructed such that the lining and internal framing was free to slide within the tracks, there were some variations.

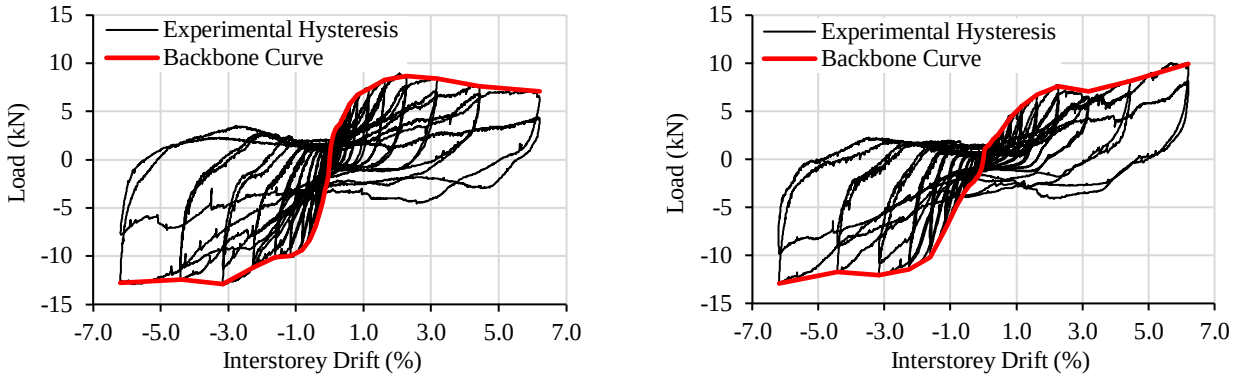

Figure 4.21 Left: Specimen 1 hysteresis; Right: Specimen 2 hysteresis.

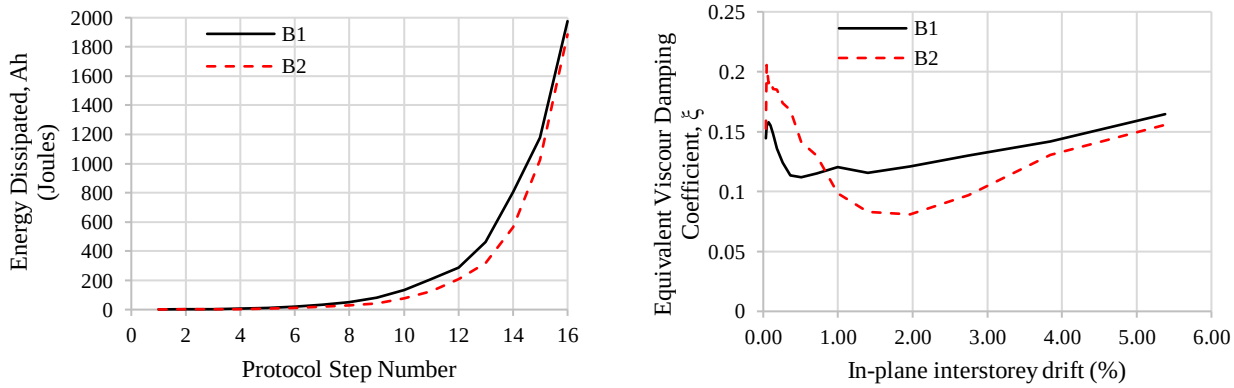

Figure 4.22 Left: Energy dissipation at each amplitude of loading; Right: Equivalent viscous damping coefficient (Equation 3).

Table 4.7 Comparison of predicted and observed damage progression in previous studies.

Author	**Lee et al. (2007)**	**Magliulo et al. (2014)**	**Tasligedik et al. (2015)**		**Pali et al. (2018)**	**This Paper**	
Dimensions							
h_c (mm)	2800	2680	2550	2550	2700	2405	2405
L (mm)	3950	2270	1200	3400	2400	2415	2410
Δh (mm)	30	16	40	40	40	22	9
Δv (mm)	-	-	26	26	20	10	5
Prediction							
DS1 (%)	1.07	0.60	1.57	1.57	1.48	0.91	0.37
DS2 (%)	-	-	3.73	2.33	2.31	1.74	0.58
Observation							
DS1 (%)	1.0	0.58	2.0	2.0	1.53	0.94	0.48
DS2 (%)	1.5	0.98	>2.5	>2.5	2.47*	1.86	0.94

* DS2 for this case is referring to the onset of corner crushing in the gypsum wallboard noting that the Pali et al. (2018) definition for DS2 includes failure of panel-to-frame fixings and collapse of dowels, which was observed at smaller drift levels than corner crushing. The average value has been taken between the two relevant specimens tested by Pali et al. (2018) (specimens #7 and #8).

The differences included variations in stud size, spacing, and material (including timber and steel); track size; fastener type and spacing; and plasterboard thickness and number of layers. In addition, all of the seismic gap systems tested in these studies were tested with structural elements at the wall ends. The studies by Lee *et al.* (2007), Tasligedik *et al.* (2015), and Pali *et al.* (2018) used quasi-static cyclic loading protocols applied in-plane to the partition wall specimens, albeit with different protocols, and the study by Magliulo *et al.* (2014) used dynamic loading. Despite the differences between the specimen designs from the previous studies and the specimens tested in this paper, it can be seen from Table 4.8 that using Equation 1 to predict the drift at the onset of DS1 is accurate in all cases. It is of particular interest that although for the specimens tested in this study loading was applied at an angle of 35° to the long wall section and the specimen was configured with return walls in a y-shape with one 45° return wall, Equation 1 still provided an accurate prediction for the drift in-plane to the wall at the onset of DS1. Therefore, for the specimens tested in this study, out-of-plane displacements or return wall configuration did not appear to significantly impact the onset of DS1b (plaster cracking).

4.6 Conclusion

Two y-shaped partition wall specimens with seismic gaps aligned at 35° to the direction of loading were subjected to quasi-static cyclic testing: one steel stud specimen with horizontal gaps at the wall ends totalling 9 mm; and one timber stud specimen with horizontal gaps totalling 22 mm. The seismic gaps in the specimens were half-filled with an acrylic gap-filler. In addition to providing drift capacities, the force-displacement behaviour has been reported, and the energy dissipation computed.

The main findings of the experimental tests are as follows:

• An equation was used to predict the formation of DS1. This equation provided an accurate estimate for DS1 in specimen 1 where plaster cracking and debonding of the gap filler material occurred simultaneously. For specimen 2 the equation accurately estimated the onset of plaster cracking but not debonding of the gap filler material, which initiated earlier.

• The gap filling material appeared to reduce the drift at the onset of DS1 for specimen 2. However, it had a beneficial effect on the re-centring behaviour of the linings. If a gap-filling material is not used, it is suggested that a pivot system is utilized in order to prevent residual gap development.

• An equation was proposed to predict the onset of DS2. This equation provided a lower bound for both specimens tested herein and when used to predict the results of previous experimental tests on seismic gap systems.

• For the specimens tested in this study, out-of-plane displacements imposed and return wall configuration did not appear to significantly impact the onset of plaster cracking in the specimens.

4.7 Acknowledgements

The authors gratefully acknowledge the funding & support offered by Ali Sahin Tasligedik; The International Collaborative Research program of the Disaster Prevention Research Institute, Kyoto University under Project Number 28W-03 (PI: Timothy Sullivan); the University of Canterbury Quake Centre; QuakeCoRE; NZ Property Council; RONDO; Winston Wallboards; Dunning Thornton Consultants; and Holmes Consulting. This project was partially supported by QuakeCoRE, a New Zealand Tertiary Education

5. POTENTIAL IMPLICATIONS FOR BUILDING PERFORMANCE

5.1 Non-structural partition involvement in PBEE loss assessment methods

An overview of the general PBEE method for buildings is provided in 1.4, however a brief description of the method is provided here also as it pertains to the involvement and influence of non-structural partition systems within the overarching process.

The overall goal of PBEE is to ensure a combination of desired system performance objectives at various levels of seismic excitation quantified by metrics that are meaningful for stakeholders, as opposed to the engineering response metrics that are conventionally used, including probabilistic estimates of repair costs, casualties, and loss-of-use duration. Loss assessment methods aim to produce an estimate of the frequency with which a particular performance metric will exceed various levels for a given design at a given location. These can be used to create probabilistic distributions of the performance measures during any planning period of interest. From the frequency and probabilistic distributions can be extracted simple point performance metrics. PEER's PBEE approach involves four stages (as shown in Figure 1.13): (1) hazard analysis requiring a corresponding hazard model, (2) structural analysis requiring a corresponding structural model, (3) damage analysis requiring a corresponding fragility model, and (4) loss analysis requiring a corresponding loss model. Within this process the influence of non-structural partitions must be considered at stages 2 to 4 by potential inclusion within the structural model by way of a non-linear hysteretic model, input of fragility models, and input of loss models.

5.2 Comparison of loss assessment inputs for traditional and low damage partition systems studied herein

To assess the varying influence of traditionally detailed and low damage partition systems, the behaviour of a traditionally detailed wall, taken from the work by Davies *et al.* (2011), is compared with experimental results for the seismic gap system and partly-sliding systems tested herein. The configuration selected from the work by Davies *et al.* (2011) is configuration 1 for test specimens 1-3, which are full-height specimens in I-shape configurations, with slip tracks at the top and bottom interfaces (Figure 5.1) , and "commercial" detailing at the junctions between return walls (Figure 5.2). The typical specimens are 3708 mm long (12'-2") and 3505 mm high (11'- 6") with 610 mm (2') long return walls at each end.

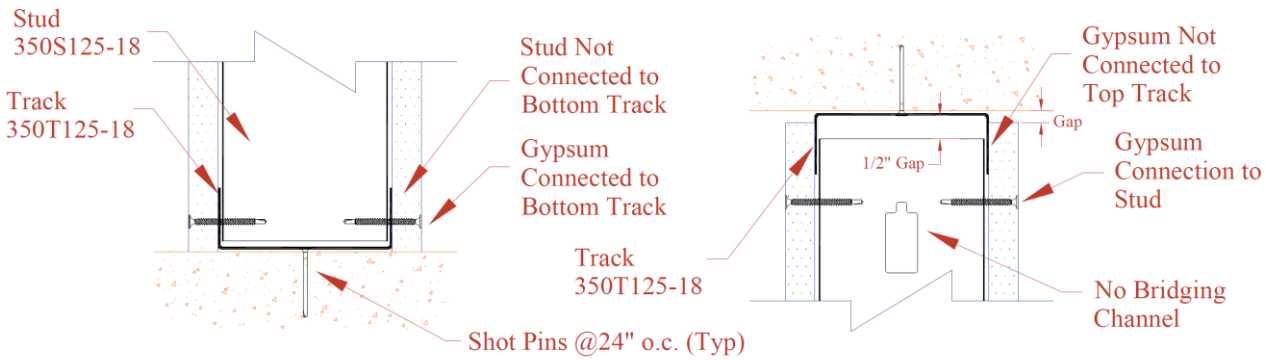

Figure 5.1 Slip track details for baseline specimens (Davies *et al.* (2011) configuration 1) at top and bottom interfaces.

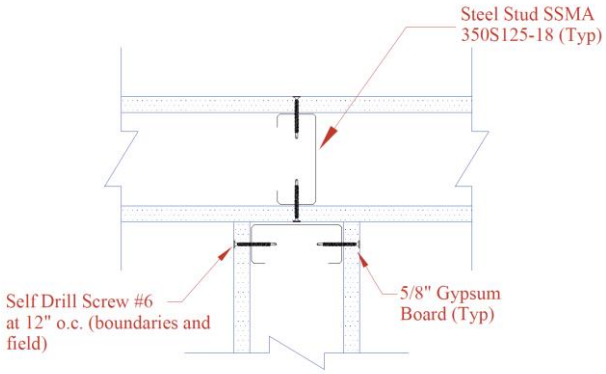

Figure 5.2 Commercial construction wall intersection detailing for baseline specimens (Davies *et al.* (2011) configuration 1).

5.2.1 Hysteretic modelling

In order to understand the effect of non-structural partition wall systems on the dynamic response of structures, the walls can be incorporated into the building model. Non-linear shear springs can be applied in conjunction with the Wayne-Stewart hysteretic model, available in Ruaumoko 2D, to model the hysteretic behaviour of partition systems. A comparison of the mean fitted Wayne-Stewart Hysteretic model parameters per linear metre for the baseline specimens from Davies *et al.* (2011) (Subgroup 1a), the three partially-sliding specimens tested in this study, and the two seismic gap partition specimens tested in this study are shown in Table 5.1. A comparison of the energy dissipation during each step of the protocol and equivalent viscous damping coefficient versus in-plane drift demand for the specimens tested within this study is shown in Figure 5.3. Note that in interpreting the results for the baseline parameters the walls are 3505 mm high versus whereas the walls in this study which are 2400 mm high. The capacity, stiffness, and overall behaviour of the wall system is related to the wall height, and so the results are not directly comparable, and the increased strength and stiffness of the specimens tested within this study is to be expected. In addition, the models represent the

hysteresis along the direction of loading. The results of the structural analysis on the building will allow the probability of a certain EDP occurring to be determined. In the case of partition walls, the critical EDP is inter-storey-drift. While studies have shown that conducting a coupled analysis with partition walls as part of the building model can significantly effect the behaviour of structures and can have significant effects on maximum inter-storey drifts, floor accelerations, strength, and collapse probability (Davies *et al.* 2011, Wood and Hutchinson 2012) for simplicity the effects of partitions have not been included within the subsequent loss assessment case studies within this chapter.

Table 5.1 Wayne-Stewart hysteretic model fit parameters per linear metre for baseline specimens (Davies *et al.* (2011) subgroup 1a specimens) and low damage systems from this study.

	Key Parameters	Baseline specimens	Partly sliding specimens	Seismic gap steel stud specimen	Seismic gap timber stud specimen
Ko	Stiffness (kN/mm):	0.12	0.46	0.33	0.15
PTRI	Tri-linear factor beyond ultimate force or moment:	-0.06	0.00	0.00	0.03
FU+	Positive ultimate force (kN):	1.60	4.10	3.62	2.81
FU-	Negative ultimate force (kN):	1.60	-4.08	-4.38	-4.67
M1	Ductility at start of degradation:	n/a	2.98	n/a	n/a
M2	Ductility at finish of degradation:	n/a	4.97	n/a	n/a
M3	Final fraction of strength:	n/a	0.78	n/a	n/a
M4	Ductility at 1% of initial strength:	n/a	Inf	n/a	n/a
FY	Yield force or moment (>0) (kN):	1.01	1.90	1.42	0.93
FI	Intercept force or moment (>0) (kN):	0.17	0.63	0.63	0.33
R	Bi-linear factor (<0.9) or Ramberg-Osgood Factor (>1):	0.48	0.26	0.40	0.52
PUNL	Unloading stiffness factor (>1):	0.93	1.50	5.00	10.00
BETA	Softening factor (>=1):	1.09	1.05	1.10	1.10
ALPHA	Pinch power factor (<=1):	0.73	0.57	0.35	0.20
IOP	0 for the unmodified loop, 1 for the modified loop:	1	1	1	1

Notes: [1] Factors M1 to M4 are parameters corresponding to strength degradation type 1, where strength degradation depends on the ductility, which is only applicable to the partly sliding specimens. [2] Positive and negative gaps size are also input parameters however, these values have all been selected as zero.

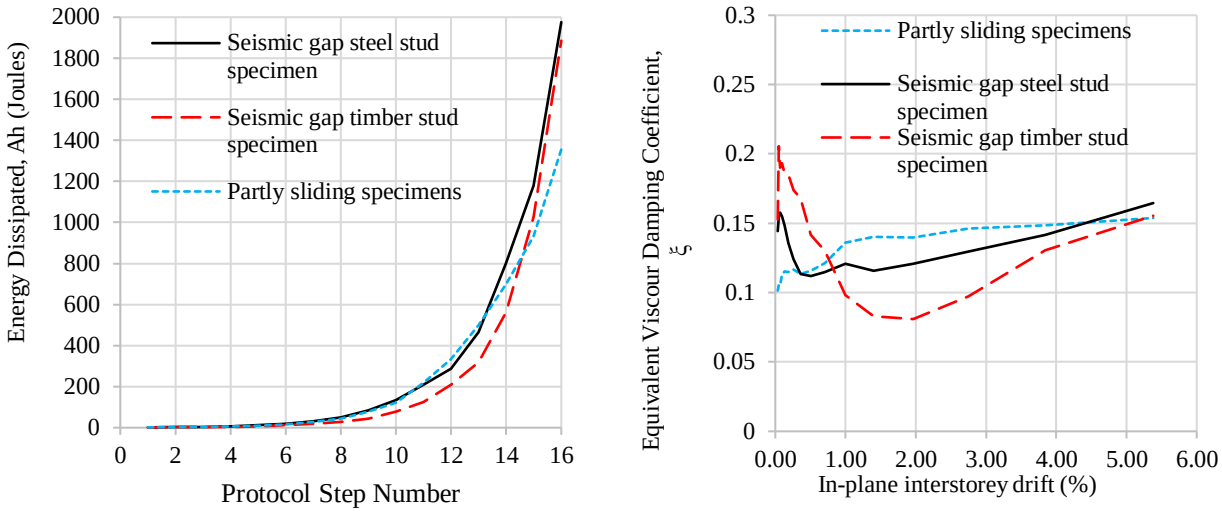

Figure 5.3 (a) Energy dissipation during each protocol step; (b) Equivalent viscous damping coefficient for each cycle versus in-plane drift demand

5.2.2 Damage progression & fragility models

Fragility models allow the level of damage in an element to be correlated to a relevant EDP. In the case of partition walls, the relevant EDP is inter-storey drift. Therefore, a fragility model allows designers to determine the probability of a particular damage state occurring in a partition system at a certain level of inter-storey drift. The fragility functions for the baseline specimens were compared with the fragility functions determined for the partly sliding specimens tested in this study (shown in chapter 3). The fragility parameters were not able to be calculated for the seismic gap systems tested in this study. This is because the empirical dispersion factor, β, which is the standard deviation of the data in log space and represents uncertainty, cannot be calculated using only two data points. In addition as the two specimens are designed to include different gap widths, gap closure will occur, by design, at different drifts, and therefore the specimens do not represent the specimen-to-specimen randomness of specimens with similar details and should not be grouped within the same fragility group. If further investigation into the effects of using the seismic gap system within a PBEE analysis framework is to be undertaken without further experimentation to determine the dispersion factor for the specimens, the median drifts at the onset of each damage state, x_m, may be assumed as the inter-storey drift at the onset of each damage state along with an assumed dispersion factor. Dispersion factors for each damage state are assumed to be the same as those for the partly-sliding specimens. These values are used as the partly sliding specimens include two identical plain wall specimens and one doorway specimen, and therefore the dispersion determined for these specimens should be higher than the dispersion determined for specimens of the same configuration.

Note that for the partly-sliding wall tests the DS3 values recorded in chapters 4 represent the final maximum drift the specimen was subject to before an inspection of the internal frame was conducted. The formation of hinges in studs, associated with DS3, was discovered during the inspection performed following the tests, which indicates that the DS was triggered during testing at an unknown drift level. The formation of hinges in studs may be related to popping out screws around the hinge or strength degradation in the hysteresis loops. However, the lowest drift level at which plasterboard panels need to be replaced corresponds to DS2 and as this type of repair work could reveal damaged studs, a lower-bound estimate for DS3 would be to adopt the same drift values as per DS2. In order to produce a more accurate estimate of DS3 for inclusion within loss assessment models, and because no observations of popping out of screws around the stud hinges was made during the testing, the drift at the onset of DS3 was estimated by tracking the strength degradation in the hysteretic loop. The backbone curves of the hysteretic loops were used and the drift in-plane to the main wall section at which the peak force was measured chosen as the estimate for the onset of DS3. The points chosen for the flexible track system are shown in Figure 5.4. The final fragility curve parameters selected for the flexible track system were calculated in the same method as described in chapter 2 and shown in Table 5.2.

For the seismic gap specimens DS3 was observed during testing. This observation was of damage to the vertical tracks at the main wall ends and also pushing out of the bottom tracks at the junctions. In order to confirm the value for DS3 and fragility parameters for inclusion within the loss assessment models, the points at which strength degradation began in the hysteretic response was tracked as shown in Figure 5.5and Figure 5.6. For the steel stud specimen the observed damage to the steel framing coincided with the strengthe degradation and so this point was deemed as OK. For the timber stud-specimen, no strength degradation in the hysteretic response can be seen. This is assumed to be because the timber studs do not buckle, and framing damage is concentrated in the vertical and horizontal steel tracks. Observations of framing damage at the end of the test also show that only one of the vertical studs ruptured in compression by the end of the test whereas most of the steel framing was damaged. Therefore, the final point chosen for DS3 was of the observed damage to the steel tracks. Final damage observation parameters used for the seismic gap partition specimens are shown in Table 5.3. A summary of the fragility parameters for the baseline specimens, partly sliding specimens, and seismic gap specimens used in the following loss assessment is shown in Table 5.4.

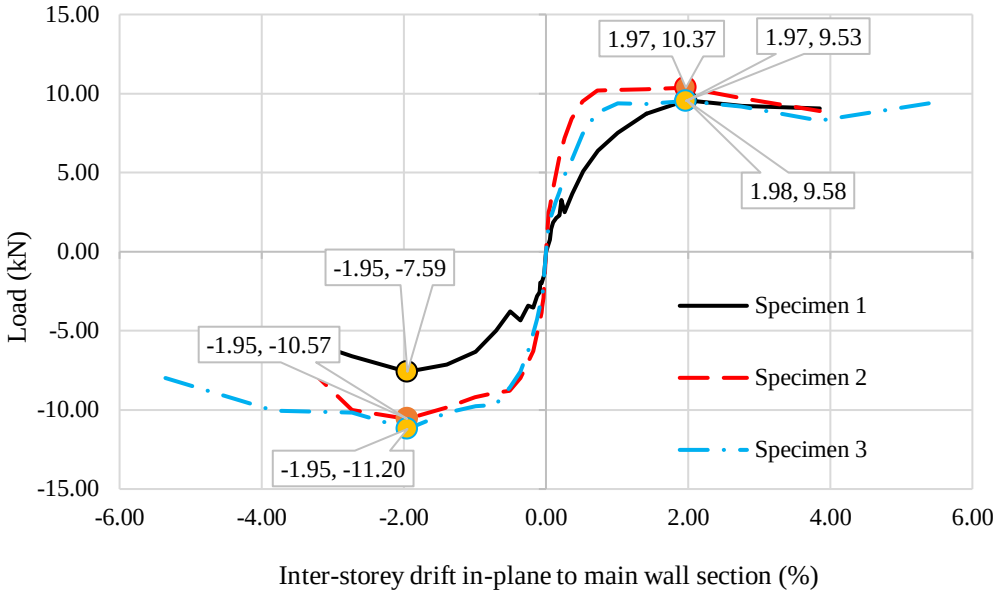

Figure 5.4 Strength degradation points chosen as likely drifts at the onset of DS3 for flexible track specimens (specimens A1-3).

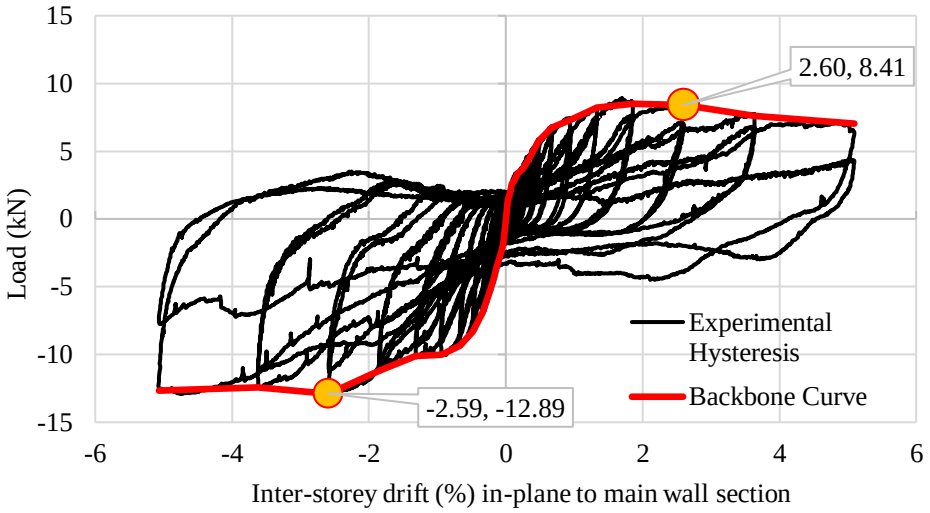

Figure 5.5 Strength degradation points chosen as likely drifts at the onset of DS3 for seismic gap steel stud specimen (specimen B1).

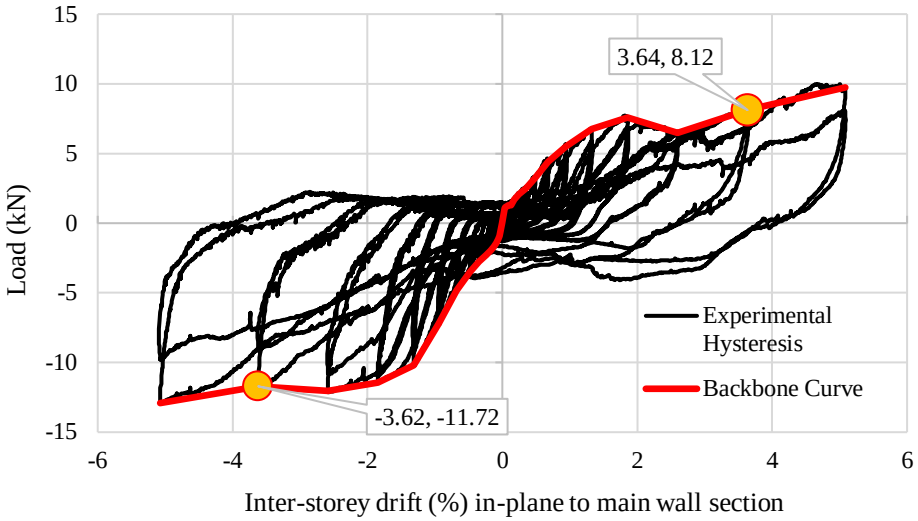

Figure 5.6 Strength degradation points chosen as likely drifts at the onset of DS3 for seismic gap timber stud specimen (specimen B2).

Table 5.2. In-plane drift %, r_i, at damage onset and fragility curve parameters for partly-sliding partition specimens.

	A1	**A2**	**A3**	**x_m**	**β**
DS1	0.36	0.26	0.26	0.29	0.35
DS2	0.36	0.26	0.26	0.29	0.35
DS3	1.95	1.95	1.95	1.95	0.3

Table 5.3. In-plane drift at damage onset for each damage state and assumed median value for fragility functions, x_m(%) for seismic gap partition system specimens.

	Steel stud specimen	**Timber stud specimen**
DS1	0.48	0.67
DS2	0.94	1.86
DS3	2.6	3.64

5.2.3 Repair Cost

As repair costs for each damage state were not estimated for the specimens tested within this study, or the baseline specimens, all specimens are assumed to have the same repair cost as that derived for partitions in Dhakal *et al.* (2016). The data derived by Dhakal *et al.* (2016) on likely cost of repair was obtained by consulting builders, partition suppliers, construction companies, and quantity surveying guides. The authors of this study acknowledge that these costs are applicable only to the Christchurch area due to the economic environment and are subject to change with variations in economic and industrial conditions. The loss function corresponds to the damage states and repair actions used within

this study. Assuming that all partition specimens have the same loss function is a limitation of the results of this assessment as each system showed a different pattern of damage progression inferring that different repair actions would be required for each system at different each damage state. However, due to the overall similarity in the design of the specimens it is thought that the loss function will provide a reasonable estimation of the actual loss function of the specimens. cost. The repair cost assumed for each partition specimen at each damage state is shown in Table 5.5. These values are presented in New Zealand Dollars (NZ$) and are converted to US Dollars (US$) in the subsequent loss assessment. The December 2017 conversion ratio of 1.4 has been assumed.

Table 5.4. Fragility curve parameters for baseline/traditional specimens and low damage systems tested within this study.

		x_m (% drift)	β
Traditional/Baseline	DS1	0.26	0.45
	DS2	0.68	0.33
	DS3	0.75	0.36
Flexible track specimens - combined	DS1	0.29	0.35
	DS2	0.29	0.35
	DS3	1.95	0.30
Seismic gap - steel stud specimen	DS1	0.48	0.35
	DS2	0.94	0.35
	DS3	2.6	0.30
Seismic gap - timber stud specimen	DS1	0.67	0.35
	DS2	1.86	0.35
	DS3	3.64	0.30

Table 5.5 Assumed loss function parameters for the partition specimens determined from Dhakal *et al.* (2016).

Damage state	Average repair cost (NZ$/m^2)	Standard deviation (NZ$/m^2)
DS1	26.6	6.99
DS2	61.8	6.27
DS3	115.9	21.07

5.3 Loss Assessment Case Study

5.3.1 Case Study Buildings

Four steel moment resisting frame case study buildings were assessed in this study. These were (1) a 4-storey building designed for the Christchurch region, (2) a 4-storey building designed for the Wellington region, (3) a 12-storey building designed for the Christchurch region, and (4) a 12-storey building designed for the wellington region. The layout of the case study buildings adopted in this study is the same as those defined in Yeow *et al.* (2018) and is shown in Figure 5.7. A short description of the

buildings is provided herein highlighting key aspects of the design, however for further details refer to Yeow *et al.* (2018).

The plan dimensions of the buildings were 40 m by 24 m for the four-storey buildings and 48 m by 32 m for the 12-storey buildings. All buildings were designed with perimeter lateral load resisting frames along each side of the building; interior gravity beams and columns; floor heights of 4.5 m on the ground floor and 3.6 m on all other floors; and bay widths of 8.0 m.

The general design of the frames was done as follows. The demands on the frames were determined according to the New Zealand loadings code, NZS1170 (Standards New Zealand 2004) and the design of the structural system was conducted according to New Zealand steel structures standard, NZS3404 (Standards New Zealand 1997). An iterative design process was used in order to determine the lightest steel frame whilst satisfying code criteria for the individual elements. The iterative process involved first assuming an initial size for the frame and then (1) checking the serviceability drift requirements under wind actions, (2) checking the serviceability requirements under earthquake actions, (3) checking that the 2.5% inter-storey drift limit was not exceeded under ultimate limit state seismic actions, and (4) checking the building strength requirements under ultimate limit state actions. Once the lightest frame had been determined an additional consideration was adopted, which was to keep the same beam section size for every three floors. This was done to reflect common practices for design, which facilitate easier construction. This was done for all floors except the top three where the beam section size was varied for each floor to ensure that the top floor beams did not have a moment capacity to demand ratio significantly larger than those on lower floors. The frame sizes were iterated until the frame size could not be decreased further and all of the design requirements were met. Traditional bolted-end-plate connections were used as these are the most common connection type used in New Zealand. The weak beam strong column method was used and to ensure the beams are the weakest link in the strength hierarchy. The governing factor for design of the buildings was the 2.5% drift requirement under ultimate limit state actions.

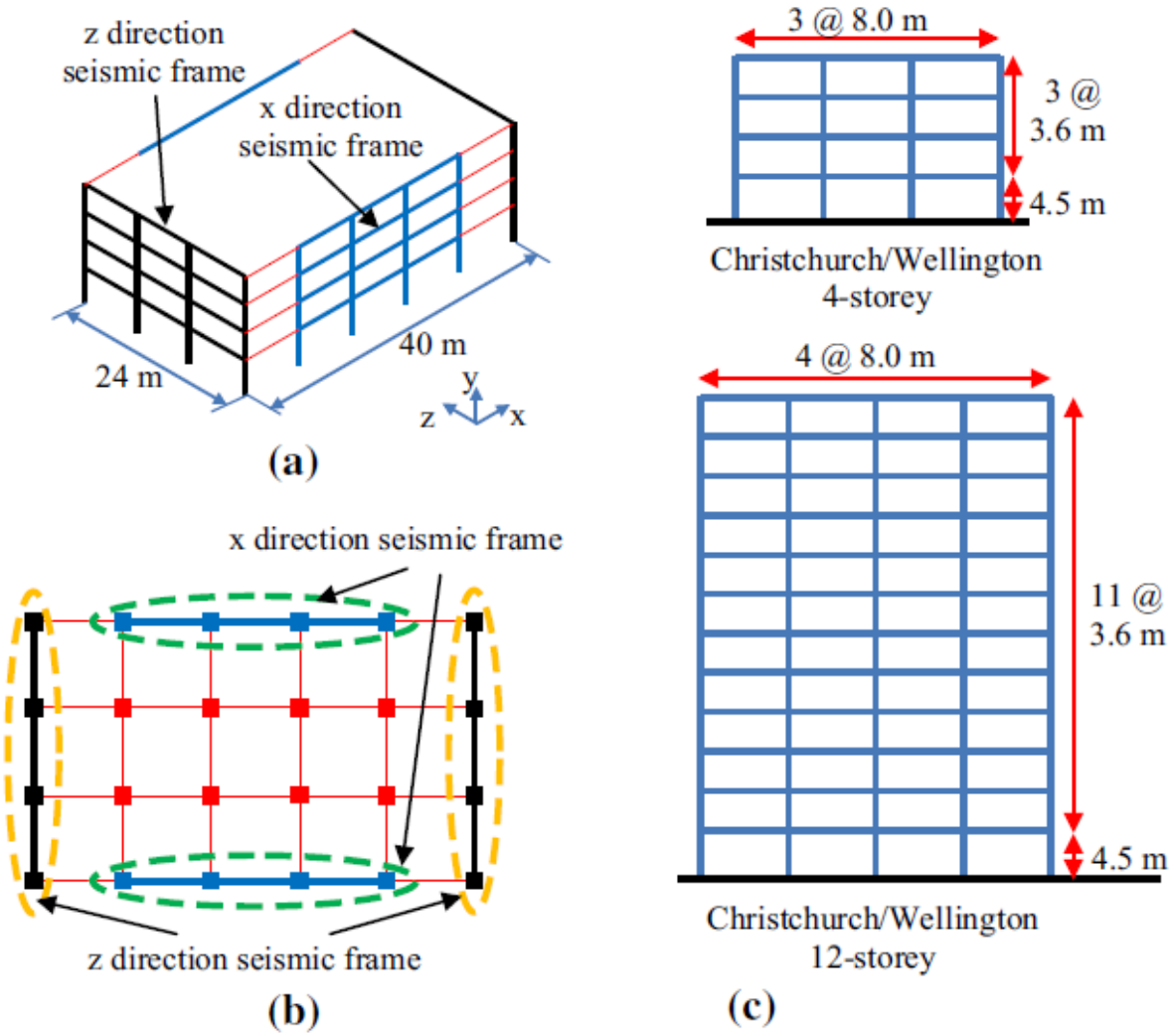

Figure 5.7 Case study building; (a) example of 4-storey isometric view, (b) example of plan view, and (c) frame elevations (Yeow *et al.* 2018).

5.3.2 Loss Assessment methodology

Loss assessment according the PEER centre's framework as described in Figure 1.13 including structural modelling, seismic hazard analysis and ground motion selection, and seismic loss estimation was performed according to the same methodology described in Yeow *et al.* (2018). A brief overview of the methodology is provided herein highlighting key aspects of the approach however for more detailed information refer to Yeow *et al.* (2018).

- Structural modelling and analysis
    - Two-dimensional inelastic structural analyses of all frames were performed in Ruaumoko 2D (Carr 2000) using large displacement analysis to account for P-delta effects and assuming Caughey (Caughey 1960) damping of 3% on all nodes.
    - For simplicity the partitions were not included within the building model

- Seismic hazard analysis and ground motion selection
    - Probabilistic seismic hazard analysis was performed for Christchurch (43.53°S, 172.64°E) for a shear wave velocity at 30 m depth (V_{s30}) of 250 m/s, Wellington (41.29°S, 174.78°E) for V_{s30} = 450 m/s on OpenSHA (Field *et al.* 2003) using New Zealand-specific rupture forecast models (Stirling *et al.* 2012) and attenuation relationships (Bradley 2013) for spectral acceleration at 1.0 s for the 4-storey buildings and 2.0 s for the 12-storey buildings.
    - Ground motion details are provided on the QuakeCore wiki page specific to this project (link in acknowledgements).
- Seismic loss estimation (including fragility and loss assessment)
    - Seismic loss estimation was performed in SLAT (Bradley 2011). The full list of component quantities (including structural components, non-structural drift sensitive components, and non-structural acceleration sensitive components), fragility functions, and consequence functions adopted in this study are provided on the QuakeCore wiki page specific to this project (link in acknowledgements). Fragility functions were obtained from literature or from PACT's (Applied Technology Council 2012) fragility library.

5.3.3 Loss Assessment results

The loss assessment was conducted for each of the four fragility parameter cases shown in Table 5.4: (1) Traditional/baseline specimens, (2) flexible track specimens, (3) seismic gap steel stud specimen, and (4) seismic gap timber stud specimen. The repair cost breakdown by component for the fourth hazard level and traditional partitions for each building type is shown in Figure 5.8. The expected annual loss as a percentage of total building replacement cost for each of the four buildings with each of the four partition wall systems is shown in Table 5.6. Noting that the building replacement value is assumed to be 25,614,000 (USD) and 5,614,000 (USD) for 12-st and 4-st case study buildings, respectively.

The expected repair cost (in USD) at each hazard level for each of the different partition types for the Christchurch 4-storey, Wellington 4-storey, Christchurch 12-storey, and Wellington 12-storey is shown in Table 5.7, Table 5.8, Table 5.9, and Table 5.10 respectively. Note the Hazard levels 1 to 9 correspond to (1) 80%, (2) 50%, (3) 20%, (4) 10%, (5) 5%, (6) 2%, (7) 1%, (8) 0.5%, and (9) 0.2% probability of exceedance in 50 years, respectively.

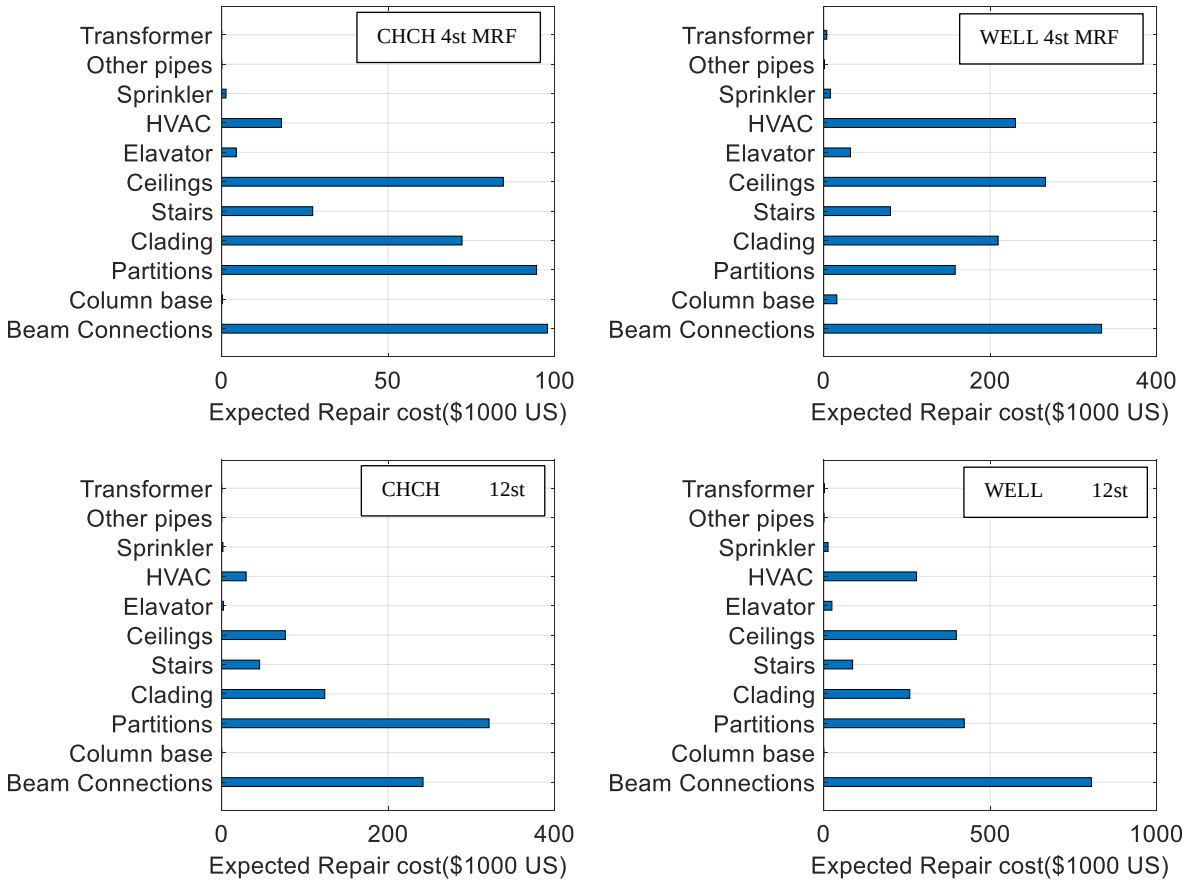

Figure 5.8. Repair cost breakdown by component for the fourth hazard level with traditional partition (return period of 500yrs)

Table 5.6. Expected annual loss (%) for each case study building with different partitions type

Case Study Building	Traditional	Flexible track	Seismic gap (steel)	Seismic gap (timber)
CHCH 4-st	0.097	0.115	0.0825	0.0775
WELL 4-St	0.00159	0.00161	0.00151	0.00148
CHCH 12-St	0.0453	0.0479	0.0341	0.0305
WELL 12-St	0.0802	0.0851	0.0780	0.0761

Table 5.7. Expected partition repair cost for CHCH 4-st case study (1000 USD)

Hazard Level	Traditional	Flexible track	Seismic gap (steel)	Seismic gap (timber)
1	22.29	50.27	7.89	3.35
2	38.08	62.53	16.16	8.08
3	51.60	66.68	24.84	14.03
4	58.47	67.35	32.24	21.23
5	61.47	67.50	36.98	28.02
6	64.22	67.55	42.70	36.91
7	65.26	67.58	46.77	43.75
8	66.41	67.54	50.31	49.83
9	68.64	68.10	55.18	57.24

Table 5.8. Expected partition repair cost for WELL 4-st case study (1000 USD)

Hazard Level	Traditional	Flexible track	Seismic gap (steel)	Seismic gap (timber)
1	6.07	10.25	1.22	0.33
2	23.44	28.18	8.32	3.64
3	56.67	43.59	29.57	15.68
4	76.62	61.15	51.46	34.45
5	95.06	81.79	73.08	55.93
6	104.86	97.32	90.50	76.92
7	108.88	102.55	96.19	83.42
8	108.39	103.75	98.36	87.24
9	136.17	125.62	117.11	99.99

Table 5.9. Expected partition repair cost for CHCH 12-st case study (1000 USD)

Hazard Level	Traditional	Flexible track	Seismic gap (steel)	Seismic gap (timber)
1	65.19	96.59	19.33	7.13
2	122.94	139.55	44.99	20.19
3	193.58	165.61	83.39	41.27
4	226.48	176.72	108.37	55.68
5	244.29	185.85	126.44	67.67
6	265.65	199.46	151.85	85.30
7	277.46	211.70	169.31	101.63
8	285.09	224.44	187.36	122.82
9	293.71	242.22	211.48	150.31

Table 5.10. Expected partition repair cost for WELL 12-st case study (1000 USD)

Hazard Level	Traditional	Flexible track	Seismic gap (steel)	Seismic gap (timber)
1	10.25	15.92	1.98	0.60
2	51.61	78.14	14.31	5.15
3	181.96	161.90	80.09	39.74
4	257.49	196.23	142.41	80.35
5	263.87	226.83	189.39	125.89
6	272.11	259.57	234.33	181.09
7	281.76	266.42	244.84	195.94
8	295.78	280.87	261.52	223.53
9	301.88	282.71	265.14	230.58

5.4 Discussion of potential implications

Figure 5.8 shows the repair cost breakdown of each of each component for each case study building for the traditional/baseline specimens following a hazard level four (500 yr return period) earthquake event. This event corresponds to the typical ULS design earthquake event for an importance level 2 building. As can be seen from this figure partitions contribute to the larger percentage of the losses in the Christchurch buildings and contribute to the most significant part of the losses of any component in the Christchurch 12-storey case study building. However, the variation in the proportion of partition repair cost to that of other elements is significant. Highlighting the fact the influence of incorporating low damage systems is suspected to be highly dependent on the building system they are to be incorporated within.

Table 5.6 presents the expected annual loss (%) for each building for each of the four systems. The expected annual loss (%) for each of the buildings followed the same pattern when including the different partition systems. The order (lowest to highest) of each system in terms of the expected annual losses of each building when incorporating the system was, (1) the seismic gap timber stud system, (2) the seismic gap steel stud system, (3) the traditional/baseline system, and (4) the flexible track system. It can be seen from Table 5.6 that there is significant variation in the impact of using the different systems on the expected annual loss for each of the case study buildings. For the seismic gap timber stud system, which incurred the greatest reduction in expected annual losses for each case study building, the reduction in expected annual losses in comparison to the losses found when using the traditional system ranged from a 5% reduction to a 30% reduction. This further reinforces that while there is a benefit to the using low damage partition systems in each building the extent of reduction in expected annual losses is significant dependent on the particular building and location.

Tables 5.7 – 5.10 report the expected partition repair cost for each of the case study buildings incorporating each of the four systems at each hazard level. At large hazard levels (Hazard level 4 - 9)

the expected repair costs in the each of the systems tends to plateau, this is likely because DS3 has been triggered in most specimens and the relatively small increasing repair cost at larger hazard levels can be attributed to the flattening of the DS3 fragility curve. The seismic gap steel and timber stud specimens begin to plateau at higher hazard levels because the median drift at the onset of DS3 for these specimens is significantly higher as can be seen in Table 5.4. It can also be seen that while the flexible track specimens have larger repair costs at hazard levels 1 and 2 in comparison to the traditional system at hazard levels 3 - 9, they typically have smaller repair costs. This can be attributed to the fact that DS2 in the flexible track systems triggers much earlier than for the traditional system but DS3 triggers at a higher level. The resulting expected annual losses for the flexible track system is higher than the traditional system which reinforces findings from past studies (Aslani and Miranda 2005, Bradley *et al.* 2009) which observed that the greatest contribution to expected annual losses arises from low to moderate intensity shaking seismic events (low hazard levels). This is one of the reasons it is suspected that the improved behaviour of the seismic gap systems at higher hazard levels in comparison to the seismic gaps steel and timber systems is not as significant as the improved behaviour at lower hazard levels.

While clear trends can be observed from the seismic loss assessment incorporating the different partition systems there are a number of limitations upon any conclusions that can be drawn from these results. Including,

- The effect of the partitions wall systems on the dynamic response of structures was not considered. As shown in Table 5.1, the hysteretic parameters are significantly different, which may impact the structural analysis results.
- Only full-height specimens have been incorporated within the modelling. In real buildings, different partition wall configurations will exist within each structure including partial-height walls, walls with window openings, walls with bookcase or other attachments (which are typically acceleration sensitive), and other configurations.
- The effects of differing wall heights on fragility has not been considered. The walls tested in this study were all approximately 2.4 m high whereas the storey height of the case study buildings are 4.5 m at the base level and 3.6 m on the storey's above.
- The loss functions for each of the walls was the same as for a traditional New Zealand partition wall within the particular economic environment of Christchurch (Dhakal *et al.* 2016).
- The repair cost are estimates made assuming that finishing, replacement of gypsum board, and replacement of framing is required at every location once a particular damage state initiates. This is not accurate for the flexible track system, as the wallboard damage observed for DS2 was highly localised, and the point at which DS2 is reported to initiate does not imply the

wallboard in every location requires replacement. Therefore, it is expected that the losses determined in this assessment overestimate the true losses that would be incurred.

- The repair cost used for the seismic gap timber stud system was made assuming the same DS1 repair action as for a traditional system. In reality, the DS1 triggered in this system was due to damage to the acrylic gap filler in the seismic gaps, requiring replacement of the gap filling material, whereas the repair cost used for traditional systems assumes the repair action required is re-plastering of the joints and re-painting, which was observed at larger drifts in the seismic gap timber stud specimen.

6. CONCLUSIONS

6.1 Findings in relation to research objectives

This research project aimed to further the development of low damage seismic systems for non-structural partition walls in order to facilitate their adoption by industry to assist with reducing the losses associated with the maintenance and repair cost of buildings across their design life. In particular, this study focused on the behaviour of steel-framed partition walls systems with novel detailing that aim to be "low-damage" and are designed according to common practice for walls used in commercial and institutional buildings in New Zealand. The findings of this study presented in respect of the three main research objectives are listed below:

1. Investigate the performance of the flexible track system proposed by Davies *et al.* (2011) and industry by experimental testing of full-scale specimens in order to:

   a. *Validate the performance of this system using NZ materials and construction practices.*

      Test specimens were designed that represent a version of the flexible track system proposed by Davies *et al.* (2011) built with NZ materials and construction practices in collaboration with Industry partners who are using this system in practice. However, a construction error was made whereby a single top track slab to concrete anchor was left in at the three-way wall junction. The experimental tests were still deemed worthwhile since such errors will also occur in practice and because the behaviour of the wall system could be examined with this fixing in mind.

   b. *Derive its fragility function for use within the PBEE framework.*

      Three specimens with partly sliding detailing, consisting of top tracks that are not bolted at intersections. This is the minimum number of specimens required for development of empirically derived fragility functions. The fragility parameter for the specimens were reported and used in a subsequent loss estimation according to the PBEE framework. In addition, the force-displacement behaviour has been reported, energy dissipation computed, and parameters of the Wayne-Stewart hysteretic model fitted to the test results. This information may be useful for those interested in undertaking refined analyses of partition walls.

c. *Investigate the performance of the system when tested under uni-directional loading applied at an oblique angle to the wall and with a unique return wall configuration including an angled return wall.*

Specimens were aligned at 30° subjected to quasi-static cyclic testing. Their y-shaped configuration meant bi-directional behaviour could be examined. No damage was observed along the field of the wall due to out-of-plane displacements (other than to sealant). The results showed that the behaviour of the wall specimens depends on the direction of loading and that the walls deform as a unit rather than separately. Therefore, bi-directional behaviour is deemed significant, even if its impact cannot be directly quantified by this test.

d. *And investigate the behaviour of a fire stop sealant used at the top boundary of the plasterboard linings under quasi-static cyclic loading.*

Damage to sealant in the specimens first occurred around areas of high deformability (i.e. at the junctions) at drifts greater than 0.36%. Whereas damage to sealant away from junctions typically occurred at higher drifts (0.7-1%) irrespective of whether this was in the primary length of the wall or in a return wall (i.e. in-plane or out-of-plane demand). Results suggest that the bond between plasterboard and sealant is important for the seismic performance. It was also noted that after the sealant had cured there was a significant number of defects in the bond to the plasterboard. Therefore, it is advised that careful quality control is maintained when applying similar products, as defects in the bond may hamper the effectiveness of their fire and acoustic performance and reduce their ability to withstand seismic movement.

2. Investigate the performance of the seismic gap partition wall systems proposed in a number of studies, in particular the detailing used in Tasligedik *et al.* (2015) further developed in this study with input from industry, by experimental testing of full-scale specimens in order to:

a. *Validate the performance of this system using NZ materials and construction practices.*

Two specimens were tested constructed using the details provided by Tasligedik *et al.* (2015) and further developed in collaboration with industry: one steel stud specimen and one timber study specimen. In addition to providing drift capacities, the force-displacement behaviour has been reported, and the energy dissipation computed.

b. *Investigate the performance of the system when tested under uni-directional loading applied at an oblique angle to the wall and with a unique return wall configuration including an angled return.*

Specimens were aligned at 35° and subjected to quasi-static cyclic testing. The y-shaped configuration meant bi-directional behaviour could be examined. Out-of-plane displacements imposed and return wall configuration did not appear to significantly impact the onset of plaster cracking in the specimens.

c. *Investigate alternate detailing of the specimens including increasing horizontal gap widths, including an intermediate joint, and using timber studs instead of steel studs.*

The steel stud specimen had horizontal gaps at the wall ends totalling 9 mm; and the timber stud specimen with horizontal gaps totalling 22 mm. Damage state 1, 2, & 3 initiated at significantly larger inter-storey drifts. An equation was used to predict the formation of DS1. This equation provided an accurate estimate for DS1 in specimen 1 where plaster cracking and debonding of the gap filler material occurred simultaneously. For specimen 2 the equation accurately estimated the onset of plaster cracking but not debonding of the gap filler material, which initiated earlier. An equation was proposed to predict the onset of DS2. This equation provided a lower bound for both specimens tested herein and when used to predict the results of previous experimental tests on seismic gap systems.

d. *Investigate the behaviour of using an acrylic gap filler within the seismic gaps and its influence on the behaviour of the system under quasi-static loading.*

The gap filling material appeared to reduce the drift at the onset of DS1 for specimen 2. However, it had a beneficial effect on the re-centring behaviour of the linings. If a gap-filling material is not used, it is suggested that a pivot system is utilized in order to prevent residual gap development.

3. Investigate the potential implications of using the systems studied herein compared with traditionally detailed partition wall systems within multi-storey buildings using the PBEE loss assessment method.

A loss assessment according to the PBEE methodology was conducted on four steel MRF case study buildings: (1) a 4-storey building designed for the Christchurch region, (2) a 4-storey building designed for the Wellington region, (3) a 12-storey building designed for the Christchurch region, and (4) a 12-storey building designed for the wellington region. The fragility parameters for a traditional partition system, the flexible track partition system, and the seismic gap steel stud and timber stud partition systems were included within the loss assessment. The order (lowest to highest) of each system in terms of the expected annual losses of each building when incorporating the system was, (1) the seismic gap timber stud system, (2) the seismic gap steel stud system, (3) the traditional/baseline system, and (4) the flexible track system.

For the seismic gap timber stud system, which incurred the greatest reduction in expected annual losses for each case study building, the reduction in expected annual losses in comparison to the losses found when using the traditional system ranged from a 5% reduction to a 30% reduction. This reinforces the fact that while there is a benefit to the using low damage partition systems in each building the extent of reduction in expected annual losses is significant dependent on the particular building and location.

The flexible track specimens had larger repair costs at small hazard levels compared to the traditional system but smaller repair costs at larger hazard levels. However, the resulting expected annual losses for the flexible track system was higher than the traditional system which reinforces findings from past studies which observed that the greatest contribution to expected annual losses arises from low to moderate intensity shaking seismic events (low hazard levels).

6.2 Limitations

This study aimed to provide an estimate of the fragility parameters and to investigate the behaviour of the flexible track system; to investigate the behaviour of the seismic gap system; and to estimate the expected annual losses of using these systems within NZ buildings in a loss assessment according to the PBEE framework. There were, however, were several limitations on the conclusions drawn from the experiments testing phase:

- The construction error made during construction of the three flexible track system specimens is suspected to have significantly altered their behaviour and therefore the results of the testing of the flexible track systems does not accurately describe the true fragility or behaviour of specimens with flexible track system detailing.
- Only three tests on the flexible track system specimens were used to derive the fragility parameters. This is the minimum required to provide an estimate of the dispersion. A more accurate estimate of the dispersion could be provided by conducting more tests.
- The derived fragility parameters for the flexible track system represent the fragility of an arbitrary wall configuration as of the three specimens tested one included a doorway. However, this excludes a number of variables that would existing within a building including different return wall configurations, window openings, or varying specimen geometry.
- Only a single specimen for the seismic gap steel system and the seismic gap timber specimen was tested. Therefore, conclusions are not able to be drawn about the probable degree of variation in response between specimens of the same detailing.
- Particle tracking results were not able to be used due to insufficiencies within the camera setup, lighting, and data recording.
- Of the five specimens tested all were designed with approximately the same wall configuration and specimen geometry. The effects of differing wall aspect ratios and heights is unknown.

And a number of limitations on the loss assessment phase of this study:

- The effect of the partitions wall systems on the dynamic response of structures was not considered in the loss assessment.
- Only full-height specimens were used to represent the partition walls within the case study buildings. In real buildings, different partition wall configurations will exist within each structure including partial-height walls, walls with window openings, walls with bookcase or other attachments (which are typically acceleration sensitive), and other configurations.
- The walls tested in this study were all approximately 2.4 m high whereas the storey height of the case study buildings is 4.5 m at the base level and 3.6 m for the storey's above. The effect of wall-height on fragility of the specimens is unknown.

- The loss functions for each of the walls was the same as for a traditional New Zealand partition wall within the particular economic environment of Christchurch and may not accurately represent the damage repair cost relationship of any of the systems studied within the loss assessment.
- The results of the loss assessment are applicable to the buildings assessed alone i.e. 4- and 12-storey steel MRF buildings located within the Christchurch and Wellington regions of New Zealand.

6.3 Recommendations for Future Work

As such, the following suggestions are made for future research on the topic of this study:

- Development of fragility functions for the seismic gap partition wall systems tested herein.
- Determination of appropriate damage to repair cost relationships for each of the tested systems to provide more accurate inputs for inclusion within loss assessments according to the PBEE methodology.
- Component testing of fire stop sealants to determine its damage deformation relationship as this has significant implications for post-earthquake fire performance and no experimental testing the author is aware of has been conducted to help determine the damage repair relationship.
- Experimental testing of partly sliding system including improved wall end details as suggested in Chapter 3.
- Testing of the additional proposed low damage partitions systems including the systems collected during Industry workshops during the initial stages of this study. Details of these specimens can be found in Appendix XX.
- Loss assessment including the effect of the partition wall systems effect on structural response; more case study buildings and locations; and with loss functions appropriate to the particular systems to be studied.

REFERENCES

Adham, S.A., Avanessian, V., Hart, G.C., Anderson, R.W., Elmlinger, J., and Gregory, J., 1990. Shear wall resistance of lightgage steel stud wall systems. Earthquake Spectra, 6 (1), 1–14.

American Society of Civil Engineers, 2006. Seismic Rehabilitation of Existing Buildings. ASCE/SE 41-06, ASCE, Reston, Virginia, USA. https://doi.org/10.1061/9780784408841

Applied Technology Council, 2007. Interim Testing Protocols for Determining the Seismic Performance Characteristics of Structural and Nonstructural Components. FEMA 461, ATC, California, USA.

Applied Technology Council, 2012. Seismic Performance Assessment of Buildings. FEMA P-58, ATC, California, USA.

Araya-Letelier, G. and Miranda, E., 2012. Novel Sliding/Frictional Connections for Improved Seismic Performance of Gypsum Wallboard Partitions. Proceedings of 15th World Conference on Earthquake Engineering, Lisbon, Portugal, 24-28 September 2012.

Arifin, F.A., Sullivan, T.J., and Macrae, G.A., 2017. Identification of Cost-Effective Retrofit and/or Rehabilitation Strategies for Steel Buildings. Master's Thesis, University of Canterbury, Christchurch, New Zealand, 306 pp. http://hdl.handle.net/10092/15010

Aslani, H. and Miranda, E., 2005. Probabilistic earthquake loss estimation and loss disaggregation in buildings, Report No. 157. John A. Blume Earthquake Engineering Centre, Stanford University, Stanford, California.

Baird, A., Tasligedik, A.S., Palermo, A., and Pampanin, S., 2014. Seismic performance of vertical nonstructural components in the 22 February 2011 Christchurch earthquake. Earthquake Spectra, 30 (1), 401–425.

Bradley, B., Dhakal, R., Cubrinovsky, M., and MacRae, G.A., 2009. Seismic loss estimation for efficient decision making. Bulletin of the New Zealand Society for Earthquake Engineering, 42 (2), 96–110.

Bradley, B.A., 2011. SLAT: seismic loss assessment tool (version 1.16). Computer Program Library, Department of Civil and Natural Resources Engineering, University of Canterbury.

Bradley, B.A., 2013. New Zealand-specific pseudospectral acceleration ground-motion prediction equation for active shallow crustal earthquakes based on foreign models. Bulletin of the Seismological Society of America, 103(3), 1801–1822. http://dx.doi.org/10.1785/0120120021

Calvi, G.M., Priestley, M.J.N., and Kowalsky, M.J., 2007. Displacement-Based Seismic Design of Structures. IUSS Press, Pavia, Italy.

Carr, A., 2000. Ruaumoko 2D: Software for inelastic dynamic analysis. Computer Program Library, Department of Civil and Natural Resources Engineering, University of Canterbury, Christchurch, New Zealand.

Carr, A., 2008. Ruaumoko Manual - Volume 5: Appendices. Department of Civil and Natural Resources Engineering, University of Canterbury, Christchurch, New Zealand. DOI: 10.13140/RG.2.1.4493.7127

Caughey, T.K., 1960. Classical normal modes in damping linear systems. Journal of Applied Mechanics, 27 (2), 269–271. https://doi.org/10.1115/1.3643949

Davies, R.D., Retamales, R., Mosqueda, G., and Filiatrault, A., 2011. Experimental Seismic Evaluation, Model Parameterization, and Effects of Cold-Formed Steel-Framed Gypsum Partition Walls on the Seismic Performance of an Essential Facility. Technical Report MCEER-11-0005. University at Buffalo, State University of New York, New York, 221 pp.

Deierlein, G.G., Krawinkler, H., and Cornell, C.A., 2003. A framework for performance-based earthquake engineering. Proceedings of 2003 Pacific Conference on Earthquake Engineering. Christchurch, New Zealand, 140–148.

Dhakal, R.P., 2010. Damage to non-structural components and contents in 2010 Darfield earthquake. Bulletin of the New Zealand Society for Earthquake Engineering, 43 (4), 404–410.

Dhakal, R.P., Pourali, A., and Saha, S.K., 2016. Simplified Seismic Loss Functions for Suspended Ceilings and Drywall Partitions. Bulletin of the New Zealand Society for Earthquake Engineering Special Issue on Seismic Performance of Non-Structural Elements (SPONSE), 49 (1), 64–78.

Field, E.H., Jordan, T.H., and Cornell, C.A., 2003. OpenSHA: A Developing Community-Modeling Environment for Seismic Hazard Analysis. Seismological Research Letters, 74, 406–419.

Filiatrault, A., Uang, C.-M., Folz, B., Chrstopoulos, C., and Gatto, K., 2001. Reconnaissance Report of the February 28, 2001 Nisqually (Seattle-Olympia) Earthquake. Structural Systems Research Project Report No. SSRP-2001/02. Department of Structural Engineering, University of California, San Diego La Jolla, California, USA.

Freeman, S.A., 1971. Third Progress Report on Racking Tests of Wall Panels. Report JAB-99-54, University of California, Berkeley, 270 pp.

Girard, J.D. and Tarpy, T.S., 1982. Shear Resistance of Steel-stud Wall Panels. Proceedings of 6th International Specialty Conference on Cold-Formed Steel Structures, Missouri, U.S.A. http://scholarsmine.mst.edu/isccss/6iccfss/6iccfss-session8/3

Jenkins, C., Soroushian, S., Rahmanishamsi, E., and Maragakis, E.M., 2016. Experimental fragility analysis of cold-formed steel-framed partition wall systems. Thin-Walled Structures, 103, 1760–1773.

Khakurel, S., Dhakal, R.P., Yeow, T.Z., and Saha, S.K., 2020. Performance Group Weighting Factors for Rapid Seismic Loss Estimation of Buildings of Different Usage. Earthquake Spectra, In Press.

Krawinkler, H., Parisi, F., Ibarra, L., Ayoub, A., and Medina, R., 2001. Development of a Testing Protocol for Woodframe Structures. CUREE Publication No. W-02, Consortium of Universities for Research in Earthquake Engineering (CUREE), Richmonda, CA, USA.

Lee, T.H., Kato, M., Matsumiya, T., Suita, K., and Nakashima, M., 2007. Seismic Performance Evaluation of Nonstructural Components: Drywall Partitions. Earthquake Engineering & Structural Dynamics, 36 (3), 367–382.

Magliulo, G., Petrone, C., Capozzi, V., Maddaloni, G., Lopez, P., and Manfredi, G., 2014. Seismic performance evaluation of plasterboard partitions via shake table tests. Bulletin of Earthquake Engineering, 12 (4), 1657–1677.

McMullin, K.M. and Merrick, D.S., 2007. Seismic Damage Thresholds for Gypsum Wallboard Partition Walls. Journal of Architectural Engineering, 13 (1), 22–29.

Miranda, E., Mosqueda, G., Retamales, R., and Pekcan, G., 2012. Performance of nonstructural components during the 27 February 2010 Chile earthquake. Earthquake Spectra, 28 (S1), S453–S471.

Mulligan, J., Sullivan, T.J., and Dhakal, R.P., 2020a. Experimental Seismic Performance of Partly-Sliding Partition Walls. Journal of Earthquake Engineering, In Press.

Mulligan, J., Sullivan, T.J., and Dhakal, R.P., 2020b. Experimental Study of the Seismic Performance of Plasterboard Partition Walls with Seismic Gaps. Bulletin of the New Zealand Society for Earthquake Engineering, In Press.

Pali, T., Bucciero, B., Terracciano, M.T., Macillo, V., Fiorino, L., and Landolfo, R., 2017. In-plane quasi-static cyclic tests on lightweight steel drywall non-structural partition walls. ce/papers, 1 (2-3), 2857–2866.

Pali, T., Macillo, V., Terracciano, M., Bucciero, B., Fiorino, L., and Landolfo, R., 2018. In-plane quasi-static cyclic tests of nonstructural lightweight steel drywall partitions for seismic performance evaluation. Earthquake Engineering & Structural Dynamics, 47 (6), 1566–1588.

Petrone, C., Magliulo, G., Lopez, P., and Manfredi, G., 2016. Out-of-Plane Seismic Performance of Plasterboard Partition Walls Via Quasi-Static Tests. Bulletin of the New Zealand Society for Earthquake Engineering, 49(1), 125-137.

Porter, K., 2018. A Beginner's Guide to Fragility, Vulnerability, and Risk. University of Colorado Boulder, USA, 136 pp. https://www.sparisk.com/pubs/Porter-beginners-guide.pdf

Porter, K., Kennedy, R., and Bachman, R., 2007. Creating fragility functions for performance-based earthquake engineering. Earthquake Spectra, 23 (2), 471–489.

Porter, K.A., 2003. An Overview of PEER's Performance-Based Earthquake Engineering Methodology. Proceedings of 9th International Conference on Applications of Statistics and Probability in Civil Engineering (ICASP9), Fransisco, California, USA, 973–980.

Restrepo, J.I. and Bersofsky, A.M., 2011. Performance characteristics of light gage steel stud partition walls. Thin-Walled Structures, 49 (2), 317–324.

Retamales, R., Davies, R., Mosqueda, G., and Filiatrault, A., 2013. Experimental Seismic Fragility of Cold-Formed Steel Framed Gypsum Partition Walls. Journal of Structural Engineering, 139 (8), 1285–1293.

Rihal, S.S., 1980. Racking Building Tests of Non-Structural Building Partitions. Report ARCE R90-1, California Polytechnic State University, San Luis Obispo, 123 pp.

Soong, T.T., Kao, A.S., and Vender, A., 1999. Nonstructural damage database. Technical Report MCEER-99-0014. University at Buffalo, State University of New York, New York, 72 pp.

Standards New Zealand, 1997. NZS3404:1997 Steel Structures Standard. Wellington.

Standards New Zealand, 2004. NZS 1170.5:2004 Structural Design Actions. Wellington.

Standards New Zealand, 2011. NZS 3604:2011 Timber-framed Buildings. Wellington.

Stirling, M.W., McVerry, G.H., and Gerstenberger, M., 2012. National Seismic Hazard Model for New Zealand: 2010 Update. Bulletin of the Seismological Society of America, 102(4), 1514–1542. https://doi.org/10.1785/0120110170

Taghavi, S. and Miranda, E., 2003. Response Assessment of Nonstructural Building Elements. Report 2003/05. Pacific Earthquake Engineering Research Centre, PEER, Berkeley, 96 pp.

Tasligedik, A.S., Pampanin, S., and Palermo, A., 2015. Low damage seismic solutions for non-structural drywall partitions. Bulletin of Earthquake Engineering, 13 (4), 1029–1050.

USGS, 1971. The San Fernando, California, earthquake of February 9, 1971; a preliminary report published jointly by the U.S. Geological Survey and the National Oceanic and Atmospheric Administration. Professional Paper 733, 254 pp. https://doi.org/10.3133/pp733

Whitman, R. V., Hong, S.-T., and Reed, J.W., 1973. Damage statistics for highrise buildings in the vicinity of the San Fernando Earthquake. Structures publication No. 363. Massachusetts Institute of Technology Department of Civil Engineering, Cambridge, 266 pp.

Winstone Wallboards, 2012. GIB® Fire Rated Systems. Winstone Wallboards, Auckland, 84 pp.

Winstone Wallboards, 2014. GIB® Site Guide. Winstone Wallboards, Auckland, 114 pp.

Wood, R.L. and Hutchinson, T.C., 2012. A Numerical Model for Capturing the In-Plane Seismic Response of Interior Metal Stud Partition Walls: Preliminary Coupled Analysis. Proceedings of 15th World Conference on Earthquake Engineering (15WCEE), Lisbon, Portugal.

Yeow, T.Z., Orumiyehei, A., Sullivan, T.J., MacRae, G.A., Clifton, G.C., and Elwood, K.J., 2018. Seismic performance of steel friction connections considering direct-repair costs. Bulletin of Earthquake Engineering. https://doi.org/10.1007/s10518-018-0421-x

APPENDICES

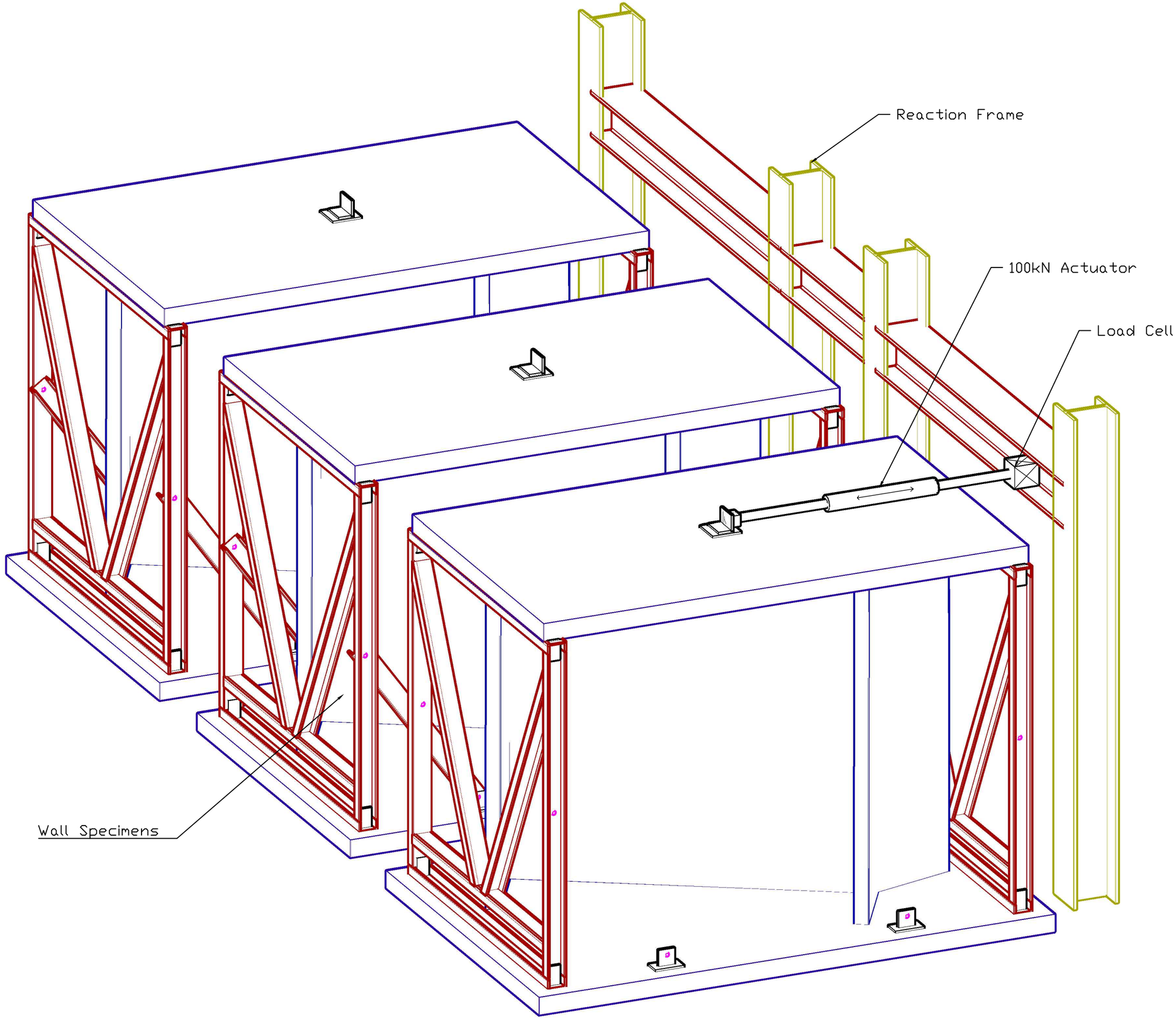

Experimental Test Setup – 3D

UNIVERSITY OF CANTERBURY
Te Whare Wānanga o Waitaha
CHRISTCHURCH NEW ZEALAND

UNIVERSITY OF CANTERBURY
Private Bag 4800
Christchurch 8140

CIVIL AND NATURAL RESOURCES ENGINEERING
69 Creyke Road
Christchurch 8140

NOTES:
Details of the reaction frame arrangement have not been confirmed

Dimensions in mm

SCALE: 1:25 @ A3

VER.	COMMENTS AND CHANGES	DATE
2	FOR CONSTRUCTION	17/DEC/17
1	Prelim	2/DEC/17

PROJECT:
Partitions Experimental Testing

DESIGNERS:
Joshua Mulligan

SUPERVISORS:
Timothy Sullivan

TITLE:
3D View of Experimental Test Setup

CODE: 64560538

DATE: 17-DEC-2017

PAGE: 001

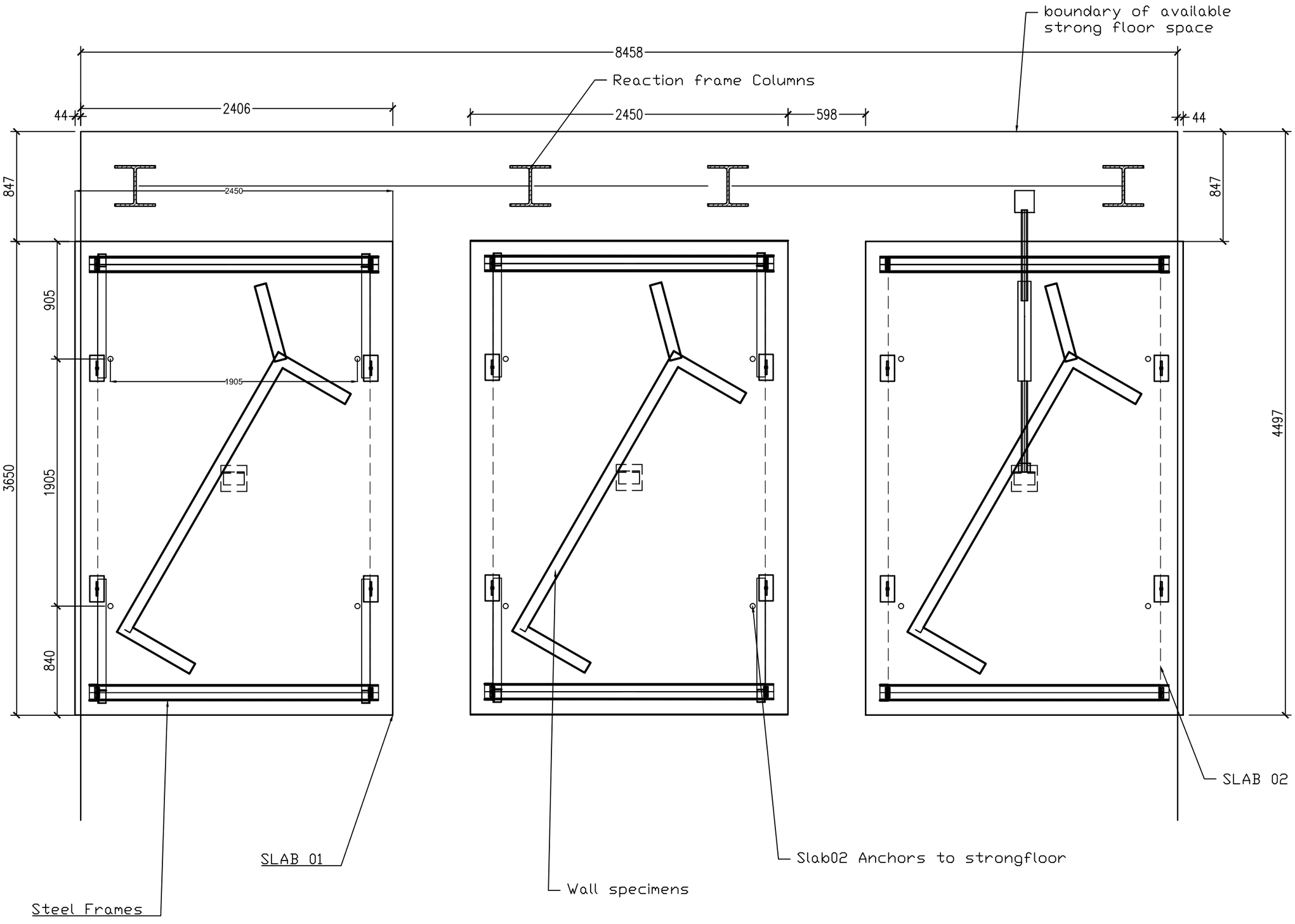

PLAN OF TEST SETUP WITH STRONGFLOOR

UNIVERSITY OF CANTERBURY
Te Whare Wānanga o Waitaha
CHRISTCHURCH NEW ZEALAND

UNIVERSITY OF CANTERBURY
Private Bag 4800
Christchurch 8140

CIVIL AND NATURAL RESOURCES ENGINEERING
69 Creyke Road
Christchurch 8140

NOTES:
Reaction frame already in lab

Dimensions in mm

SCALE: 1:30 @ A3

VER.	COMMENTS AND CHANGES	DATE
2	FOR CONSTRUCTION	17/DEC/17
1	Prelim	2/DEC/17

PROJECT:
Partitions Experimental Testing

DESIGNERS:
Joshua Mulligan

SUPERVISORS:
Timothy Sullivan

TITLE:
TESTING SETUP PLAN

CODE: 64560538

DATE: 17-DEC-2017

PAGE: 002

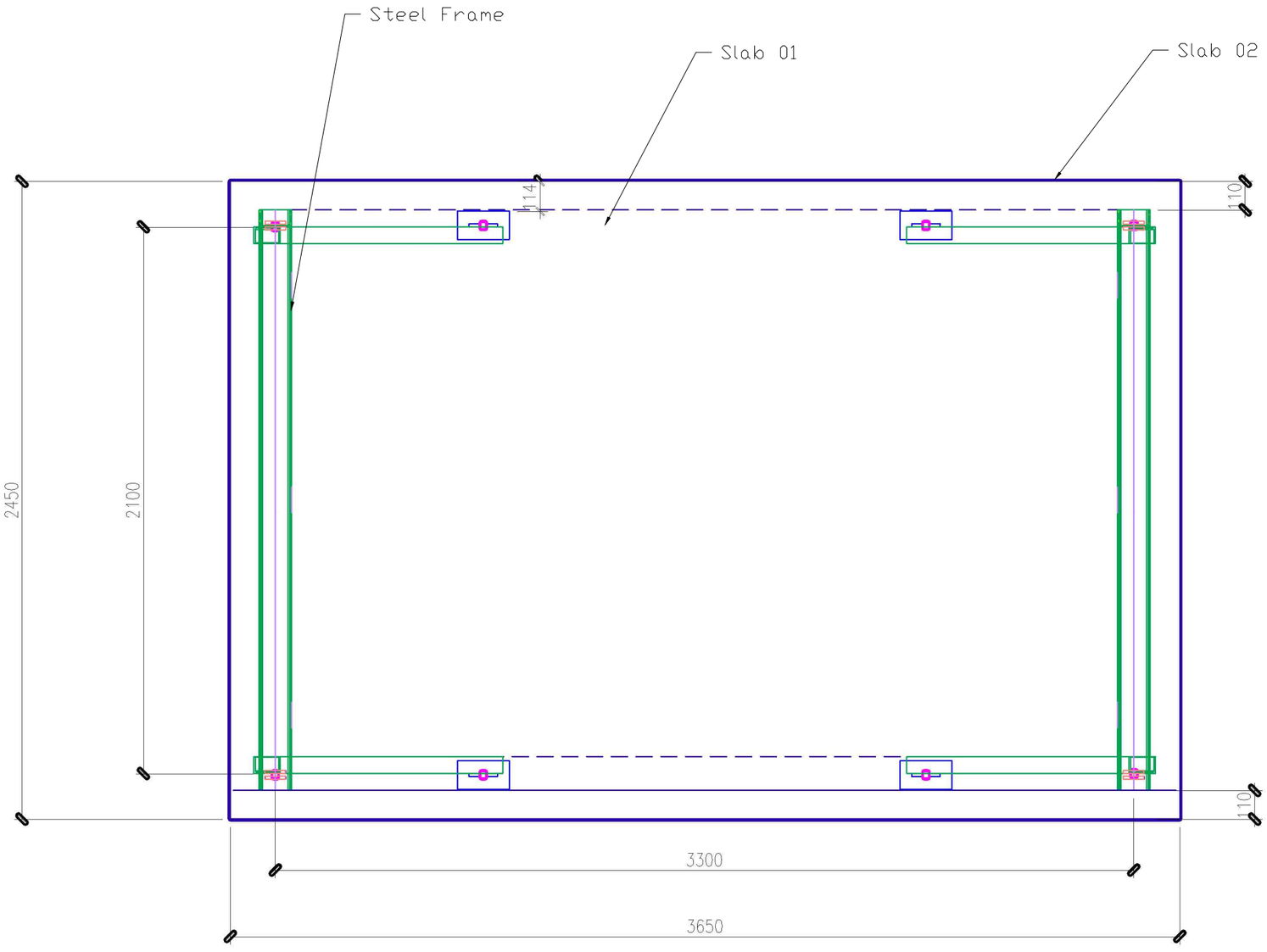

PLAN

UNIVERSITY OF CANTERBURY
Te Whare Wānanga o Waitaha
CHRISTCHURCH NEW ZEALAND

UNIVERSITY OF CANTERBURY
Private Bag 4800
Christchurch 8140

CIVIL AND NATURAL RESOURCES ENGINEERING
69 Creyke Road
Christchurch 8140

NOTES:
All frame members are 125x65 PFC steel sections

tolerances shall be +- 2mm

Dimensions in mm

SCALE: 1:20 @ A3

VER.	COMMENTS AND CHANGES	DATE
2	FOR CONSTRUCTION	17/DEC/17
1	Prelim	2/DEC/17

PROJECT:
Partitions Experimental Test Setup

DESIGNERS:
Joshua Mulligan

SUPERVISORS:
Timothy Sullivan

TITLE:
Testing Frame Plan

CODE: 64560538

DATE: 17-DEC-2017

PAGE: 003

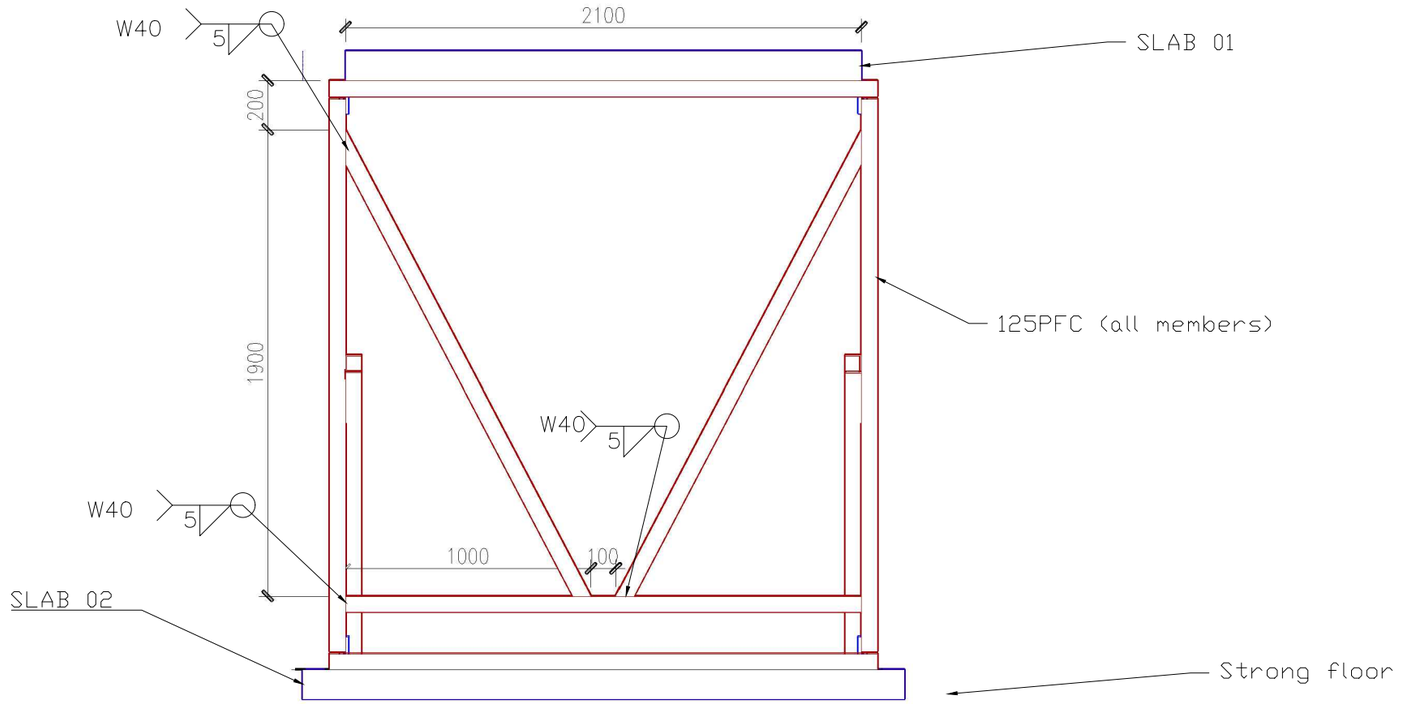

East Elevation

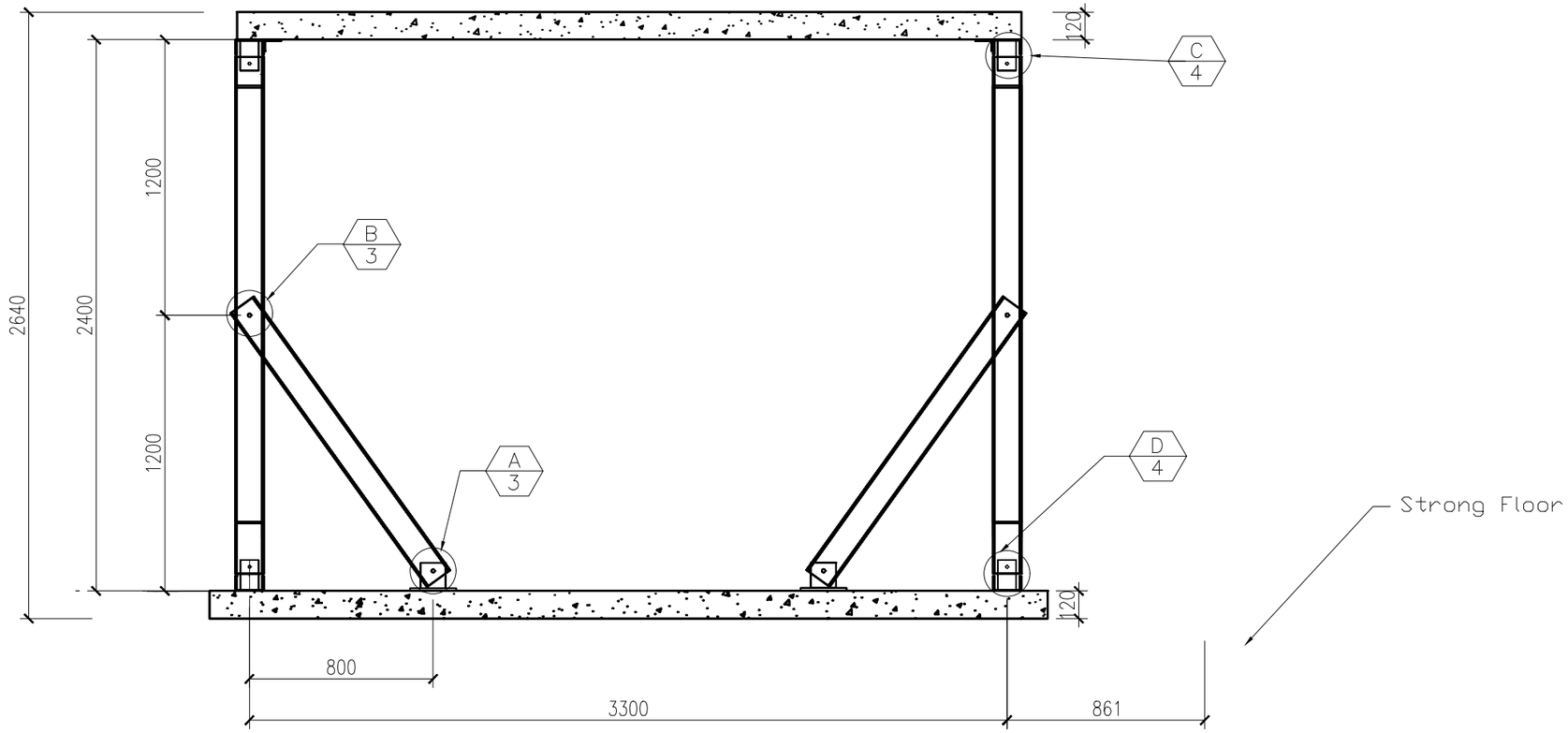

North Elevation

UNIVERSITY OF CANTERBURY
Te Whare Wānanga o Waitaha
CHRISTCHURCH NEW ZEALAND

UNIVERSITY OF CANTERBURY
Private Bag 4800
Christchurch 8140

CIVIL AND NATURAL RESOURCES ENGINEERING
69 Creyke Road
Christchurch 8140

NOTES:

All steel frame members are 125 PFC

Steel Frames are identical

Dimensions in mm

SCALE: 1:25 @ A3

VER.	COMMENTS AND CHANGES	DATE
2	FOR CONSTRUCTION	17/DEC/17
1	Prelim	2/DEC/17

PROJECT:
Partitions Experimental Test Setup

DESIGNERS:
Joshua Mulligan

SUPERVISORS:
Timothy Sullivan

TITLE:
Steel Testing Frame Elevations

CODE: 64560538

DATE: 17-DEC-2017

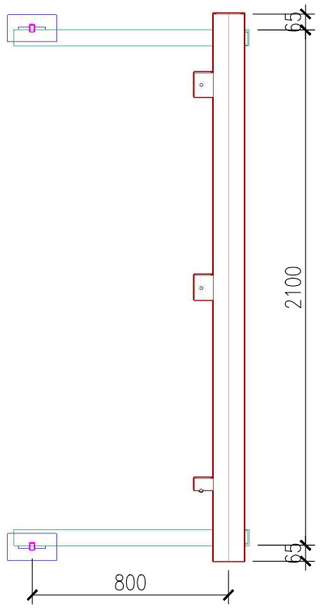

Steel Frame Plan

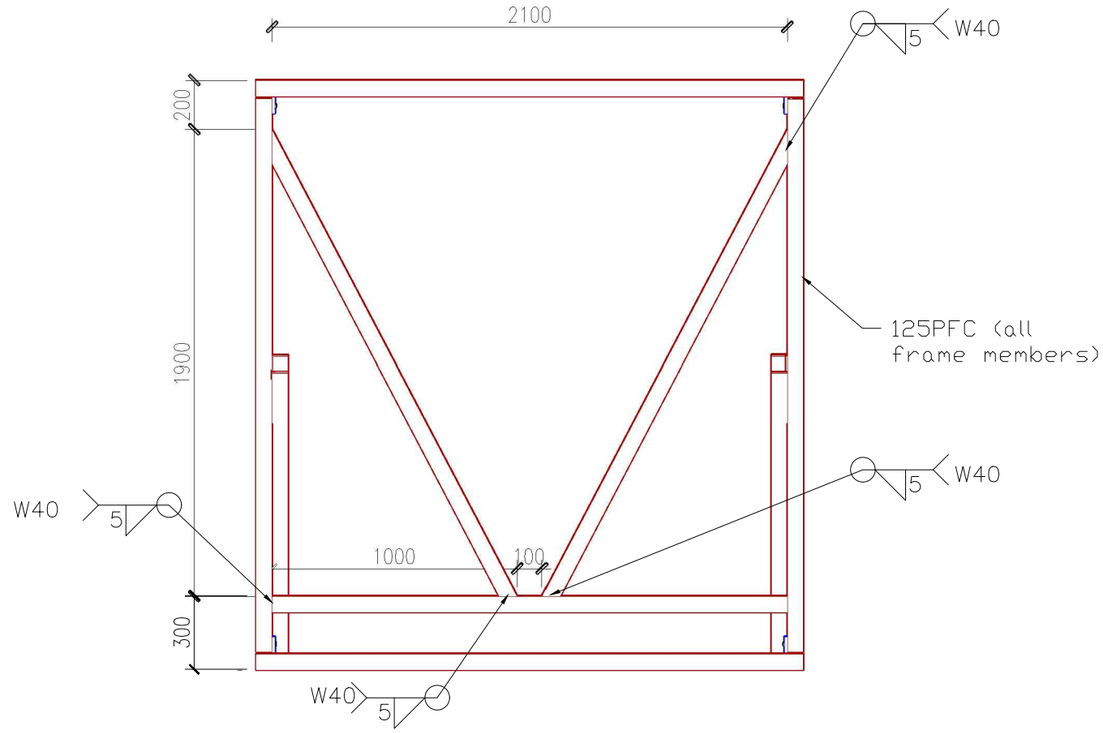

Steel Frame Front Elevation

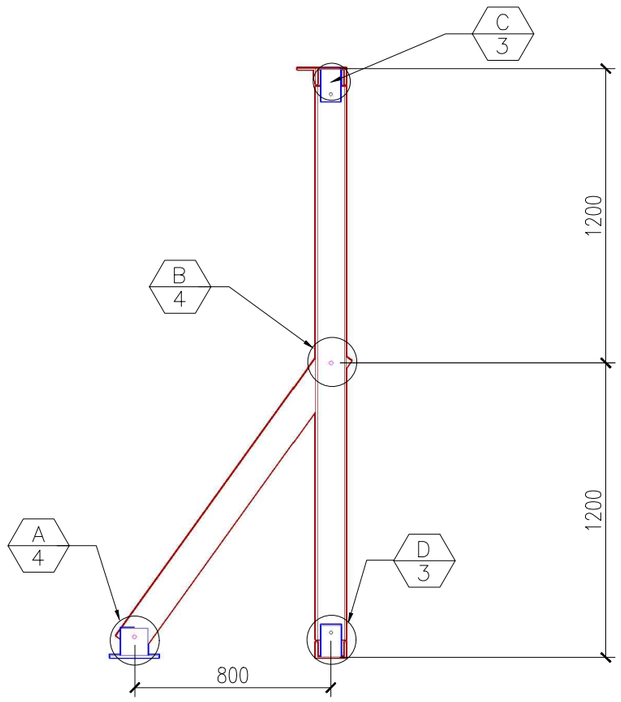

Steel Frame Side Elevation

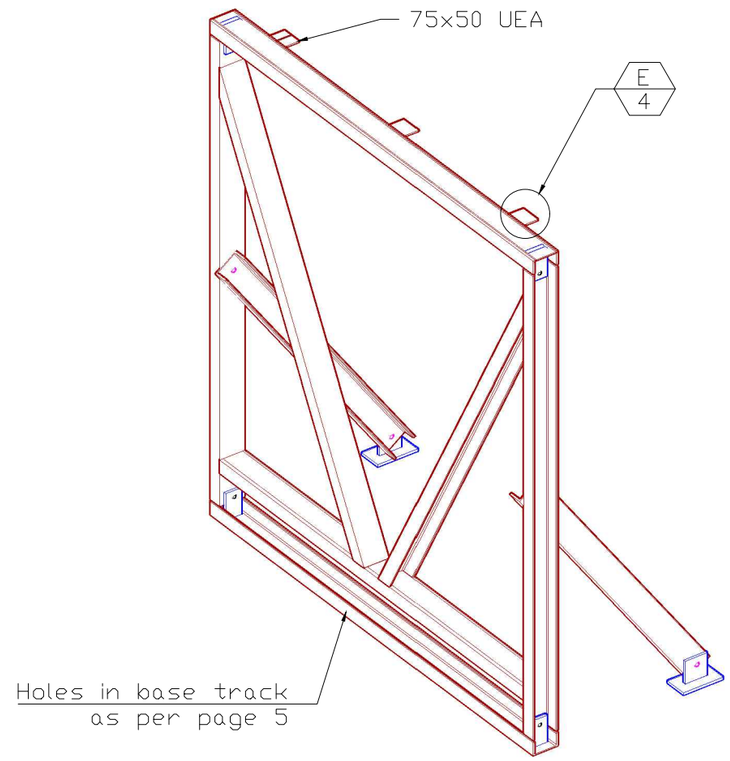

Steel Frame 3D

UNIVERSITY OF CANTERBURY
Te Whare Wānanga o Waitaha
CHRISTCHURCH NEW ZEALAND

UNIVERSITY OF CANTERBURY
Private Bag 4800
Christchurch 8140

CIVIL AND NATURAL
RESOURCES ENGINEERING
69 Creyke Road
Christchurch 8140

NOTES:

All steel frame members are 125 PFC

Steel Frames are symmetric about the centre

All welds are SP

Dimensions in mm

SCALE: 1:25 @ A3

VER.	COMMENTS AND CHANGES	DATE
1	FOR CONSTRUCTION	7/JAN/18
1	FOR TENDER	19/DEC/17

PROJECT:
Partitions Experimental Test Setup

DESIGNERS:
Joshua Mulligan

SUPERVISORS:
Timothy Sullivan

TITLE:
Steel Testing Frame

CODE: 64560538

DATE: 07-JAN-2018

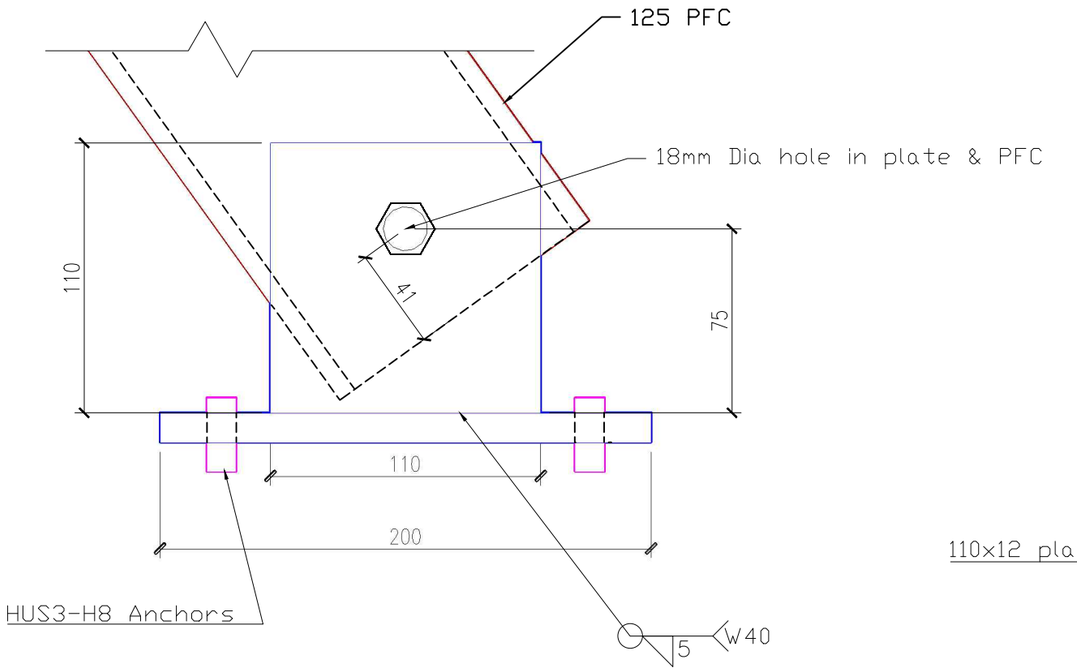

Connection A.1

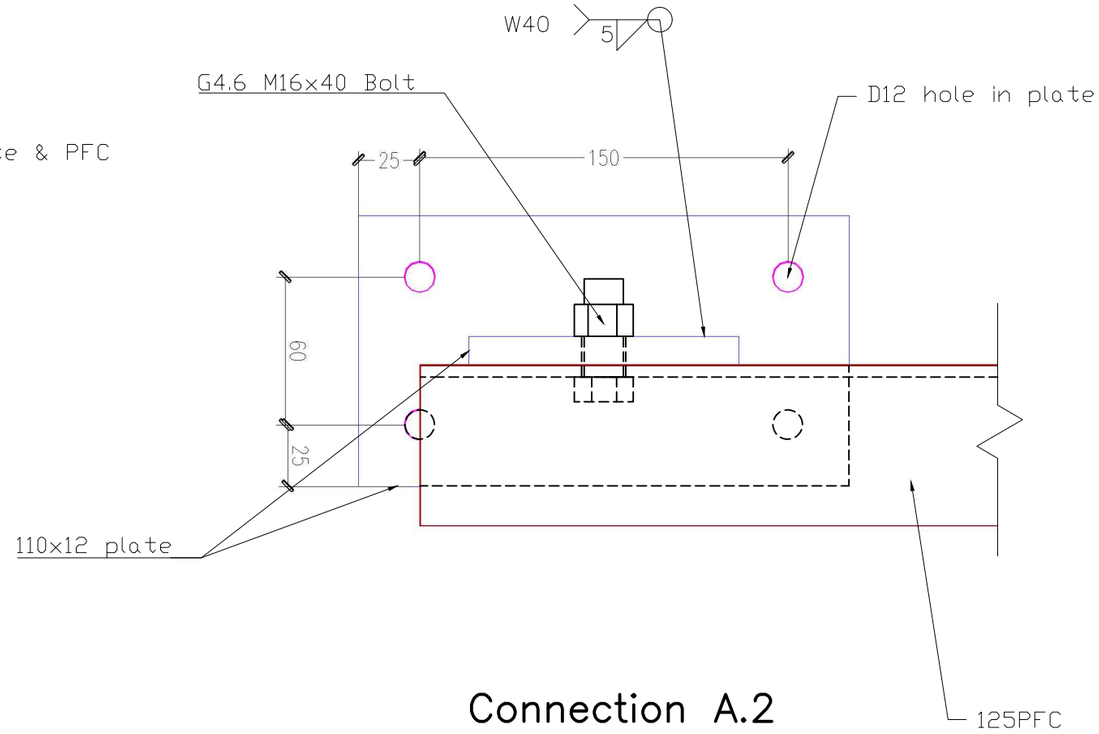

Connection A.2

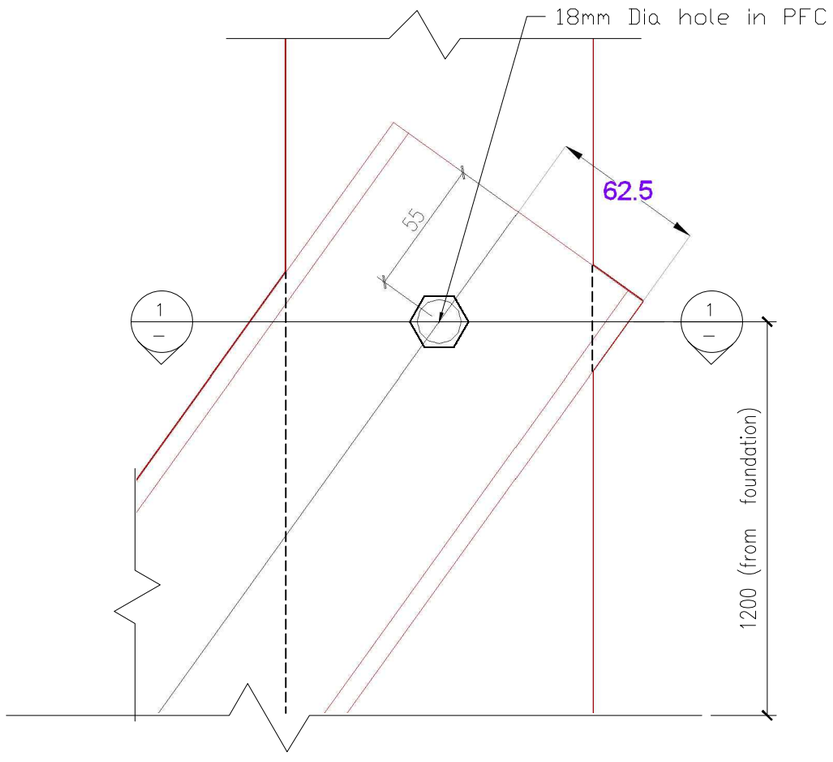

Connection B.1

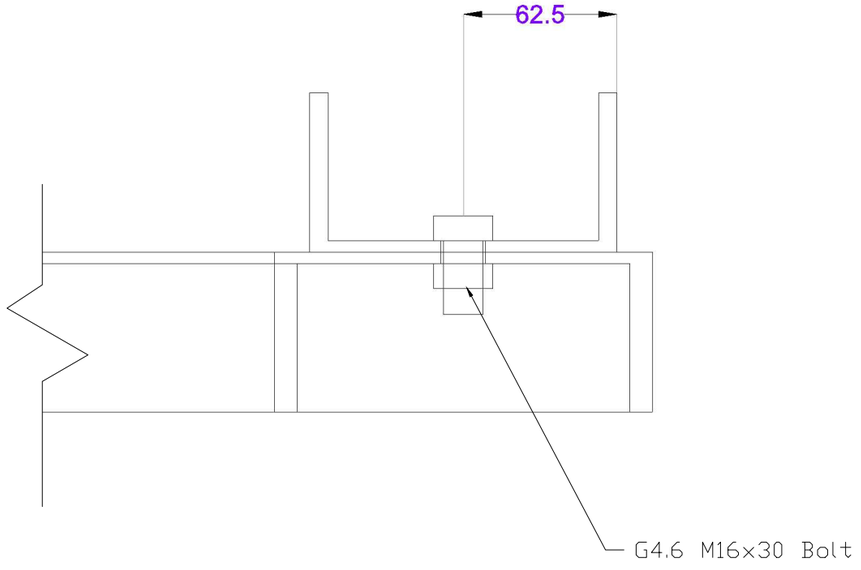

Connection B.2 Section 1

UNIVERSITY OF CANTERBURY
Te Whare Wānanga o Waitaha
CHRISTCHURCH NEW ZEALAND

UNIVERSITY OF CANTERBURY
Private Bag 4800
Christchurch 8140

CIVIL AND NATURAL RESOURCES ENGINEERING
69 Creyke Road
Christchurch 8140

NOTES:

All frame members are 125x65 PFC steel sections

Concrete anchors:
HILTI HUS-H8 Screw Anchors

Weld specifications:
SP
tw = 5mm
W40X

NB:
Connection B is identical for each brace connection

Bolts provided separately (not in tender)

Dimensions in mm

SCALE: 1:2.5 @A3

VER.	COMMENTS AND CHANGES	DATE
1	FOR CONSTRUCTION	7/JAN/18
1	FOR TENDER	19/DEC/17

PROJECT:
Partitions Experimental Testing

DESIGNERS:
Joshua Mulligan

SUPERVISORS:
Timothy Sullivan

TITLE:
Connection Detailing 1

CODE: 64560538
PAGE: 006

DATE: 07-JAN-2018

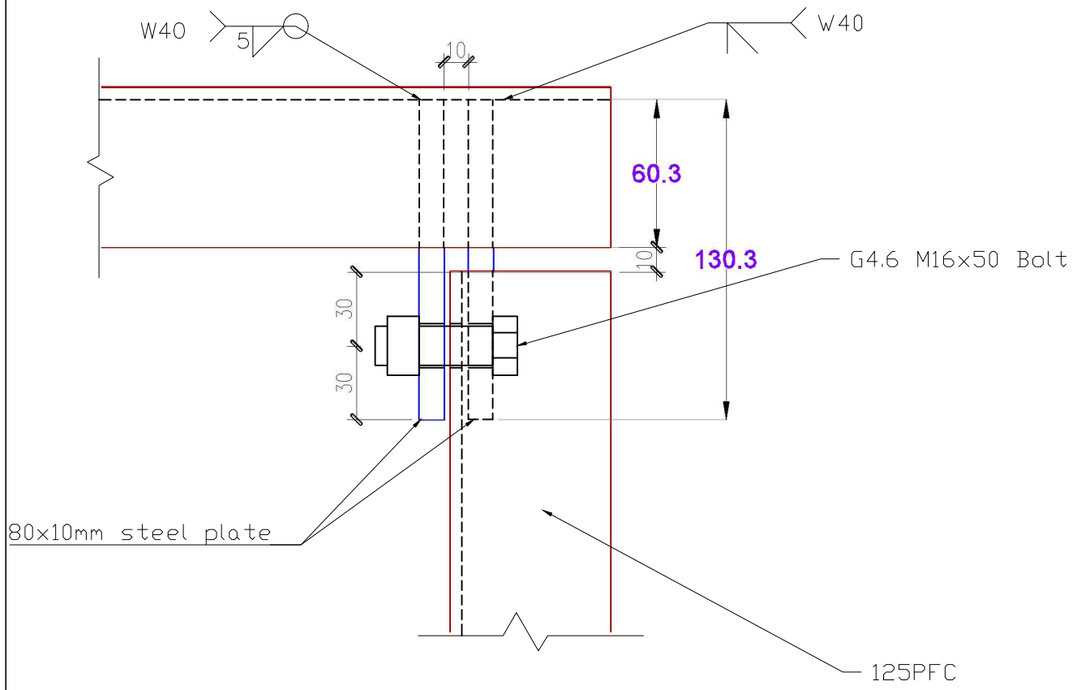

Connection C.1

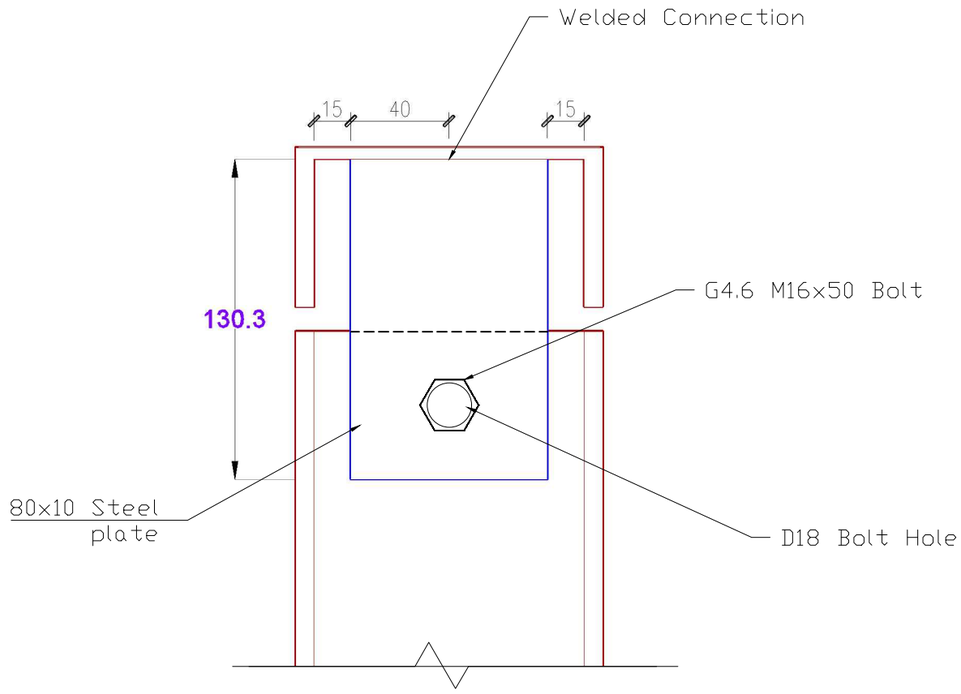

Connection C.2

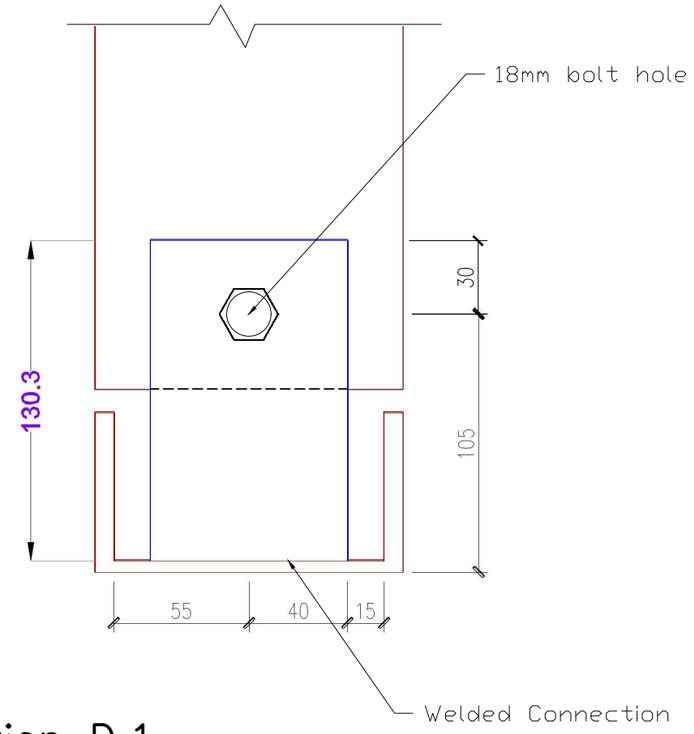

Connection D.1

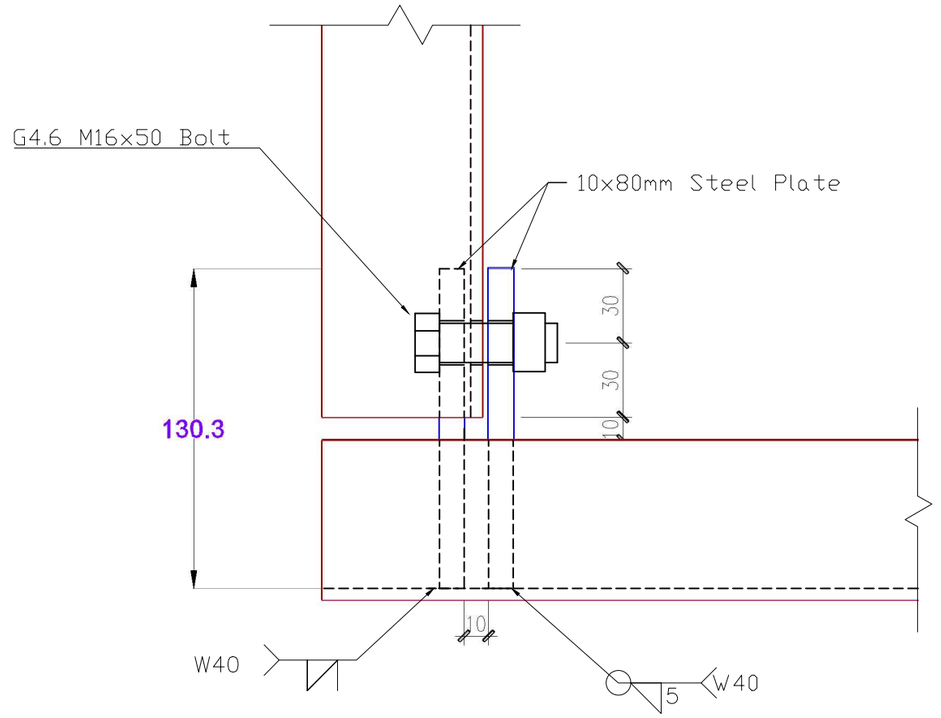

CONNECTION D.2

UNIVERSITY OF CANTERBURY
Te Whare Wānanga o Waitaha
CHRISTCHURCH NEW ZEALAND

UNIVERSITY OF CANTERBURY
Private Bag 4800
Christchurch 8140

CIVIL AND NATURAL RESOURCES ENGINEERING
69 Creyke Road
Christchurch 8140

NOTES:

All frame members are 125x65 PFC steel sections

All Weld specifications:
SP
tw = 5 mm
W40X

Bolts provided separately (not in tender)

Dimensions in mm

SCALE: 1:2.5 @ A3

VER.	COMMENTS AND CHANGES	DATE
1	FOR CONSTRUCTION	7/JAN/18
1	FOR TENDER	19/DEC/17

PROJECT:
Partitions Experimental Testing

DESIGNERS:
Joshua Mulligan

SUPERVISORS:
Timothy Sullivan

TITLE:
Connection Detailing 2

CODE: 64560538

DATE: 07-JAN-2018

PAGE: 007

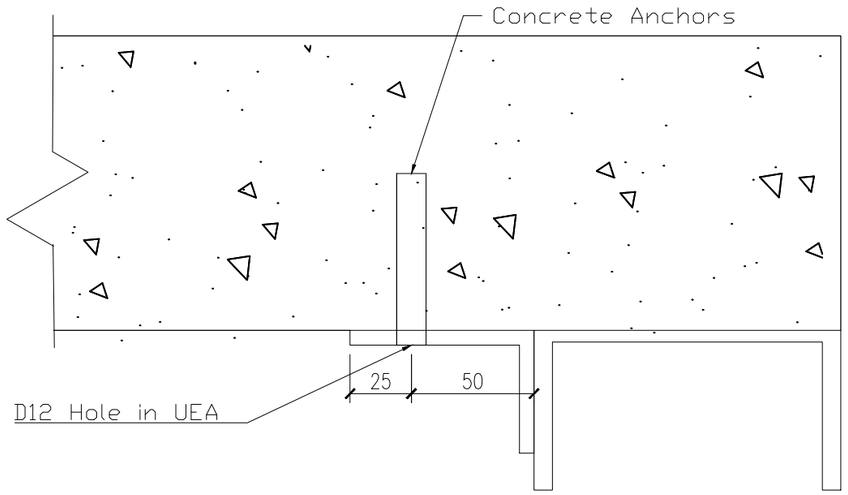

Connection E.1

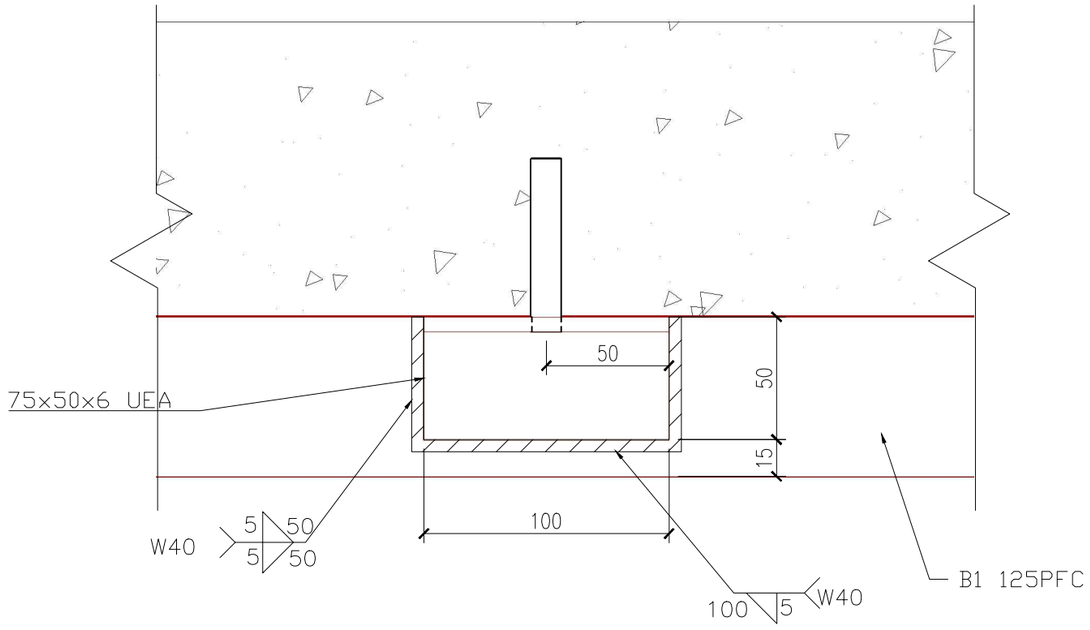

Connection E.2

UNIVERSITY OF CANTERBURY
Te Whare Wānanga o Waitaha
CHRISTCHURCH NEW ZEALAND

UNIVERSITY OF CANTERBURY
Private Bag 4800
Christchurch 8140

CIVIL AND NATURAL RESOURCES ENGINEERING
69 Creyke Road
Christchurch 8140

NOTES:

All frame members are 125x65 PFC steel sections

All Weld specifications:
SP
tw = 5 mm
W40X

Anchor bolts to be provided separately (not in tender)

Dimensions in mm

SCALE: 1:2.5 @ A3

VER.	COMMENTS AND CHANGES	DATE
1	FOR CONSTRUCTION	7/JAN/18
1	FOR TENDER	19/DEC/17

PROJECT:
Partitions Experimental Testing

DESIGNERS:
Joshua Mulligan

SUPERVISORS:
Timothy Sullivan

TITLE:
Connection Detailing 3

CODE: 64560538

DATE: 07-JAN-2018

PAGE: 008

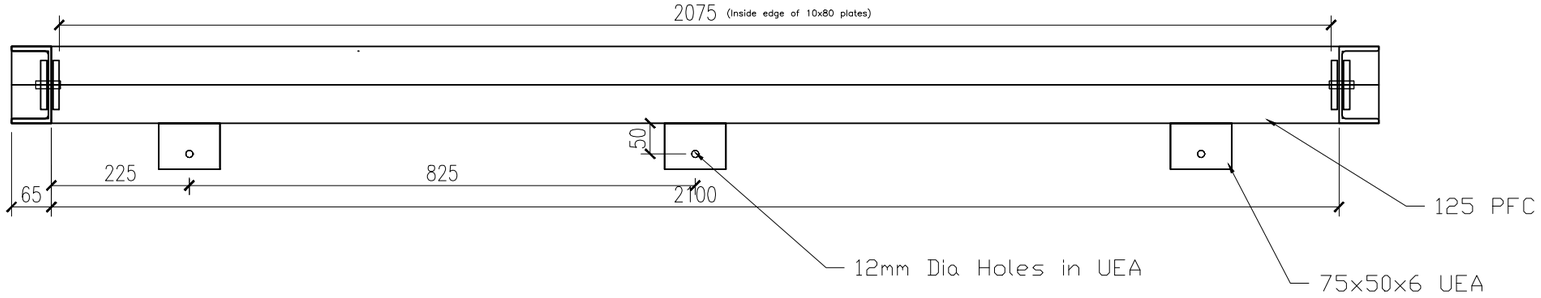

TOP TRACK PLAN

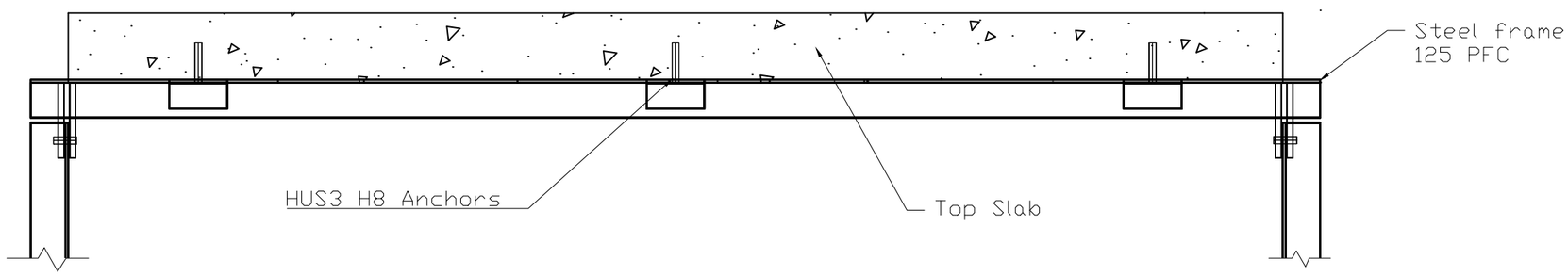

TOP TRACK SECTION

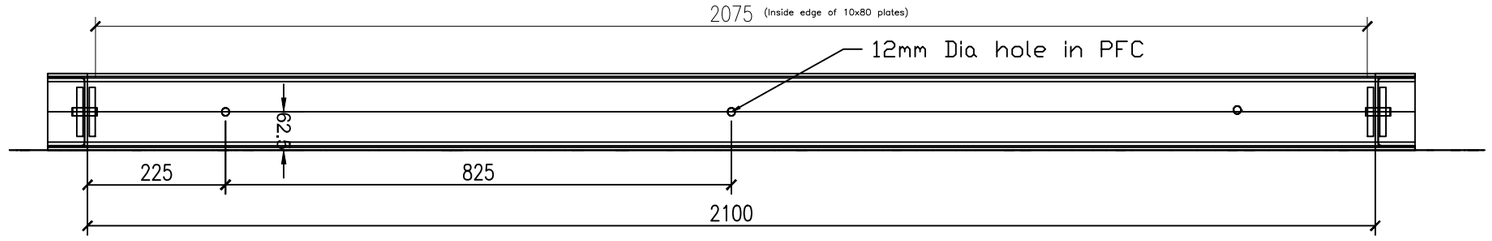

BOTTOM TRACK PLAN

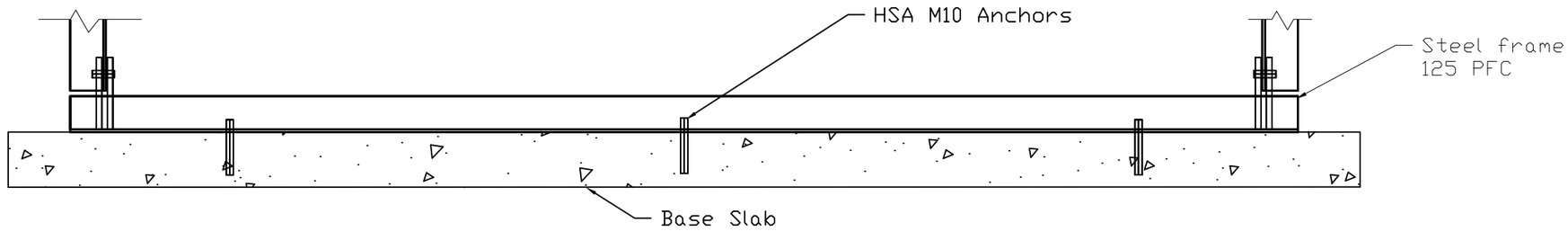

BOTTOM TRACK SECTION

UNIVERSITY OF CANTERBURY
Private Bag 4800
Christchurch 8140

CIVIL AND NATURAL RESOURCES ENGINEERING
69 Creyke Road
Christchurch 8140

NOTES:

Top Anchors are HUS3 H8 HILTI screw anchors to be installed according to HILTI specifications

Bottom Anchors are HSA M10 HILTI mechanical fasteners

Anchors are to be supplied separately (not in tender)

Dimensions in mm

SCALE: 1:10 @ A3

VER.	COMMENTS AND CHANGES	DATE
1	FOR CONSTRUCTION	7/JAN/18
1	FOR TENDER	19/DEC/17

PROJECT:
Partitions Experimental Testing

DESIGNERS:
Joshua Mulligan

SUPERVISORS:
Timothy Sullivan

TITLE:
Frame anchor details

CODE: 64560538

DATE: 07-JAN-2018

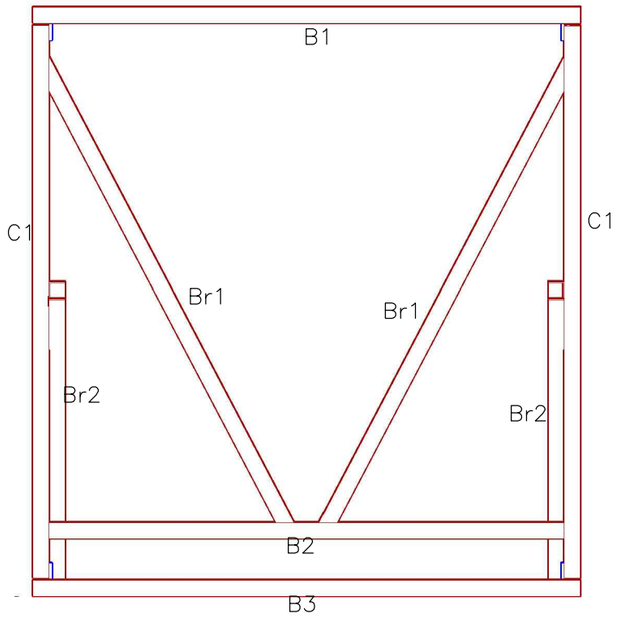

Member Schedule per Frame					
member	Section	length	number per frame	Weight (kg)	Notes
B1	125PFC	2230	1	26.5	
B2	125PFC	2100	1	25	
B3	125PFC	2230	1	26.5	Holes as per p5
C1	125PFC	2250	2	53.6	
Br1	125PFC	2147	2.0	51.1	ends cut as per Br1 detail (p7)
Br2	125PFC	1370	2.0	32.6	
			total	215.3	

TOTAL OF SIX FRAMES TO BE PROVIDED.

TOTAL WEIGHT = 1291.8 KG

Steel Frame East Elevation Members

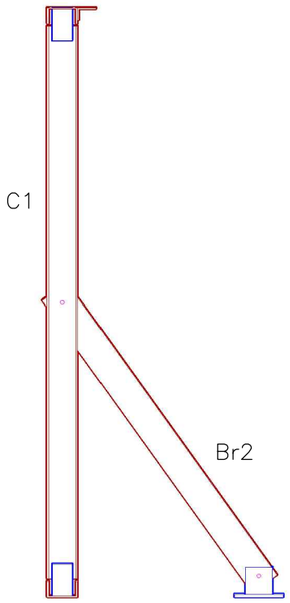

Steel Frame Side Elevation Members

UNIVERSITY OF CANTERBURY
Te Whare Wānanga o Waitaha
CHRISTCHURCH NEW ZEALAND
UNIVERSITY OF CANTERBURY
Private Bag 4800
Christchurch 8140
CIVIL AND NATURAL RESOURCES ENGINEERING
69 Creyke Road
Christchurch 8140

NOTES:

Dimensions in mm

SCALE: 1:25 @ A3

VER.	COMMENTS AND CHANGES	DATE
1	FOR CONSTRUCTION	7/JAN/18
1	FOR TENDER	19/DEC/17

PROJECT:
Partitions Experimental Testing

DESIGNERS:
Joshua Mulligan

SUPERVISORS:
Timothy Sullivan

TITLE:
Steel Member Schedule

CODE: 64560538

DATE: 07-JAN-2018

PAGE: 0010

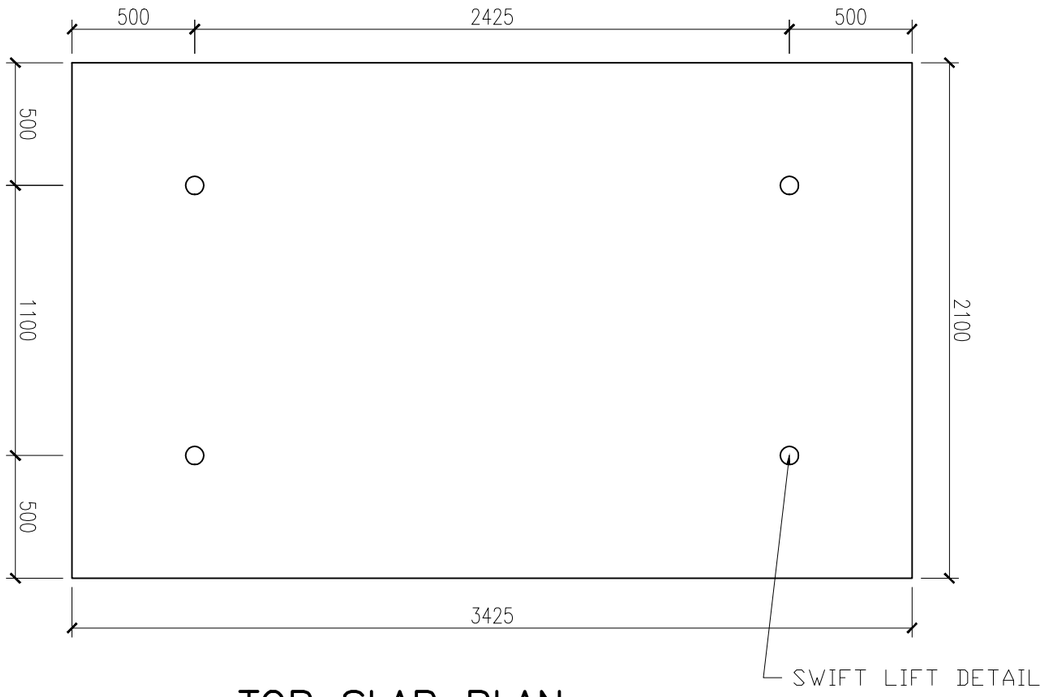

TOP SLAB PLAN

SCALE: 1:25

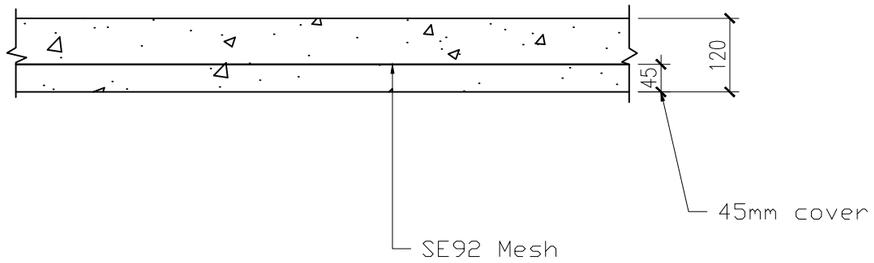

TOP SLAB SECTION

SCALE: 1:10

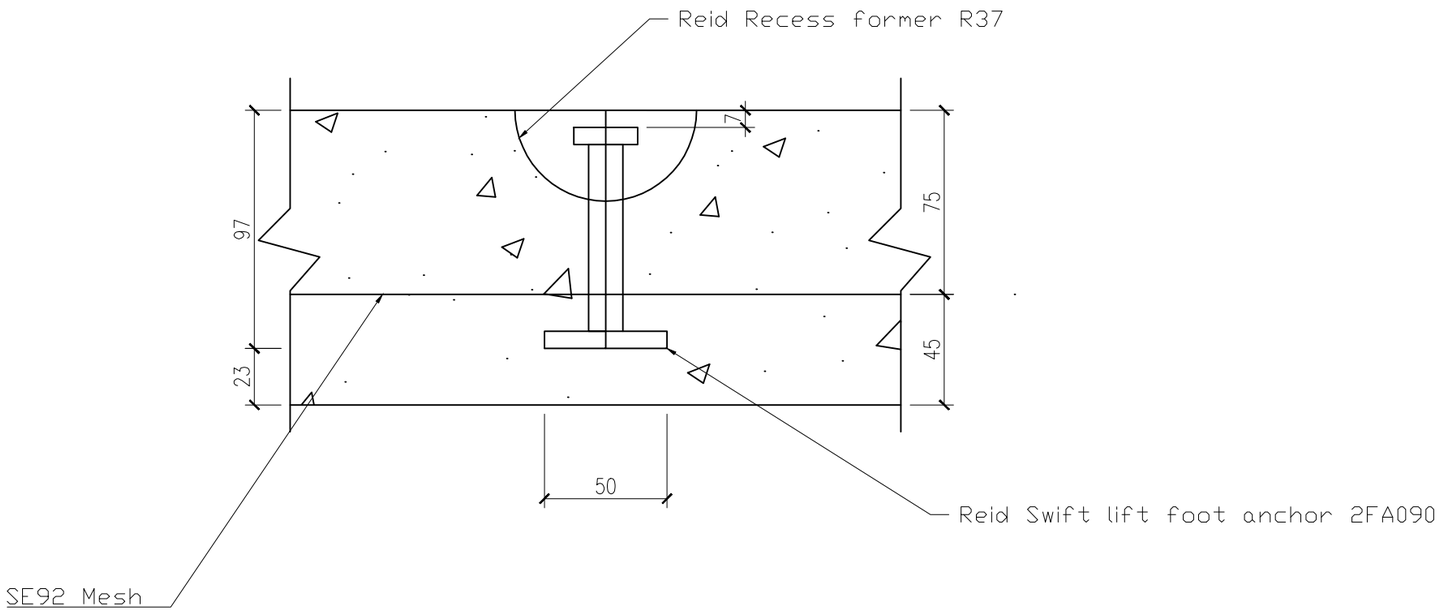

TOP SLAB SWIFT LIFT DETAIL

SCALE: 1:2.5

UNIVERSITY OF CANTERBURY
Private Bag 4800
Christchurch 8140

CIVIL AND NATURAL RESOURCES ENGINEERING
69 Creyke Road
Christchurch 8140

NOTES:

Concrete specifications:
at least 25MPa f'c
Standard concrete
No requirement on aggregate size

Reinforcing:
45mm cover
Reinforcing for slab 01 is seismic mesh 9mm diam 200 spacing (SE92)

Reid Lifting Anchors:
Swift lift anchor is a 2FA090
Recess former is a 2FA90PR
Clutch is 2LE

Dimensions in mm

SCALE: 1:10, 1:25 @ A3

VER.	COMMENTS AND CHANGES	DATE
3	FOR CONSTRUCTION	14/DEC/17
2	FOR TENDER	13/DEC/17
1	Prelim	22/NOV/17

PROJECT:
Partitions Experimental Testing Setup

DESIGNERS:
Joshua Mulligan

SUPERVISORS:
Timothy Sullivan

TITLE:
TOP CONCRETE SLAB FOR CONSTRUCTION

CODE: 64560538
DATE: 14-DEC-2017
PAGE: 011

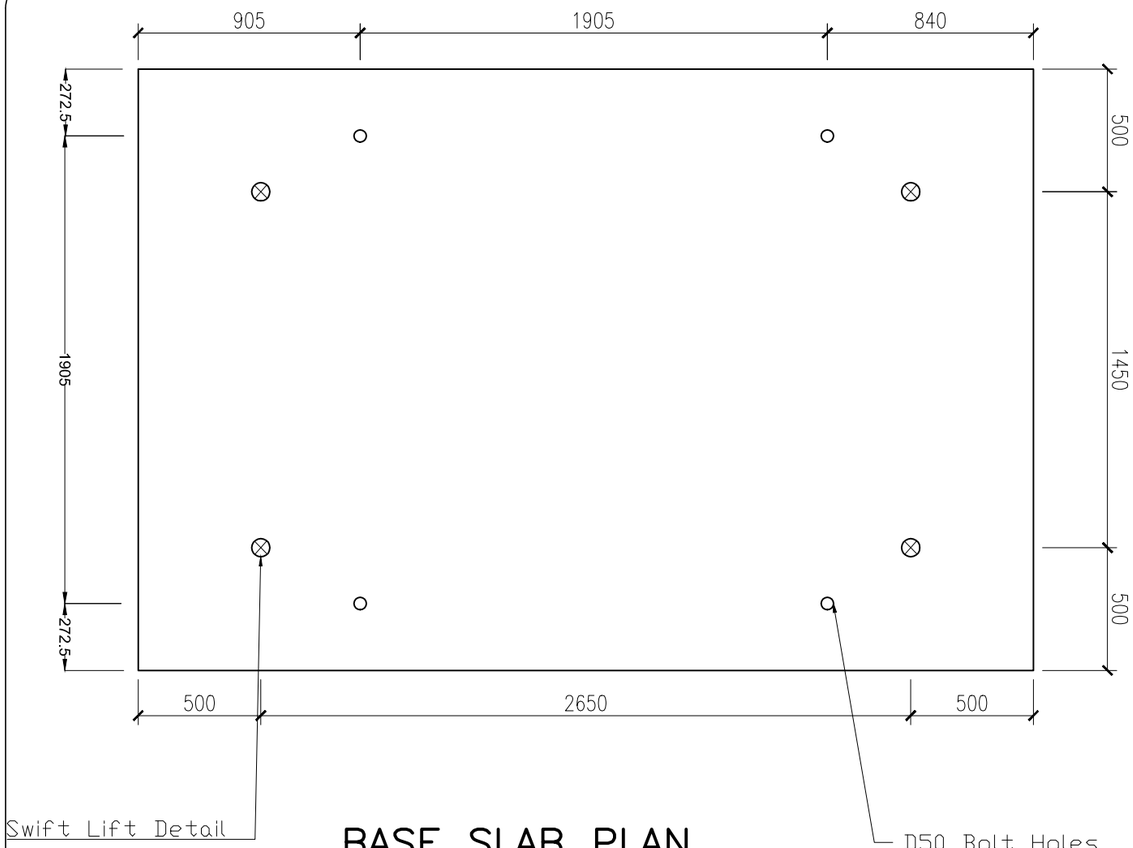

BASE SLAB PLAN

SCALE: 1:25

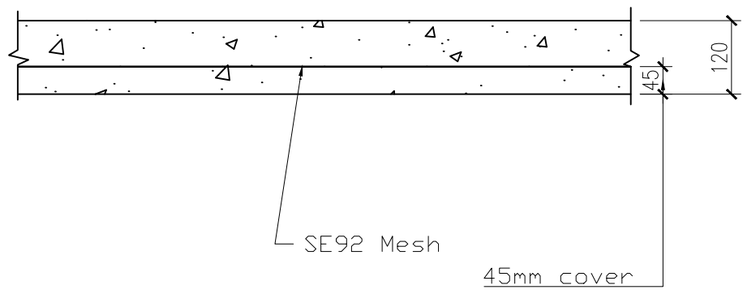

BASE SLAB SECTION

SCALE: 1:10

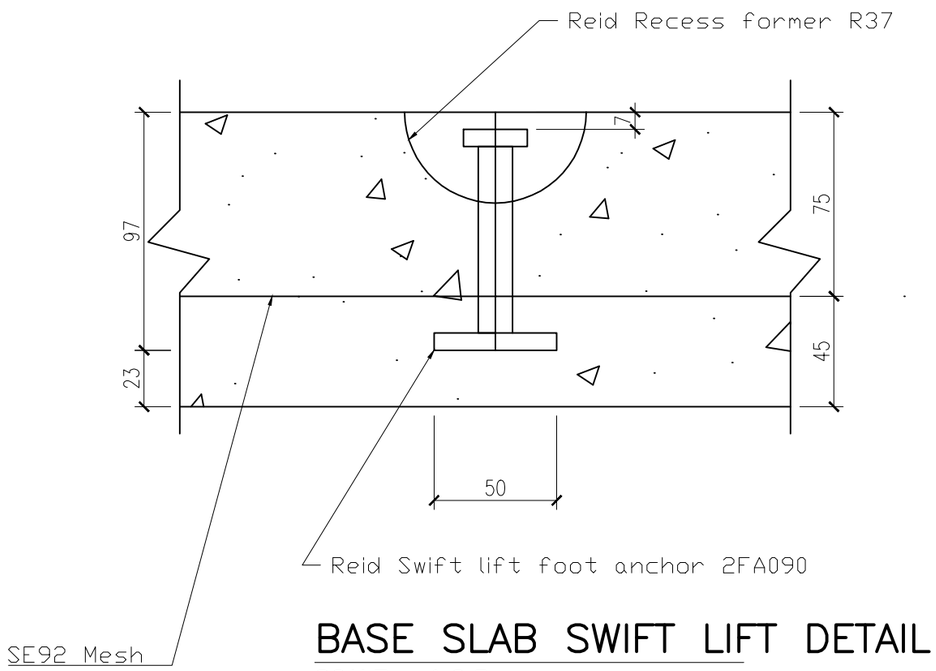

BASE SLAB SWIFT LIFT DETAIL

SCALE: 1:2.5

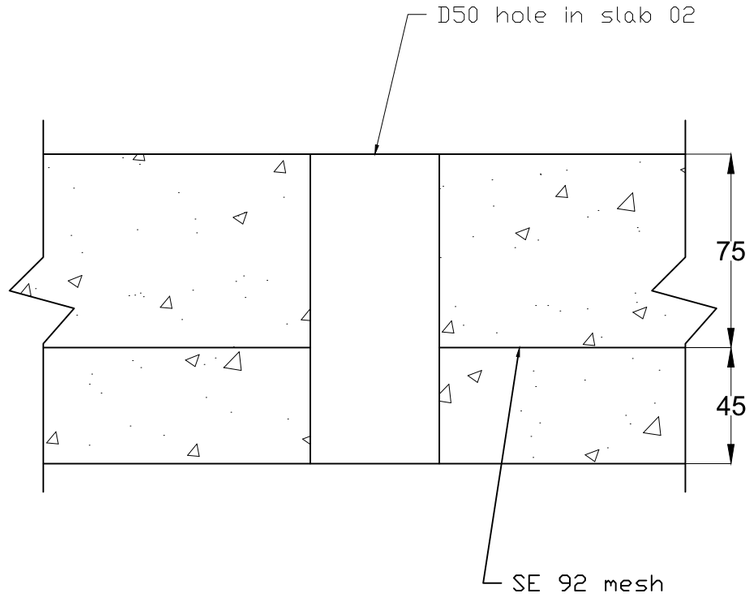

BASE SLAB BOLT HOLE DETAIL

SCALE: 1:2.5

UNIVERSITY OF CANTERBURY
Private Bag 4800
Christchurch 8140

CIVIL AND NATURAL RESOURCES ENGINEERING
69 Creyke Road
Christchurch 8140

NOTES:

Concrete Geometry:
plan dimensions 3650x2450mm
thickness 120mm

Concrete specifications:
at least 25MPa f'c
Standard concrete
No requirement on aggregate size

Reinforcing:
45mm cover
Reinforcing is seismic mesh 9mm diam 200 spacing (SE92)

Reid Lifting Anchors:
Swift lift anchor is a 2FA090
Recess former is a 2FA90PR
Clutch is 2LE

Dimensions in mm

SCALE: AS PER DETAIL

VER.	COMMENTS AND CHANGES	DATE
3	FOR CONSTRUCTION	14/DEC/17
2	FOR TENDER	13/DEC/17
1	Prelim	22/NOV/17

PROJECT:
Partitions Experimental Testing Setup

DESIGNERS:
Joshua Mulligan

SUPERVISORS:
Timothy Sullivan

TITLE:
BASE CONRETE SLAB FOR CONSTRUCTION

CODE: 64560538
DATE: 14-DEC-2017
PAGE: 012

Appendix B Flexible Track System Data

Specimen Construction Drawings

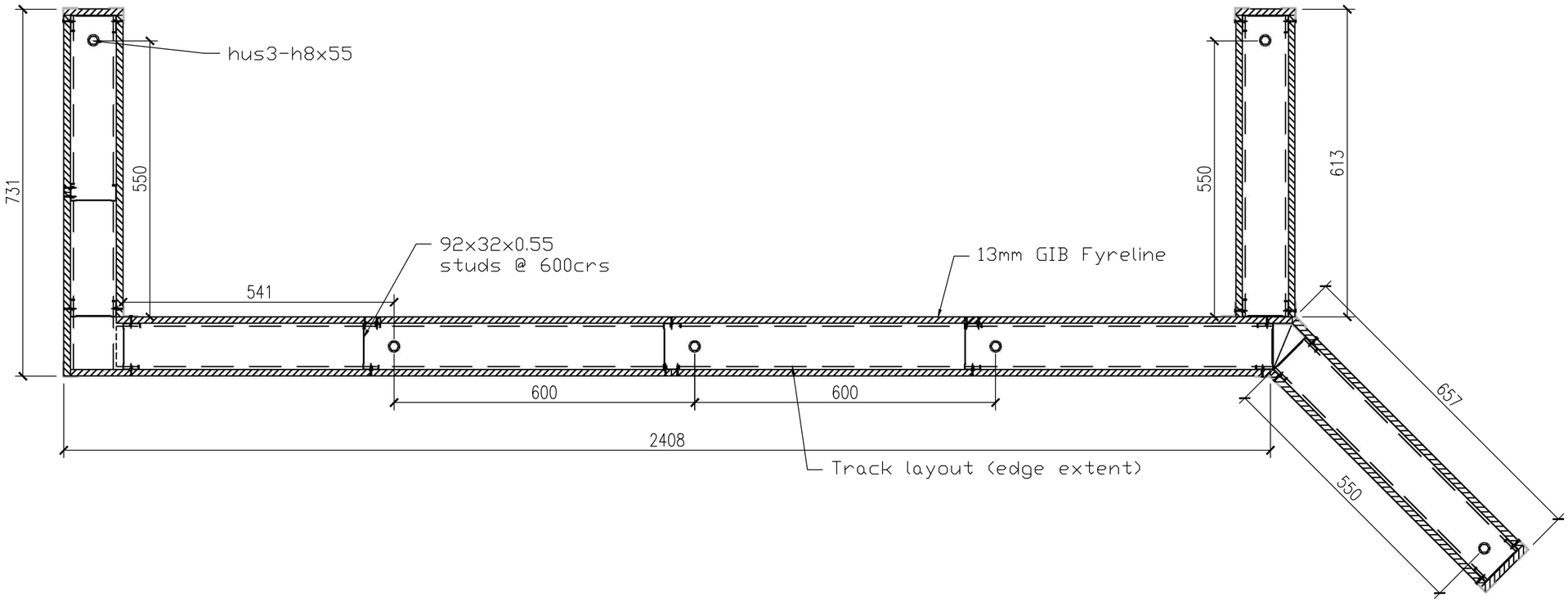

DUNNING THORNTON – TOP TRACK ANCHORS PLAN

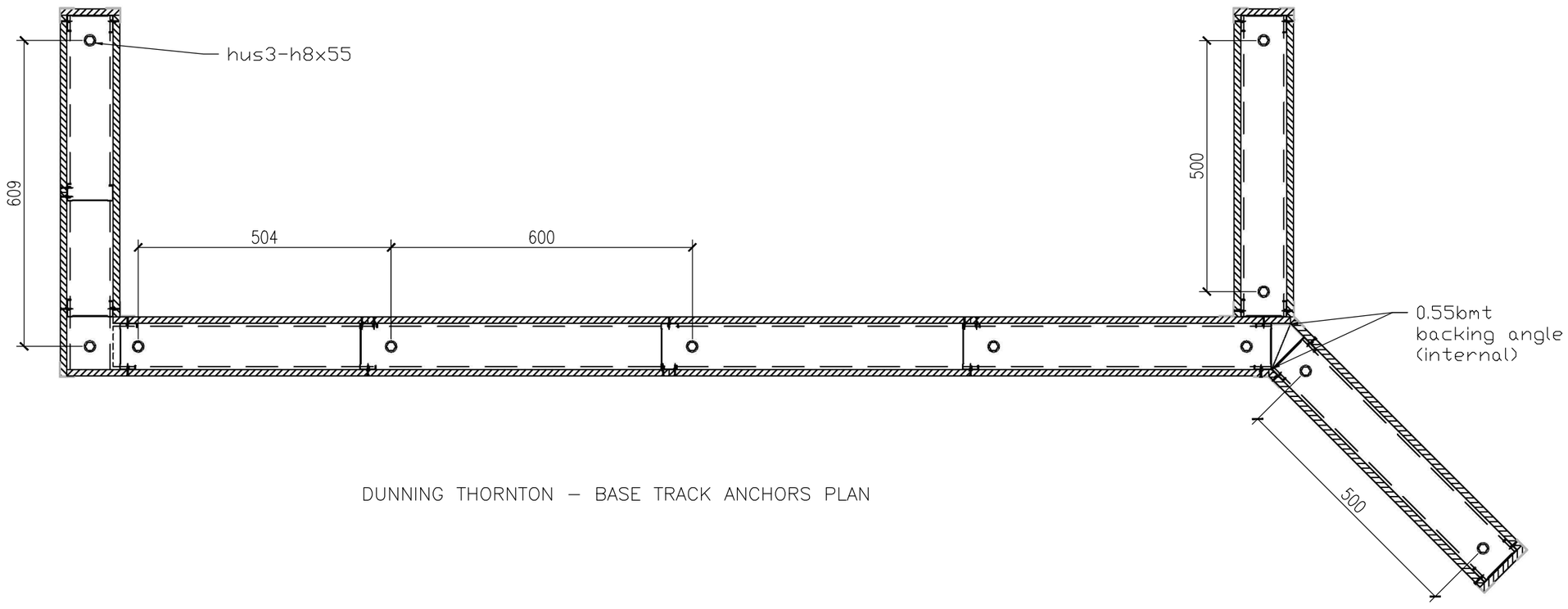

DUNNING THORNTON – BASE TRACK ANCHORS PLAN

UNIVERSITY OF CANTERBURY
Te Whare Wānanga o Waitaha
CHRISTCHURCH NEW ZEALAND

UNIVERSITY OF CANTERBURY
Private Bag 4800
Christchurch 8140

CIVIL AND NATURAL RESOURCES ENGINEERING
69 Creyke Road
Christchurch 8140

NOTES:

track anchors are HILTI HUS3-H8x55 screw anchors one at each location

NO top track anchors within 500mm of corners or junctions

Drywalls finished as per GIB site guide specifications to a level 4 finish with a single coat of paint.

All, corners junctions are to be finished with GIB ultraflex no coat 82mm tape

Dimensions in mm

SCALE: 1:10 @ A3

VER.	COMMENTS AND CHANGES	DATE
4	As-built	14/Aug/18
3	Construction	15/MAR/18
2	Preliminary	23/FEB/18
1	Preliminary	30/JAN/18

PROJECT:
Partitions Experimental Testing

DESIGNERS:
Joshua Mulligan

SUPERVISORS:
Timothy Sullivan

TITLE:
DUNNING THORNTON SERIES
y-SHAPE PLAN

CODE: 64560538

DATE: 14-Aug-2018

PAGE: 001

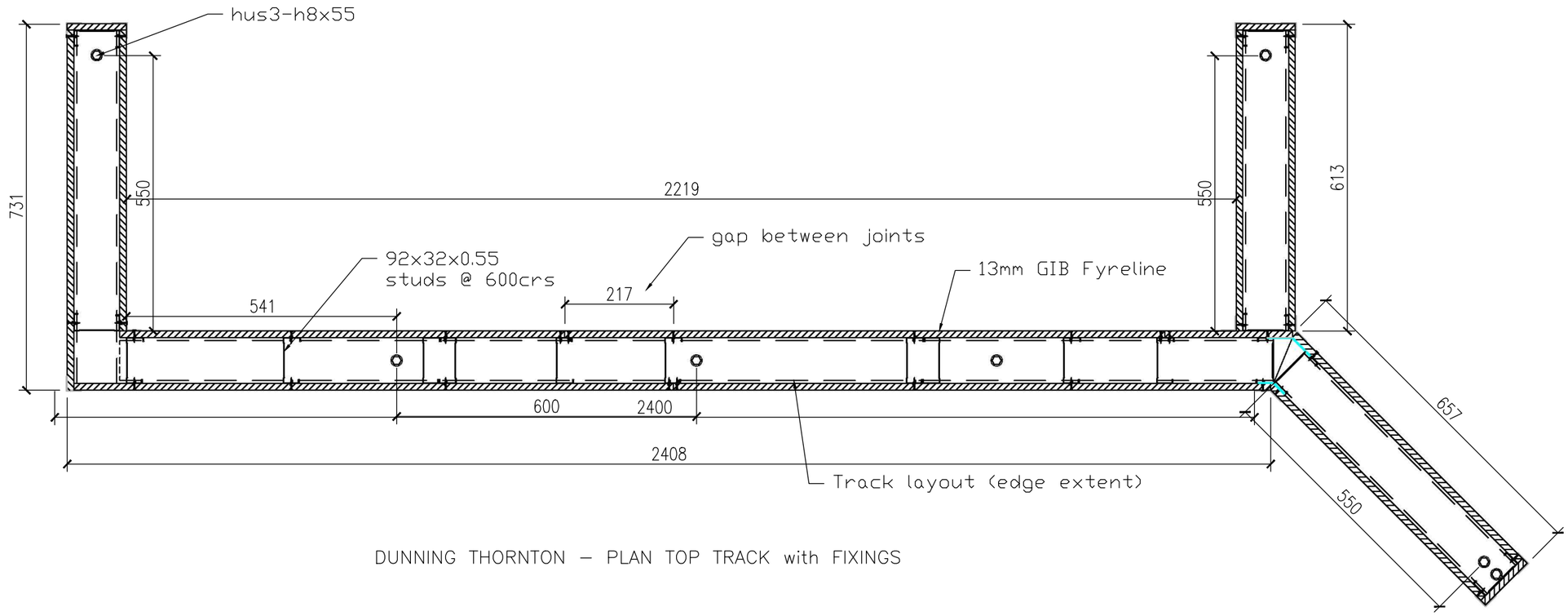

DUNNING THORNTON – PLAN TOP TRACK with FIXINGS

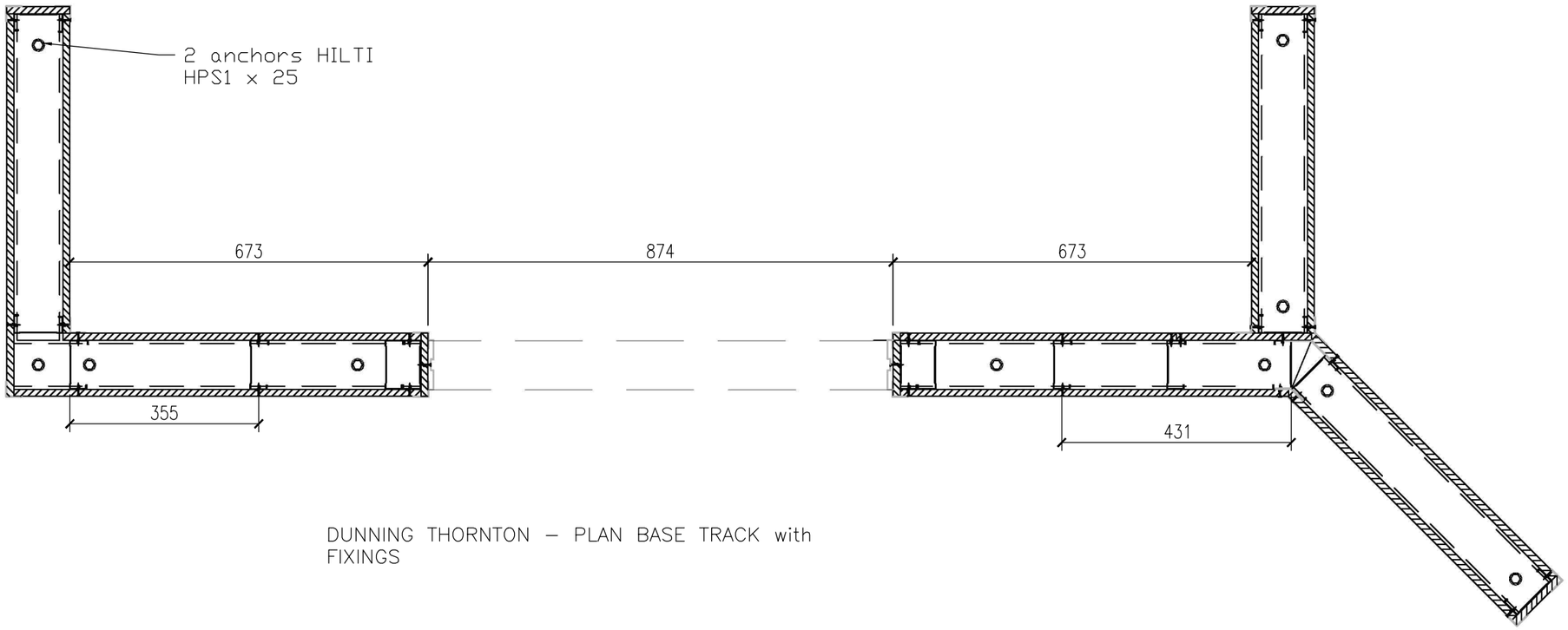

DUNNING THORNTON – PLAN BASE TRACK with FIXINGS

UNIVERSITY OF CANTERBURY
Private Bag 4800
Christchurch 8140

CIVIL AND NATURAL RESOURCES ENGINEERING
69 Creyke Road
Christchurch 8140

NOTES:

top track anchors are HILTI HUS3-H8x55 screw anchors one at each location

base track anchors are HILTI HPS1x25 impact anchors two at each location

Remove top track anchors within 500mm of corners or junctions

Drywalls finished as per GIB site guide specifications to a level 4 finish with a single coat of paint.

All, corners junctions are to be finished with GIB ultraflex no coat 82mm tape

Dimensions in mm

SCALE: 1:10 @ A3

VER.	COMMENTS AND CHANGES	DATE
2	As-built	14/Aug/18
2	Preliminary	23/FEB/18
1	Preliminary	30/JAN/18

PROJECT:
Partitions Experimental Testing

DESIGNERS:
Joshua Mulligan

SUPERVISORS:
Timothy Sullivan

TITLE:
DUNNING THORNTON
SPECIMEN DOORWAY PLAN

CODE: 64560538

DATE: 14-Aug-2018

PAGE: 002

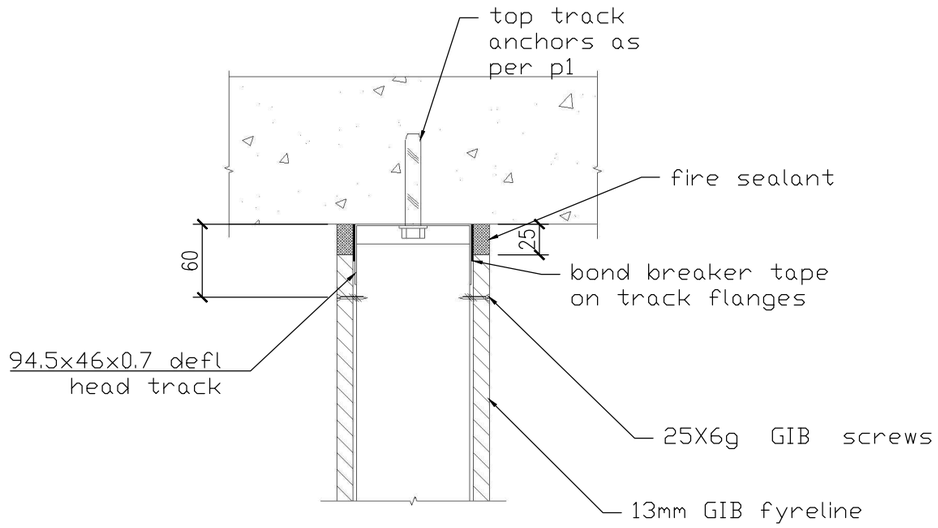

DT SYSTEM – TOP SLAB TO WALL CONNECTION

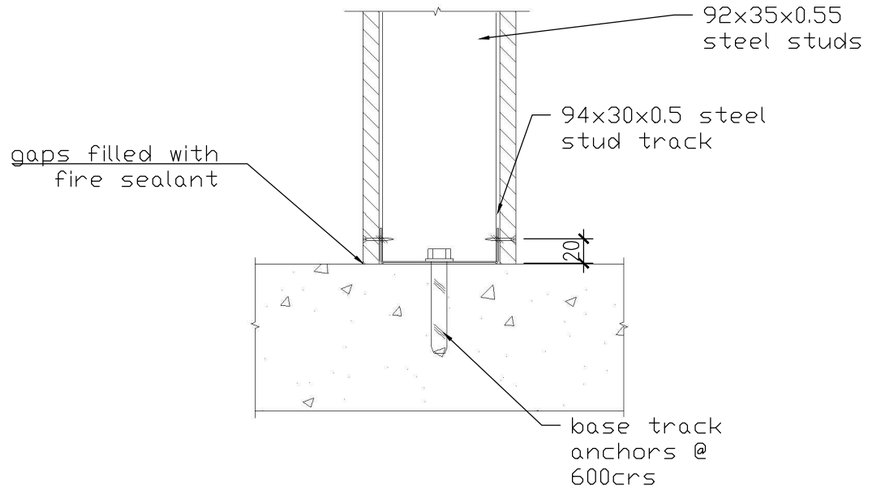

DT SYSTEM – BASE SLAB TO WALL CONNECTION GIB

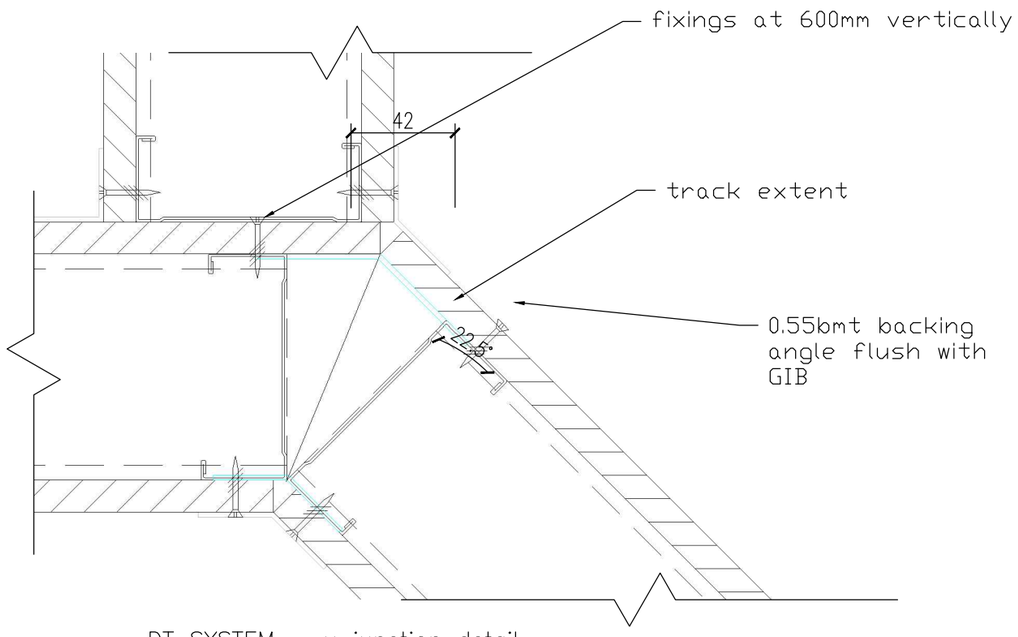

DT SYSTEM – y junction detail

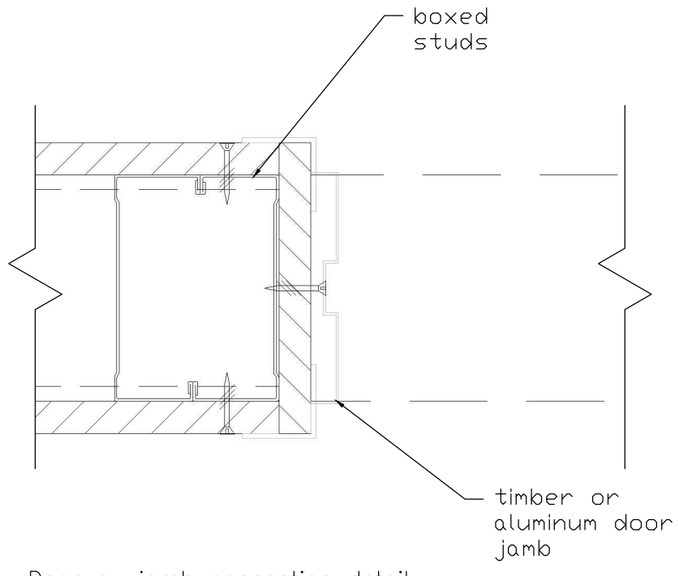

Doorway jamb connection detail

UNIVERSITY OF CANTERBURY
Private Bag 4800
Christchurch 8140

CIVIL AND NATURAL RESOURCES ENGINEERING
69 Creyke Road
Christchurch 8140

NOTES:

top track anchors are HILTI HUS3-H8x55 screw anchors one at each location

base track anchors are HILTI HPS1x25 impact anchors two at each location

Dimensions in mm

SCALE: 1:2.5 @ A3

VER.	COMMENTS AND CHANGES	DATE
4	As-built	14/Aug/18
3	Revised	23/FEB/18
2	Preliminary	06/FEB/18
1	Preliminary	30/JAN/18

PROJECT:
Low Damage Partitions Experimental Testing

DESIGNERS:
Joshua Mulligan

SUPERVISORS:
Timothy Sullivan

TITLE:
DT SPECIMENS - DETAILS

CODE: 64560538

DATE: 14-Aug-2018

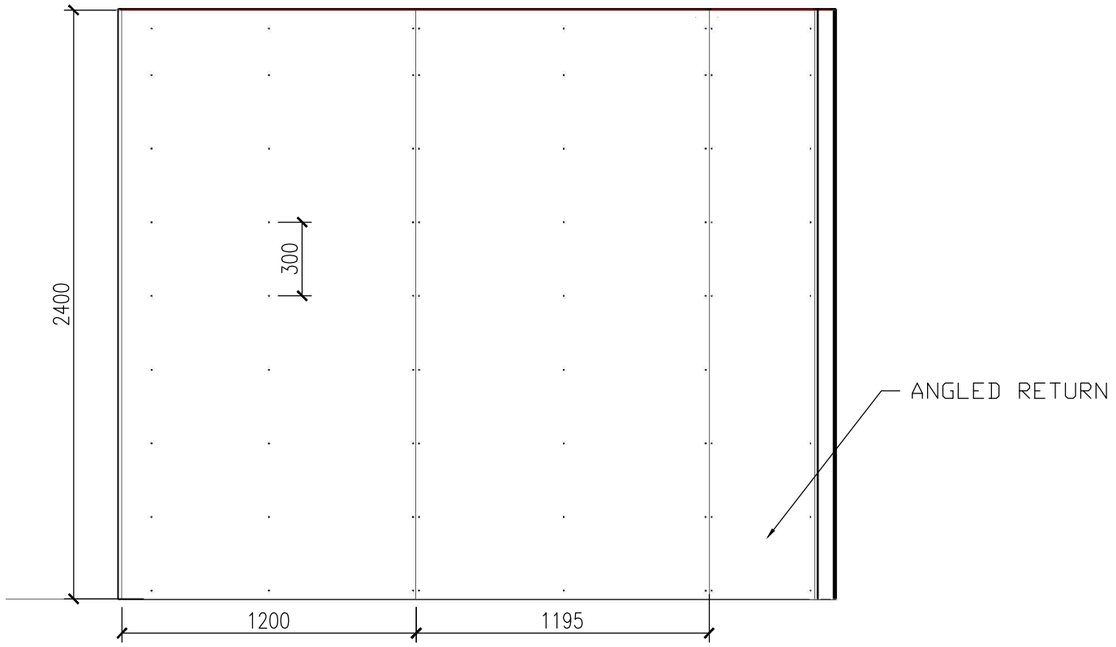

DT Specimen South Face elevation

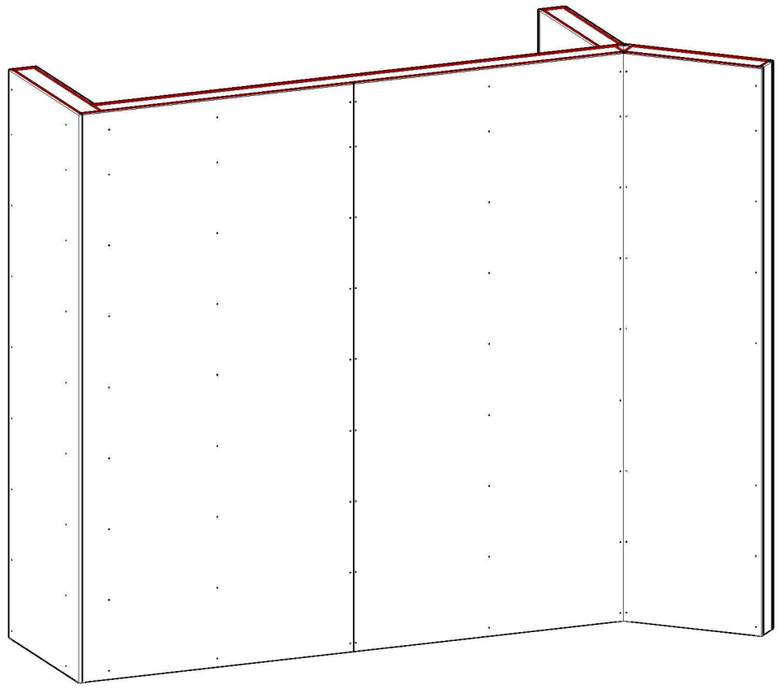

DT Specimen Plain Wall – Perspective

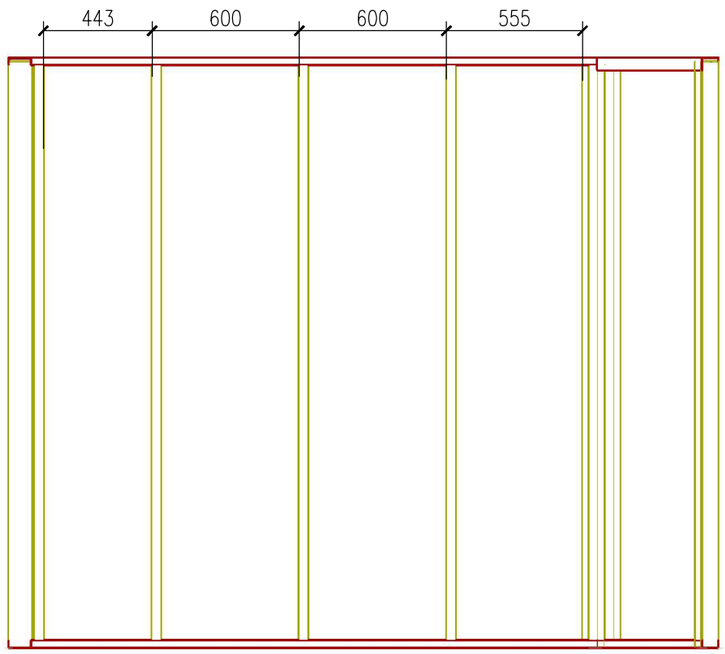

DT Specimen Plain Wall – South Face elevation

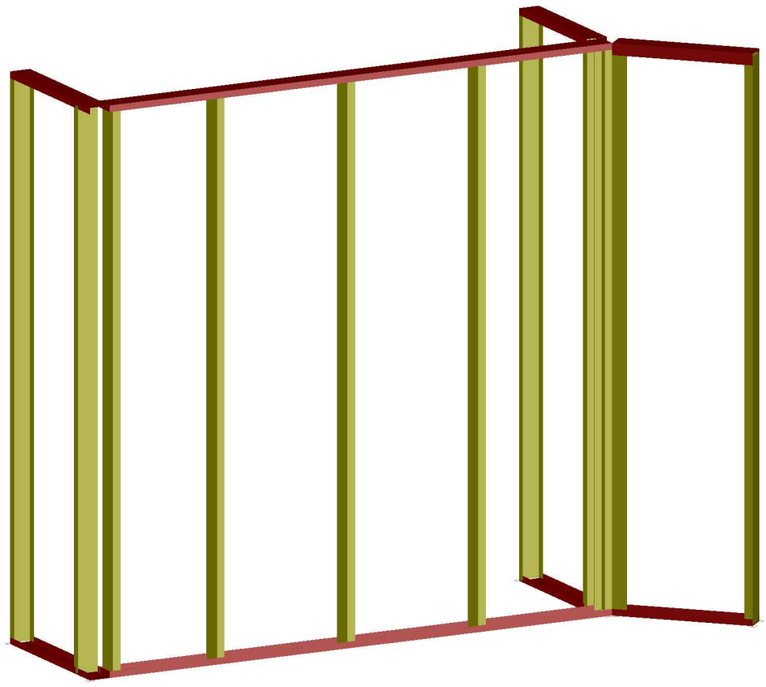

DT Specimen Plain Wall Framing – Perspective

UNIVERSITY OF CANTERBURY
Te Whare Wānanga o Waitaha
CHRISTCHURCH NEW ZEALAND

UNIVERSITY OF CANTERBURY
Private Bag 4800
Christchurch 8140

CIVIL AND NATURAL RESOURCES ENGINEERING
69 Creyke Road
Christchurch 8140

NOTES:

Dimensions in mm

SCALE: 1:25 @ A3

VER.	COMMENTS AND CHANGES	DATE
3	As-built	14/Aug/18
3	Revised	23/FEB/18
2	Revised	15/FEB/18
1	Preliminary	09/JAN/18

PROJECT:
Partitions Experimental Testing

DESIGNERS:
Joshua Mulligan

SUPERVISORS:
Timothy Sullivan

TITLE:
WALL TEST SPECIMEN
DUNNING THORNTON SYSTEM - ELEVATIONS

CODE: 64560538

DATE: 14-Aug-2018

PAGE: 004

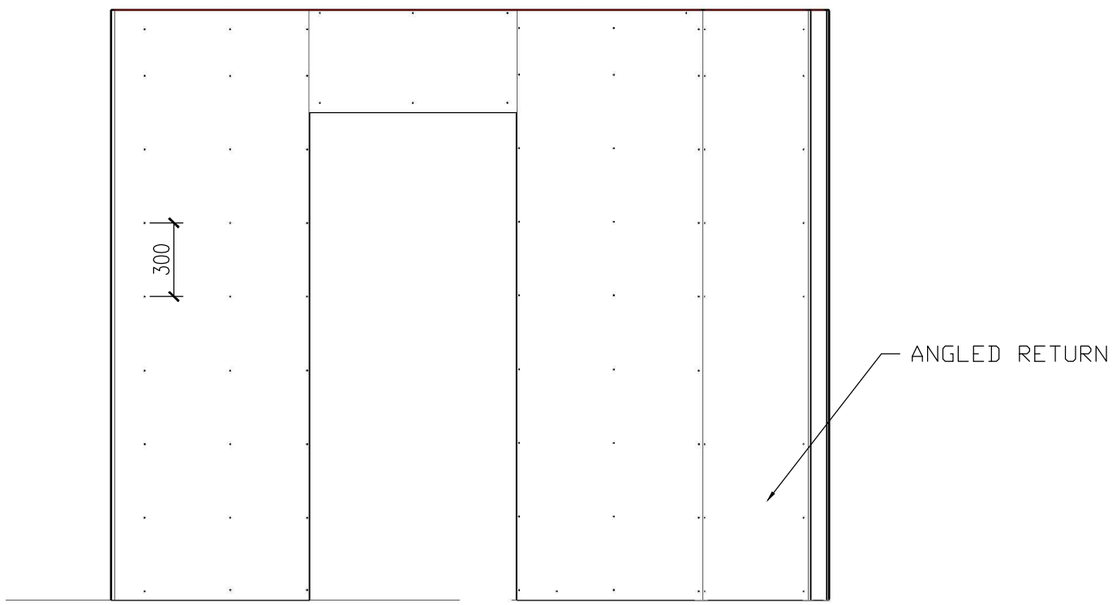

DT Specimen Doorway – South face elevation

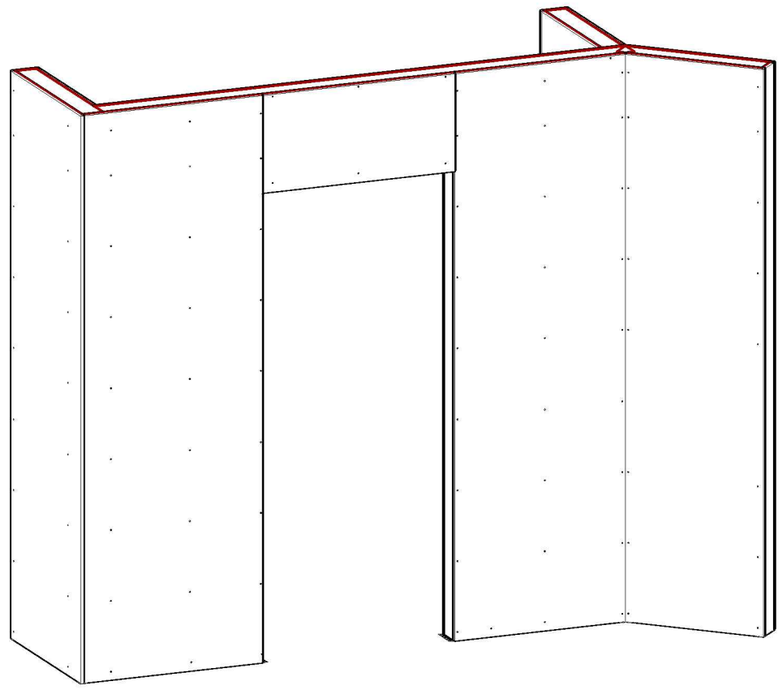

DT Specimen Doorway – Perspective

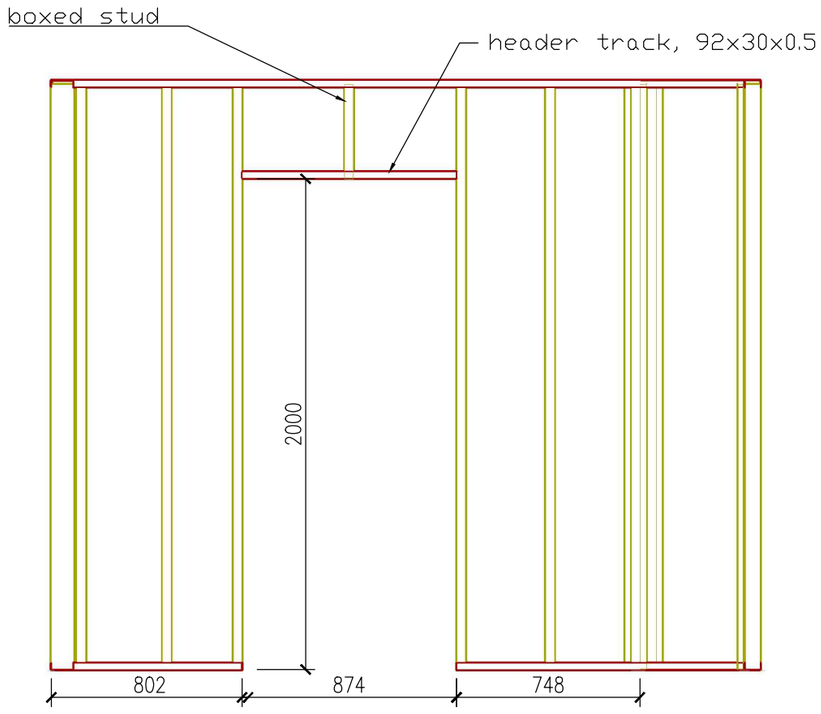

DT Specimen Doorway Framing – South face elevation

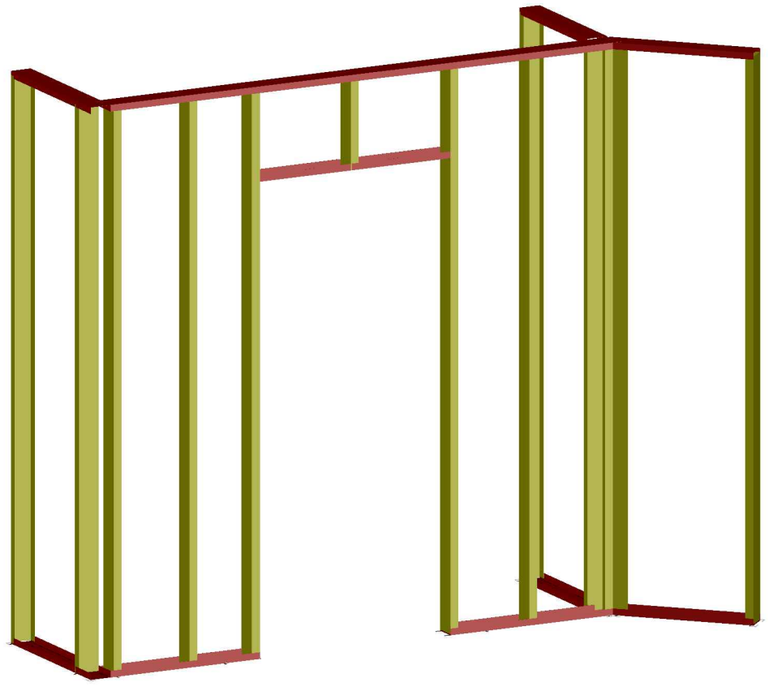

DT Specimen Doorway Framing – Perspective

UNIVERSITY OF CANTERBURY
Private Bag 4800
Christchurch 8140

CIVIL AND NATURAL RESOURCES ENGINEERING
69 Creyke Road
Christchurch 8140

NOTES:

Dimensions in mm

SCALE: 1:25 @ A3

VER.	COMMENTS AND CHANGES	DATE
3	As-built	14/Aug/18
2	Revised	23/FEB/18
1	Preliminary	09/JAN/18

PROJECT:
Partitions Experimental Testing

DESIGNERS:
Joshua Mulligan

SUPERVISORS:
Timothy Sullivan

TITLE:
WALL TEST SPECIMEN
DUNNING THORNTON SYSTEM - ELEVATIONS Doorway

CODE: 64560538

DATE: 14-Aug-2018

PAGE: 005

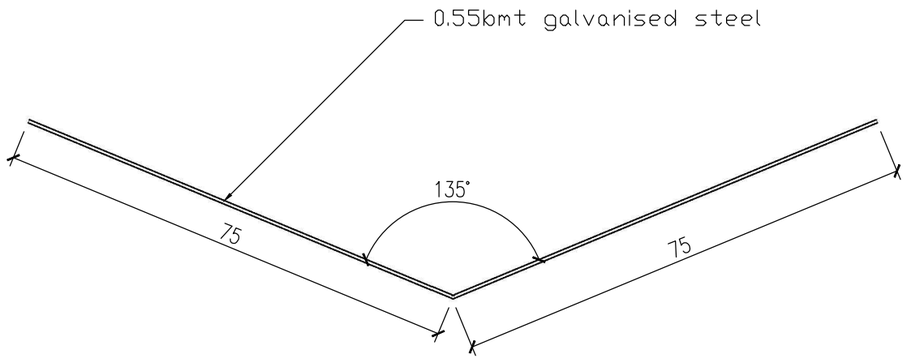

135o 0.55bmt steel backing angle 75mm

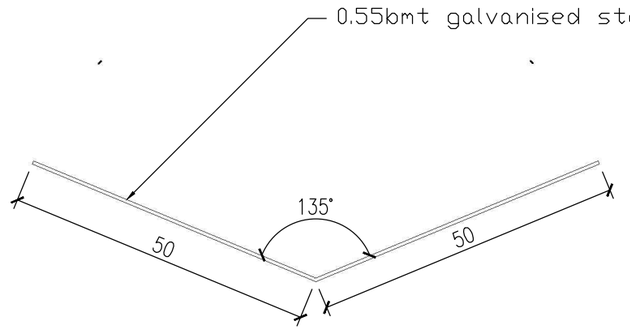

135o 0.55bmt steel backing angle 50mm

Table of quantities			
member	Material	length	number required
135o 0.55x75 angle	CFS	2400	3
135o 0.55x50 angle	CFS	2400	3

UNIVERSITY OF CANTERBURY
Te Whare Wānanga o Waitaha
CHRISTCHURCH NEW ZEALAND

UNIVERSITY OF CANTERBURY
Private Bag 4800
Christchurch 8140

CIVIL AND NATURAL RESOURCES ENGINEERING
69 Creyke Road
Christchurch 8140

NOTES:

each steel angle is to be 2.4m long and folded from 0.55bmt cfs sheet

Dimensions in mm

SCALE: 1:1 @ A3

VER.	COMMENTS AND CHANGES	DATE
1	As-built	14/Aug/18
1	FOR TENDER	15/MAR/18

PROJECT:
Low Damage Partitions Experimental Testing

DESIGNERS:
Joshua Mulligan

SUPERVISORS:
Timothy Sullivan

TITLE:
Steel Backing angle

CODE: 64560538

DATE: 14-Aug-2018

PAGE: 001

Detailed Damage Development Observations

A summary of the damage progression in each of the specimens is shown here. The damage progression is described in terms of the damage states in table Table B.1 and with reference to the locations in figure Figure B.1. This appendix is designed to be able to be interpreted independent of the main body of writing.

Table B.1 Damage states for flexible track system specimens

Damage State	Description	Repair Action
0	Hairline cracking of paint at joints	Barely visible damage, deemed not requiring repair.
1.a	Sealant de-bonding	Remove and re-apply sealant
1.b	Cracking in plaster and paint along trim	Scrape out minor cracks, and reapply plaster and paint.
1.c	Screw damage, pull through, popping, shearing	Refix or tighten any existing loose fasteners and place additional fasters near original. Finish with plaster, and sand and paint.
2	Wallboard damage - paper face separating, crushing, cracking, spalling	Requires replacement of linings or local repairs of linings. Breakages can be ground out and patch fixed, using plastering and paper tape.
3	Framing damage - flanges bent, buckling, hinging	Both linings and framing must be removed and replaced. Thus, complete demolition and replacement of the wall is required.

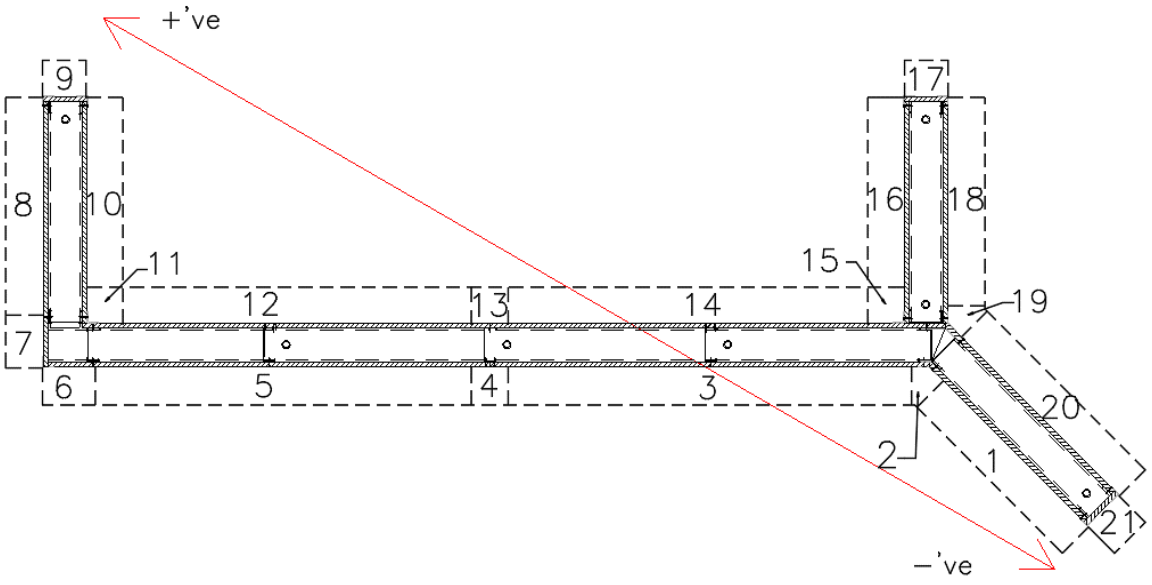

Figure B.1 Specimen location reference for damage progression tables. Axis of loading a definition of positive loading direction shown in red.

Specimen A1

Table B.2 Detailed damage progression for specimen A1 described in relation to damage states listed in Table B.1.

	STEP	6	7	8	9	10	11	12	13	14	15
Drift (%)	loading dir.	0.21	0.3	0.42	0.59	0.82	1.15	1.62	2.27	3.17	4.44
	45° wall	0.20	0.29	0.41	0.57	0.79	1.11	1.56	2.19	3.06	4.29
	90° walls	0.11	0.15	0.21	0.30	0.41	0.58	0.81	1.14	1.59	2.22
	long wall	0.18	0.26	0.36	0.51	0.71	1.00	1.40	1.97	2.75	3.85
Location	**1**	-	-	-	-	-	-	-	1a,1c	-	2
	2	-	-	-	-	-	-	-	-	1a	-
	3	-	-	-	-	-	-	1a	1c	-	2
	4	-	-	-	-	-	1c	-	-	1a	2
	5	-	-	-	-	-	1c	-	-	1a	-
	6	-	-	-	-	-	-	-	1a,2	-	1b
	7	-	-	-	-	-	1a, 2		-	-	1c
	8	-	-	-	-	-	-	1a	-	-	-
	9	-	-	-	-	-	1a, 2	-	-	-	-
	10	-	-	-	-	-	-	1c	1a	-	1b
	11	0	-	1a,1b	-	-	-	-	2	-	-
	12	-	-	-	-	1a	-	-	1c,2	-	-
	13	-	-	-	-	-	-	-	1a	-	-
	14	-	-	-	-	-	-	-	1a	-	-
	15	-	0	1a	1b	-	-	-	-	-	2
	16	-	-	-	-	1a	-	-	-	2	-
	17	-	-	-	-	-	-	-	1a,2	-	1b
	18	-	-	-	-	1a	-	-		-	1b
	19	-	-	-	-	-	1b	-		1a	-
	20	-	-	-	-	-	-	-	1c	1a	-
	21	-	-	1a,2	-	-	-	-	-	1a	-

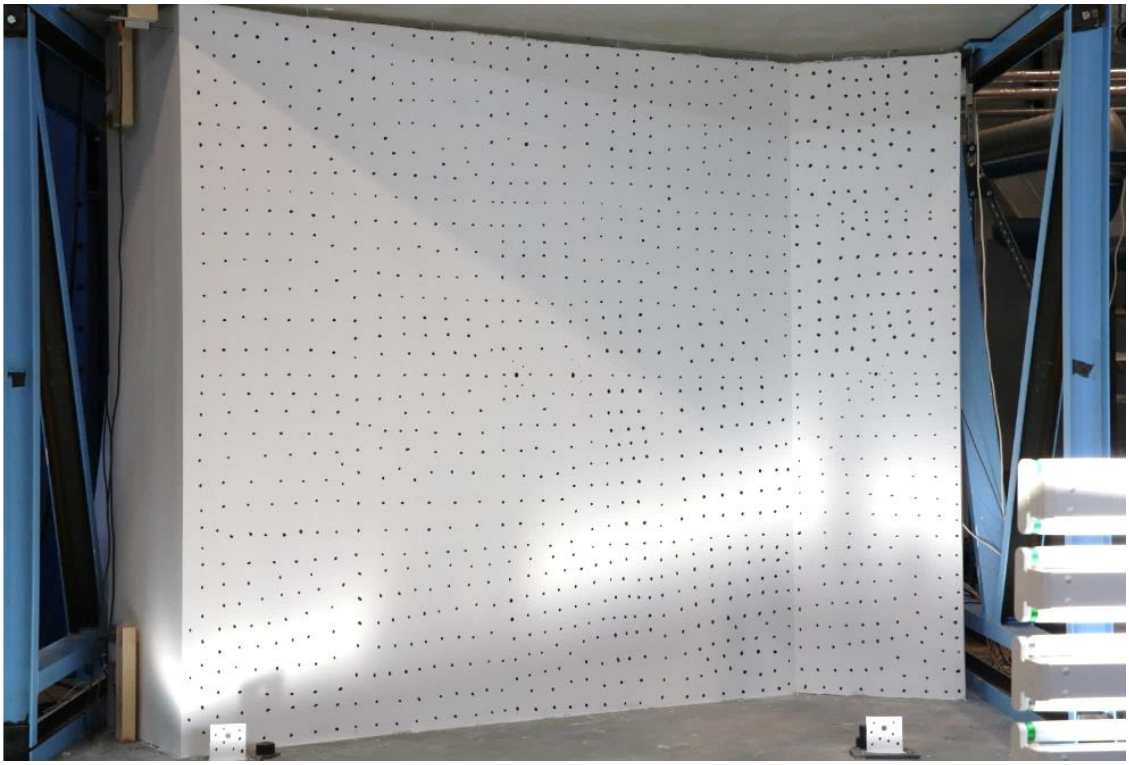

Figure B.2 Specimen A1 – Specimen condition prior to test start

Figure B.3 Specimen A1 – Prior to test start - Defects in sealant bond - location 7

Figure B.4 Specimen A1 – Prior to test start - Defects in sealant bond - location 13

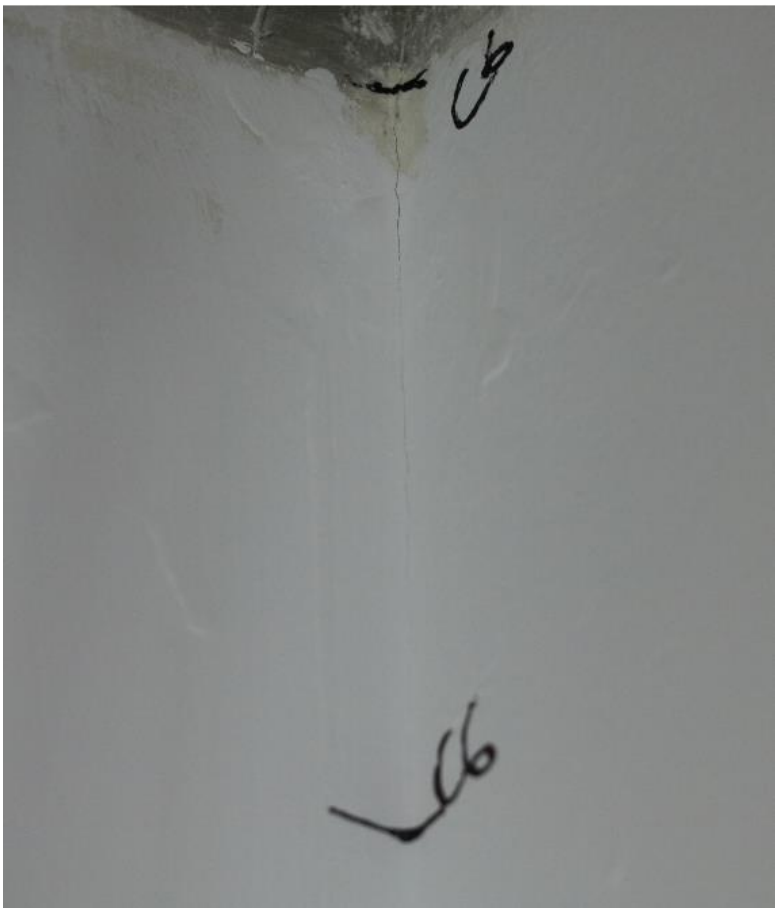

Figure B.5 Specimen A1 – Step 6 – DS0: Hairline paint cracking – location 11

Figure B.6 Specimen A1 – Step 8 – DS1b: Plaster cracking and joint tape – location 11

Figure B.7 Specimen A1 – Step 8 – DS1a: Sealant debonding at corner junction – location 15

Figure B.8 Specimen A1 - Step 8 - DS2: cracking of wallboard at wall end from pushing from track – location 21

Figure B.9 Specimen A1 - Step 8 to 9 – stiffening of reaction frame to reduce hysteretic noise

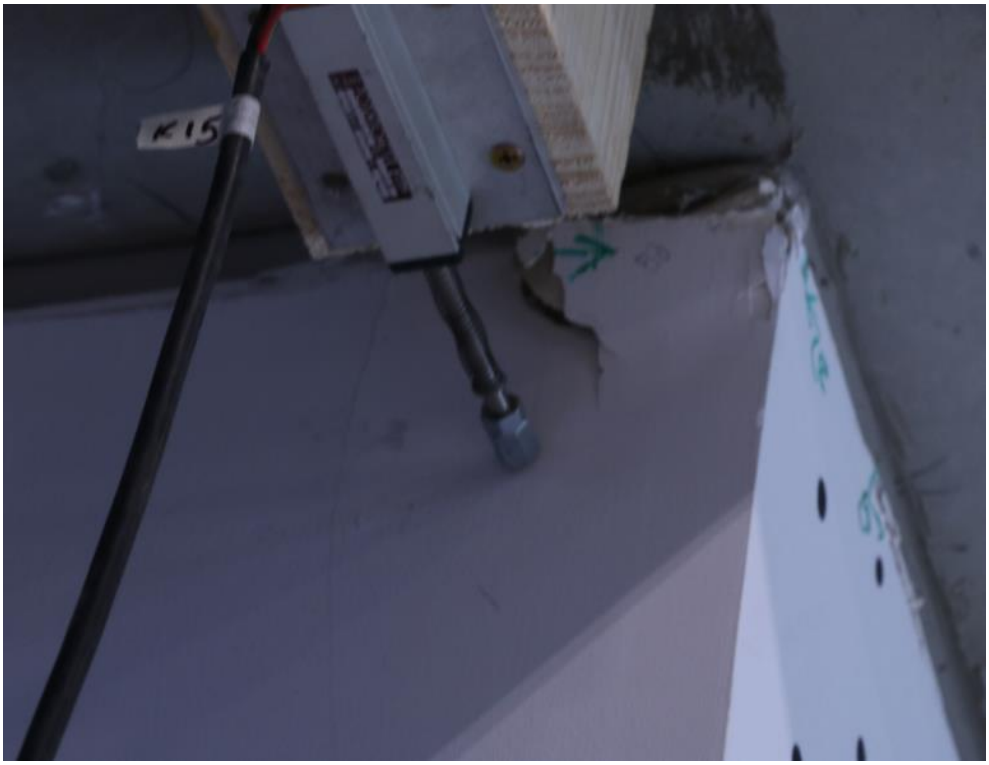

Figure B.10 Specimen A1 – Step 11 – DS2: cracking at wall end from pushing through of track – location 7

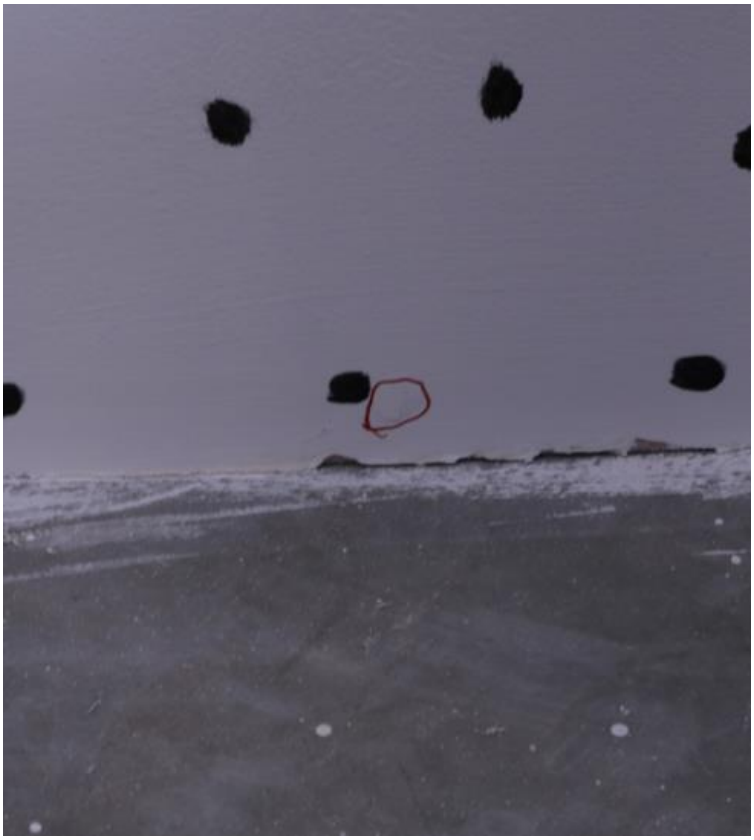

Figure B.11 Specimen A1 – Step 11 – DS1c: Popping of bottom track screw fixing head– location 3

Figure B.12 Specimen A1 – Step 11 – DS2: wallboard damage due to top track pushing through– location 9

Figure B.13 Specimen A1 - Step 12 –-further development of DS2: cracking of wallboard at wall end from pushing of track – location 21

Figure B.14 Specimen A1 - Step 8 – 0.36% drift - DS1a: onset of sealant debonding requiring replacement

Figure B.15 Specimen A1 - Step 13 –- DS2: wallboard damage – location 11

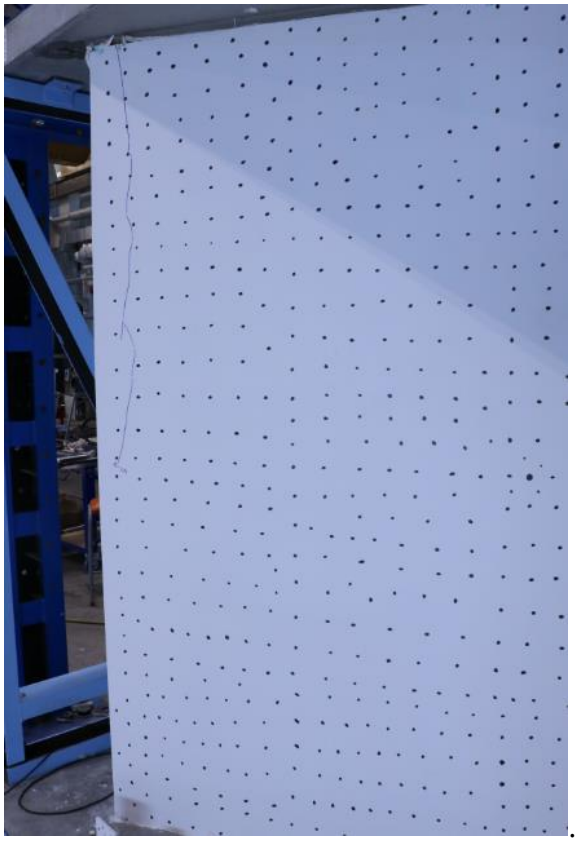

Figure B.16 Specimen A1 - Step 14 –- DS2: wallboard damage – location 6

Figure B.17 Specimen A1 - Step 14 –-A number of different forms of damage including rupturing of sealant along length of wall– locations 14-17

Figure B.18 Specimen A1 - Step 15 –-Near collapse – locations 6-11

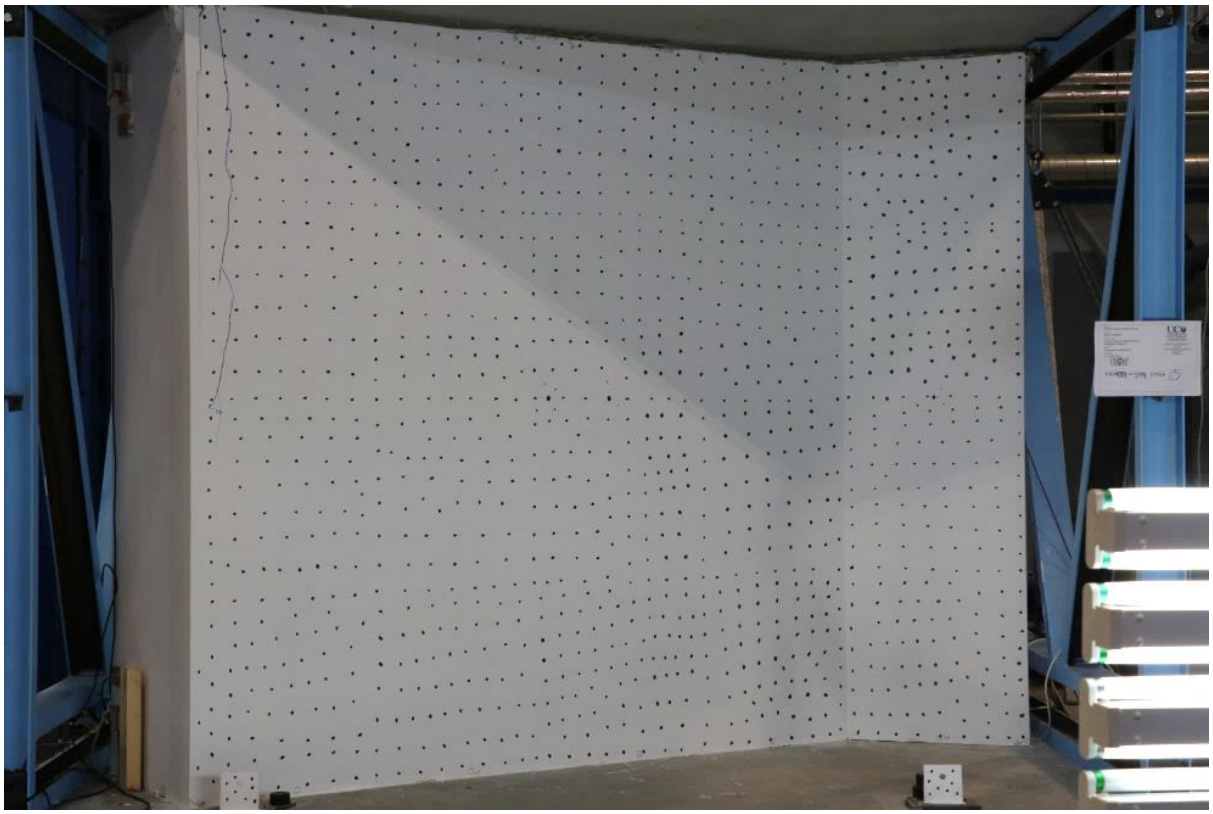

Figure B.19 Specimen A1 – Specimen condition post-test prior to removal of linings

Figure B.20 Specimen A1 – Post-test framing inspection –-buckling of studs at Y-junction and end of angled wall– locations 2, 15, 19, & 21

Figure B.21 Specimen A1 – Post-test framing inspection – bending of stud and track flanges at top including construction error – location 15 & 19

No further photos showing damage progression in this specimen or potentiometer readings are shown herein.

Specimen A2

Table B.3 Detailed damage progression for specimen A2 described in relation to damage states listed in Table B.1.

	STEP	6	7	8	9	10	11	12	13	14	15
Drift (%)	loading dir.	0.21	0.3	0.42	0.59	0.82	1.15	1.62	2.27	3.17	4.44
	45°	0.20	0.29	0.41	0.57	0.79	1.11	1.56	2.19	3.06	4.29
	90°	0.11	0.15	0.21	0.30	0.41	0.58	0.81	1.14	1.59	2.22
	long wall	0.18	0.26	0.36	0.51	0.71	1.00	1.40	1.97	2.75	3.85
Location	**1**	-	-	-	-	-	-	-	1a	-	1b
	2	-	-	-	-	-	-	-	1a	-	1b
	3	-	-	-	-	-	-	1a	-	-	-
	4	-	-	-	-	-	-	1a	-	-	-
	5	-	-	-	-	-	1a	-	-	-	-
	6	-	-	-	-	-	2	-	-	-	-
	7	-	2	-	-	-	-	-	-	-	-
	8	-	-	-	-	-	1a	-	-	-	-
	9	-	-	-	-	1a	2	-		-	-
	10	-	-	-	-	-	1a	-	-	-	-
	11	-	-	-	-	0	-	-	-	1b	2
	12	-	-	-	1a	-	-	-	-	-	-
	13	-	-	-	-	-	-	-	1a	-	-
	14	-	-	-	-	-	-	-	1a	-	-
	15	-	0	-	-	-	1a,1b	2	-	-	-
	16	-	-	-	-	-	-	2	-	-	-
	17	-	-	-	-	-	-	2	-	-	-
	18	-	-	-	-	-	-	1a	-	2	1c
	19	-	-	-	-	1a	0	-	-	1c	1b,2
	20	-	-	-	-	-	-	1a	-	2	-
	21	-	-	-	2	-	-	-	-	-	-

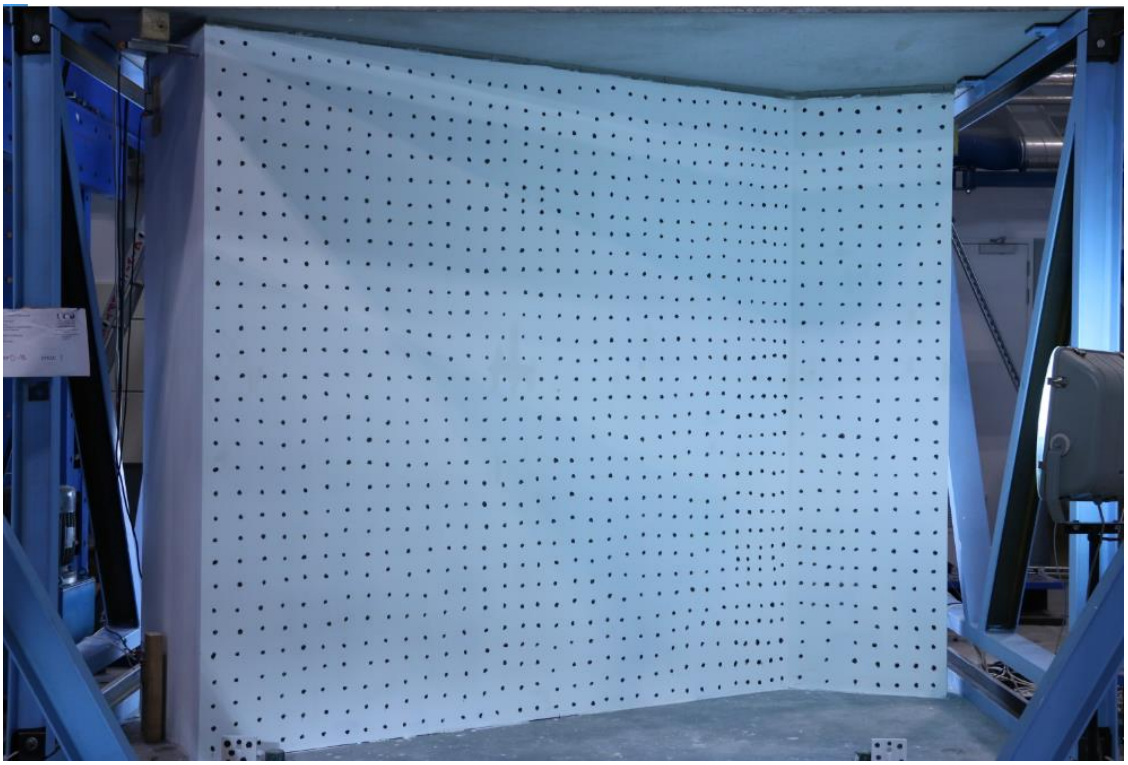

Figure B.22 Specimen A2 – Condition prior to test start

Figure B.23 Specimen A2 – Prior to test start –Defects in sealant bonding at corner junction – location 15

Figure B.24 Specimen A2 – Step 7– DS2: wallboard damage - location 7

Figure B.25 Specimen A2 – Step 7– DS0: hairline paint cracking (behind blue marker)- location 15

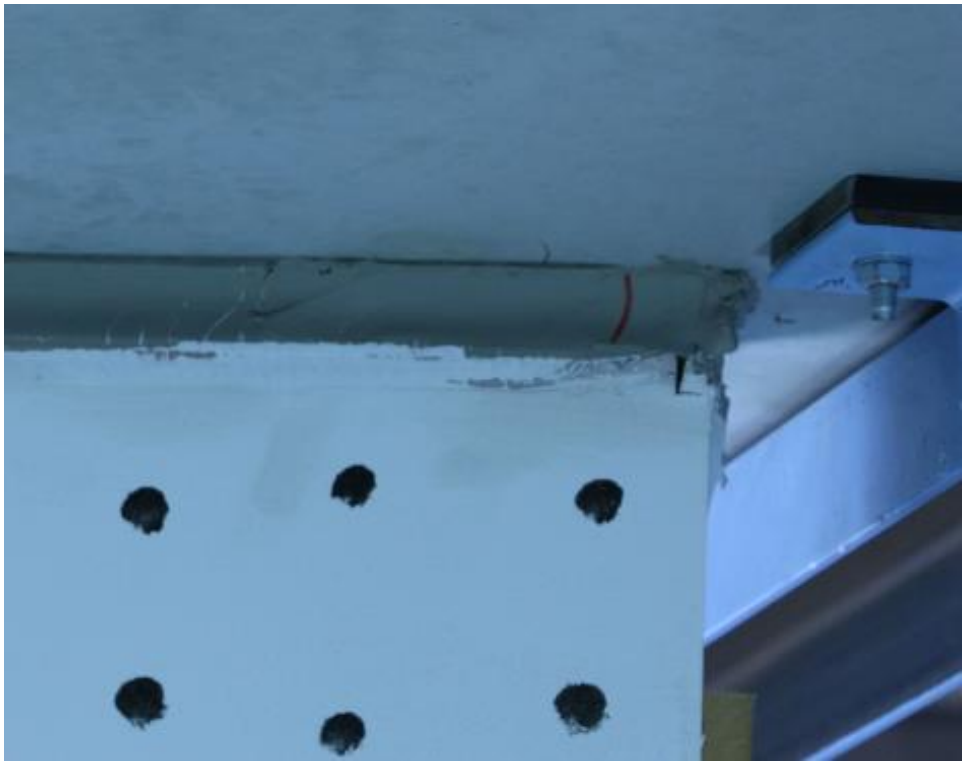

Figure B.26Specimen A2 – Step 9 – DS1a: Sealant debonding – location 1

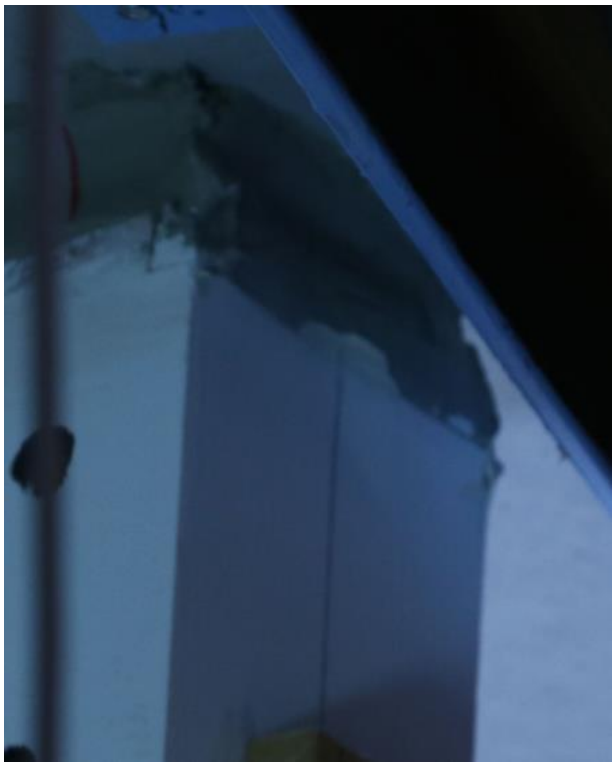

Figure B.27 Specimen A2 – Step 9 – DS2: Wallboard Damage – location 21

Figure B.28 Specimen A2 – Step 10 – DS0: Hairline paint cracking – location 11

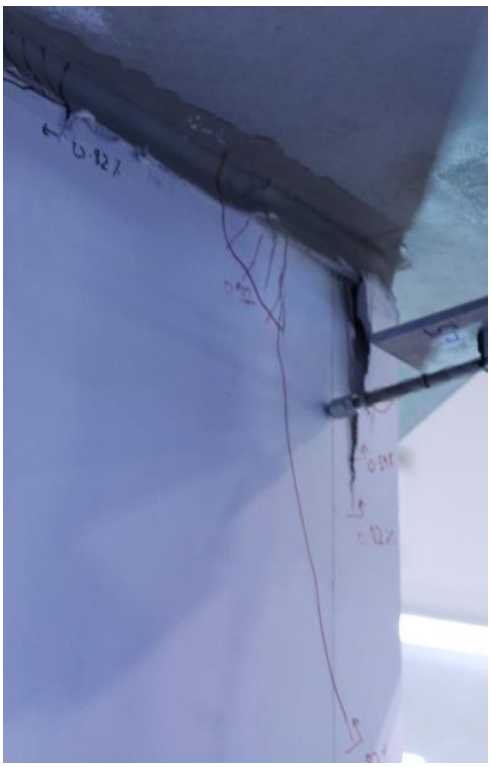

Figure B.29 Specimen A2 - Step 10 - DS2: Progression of cracking of wallboard at wall end from pushing from track – location 7

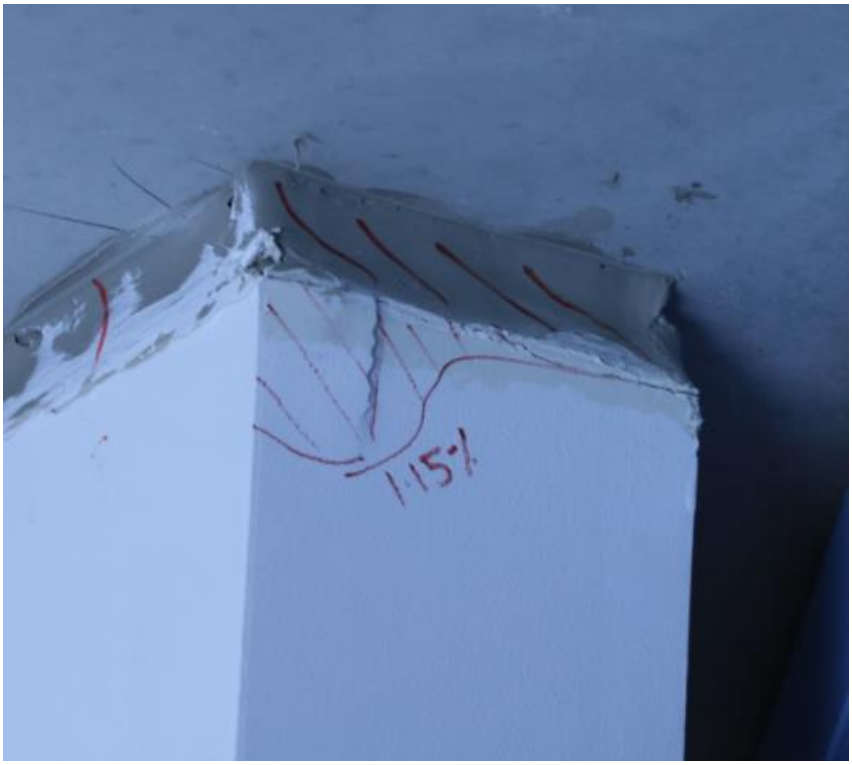

Figure B.30 Specimen A2 - Step 11 - DS2: Cracking of wallboard at wall end – location 9

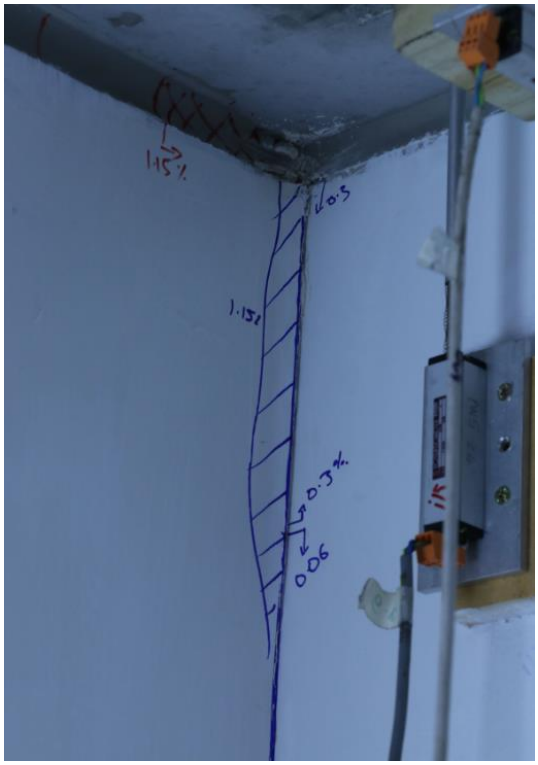

Figure B.31 Specimen A2 – Step 11 – DS1a,b: debonding of sealant at plaster cracking at intersection – location 15

Figure B.32 Specimen A2 – Step 12 – DS2: Wallboard Damage– location 15 & 16

Figure B.33 Specimen A2 – Step 12 – DS2: wallboard damage due to top track pushing through– location 16

Figure B.34 Specimen A2 - Step 13 –-DS1a: Sealant rupturing in shear (ass opposed to debonding)– location 13

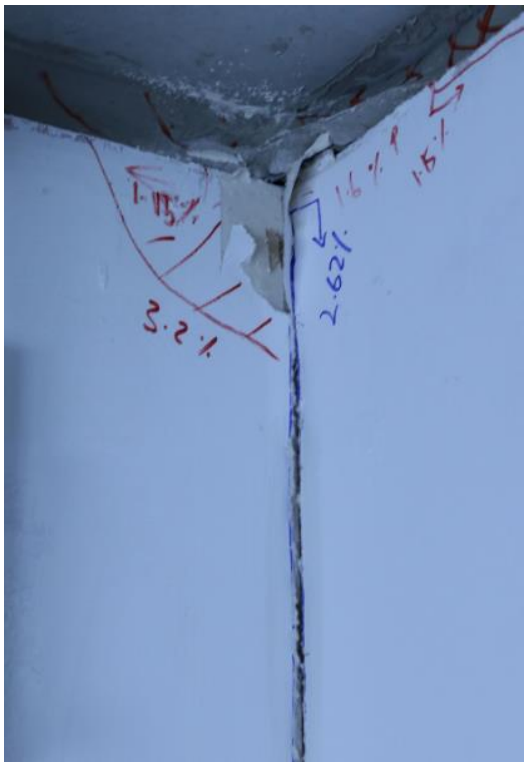

Figure B.35 Specimen A2 - Step 14 – DS1b: paper tape detaching and plaster cracking – location 11

Figure B.36 Specimen A2 - Step 14 –- DS1a: sealant rupturing– locations 12 to 14

.

Figure B.37 Specimen A2 - Step 15 –- DS2: wallboard damage – location 11

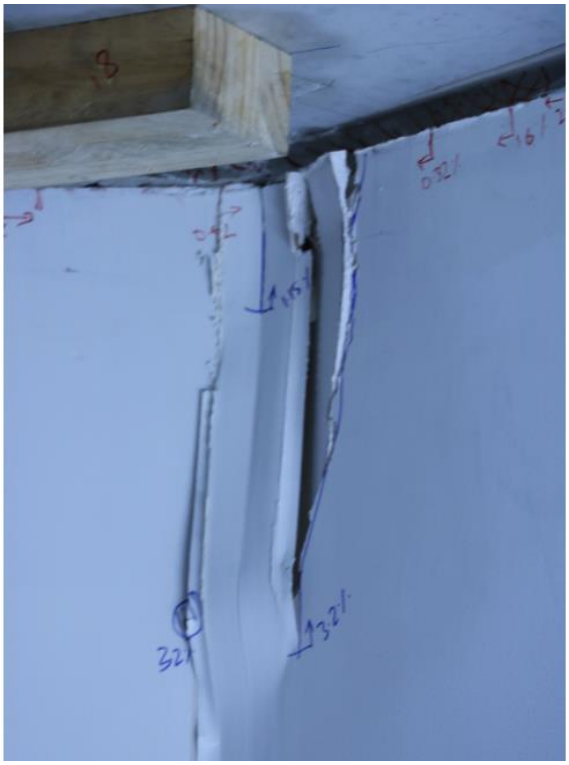

Figure B.38 Specimen A2 - Step 15 – DS2: Wallboard damage – location 19

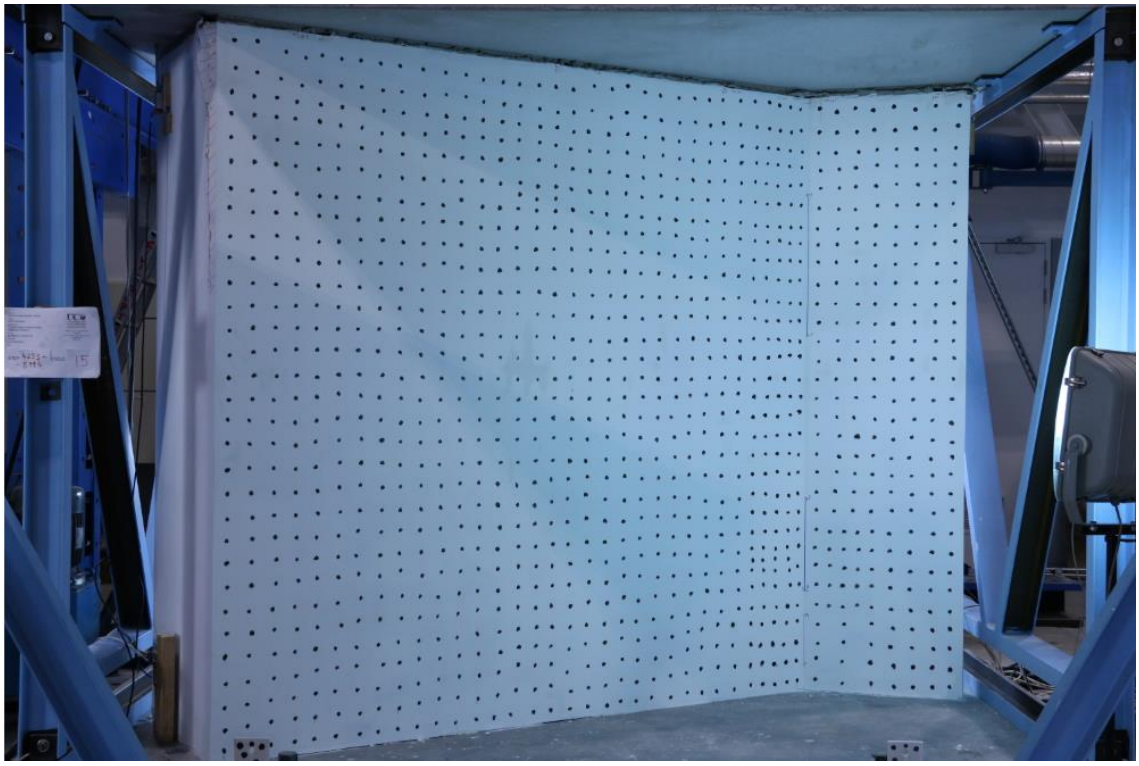

Figure B.39 Specimen A2 – Specimen after completion of test prior to removal of linings

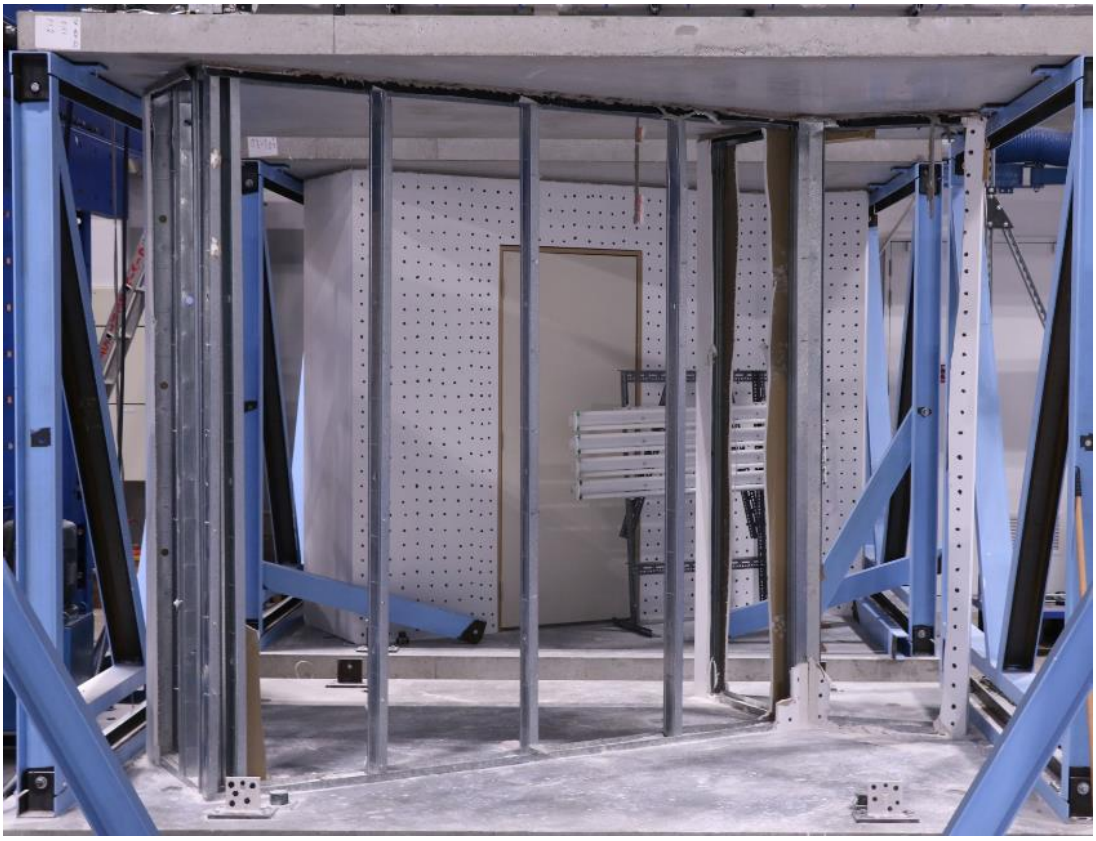

Figure B.40 Specimen A2 – Post-test framing inspection –-steel framing with linings removed

Figure B.41 Specimen A2 – Post-test framing inspection –-buckling of studs at Y-junction in angled wall– locations 2 & 19

Figure B.42 Specimen A2 – Post-test framing inspection – buckling of stud at end of angled wall– location 21

Figure B.43 Specimen A2 – Post-test framing inspection – bending of stud and track flanges at top including construction error – location 15 & 19

No further photos showing damage progression in this specimen or potentiometer readings are shown herein.

Specimen A3

Table B.4 Detailed damage progression for specimen A3 described in relation to damage states listed in Table B.1.

	STEP	6	7	8	9	10	11	12	13	14	15	16
Drift (%)	loading dir.	0.21	0.3	0.42	0.59	0.82	1.15	1.62	2.27	3.17	4.44	6.22
	45° wall	0.20	0.29	0.41	0.57	0.79	1.11	1.56	2.19	3.06	4.29	6.00
	90° walls	0.11	0.15	0.21	0.30	0.41	0.58	0.81	1.14	1.59	2.22	3.11
	long wall	0.18	0.26	0.36	0.51	0.71	1.00	1.40	1.97	2.75	3.85	5.38
Location	**1**	-	-	-	-	-	-	-	-	1a	1c,2	1b
	2	-	-	-	-	-	-	-	-	1a	1b	2
	3	-	-	-	-	-	-	-	-	1a	1b,1c	2
	4	**0**	2	-	-	-	-	-	-	1a, 3*	-	3
	5	-	-	-	-	-	-	-	1a	-	-	-
	6	-	-	-	-	-	-	-	1a	-	1c,2	-
	7	-	-	-	-	-	-	-	1a	2	-	-
	8	-	-	-	-	-	-	-	-	1a,1c	-	-
	9	-	-	-	-	-	1a,2	-	-	-	-	-
	10	-	-	-	-	-	-	-	2	-	-	-
	11	-	-	-	0	1b	2	-	-	-	-	-
	12	-	-	-	-	-	-	-	1a	-	-	1c,2
	13	**0**	2	-	-	-	-	-	1a	-	-	-
	14	-	-	-	-	-	1a	-	-	-	-	1c,2
	15	-	-	-	0	1b	-	2	-	-	-	-
	16	-	-	-	-	-	1a	-	-	-	-	-
	17	-	-	-	-	-	-	1a	-	2	-	-
	18	-	-	-	-	-	1a	-	1b	2	1c	-
	19	-	-	-	-	-	-	-	1b	2	-	-
	20	-	-	-	-	-	1a	-	-	1b	2	-
	21	-	-	-	1b	2	-	-	-	-	-	-

Note: 3* refers to damage of the doorframe at which point the door could not be closed

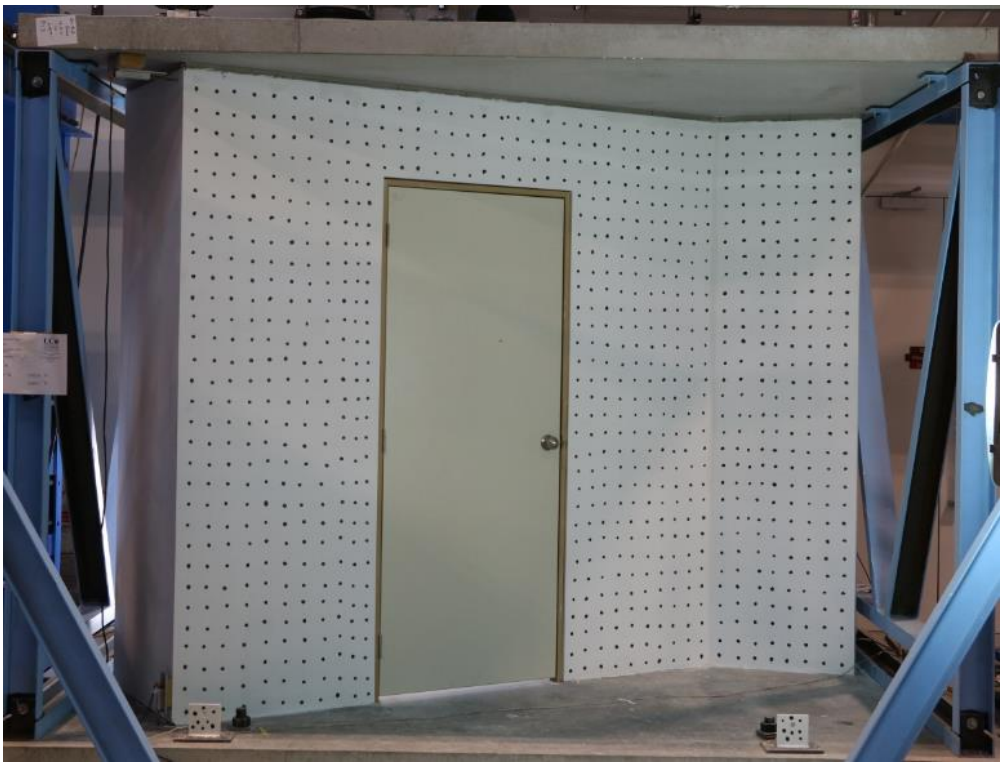

Figure B.44 Specimen A3 – Specimen prior to test start

Figure B.45 Specimen A3 – Prior to test start –Defects in sealant bonding at corner junction – location 15

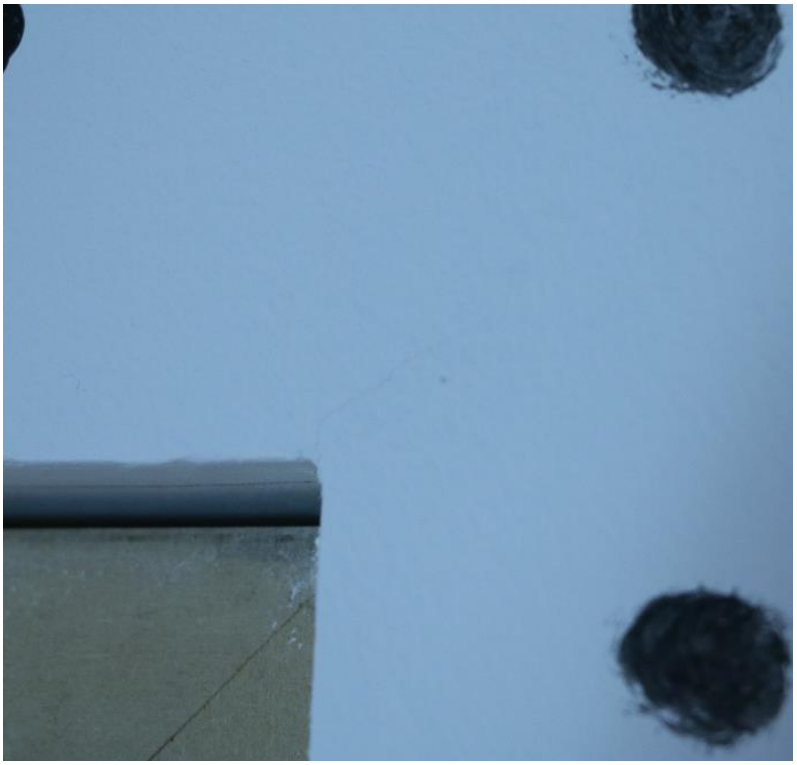

Figure B.46 Specimen A3 – Prior to test start– DS0: hairline paint cracking at the corner of door frame - location 13

Figure B.47 Specimen A3 – Step 3– DS0: hairline paint cracking - location 13

Figure B.48 Specimen A3 – Step 6 – DS00: Hairline paint cracking – location 4

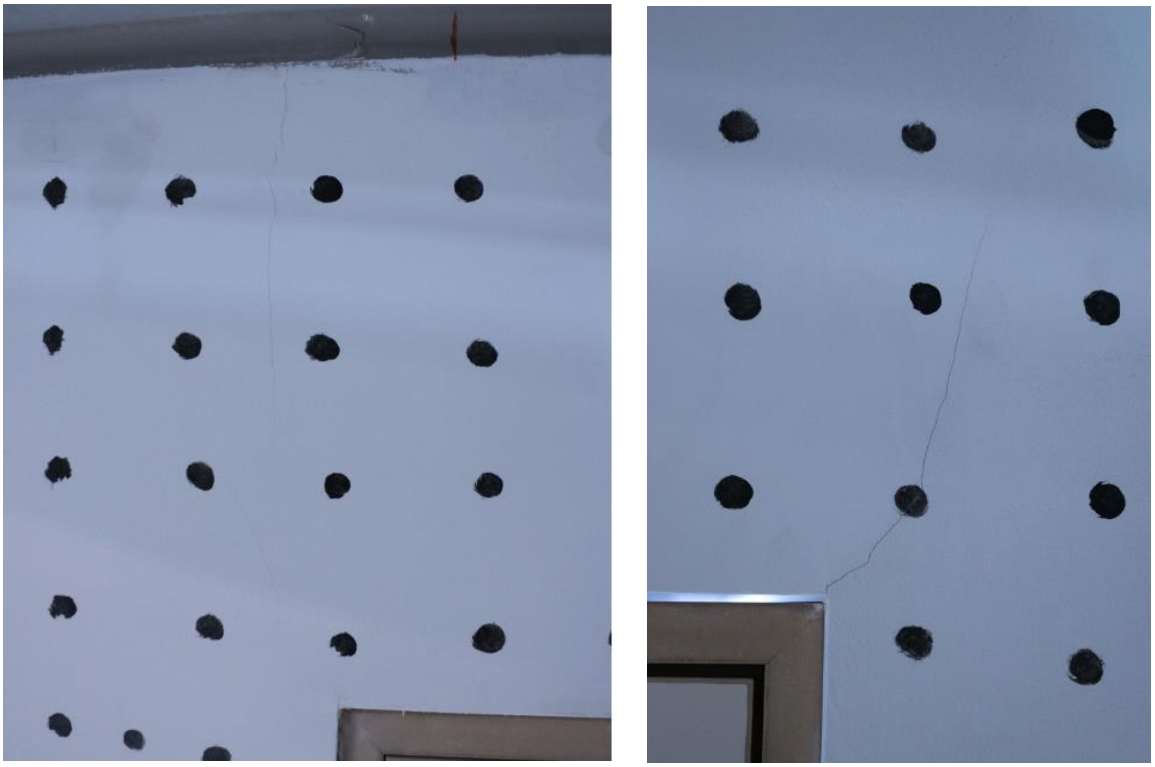

Figure B.49 Specimen A3 – Step 7 – DS2: Wallboard Damage – location 4 (either side of doorway)

Figure B.50 Specimen A3 – Step 7 – DS2: Wallboard Damage – location 13

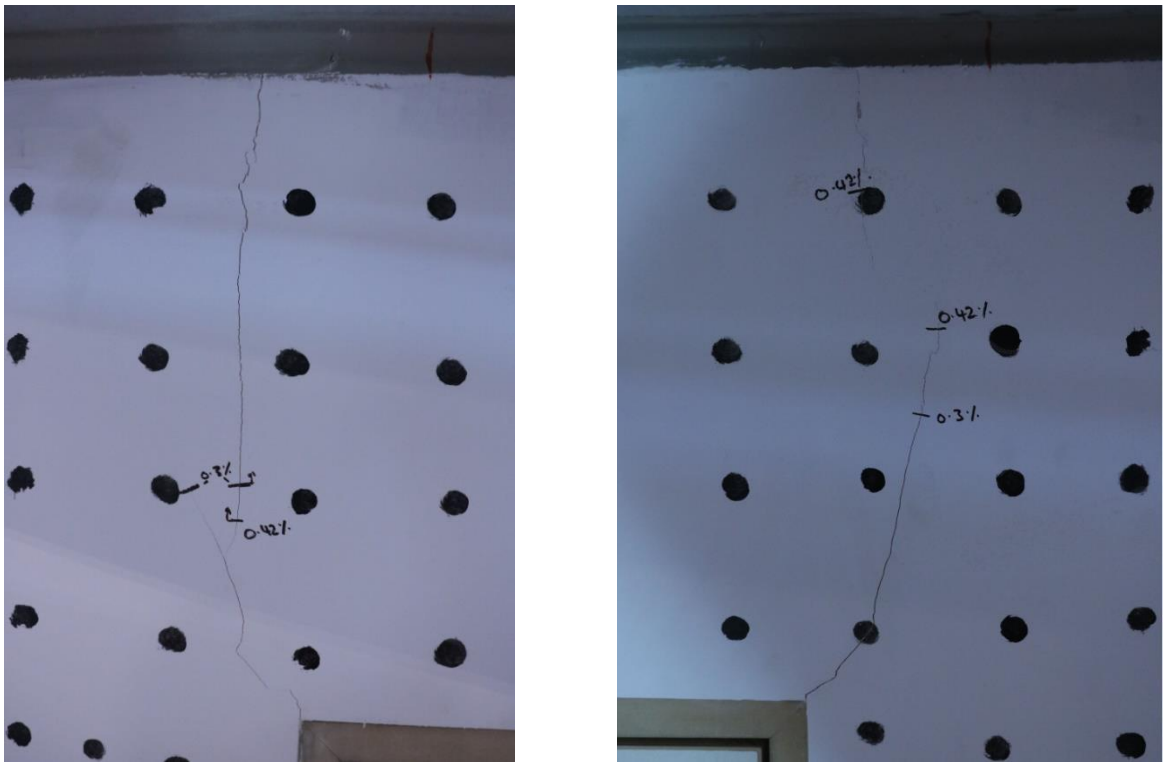

Figure B.51 Specimen A3 – Step 9 –Progression of wallboard damage – location 4 (either side of doorway)

Figure B.52 Specimen A2 – Step 9 – DS1b: Plaster damage– location 21

Figure B.53 Specimen A3 - Step 10 – DS1b: Plaster cracking – location 11

Figure B.54 Specimen A3 – Step 21 – DS2: Wallboard Damage– location 21

Figure B.55 Specimen A3 – Step 11 – DS2: wallboard damage due to top track pushing through– location 9

Figure B.56 Specimen A3 - Step 11 –-DS2: Wallboard damage – location 11

Figure B.57 Specimen A3 - Step 11 – DS1a: Separation of sealant from plasterboard lining – location 18

Figure B.58 Specimen A3 - Step 12 –- DS2: Wallboard damage – location 15

Figure B.59 Specimen A3 - Step 13 –- DS1a: Sealant debonding – location 6

Figure B.60 Specimen A3 - Step 14– DS1a: Debonding of sealant– location 4

Figure B.61 Specimen A3 - Step 14 – DS3*: damage to door framing – location 4

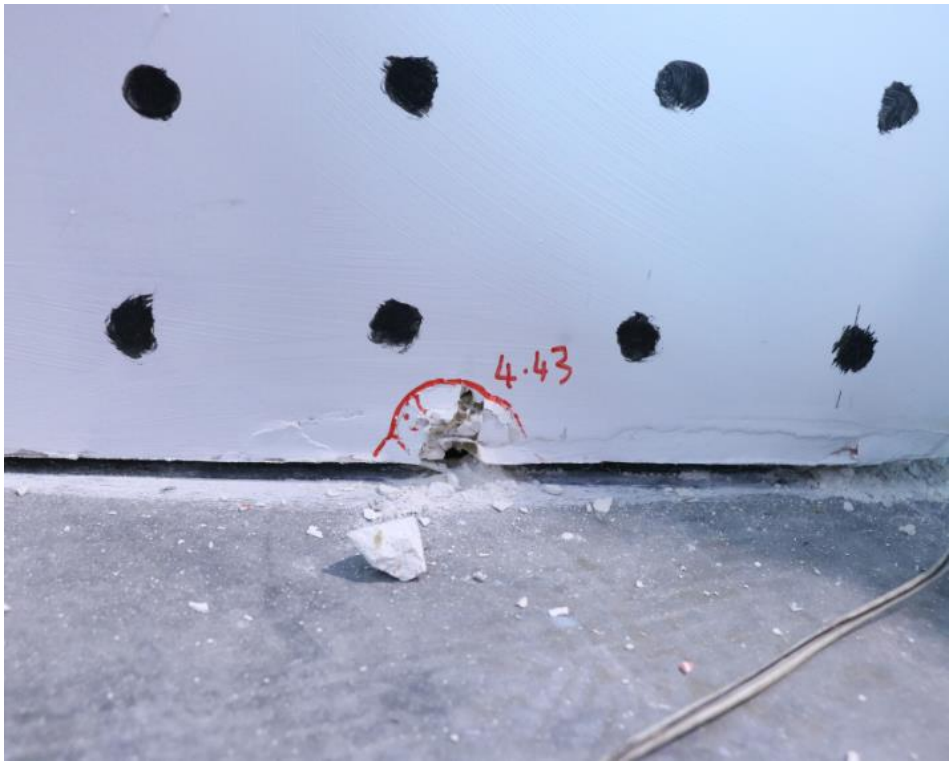

Figure B.62 Specimen A3 - Step 15– DS1c & 2: screw damage and wallboard damage around screw head– location 1

Figure B.63 Specimen A3 - Step 16– DS3: spalling of wallboard revealing buckling of studs above door frame– location 4

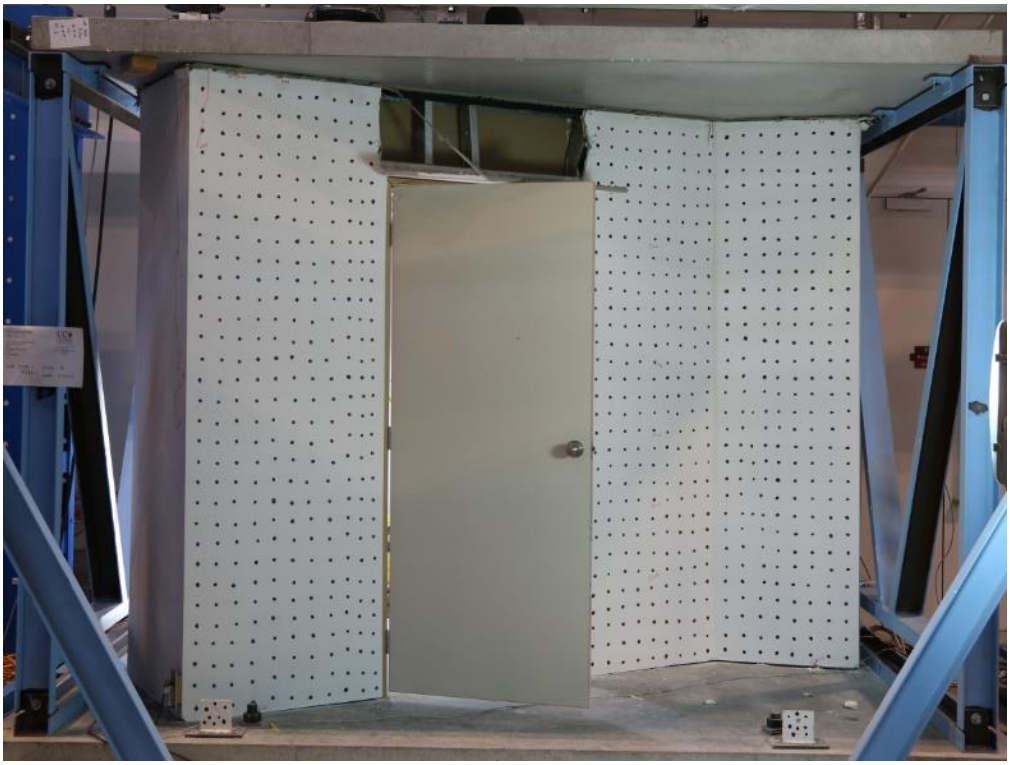

Figure B.64 Specimen A3 - Step 16 – specimen after completion of test prior to removal of linings

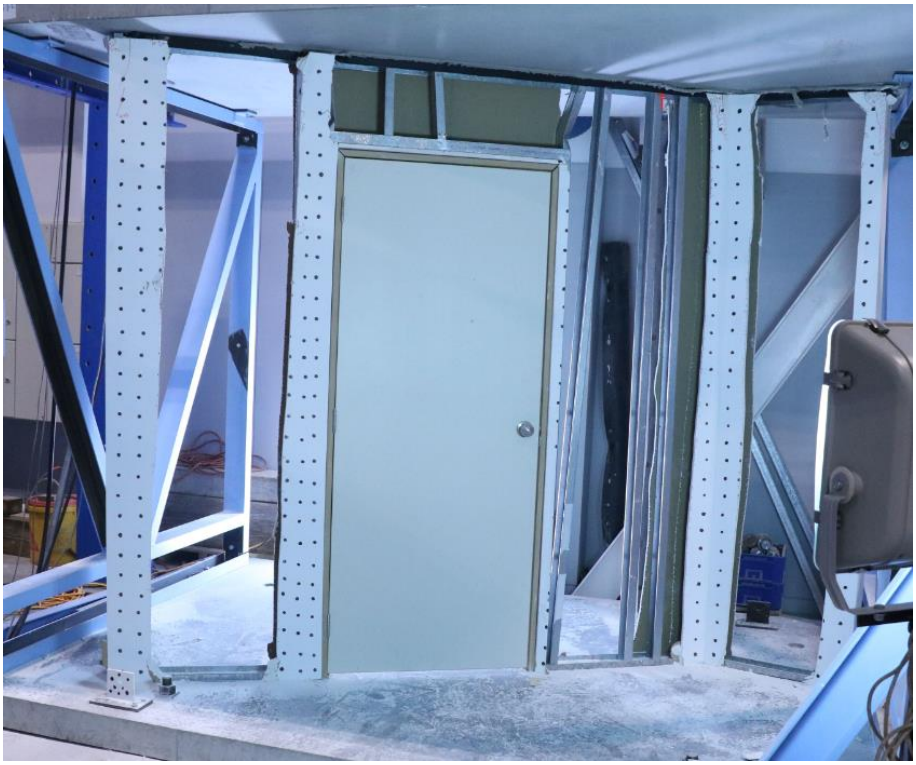

Figure B.65 Specimen A3 – Post-test framing inspection –-steel framing with linings removed

Figure B.66 Specimen A2 – Post-test framing inspection –-buckling of studs at L-junction – locations 6

Figure B.67 Specimen A2 – Post-test framing inspection – buckling and bending of study flanges of stud at end of main wall at Y-junction – location 2 & 15

Figure B.68 Specimen A2 – Post-test framing inspection – bending of stud and track flanges at top including construction error – location 15 & 19

No further photos showing damage progression in this specimen or potentiometer readings are shown herein.

Appendix C Seismic Gap System Data

Specimen Construction Drawings

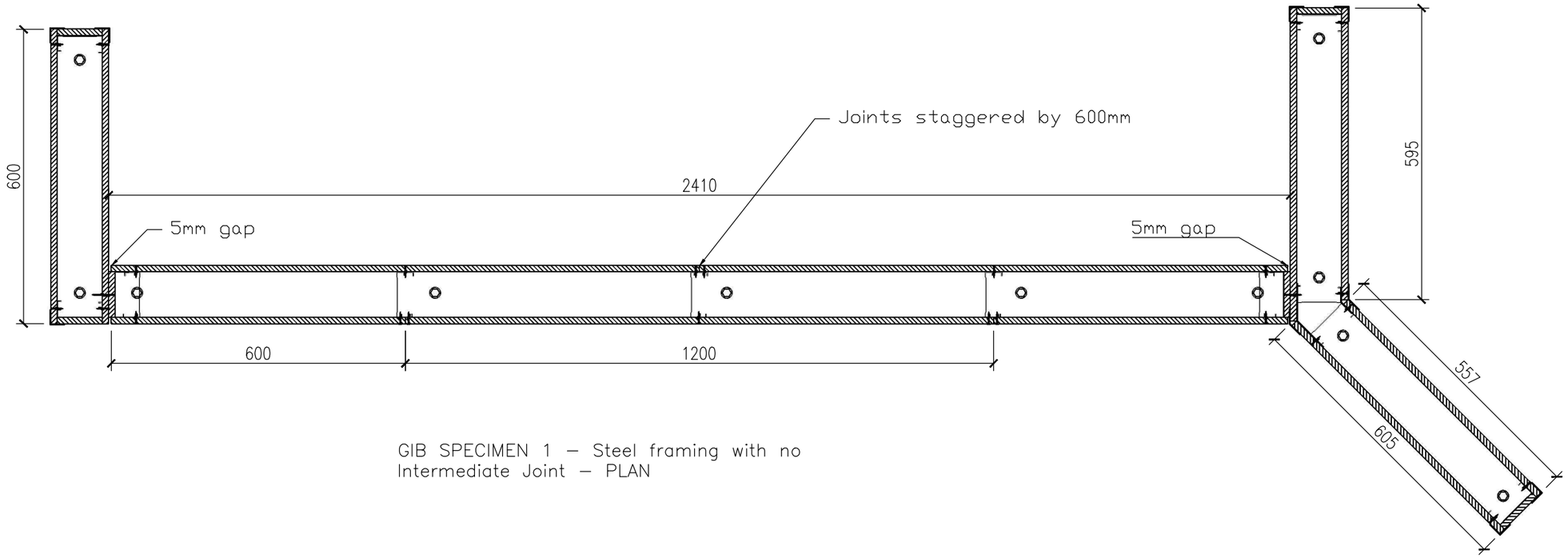

GIB SPECIMEN 1 – Steel framing with no Intermediate Joint – PLAN

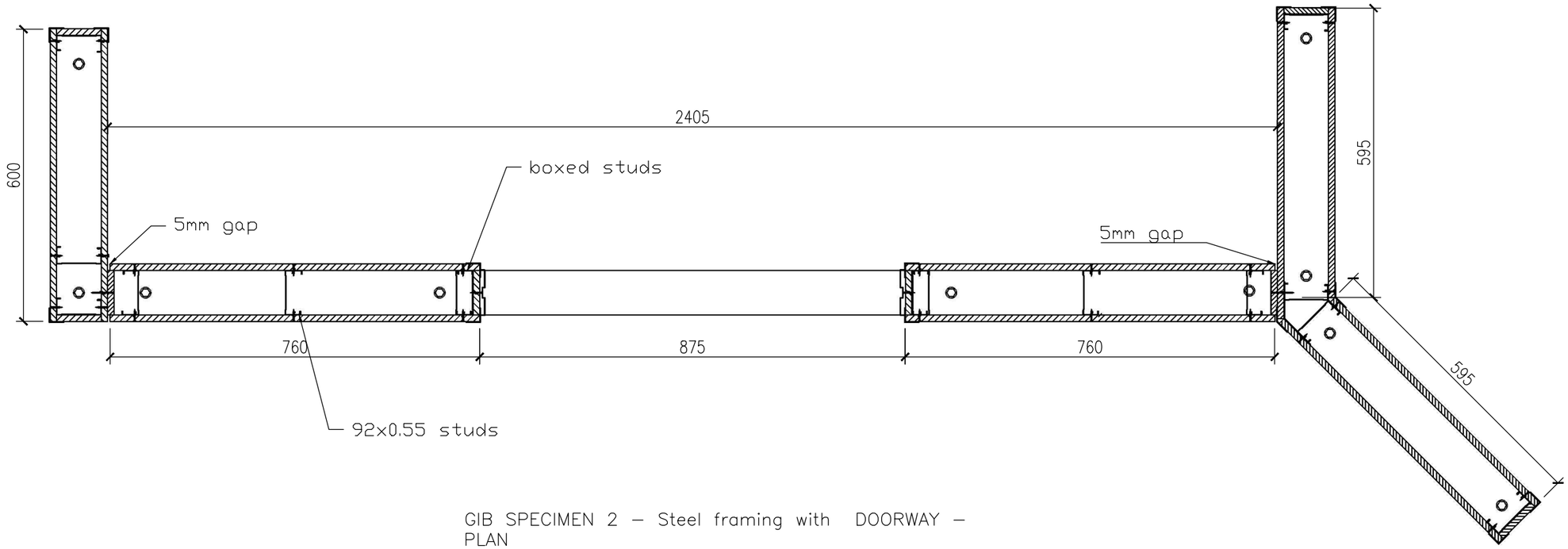

GIB SPECIMEN 2 – Steel framing with DOORWAY – PLAN

UNIVERSITY OF CANTERBURY
Te Whare Wānanga o Waitaha
CHRISTCHURCH NEW ZEALAND

UNIVERSITY OF CANTERBURY
Private Bag 4800
Christchurch 8140

CIVIL AND NATURAL RESOURCES ENGINEERING
69 Creyke Road
Christchurch 8140

NOTES:

track anchors are HILTI FIXING HUS-10 OR SIMILAR

track are to be anchored at same locations top and bottom

Drywalls finished as per GIB site guide specifications to a level 4 finish with a single coat of paint.

All, corners junctions are to be finished with GIB ultraflex no coat 82mm tape

All studs are 92x0.55bmt
All tracks are 94x0.5bmt

Dimensions in mm

SCALE: 1:10 @ A3

VER.	COMMENTS AND CHANGES	DATE
5	FOR CONSTRUCTION	20/MAY/18
4	Revision 3	11/MAY/18
3	Revision 2	01/MAY/18
2	Revised following meeting	23/APR/18
1	Preliminary	29/JAN/18

PROJECT:
Partitions Experimental Testing

DESIGNERS:
Joshua Mulligan

SUPERVISORS:
Timothy Sullivan

TITLE:
GIB System Specimens 1 and 2 Plan

CODE: 64560538

DATE: 20-MAY-2018

PAGE: 001

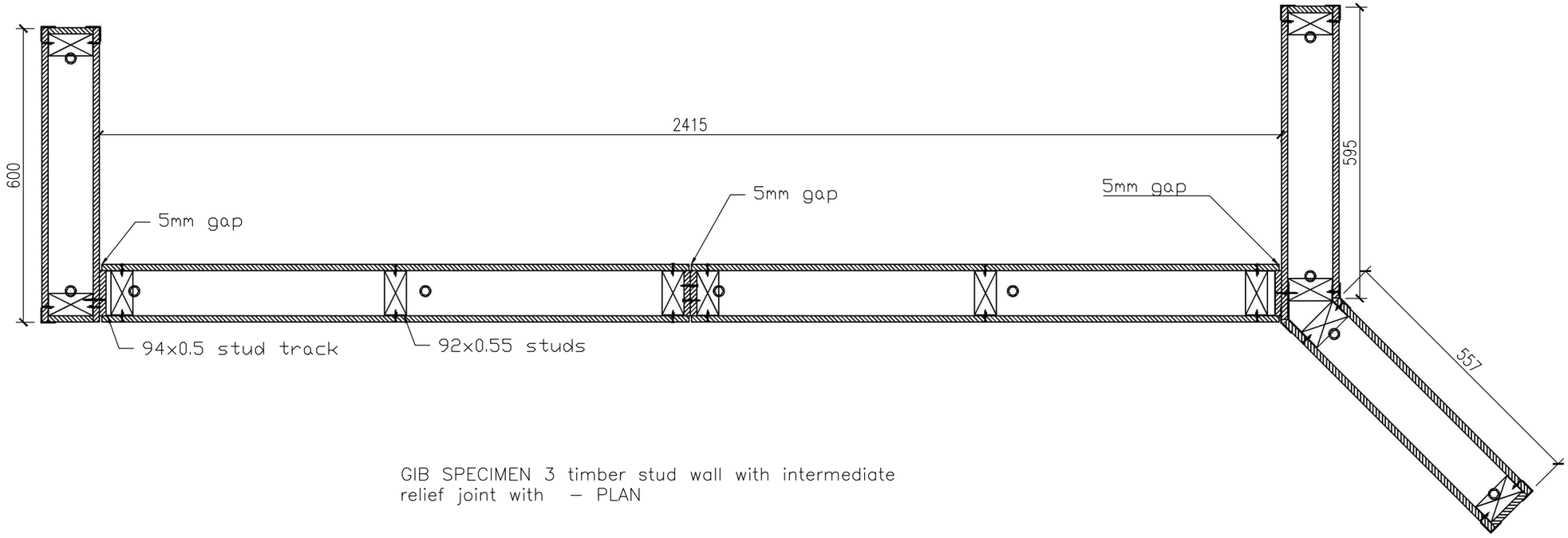

GIB SPECIMEN 3 timber stud wall with intermediate relief joint with – PLAN

UNIVERSITY OF CANTERBURY
Te Whare Wānanga o Waitaha
CHRISTCHURCH NEW ZEALAND

UNIVERSITY OF CANTERBURY
Private Bag 4800
Christchurch 8140

CIVIL AND NATURAL RESOURCES ENGINEERING
69 Creyke Road
Christchurch 8140

NOTES:

track anchors are HILTI FIXING HUS-10 OR SIMILAR

track are to be anchored at same locations top and bottom

Drywalls finished as per GIB site guide specifications to a level 4 finish with a single coat of paint.

All, corners junctions are to be finished with GIB ultraflex no coat 82mm tape

All studs are 92x0.55bmt
All tracks are 94x0.5bmt

Dimensions in mm

SCALE: 1:10 @ A3

VER.	COMMENTS AND CHANGES	DATE
5	FOR CONSTRUCTION	20/MAY/18
4	Revision 3	11/MAY/18
3	Revision 2	01/MAY/18
2	Revised following meeting	23/APR/18
1	Preliminary	29/JAN/18

PROJECT:
Partitions Experimental Testing

DESIGNERS:
Joshua Mulligan

SUPERVISORS:
Timothy Sullivan

TITLE:
GIB System Specimens 3 - Plan

CODE: 64560538

DATE: 20-May-2018

PAGE: 002

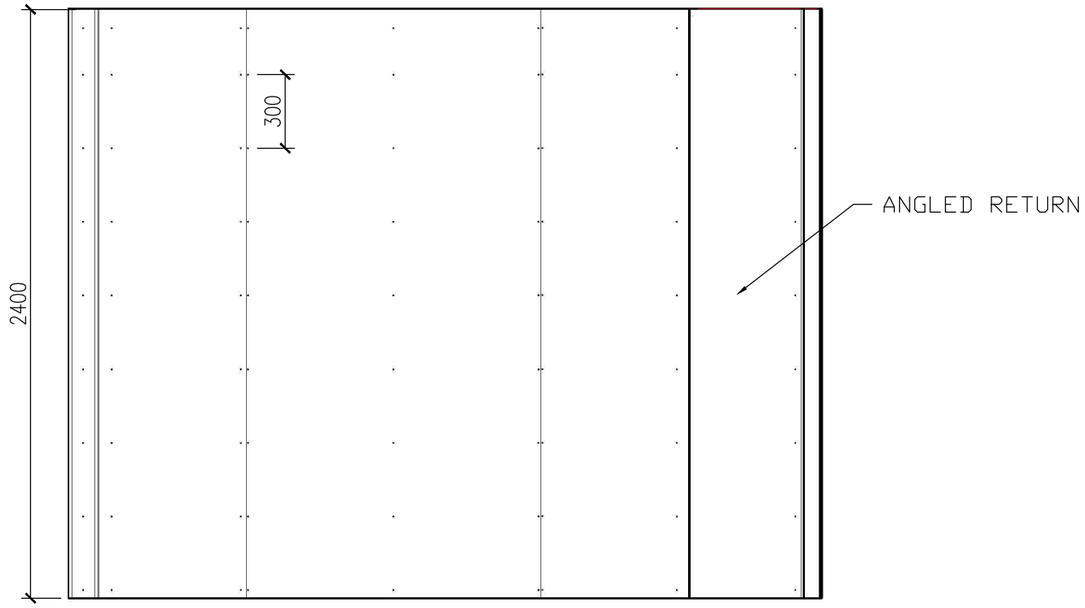

GIB Specimen 1 – ELEVATION 1

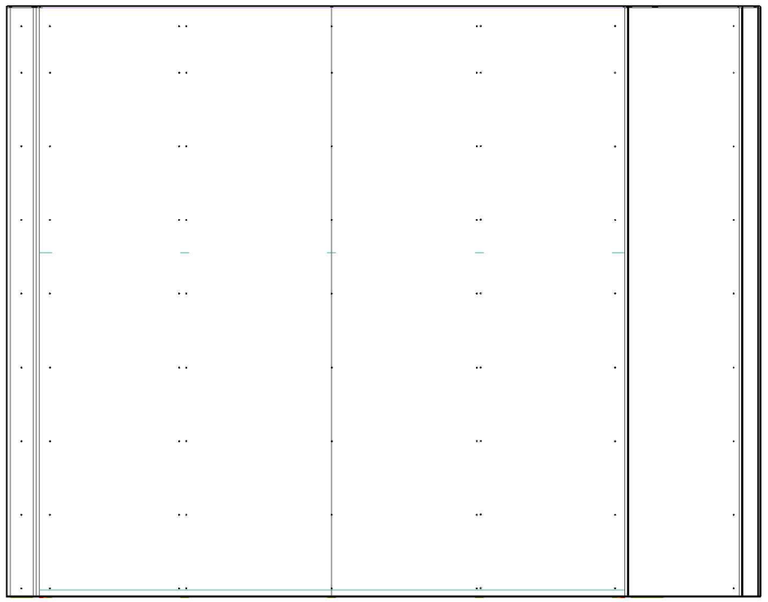

GIB Specimen 1 – ELEVATION 2

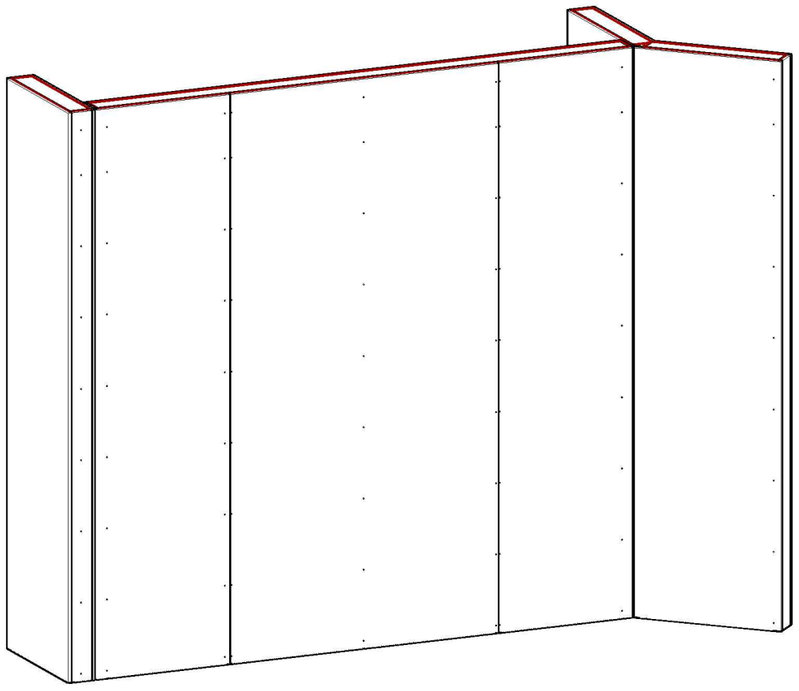

GIB Specimen 1 – perspectve

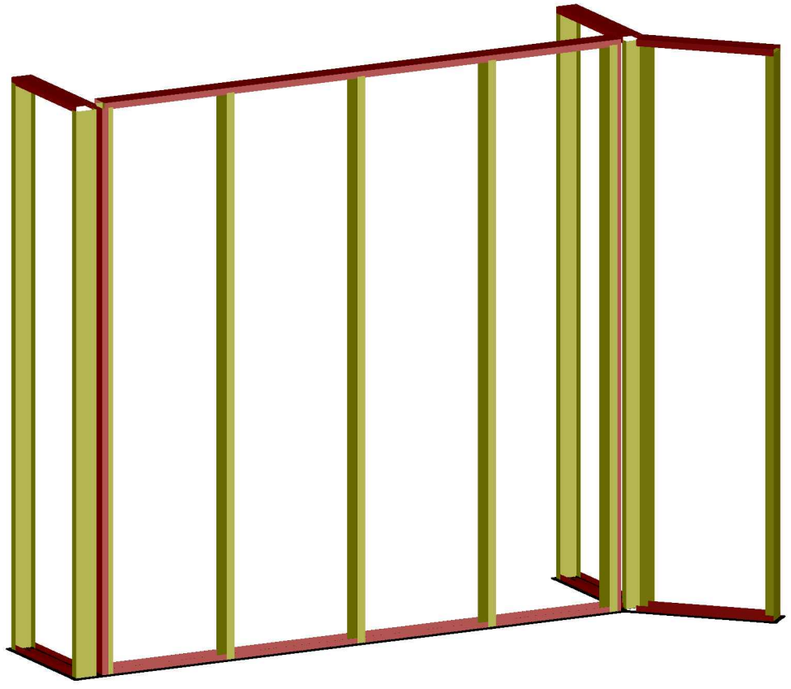

GIB Specimen 1 framing – perspective

UNIVERSITY OF CANTERBURY
Private Bag 4800
Christchurch 8140

CIVIL AND NATURAL RESOURCES ENGINEERING
69 Creyke Road
Christchurch 8140

NOTES:

All studs are 92x0.55bmt
All tracks are 94x0.5bmt

Dimensions in mm

SCALE: 1:25 @ A3

VER.	COMMENTS AND CHANGES	DATE
4	Revision 3	11/May/18
3	Revision 2	01/May/18
2	Revision 1	23/APR/18
1	Preliminary	09/JAN/18

PROJECT:
Partitions Experimental Testing

DESIGNERS:
Joshua Mulligan

SUPERVISORS:
Timothy Sullivan

TITLE:
WALL TEST SPECIMEN GIB
Elevation 1 - plain wall with no intermediate joint

CODE: 64560538

DATE: 11-May-2018

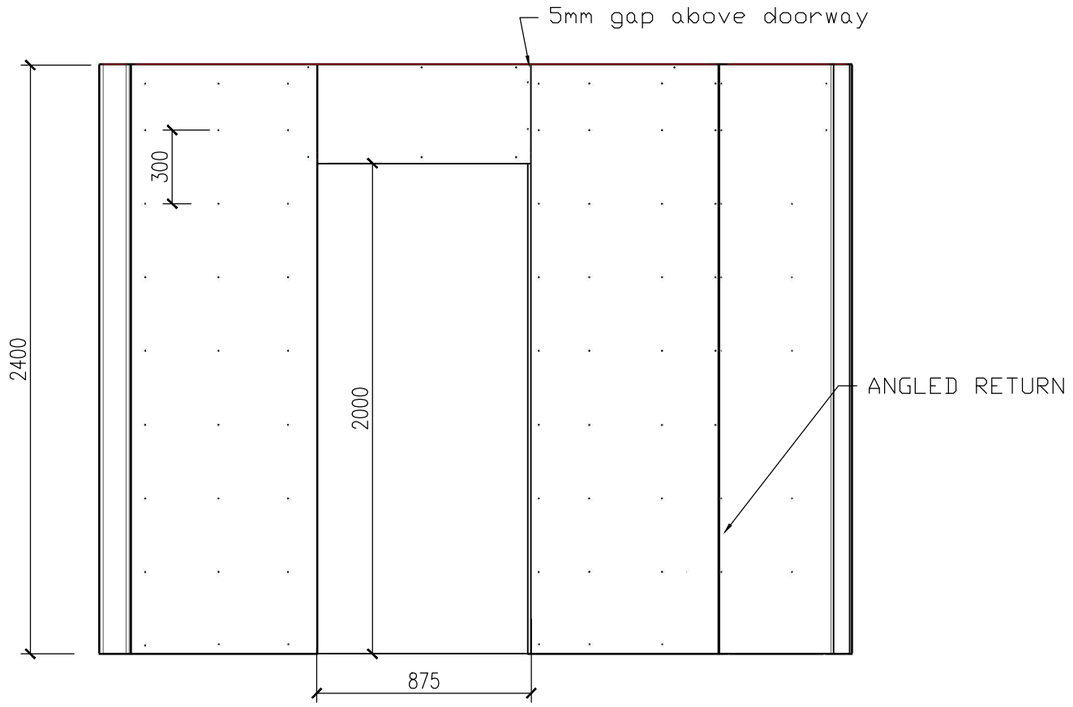

GIB specimen 2 – ELEVATION 1

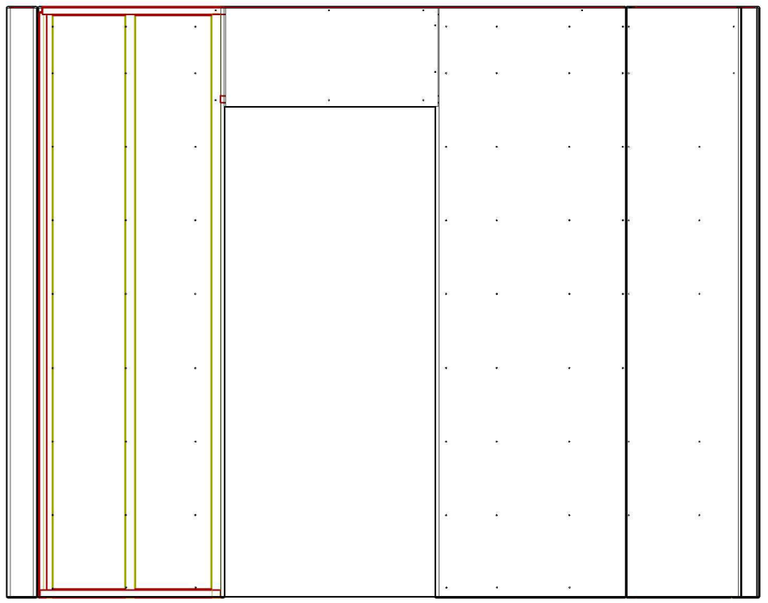

GIB Specimen 2 – ELEVATION 2

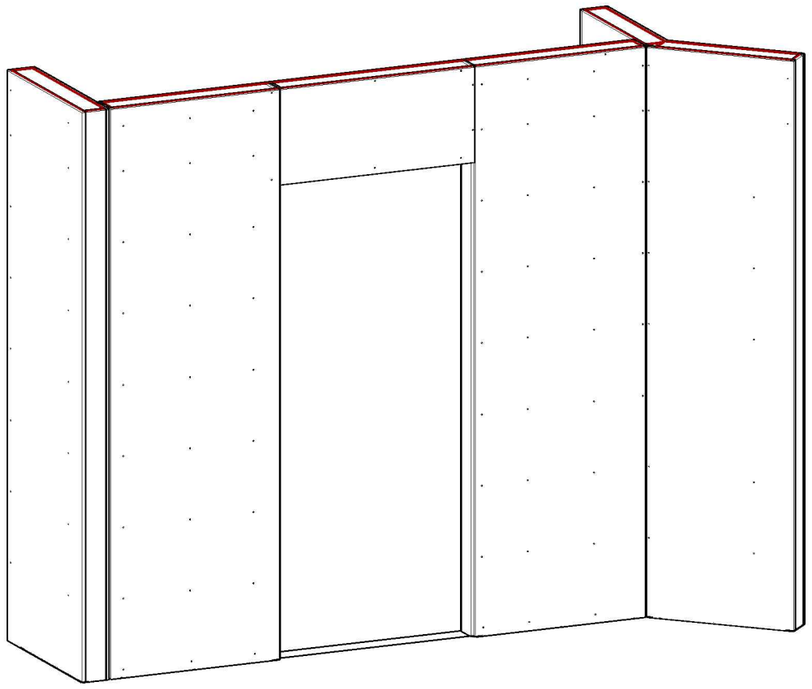

GIB Specimen 2 – Perspective

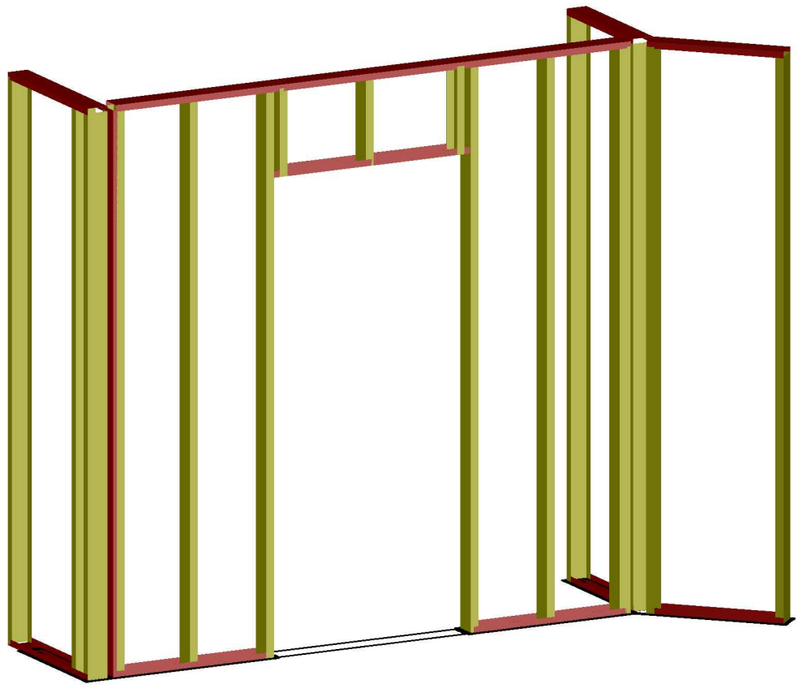

GIB Specimen 2 Framing – Perspective

UNIVERSITY OF CANTERBURY
Te Whare Wānanga o Waitaha
CHRISTCHURCH NEW ZEALAND

UNIVERSITY OF CANTERBURY
Private Bag 4800
Christchurch 8140

CIVIL AND NATURAL RESOURCES ENGINEERING
69 Creyke Road
Christchurch 8140

NOTES:

All studs are 92x0.55bmt
All tracks are 94x0.5bmt

Dimensions in mm

SCALE: 1:25 @ A3

VER.	COMMENTS AND CHANGES	DATE
4	Revision 3	11/May/18
3	Revision 2	01/May/18
2	Revision 1	23/APR/18
1	Preliminary	09/JAN/18

PROJECT:
Partitions Experimental Testing

DESIGNERS:
Joshua Mulligan

SUPERVISORS:
Timothy Sullivan

TITLE:
WALL TEST SPECIMEN GIB
Elevations - specimen 2 - steel stud wall with doorway

CODE: 64560538

DATE: 11-May-2018

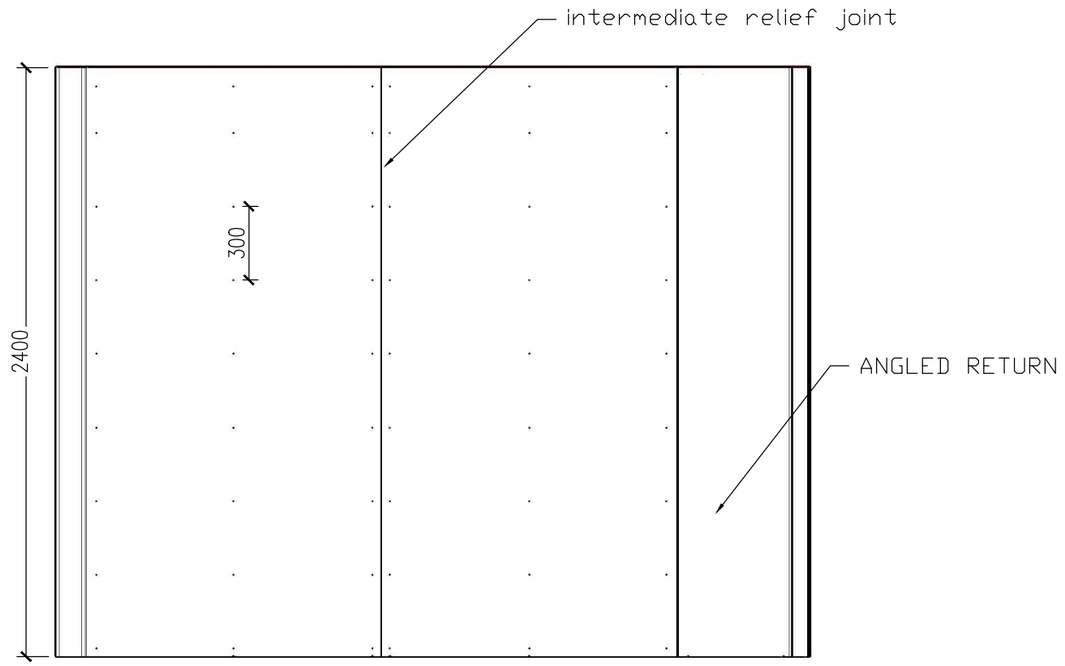

GIB Specimen 3 – ELEVATION 1

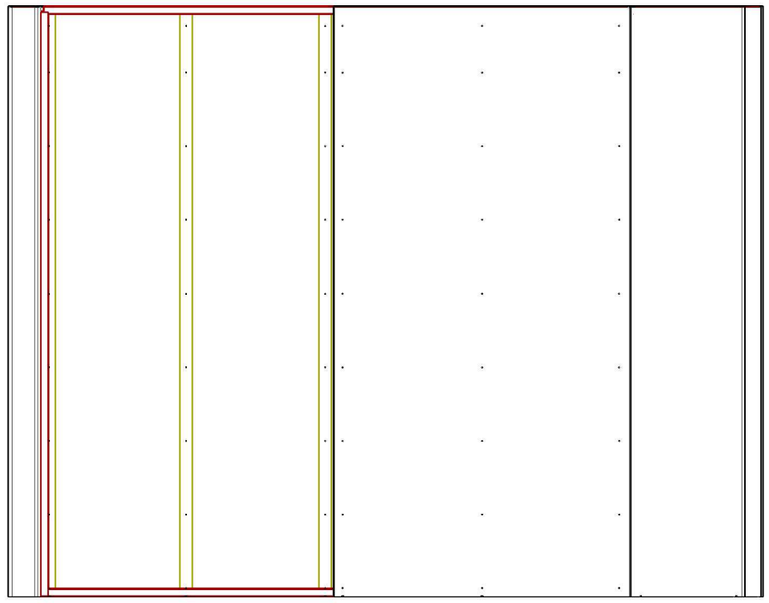

GIB Specimen 3– ELEVATION 2

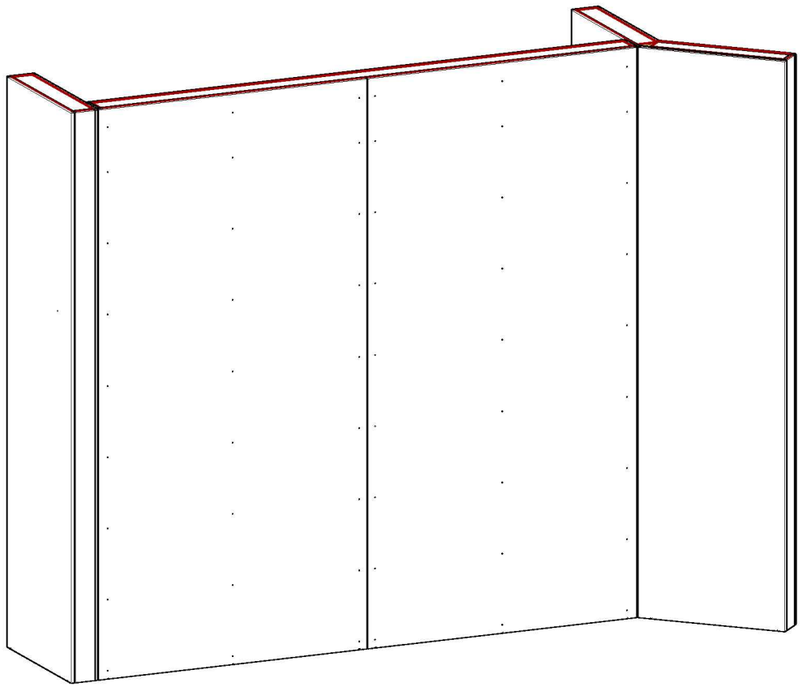

GIB Specimen 3 – Perspective

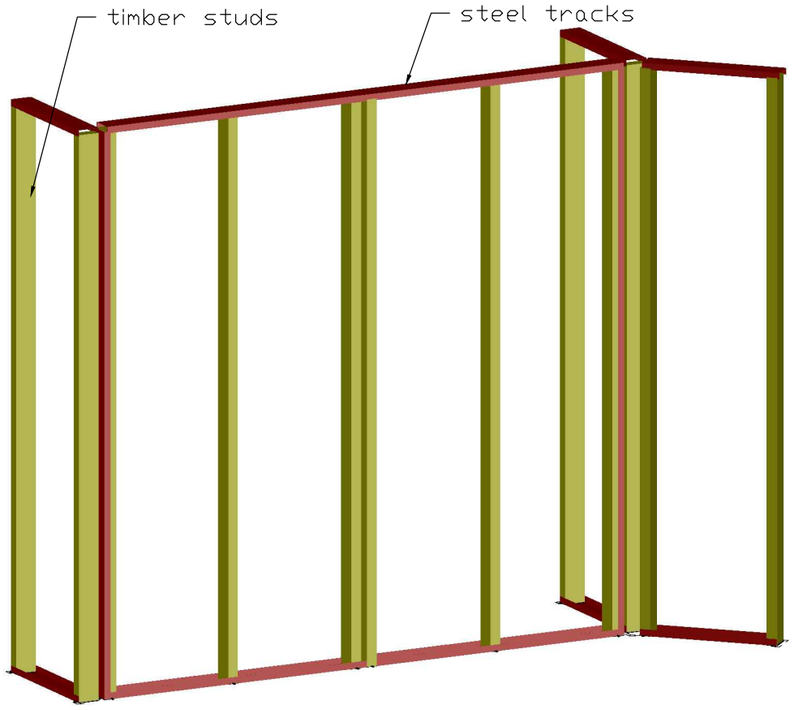

GIB Specimen 3 framing – Perspective

UNIVERSITY OF CANTERBURY
Te Whare Wānanga o Waitaha
CHRISTCHURCH NEW ZEALAND

UNIVERSITY OF CANTERBURY
Private Bag 4800
Christchurch 8140

CIVIL AND NATURAL RESOURCES ENGINEERING
69 Creyke Road
Christchurch 8140

NOTES:

All studs are 92x0.55bmt
All tracks are 94x0.5bmt

Dimensions in mm

SCALE: 1:25 @ A3

VER.	COMMENTS AND CHANGES	DATE
4	Revision 3	11/May/18
3	Revision 2	01/May/18
2	Revised following meeting	23/APR/18
1	Preliminary	09/JAN/18

PROJECT:
Partitions Experimental Testing

DESIGNERS:
Joshua Mulligan

SUPERVISORS:
Timothy Sullivan

TITLE:
WALL TEST SPECIMEN GIB
Elevation 3 - plain timber stud wall with intermediate relief joint

CODE: 64560538

DATE: 11-May-2018

PAGE: 005

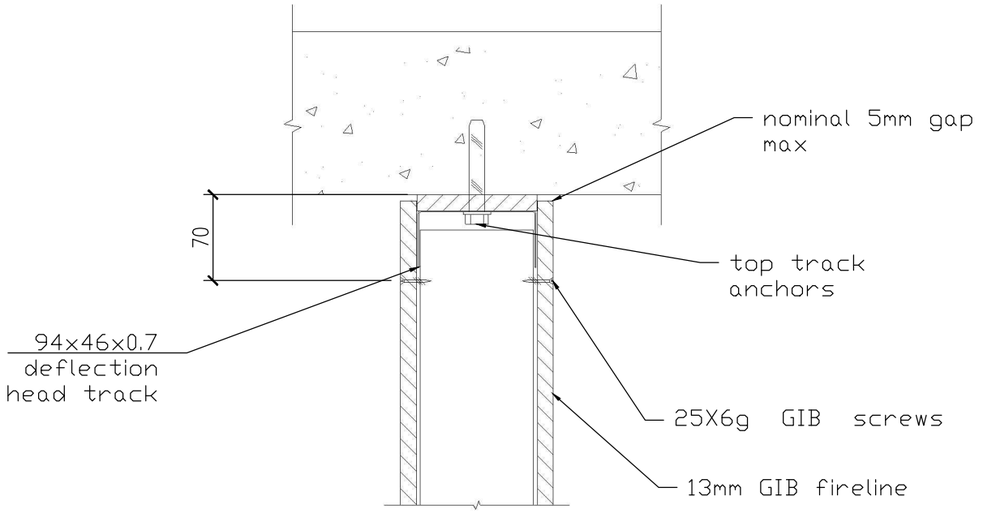

TOP SLAB TO WALL CONNECTION Detail
scale 1:5

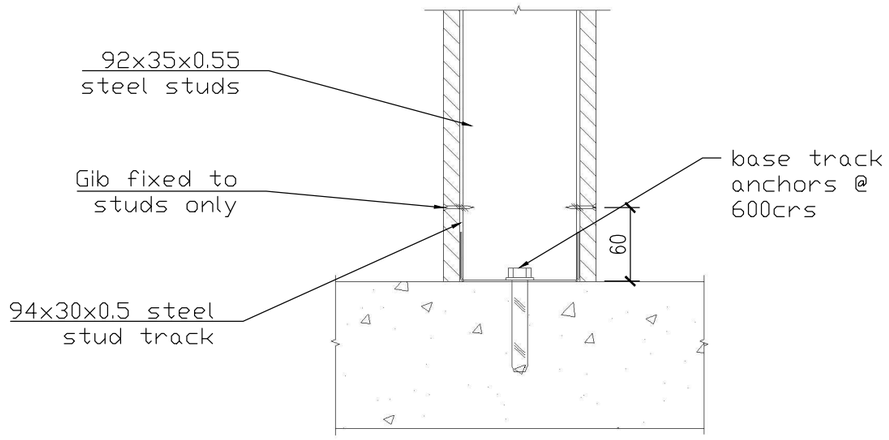

BASE SLAB TO WALL CONNECTION Detail
Scale 1:5

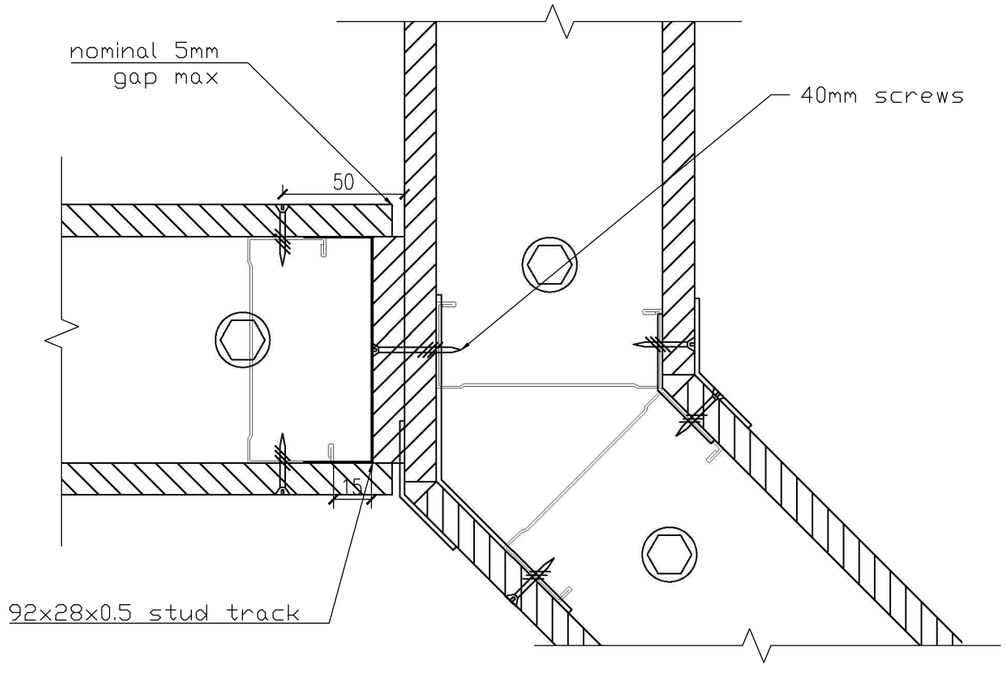

y-junction detail
Scale 1:2.5

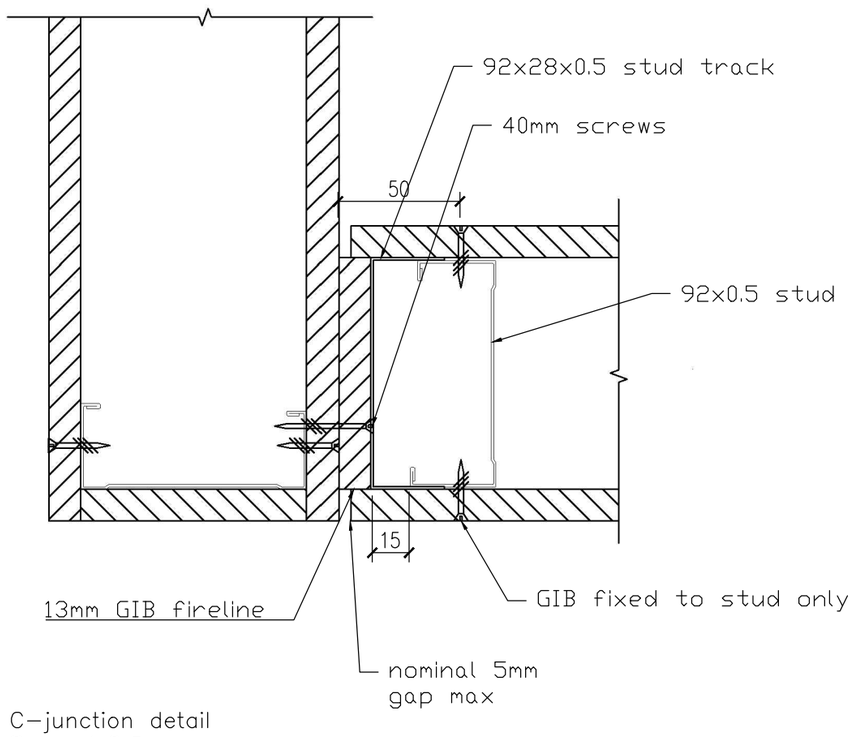

C-junction detail
Scale 1:2.5

UNIVERSITY OF CANTERBURY
Te Whare Wānanga o Waitaha
CHRISTCHURCH NEW ZEALAND

UNIVERSITY OF CANTERBURY
Private Bag 4800
Christchurch 8140

CIVIL AND NATURAL RESOURCES ENGINEERING
69 Creyke Road
Christchurch 8140

NOTES:

top & base track anchors are HILTI FIXING HUS-10 OR SIMILAR

Gib to stud fasteners are 25x6g GIB self tapping screws

Fasteners at wall junctions are to be longer than 40mm. Could use GIB Grabber self tapping 7gx51mm

For fasteners at wall control joints, to connect stud to packers to stud, screws longer than 30mm will be required. Could use GIB Grabber screw 6gx41mm or longer

All studs are 92x0.55bmt
All tracks are 94x0.5bmt

Dimensions in mm

SCALE: 1:5,1:2.5 @ A3

VER.	COMMENTS AND CHANGES	DATE
4	Revision 3	11/May/18
3	Revision 2	01/May/18
2	Revision 1	23/APR/18
1	Preliminary	09/JAN/18

PROJECT:
Low Damage Partitions Experimental Testing

DESIGNERS:
Joshua Mulligan

SUPERVISORS:
Timothy Sullivan

TITLE:
GIB System Steel Stud Sections 1

CODE: 64560538

DATE: 11-May-2018

PAGE: 006

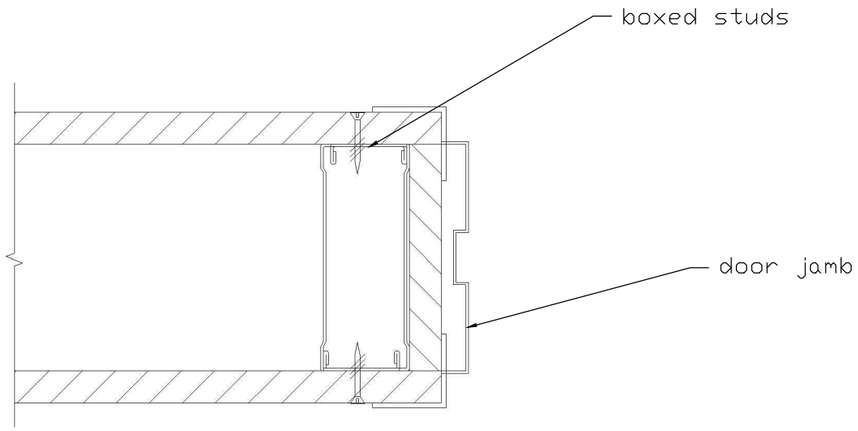

door jamb detail
scale 1:2.5

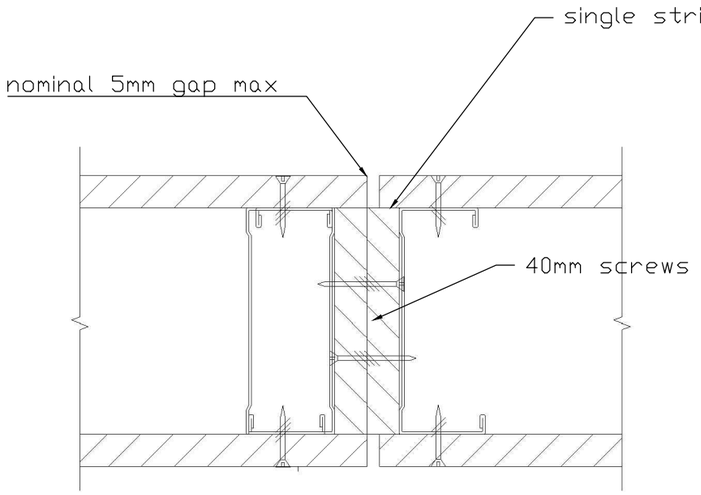

door lintel relief joint detail
scale 1:2.5

UNIVERSITY OF CANTERBURY
Private Bag 4800
Christchurch 8140

CIVIL AND NATURAL RESOURCES ENGINEERING
69 Creyke Road
Christchurch 8140

NOTES:

top & base track anchors are HILTI FIXING HUS-10 OR SIMILAR

Gib to stud fasteners are 25x6g GIB self tapping screws

Fasteners at wall junctions are to be longer than 40mm. Could use GIB Grabber self tapping 7gx51mm

For fasteners at wall control joints to connect stud to packers to stud need screw longer than 30mm. Could use GIB Grabber screw 6gx41mm or longer

All studs are 92x0.55bmt
All tracks are 94x0.5bmt

Dimensions in mm

SCALE: 1:5,1:2.5 @ A3

VER.	COMMENTS AND CHANGES	DATE
4	Revision 3	11/MAY/18
3	Revision 2	01/MAY/18
2	Revision 1	23/APR/18
1	Preliminary	09/JAN/18

PROJECT:
Low Damage Partitions
Experimental Testing

DESIGNERS:
Joshua Mulligan

SUPERVISORS:
Timothy Sullivan

TITLE:
GIB System Steel Stud Sections 2

CODE: 64560538

DATE: 11-May-2018

PAGE: 007

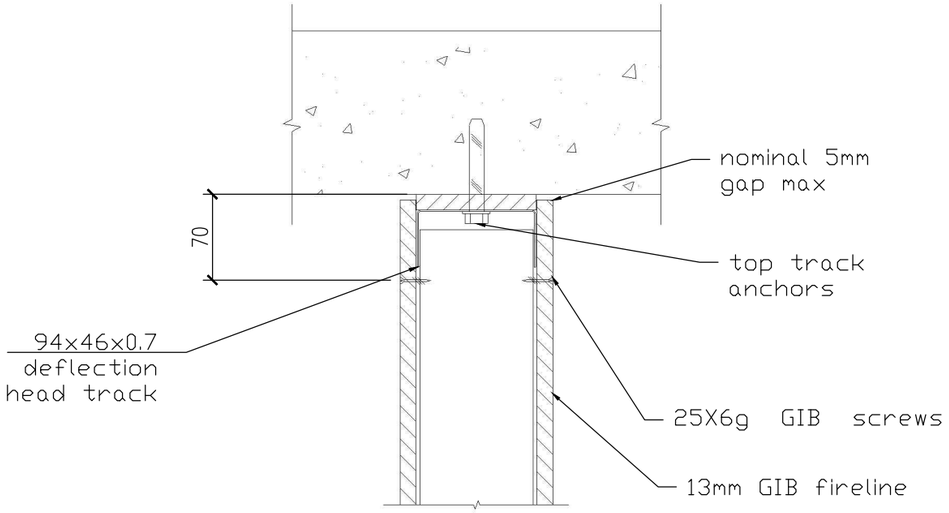

TOP SLAB TO WALL CONNECTION Detail
scale 1:5

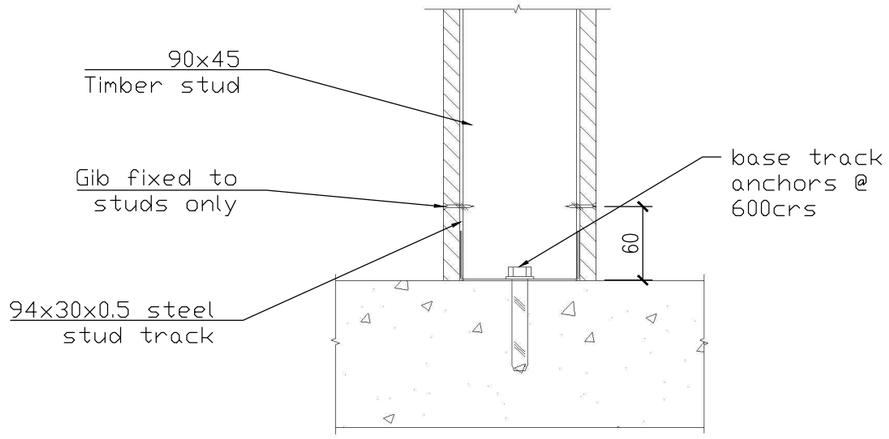

BASE SLAB TO WALL CONNECTION Detail
Scale 1:5

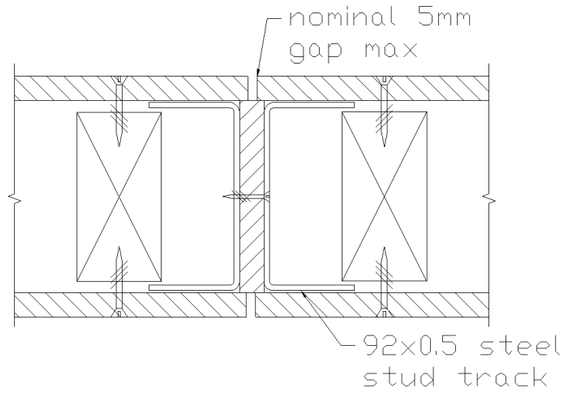

Intermediate relief joint detail
scale 1:2.5

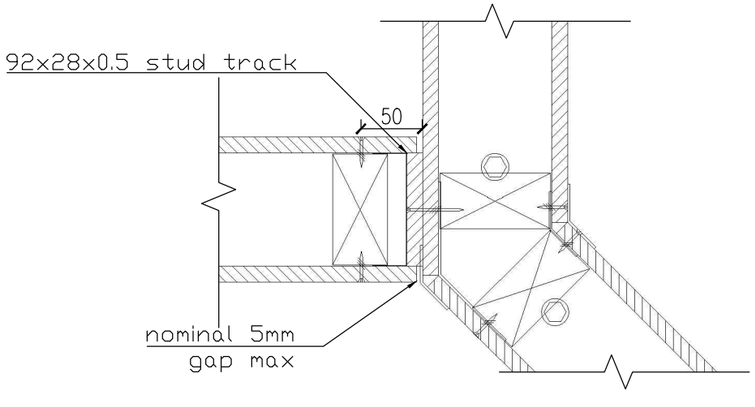

y-junction detail
Scale 1:5

C-junction detail
Scale 1:2.5

UNIVERSITY OF CANTERBURY
Te Whare Wānanga o Waitaha
CHRISTCHURCH NEW ZEALAND

UNIVERSITY OF CANTERBURY
Private Bag 4800
Christchurch 8140

CIVIL AND NATURAL
RESOURCES ENGINEERING
69 Creyke Road
Christchurch 8140

NOTES:

top & base track anchors are HILTI FIXING HUS-10 OR SIMILAR

Gib to stud fasteners are 25x6g GIB self tapping screws

Fasteners at wall junctions are to be longer than 40mm. Could use GIB Grabber self tapping 7gx51mm

For fasteners at wall control joints, to connect stud to packers to stud, screws longer than 30mm will be required. Could use GIB Grabber screw 6gx41mm or longer

All steel studs are 92x0.55bmt
Timber studs are 90x45
All tracks are 94x0.5bmt

Dimensions in mm

SCALE: 1:5,1:2.5 @ A3

VER.	COMMENTS AND CHANGES	DATE
4	Revision 3	11/May/18
3	Revision 2	01/May/18
2	Revision 1	23/APR/18
1	Preliminary	09/JAN/18

PROJECT:
Low Damage Partitions
Experimental Testing

DESIGNERS:
Joshua Mulligan

SUPERVISORS:
Timothy Sullivan

TITLE:
GIB System Timber Stud Sections

CODE: 64560538

DATE:
11-May-2018

PAGE: 008

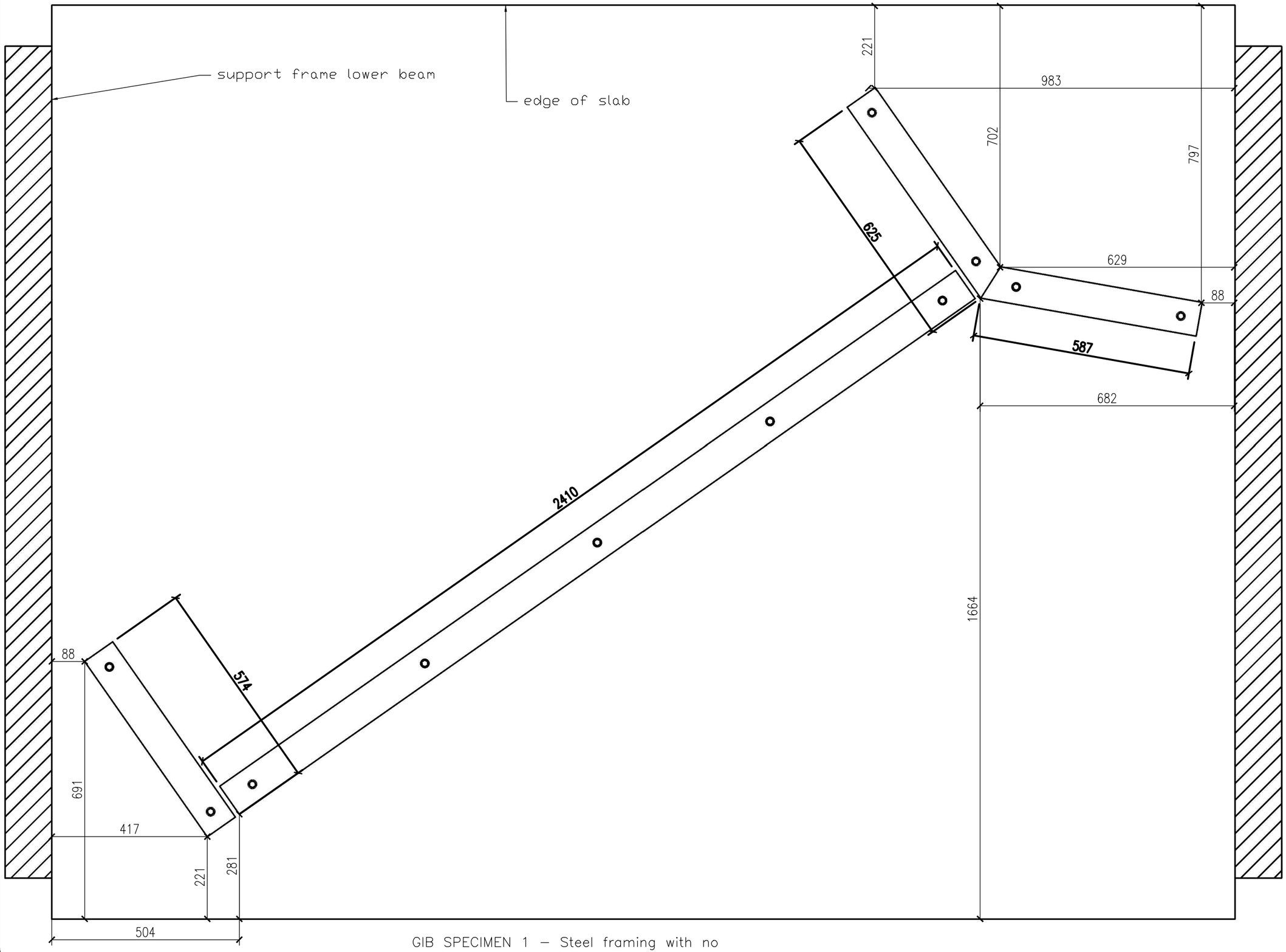

GIB SPECIMEN 1 – Steel framing with no Intermediate Joint – PLAN Track Layout

UNIVERSITY OF CANTERBURY
Te Whare Wānanga o Waitaha
CHRISTCHURCH NEW ZEALAND

UNIVERSITY OF CANTERBURY
Private Bag 4800
Christchurch 8140

CIVIL AND NATURAL RESOURCES ENGINEERING
69 Creyke Road
Christchurch 8140

NOTES:

track anchors are HILTI FIXING HUS-10 OR SIMILAR

track are to be anchored at same locations top and bottom

Drywalls finished as per GIB site guide specifications to a level 4 finish with a single coat of paint.

All, corners junctions are to be finished with GIB ultraflex no coat 82mm tape

All studs are 92x0.55bmt
All tracks are 94x0.5bmt

Dimensions in mm

SCALE: 1:10 @ A3

VER.	COMMENTS AND CHANGES	DATE
1	Construction	20/MAY/18

PROJECT:
Partitions Experimental Testing

DESIGNERS:
Joshua Mulligan

SUPERVISORS:
Timothy Sullivan

TITLE:
GIB System Specimens 1 - Plan Track Layout

CODE: 64560538

DATE: 20-May-2018

PAGE: 002

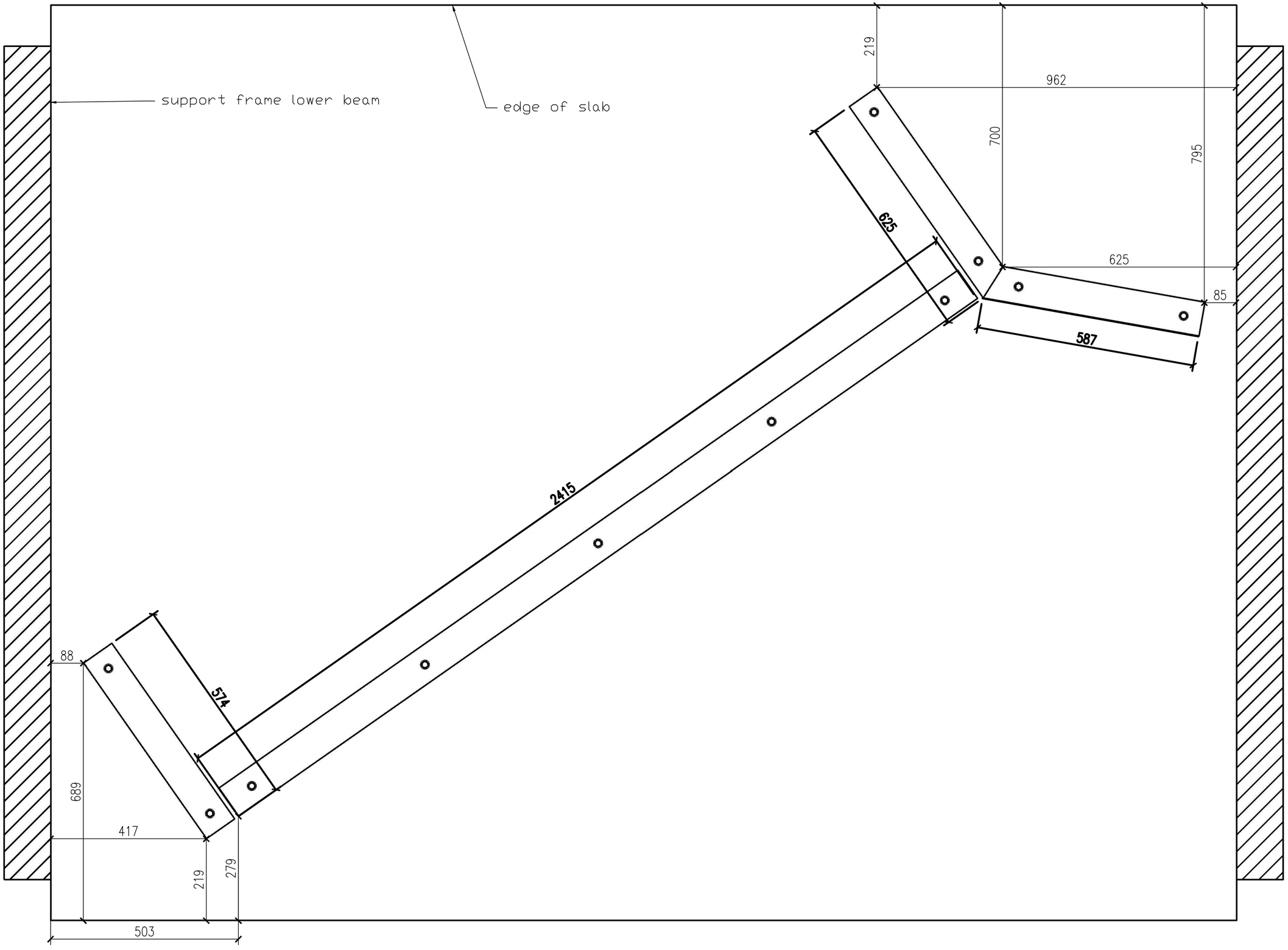

GIB SPECIMEN 3 timber stud wall with intermediate relief joint with – PLAN Track Layout

UNIVERSITY OF CANTERBURY
Te Whare Wānanga o Waitaha
CHRISTCHURCH NEW ZEALAND

UNIVERSITY OF CANTERBURY
Private Bag 4800
Christchurch 8140

CIVIL AND NATURAL RESOURCES ENGINEERING
69 Creyke Road
Christchurch 8140

NOTES:

track anchors are HILTI FIXING HUS-10 OR SIMILAR

track are to be anchored at same locations top and bottom

Drywalls finished as per GIB site guide specifications to a level 4 finish with a single coat of paint.

All, corners junctions are to be finished with GIB ultraflex no coat 82mm tape

All studs are 92x0.55bmt
All tracks are 94x0.5bmt

Dimensions in mm

SCALE: 1:10 @ A3

VER.	COMMENTS AND CHANGES	DATE
4	Revision 3	11/MAY/18
3	Revision 2	01/MAY/18
2	Revised following meeting	23/APR/18
1	Preliminary	29/JAN/18

PROJECT:
Partitions Experimental Testing

DESIGNERS:
Joshua Mulligan

SUPERVISORS:
Timothy Sullivan

TITLE:
GIB System Specimens 3

CODE: 64560538

DATE:
11-MAY-2018

PAGE: 001

Detailed Damage Development Observations

A summary of the damage progression in each of the specimens is shown here. The damage progression is described in terms of the damage states in Table C.1 and with reference to the locations in Figure C.1. This appendix is designed to be able to be interpreted independent of the main body of writing.

Table C.1 Damage states for seismic gap system specimens

Damage State	Description	Repair Action
0	Hairline cracking of paint at joints	Barely visible damage deemed not requiring repair.
1.a	Sealant de-bonding	Remove and re-apply gap filler
1.b	Cracking in plaster and paint along trim	Scrape out minor cracks and reapply plaster and paint.
1.c	Screw damage - pull through, popping, or shearing	Re-fix or tighten any existing loose fasteners and place additional fasters near original. Finish with plaster, and sand and paint.
2.a	Wallboard damage - paper face separating, crushing, cracking, or spalling	Requires replacement of linings or local repairs of linings. Breakages can be ground out and patch fixed, using plastering and paper tape.
2.b	Residual gap at joints	Replace linings
3	Framing damage - flanges bent, buckling, or hinging	Both linings and framing must be removed and replaced. Thus, complete demolition and replacement of the wall is required.

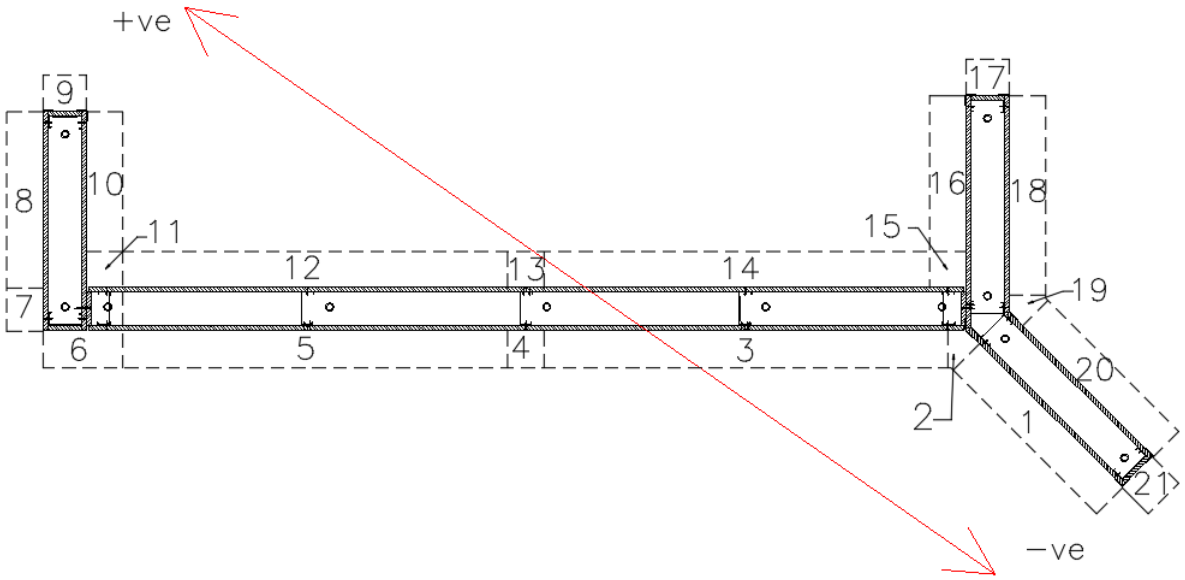

Figure C.1 Specimen location references for damage progression tables. Axis of loading a definition of positive loading direction shown in red.

Specimen B1

Table C.2 Specimen 1 damage progression described in relation to damage states defined in relation to the damage states defined in Table C.1.

	STEP	8	9	10	11	12	13	14	15	16
Drift (%)	loading	0.42	0.59	0.82	1.15	1.62	2.27	3.17	4.44	6.21
	45° wall	0.41	0.58	0.81	1.13	1.60	2.23	3.12	4.37	6.12
	90° walls	0.24	0.34	0.47	0.66	0.93	1.30	1.82	2.55	3.56
	long wall	0.34	0.48	0.67	0.94	1.33	1.86	2.60	3.64	5.09
Location	1	-	-	1b	-	-	2a	-	-	-
	2	-	-	-	1a	1b	-	2a	-	1c
	3	-	-	-	-	-	-	-	1b	-
	4	-	-	-	-	-	-	-	-	-
	5	-	-	-	-	-	-	-	-	-
	6	0	1a	-	2b	-	-	1b,2a,3	-	-
	7	-	-	-	-	1b	-	-	-	-
	8	-	-	-	-	1b	-	-	-	-
	9	-	-	-	1b	-	-	-	-	2a
	10	-	-	-	1b,2a	-	-	-	-	1c
	11	0	1a,1b	-	2a	-	2b	3	-	1c
	12	-	-	-	-	-	1b	-	-	1c
	13	-	-	-	-	-	-	-	-	-
	14	-	-	-	-	-	-	-	-	-
	15	-	0,1a	1b	2a	-	-	-	-	-
	16	-	-	-	1b	-	-	2a	-	-
	17	-	-	-	1b	-	-	-	-	2a
	18	-	-	-	-	-	-	1b	2a	-
	19	-	-	0	-	-	-	1b	-	2a
	20	-	-	-	1b,2a	-	-	-	-	-
	21	-	-	-	1b,2a	-	-	-	-	3

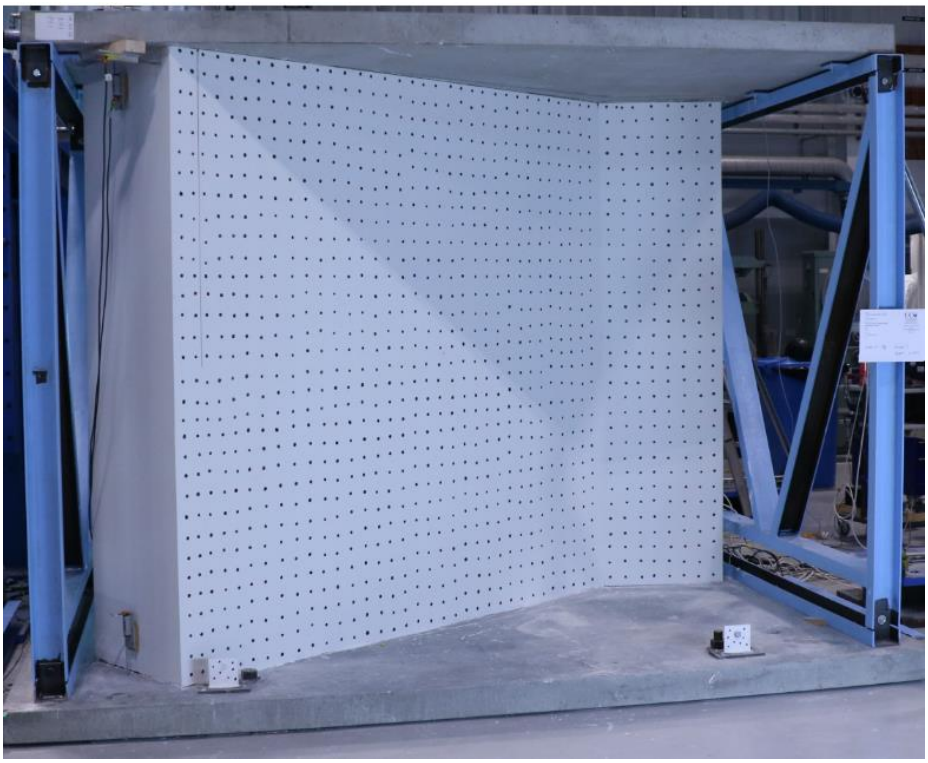

Figure C.2 Specimen B1 – Prior to test start

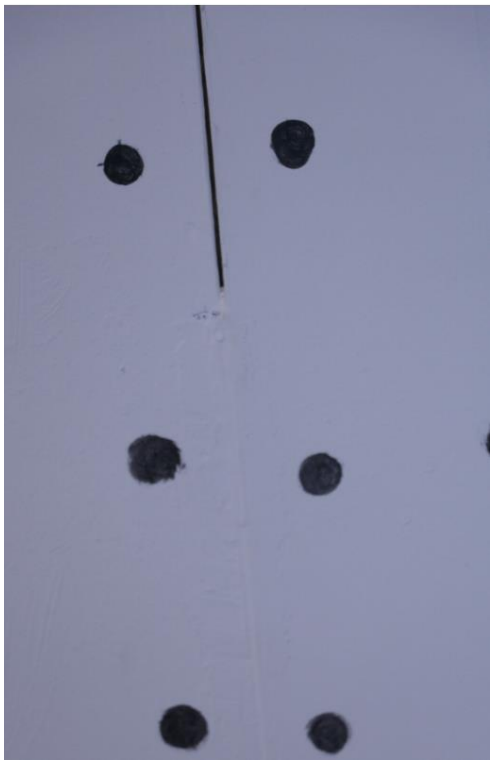

Figure C.3 Specimen B1 – Prior to test start – Half-filled seismic gap at L-junction – location 6

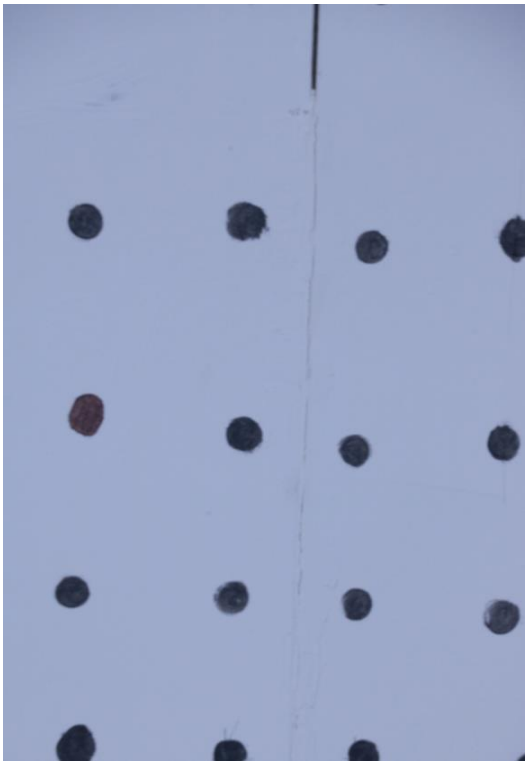

Figure C.4 Specimen B1 – Step 8 – DS0: Hairline paint cracking at Y-junction - location 2

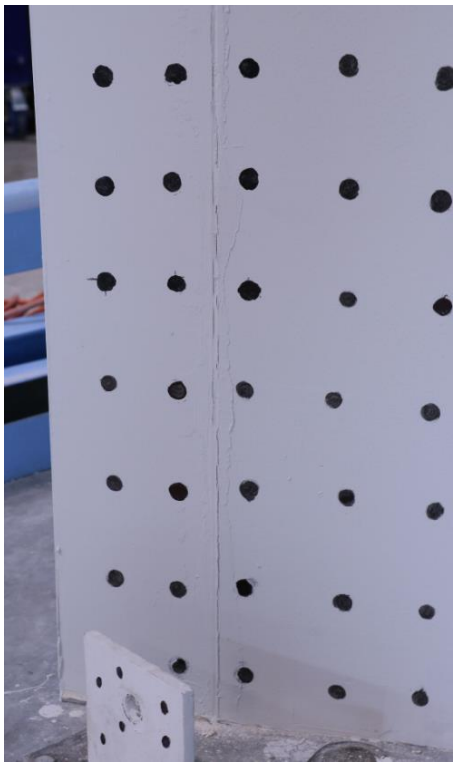

Figure C.5 Specimen B1 – Step 8 – DS0: Hairline paint cracking at L-junction - location 6

Figure C.6 Specimen B1 – Step 8 – DS0: Hairline paint cracking at L-junction - location 11

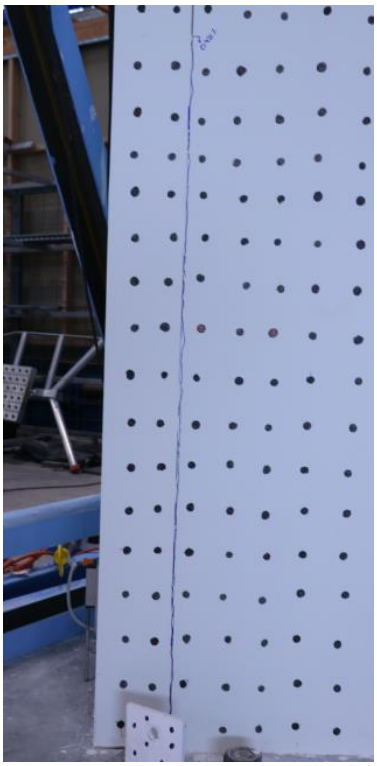

Figure C.7 Specimen B1 – Step 9 – DS1a: Debonding of gap-filler material (behind blue marker) at L-junction - location 6

Figure C.8 Specimen B1 – Step 9 – DS1b: Plaster cracking at L-junction top corner- location 11

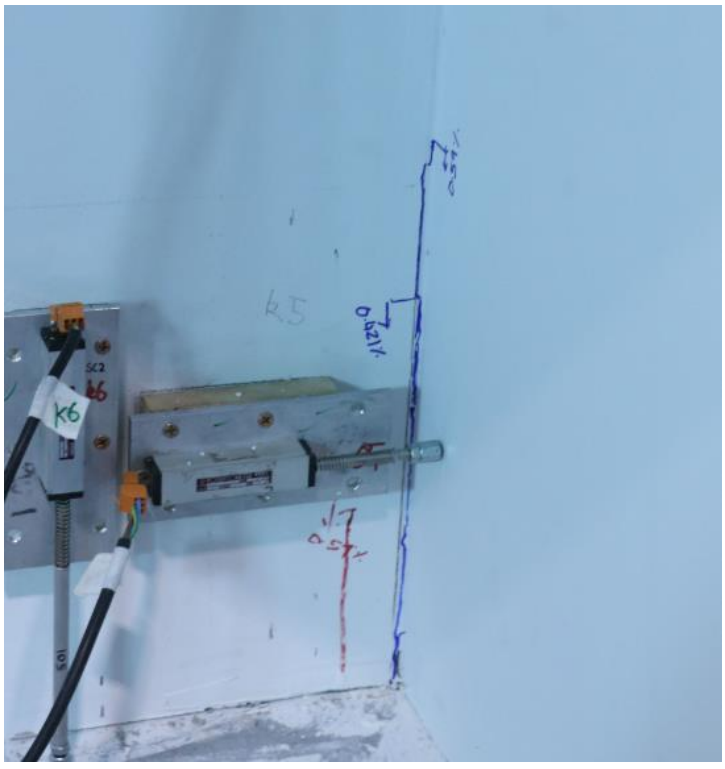

Figure C.9 Specimen B1 – Step 9 – DS1a & b: Debonding of gap filler and plaster cracking along L-trim at L-junction bottom corner- location 11

Figure C.10 Specimen B1 – Step 10 – DS1b: Plaster cracking at Y-junction top corner- location 15

Figure C.11 Specimen B1 – Step 10 – DS1a & b: Debonding of gap filler and plaster cracking along L-trim at Y-junction bottom corner- location 15

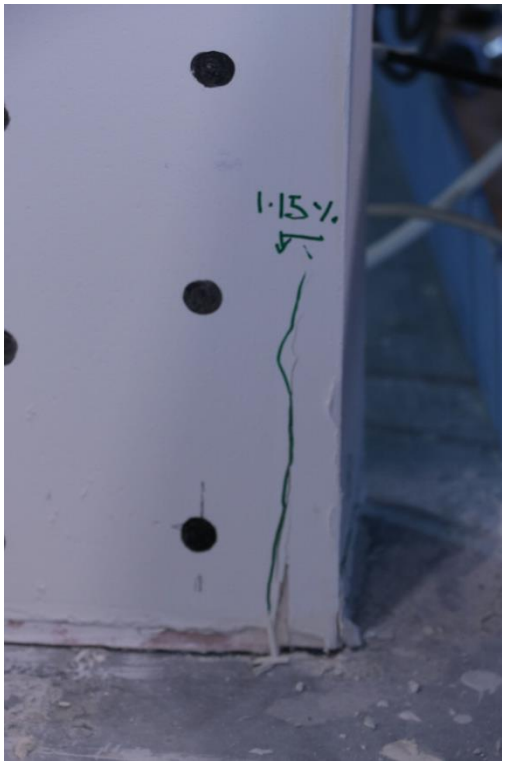

Figure C.12 Specimen B1 – Step 11 – DS1b: Plaster cracking along L-trim at bottom corner of wall end- location 1/21

Figure C.13 Specimen B1 – Step 11 – DS2b: Excessive residual gap development at L-junction – location 6

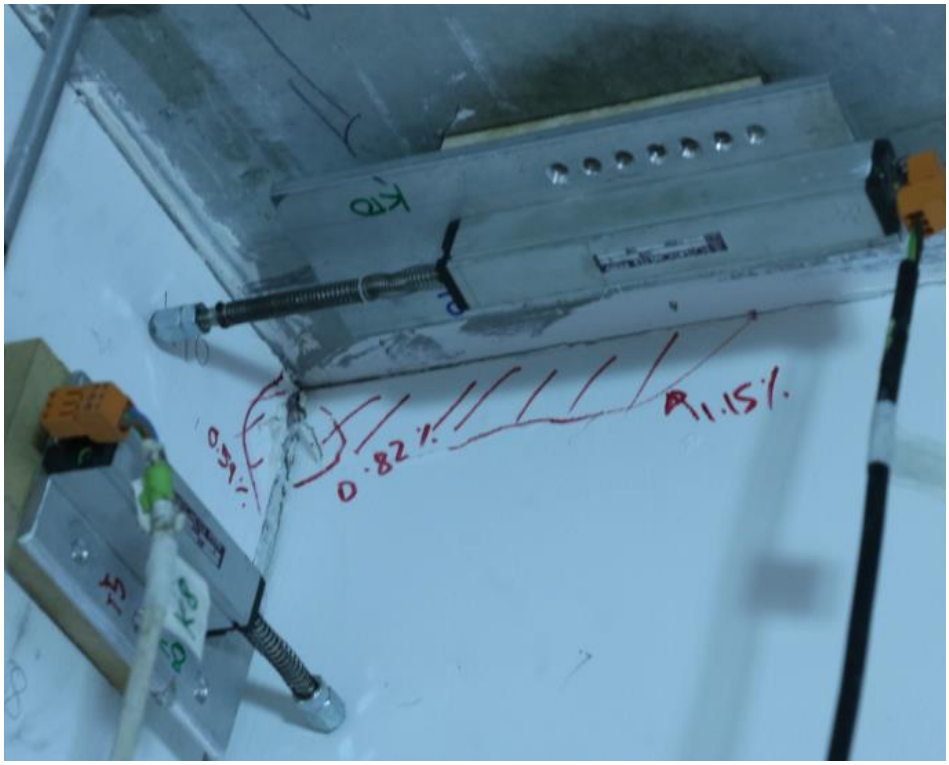

Figure C.14 Specimen B1 – Step 11 – DS1b & 2a: Cracking of plaster along L-trim and damage to wallboard– location 10

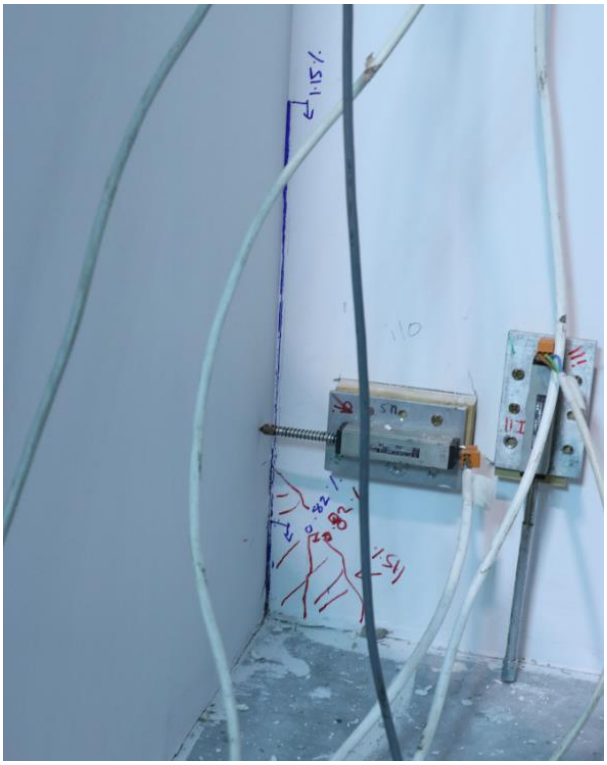

Figure C.15 Specimen B1 – Step 11 – DS2a: Wallboard crushing at toe – location 15

Figure C.16 Specimen B1 – Step 11 – DS2a: Wallboard crushing at toe – location 21

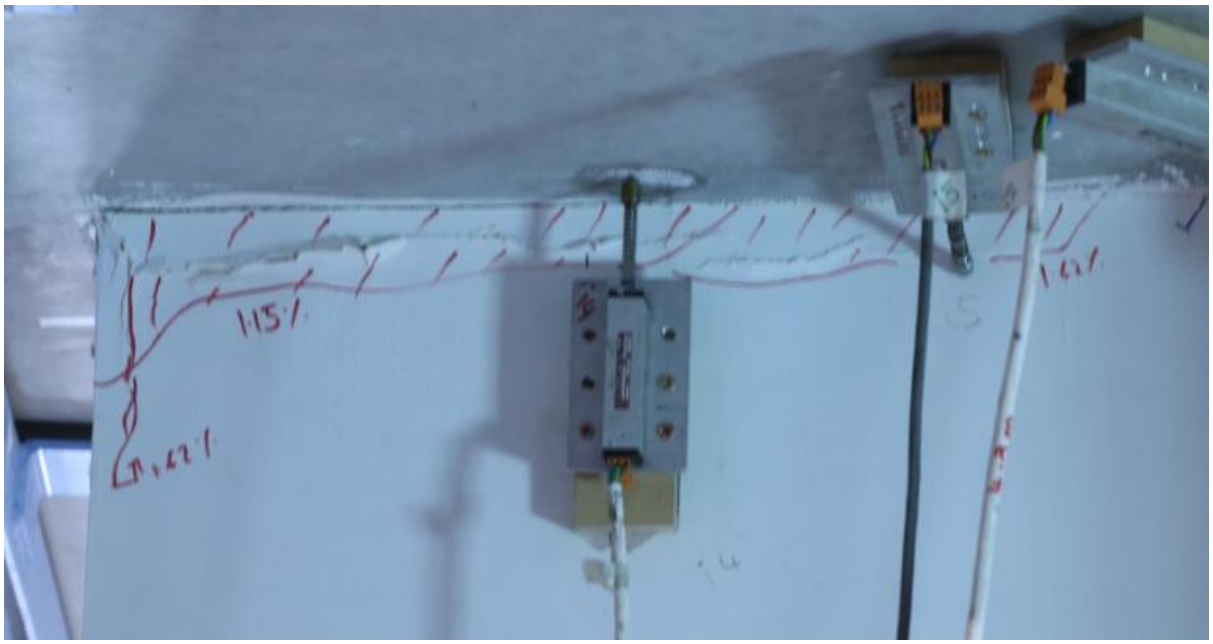

Figure C.17 Specimen B1 – Step 12 – DS1b: Plaster cracking along L-Trim – location 20

Figure C.18 Specimen B1 – Step 13 – DS1b: Plaster cracking along L-Trim – location 13

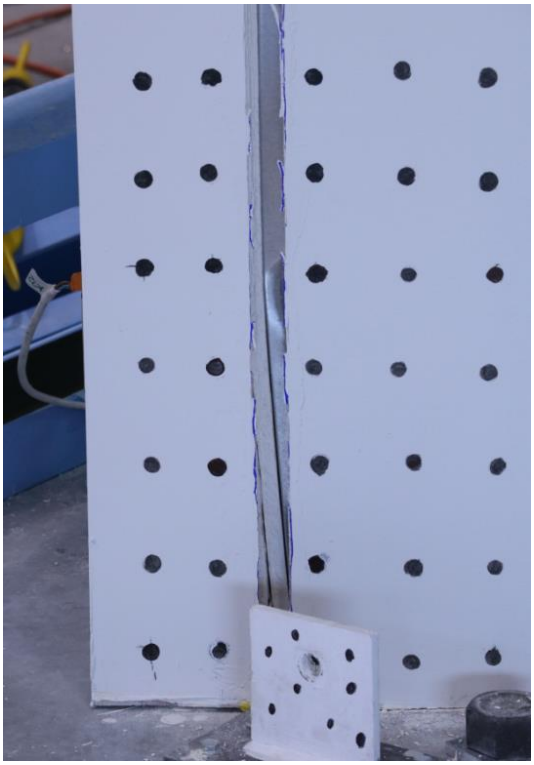

Figure C.19 Specimen B1 – Step 14 – DS2a & 3: Wallboard damage to internal plasterboard packing strips and buckling of vertical steel tracks – location 6

Figure C.20 Specimen B1 – Step 14 – DS3: evidence that bottom track in return wall at L-junction has been damaged as main wall has pushed over bottom track – location 11

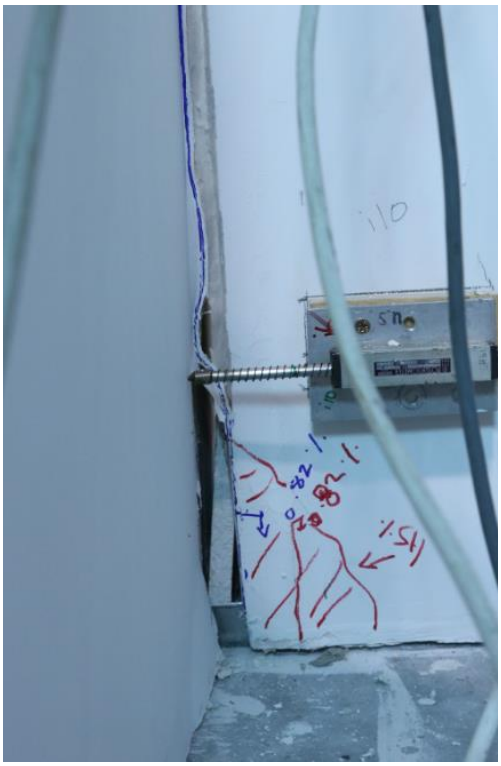

Figure C.21 Specimen B1 – Step 14 – DS2a: damage to vertical plasterboard packing strips – location 15

Figure C.22 Specimen B1 – Step 15 – separation of main wall from return wall – location 6 (left) & 11 (right)

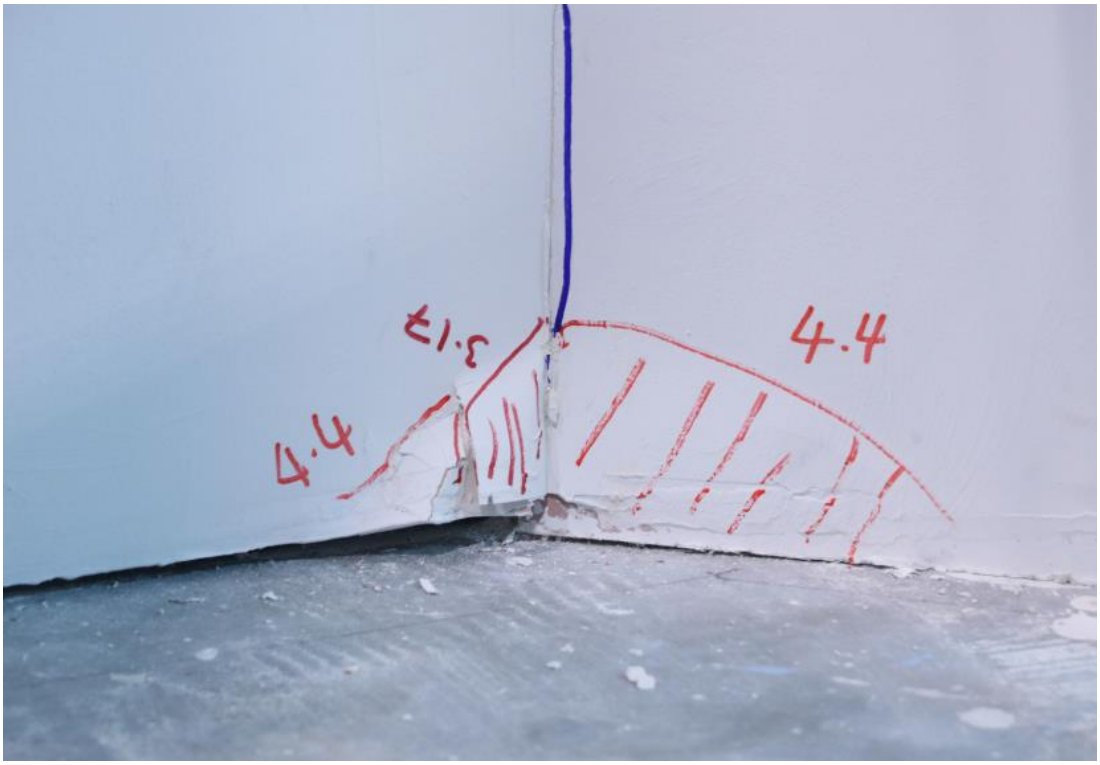

Figure C.23 Specimen B1 – Step 15 –DS2a: Damage to wallboard at Y-junction – location 19

Figure C.24 Specimen B1 – Step 16 –DS1c: linings detached from studs – location 2

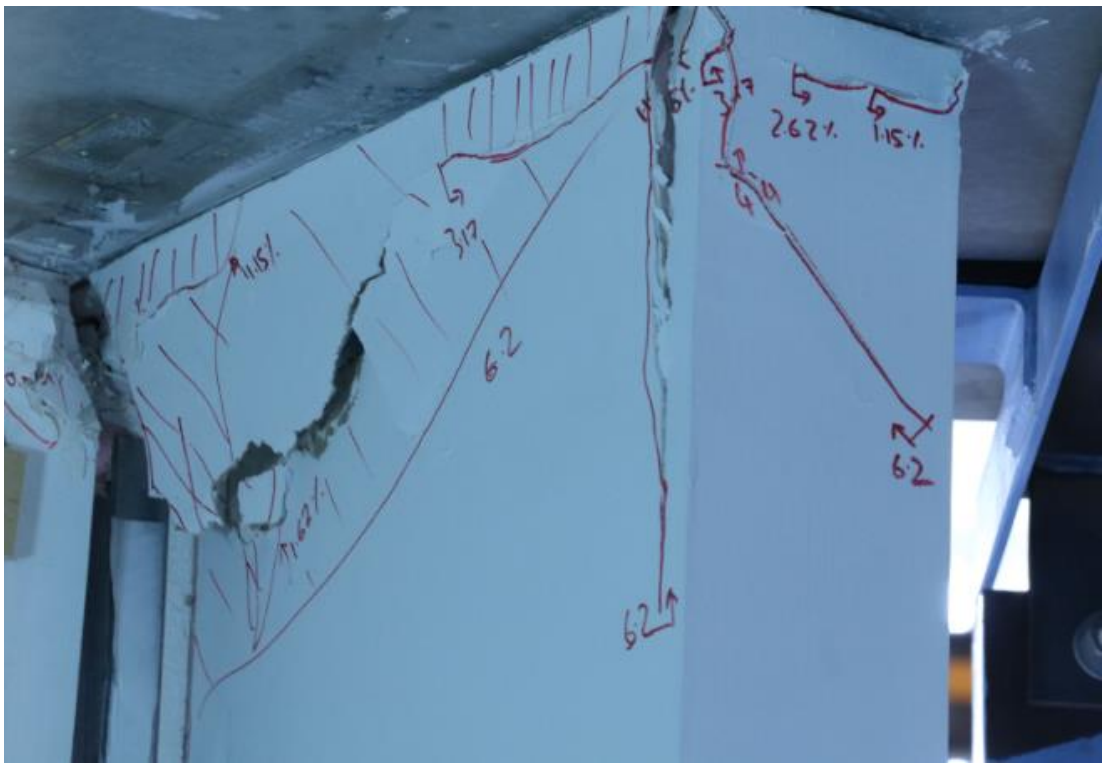

Figure C.25 Specimen B1 – Step 16 –linings spalling – location 9 to 11

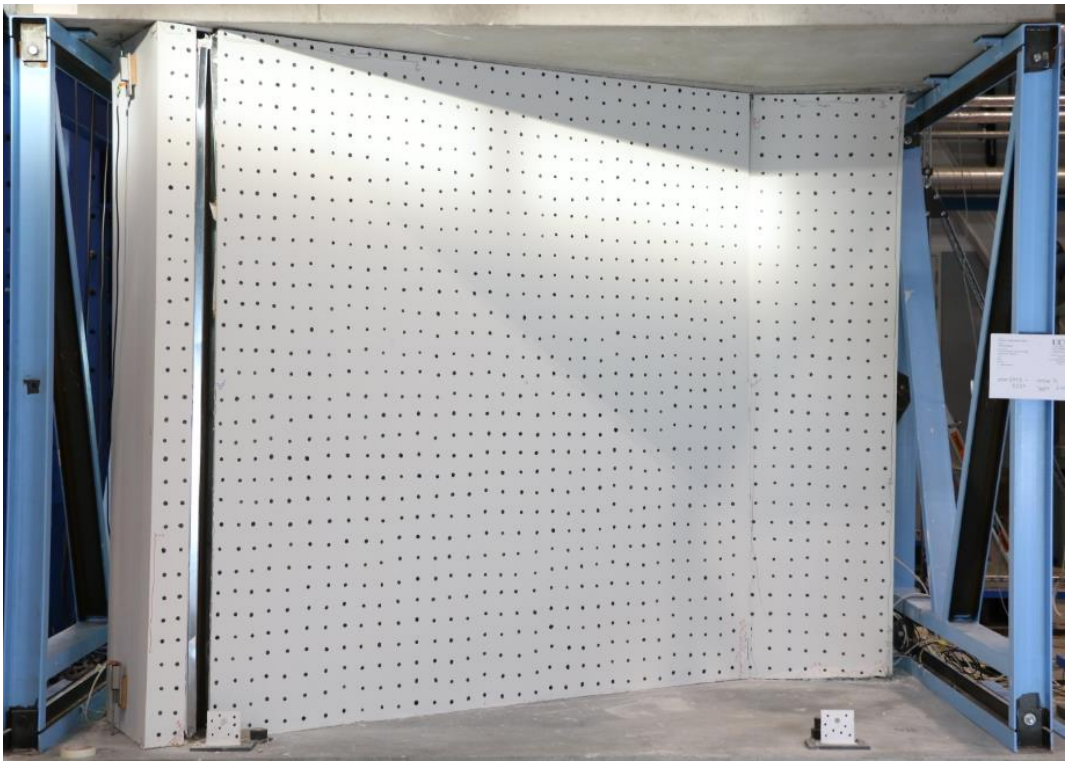

Figure C.26 Specimen B1 – Step 16 – photograph after completion of test

Figure C.27 Specimen B1 – Post-test framing inspection –-wall after removal of linings

Figure C.28 Specimen B1 – Post-test framing inspection –-bending of stud and track flanges at top of L-junction – locations 6, 7, & 11

Figure C.29 Specimen B1 – Post-test framing inspection –-bending of stud web at bottom due to pushing against bottom rack anchor bolt heads – locations 5 & 12

Figure C.30 Specimen B1 – Post-test framing inspection –-bending of stud webs and bottom track flanges due to pushing of the main wall against the Y- junction – locations 2, 15, & 19

Figure C.31 Specimen B1 – Post-test framing inspection –-buckling of studs at bottom of end of angled wall – location 21

No further photos showing damage progression in this specimen or potentiometer readings are shown herein.

Specimen B2

Table C.3 Detailed damage progression for specimen B2 described in relation to damage states listed in Table C.1.

	STEP	8	9	10	11	12	13	14	15	16
Drift (%)	loading	0.42	0.59	0.82	1.15	1.62	2.27	3.17	4.44	6.21
	45° wall	0.41	0.58	0.81	1.13	1.60	2.23	3.12	4.37	6.12
	90° walls	0.24	0.34	0.47	0.66	0.93	1.30	1.82	2.55	3.56
	long wall	0.34	0.48	0.67	0.94	1.33	1.86	2.60	3.64	5.09
Location	1	-	-	-	1b	-	-	2a	-	-
	2	-	0	1a	-	-	-	2b	-	1c
	3	-	-	-	-	-	-	-	-	1b,1c
	4	-	-	0	-	1a	-	2b	-	-
	5	-	-	-	-	-	-	-	-	1b
	6	-	0	1a	-	-	-	2b	2a,3	1c
	7	-	-	-	-	-	1b	2a	3	-
	8	-	-	-	-	-	1b	2a	-	-
	9	-	-	-	-	1b	-	-	3	2a
	10	-	-	-	-	-	1b,2a	-	-	-
	11	-	0	1a	1b	-	-	2b	2a,3	-
	12	-	-	-	1b	-	-	2a	-	-
	13	-	-	0	-	1a	-	2b	-	-
	14	-	-	-	-	-	-	1b,2a	-	-
	15	-	0	1a	-	1b	-	2b	-	-
	16	-	-	-	1b	-	-	-	2a	-
	17	-	-	-	1b	-	-	-	2a	-
	18	-	-	-	-	-	-	1b	2a	-
	19	-	-	-	-	-	-	1b	2a	-
	20	-	-	-	1b	-	-	1b,2a	-	-
	21	-	-	-	1b	-	-	2a	-	-

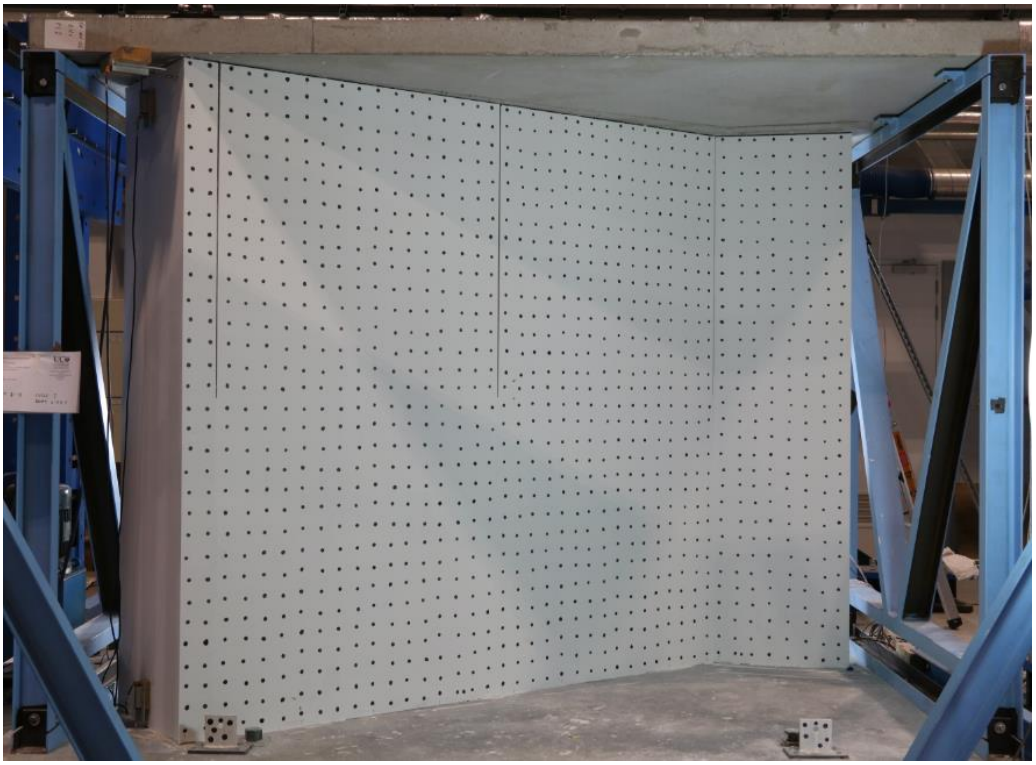

Figure C.32 Specimen B2 – Prior to test start

Figure C.33 Specimen B2 – Prior to test start – DS0: hairline paint cracking sealant at seismic gap– location 11

Figure C.34 Specimen B2 –Prior to test start – Poor finishing of gap filling material at intermediate joint - location 13

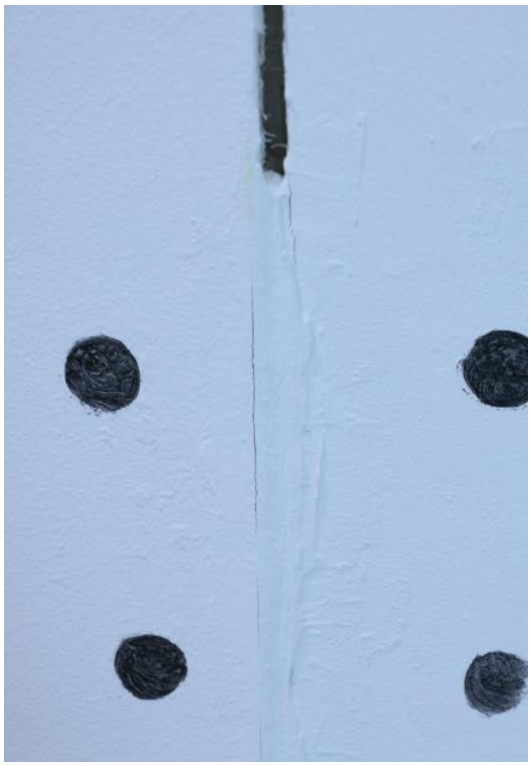

Figure C.35 Specimen B2 – Step 9 – DS0: Hairline paint cracking at L-junction - location 6

Figure C.36 Specimen B2 – Step 9 – DS0: Hairline paint cracking at Y-junction - location 15

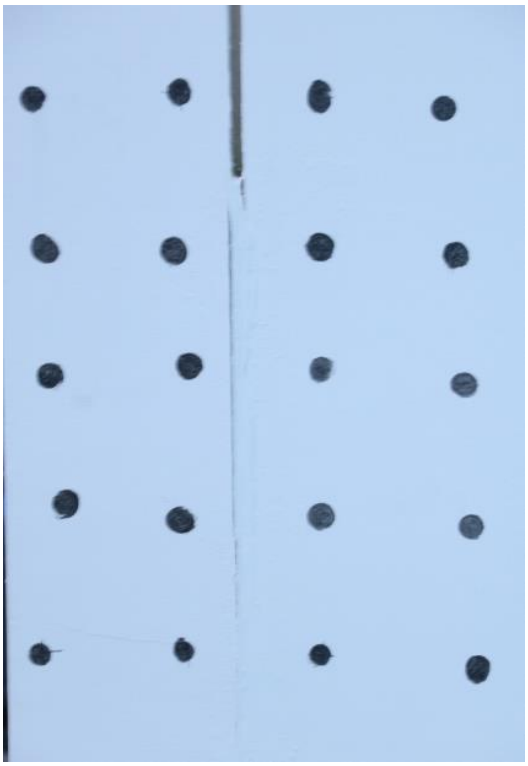

Figure C.37 Specimen B2 – Step 10 – DS1a: Debonding of gap-filler material at L-junction - location 6

Figure C.38 Specimen B2 – Step 10 – DS1a: Debonding of gap-filler material at Y-junction - location 11 (photo taken during peak excursion)

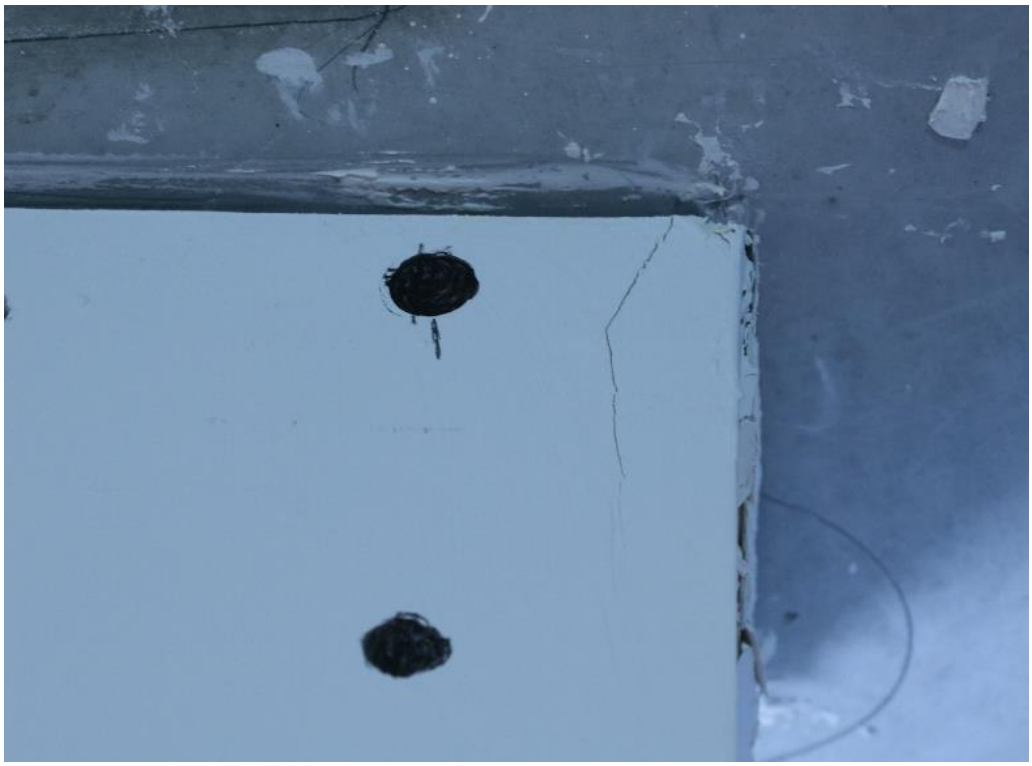

Figure C.39 Specimen B2 – Step 11 – DS1b: Plaster cracking along L-trim - location 1

Figure C.40 Specimen B2 – Step 11 – DS1b: Plaster cracking along L-trim - location 111

Figure C.41 Specimen B2 – Step 11 – DS1b: Plaster cracking along L-trim at wall end - location 21

Figure C.42 Specimen B2 – Step 12 – DS1b: Plaster cracking along L-trim at wall end- location 9

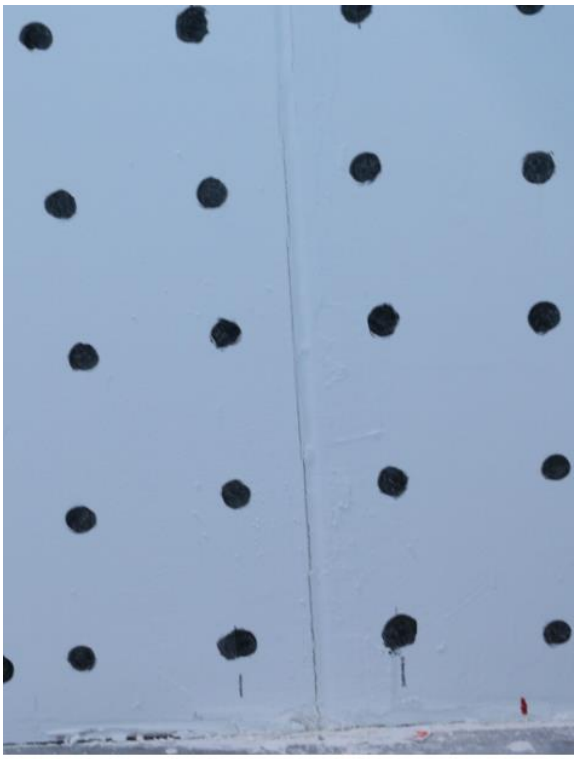

Figure C.43 Specimen B2 – Step 12 – DS1b: Gap filler material dedonding at intermediate joint – location 4

Figure C.44 Specimen B2 – Step 13 – DS1b: Cracking of plaster along L-trim – location 8

Figure C.45 Specimen B2 – Step 13 – DS2a: Wallboard damage in return wall at L-junction – location 10/11

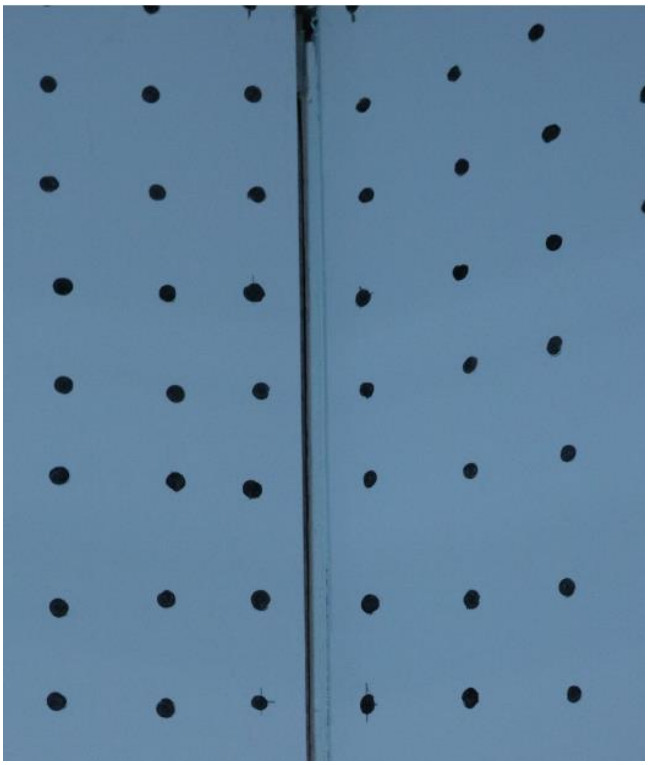

Figure C.46 Specimen B2 – Step 14 – DS2b: Excessive gap size developing at wall ends – location 2

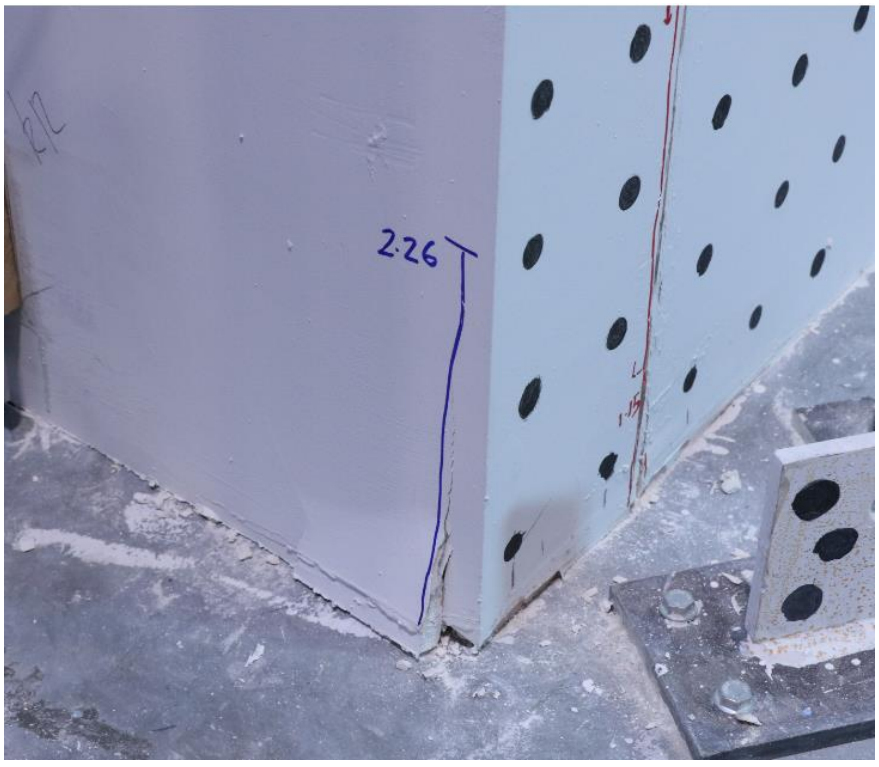

Figure C.47 Specimen B2 – Step 14 – DS2a: Wallboard damage – location 7

Figure C.48 Specimen B2 – Step 14 – DS2a: Wallboard crushing at toe at Y-junction – location 15

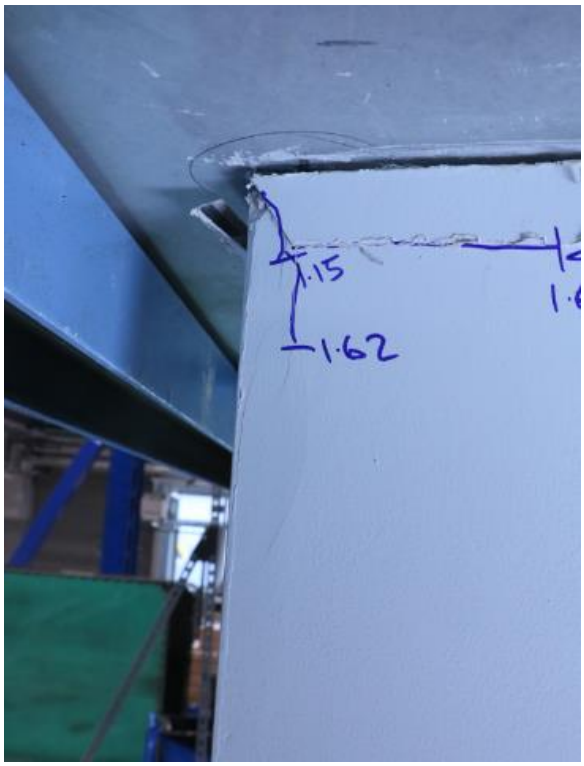

Figure C.49 Specimen B2 – Step 14 – DS2a: Wallboard damage to end wall – location 20/21

Figure C.50 Specimen B2 – Step 15 – DS2a & 3: Excessive residual gap development and bent flanges of vertical steel track – location 6

Figure C.51 Specimen B2 – Step 15 – DS2a & 3: Excessive residual gap development and bent flanges of bottom steel track in return wall – location 11

Figure C.52 Specimen B2 – Step 15 – DS2a: crushing of wallboard at the base of the Y-junction – location 19

Figure C.53 Specimen B2 – Step 16 – development of damage at L-junction – location 10/11

Figure C.54 Specimen B2 – Step 16 –DS1c: Popping out of screws along end stud– location 20/21

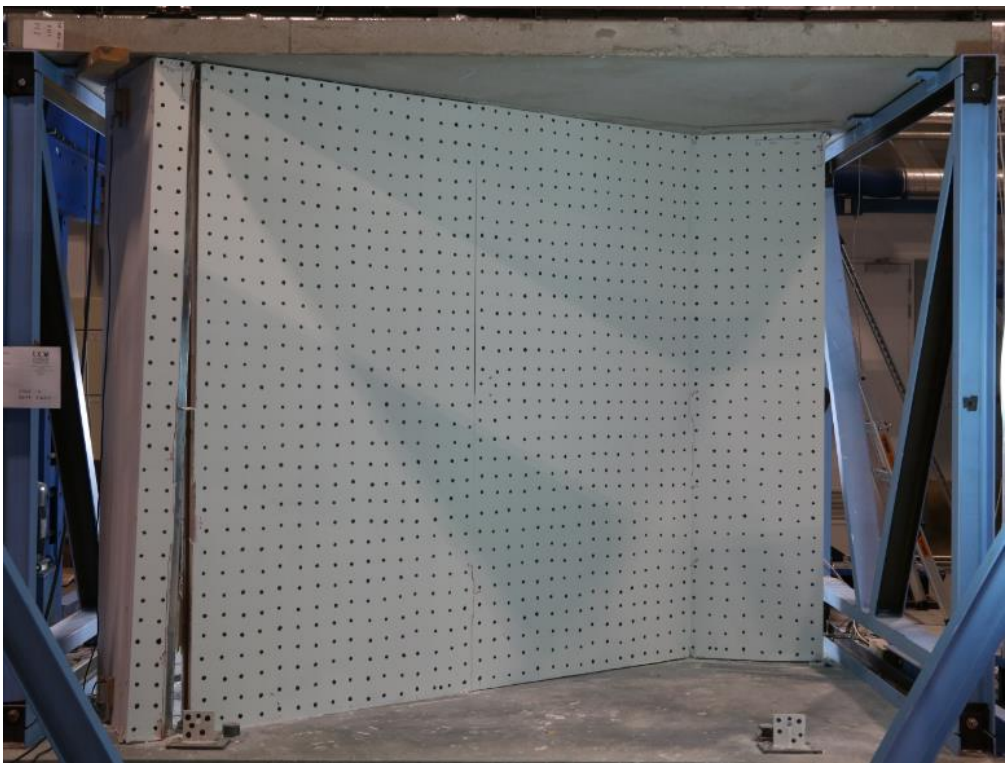

Figure C.55 Specimen B2 – Step 16 – state of specimen after completion of test

Figure C.56 Specimen B2 – Post-test framing inspection –-wall after removal of linings

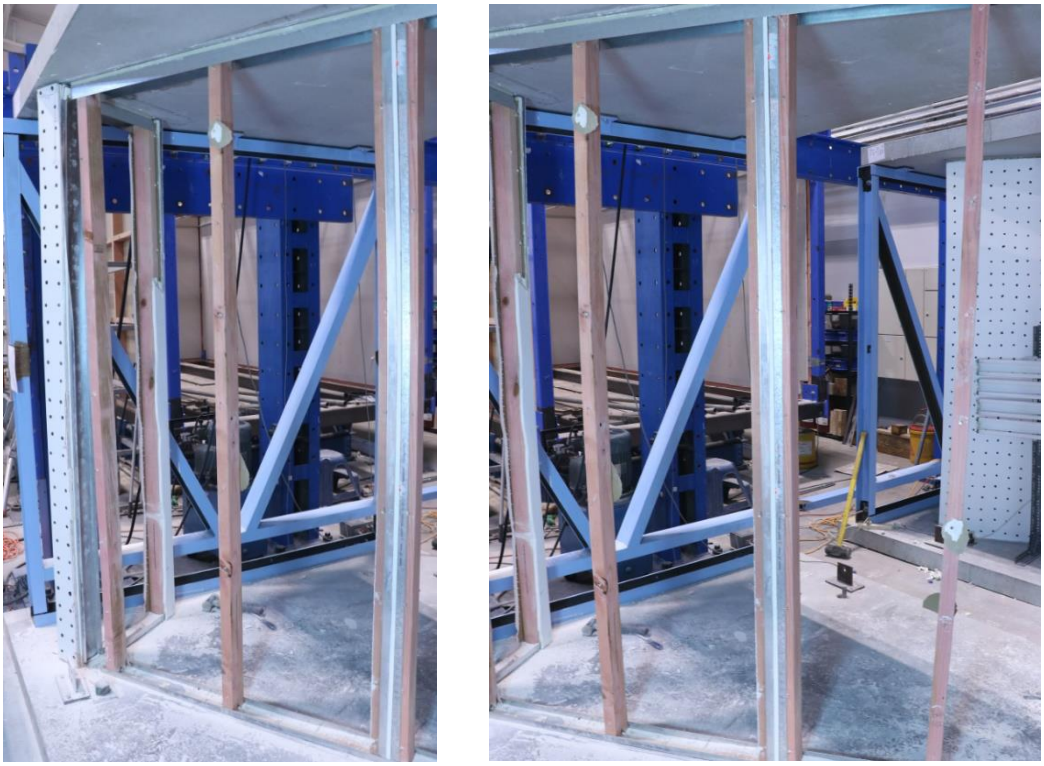

Figure C.57 Specimen B2 – Post-test framing inspection –-showing timber studs mostly in good condition (could be re-used)

Figure C.58 Specimen B2 – Post-test framing inspection –-bending of bottom track flanges in return wall at L-junction – locations 6, 7, & 11

Figure C.59 Specimen B2 – Post-test framing inspection –-Axial compression damage to timber stud at end of angled wall – locations 21

Figure C.60 Specimen B2 – Post-test framing inspection –-bending of bottom track flanges due to pushing of the main wall against the Y- junction – locations 2, 15, & 19

No further photos showing damage progression in this specimen or potentiometer readings are shown herein.